DOCTOR OF PHILOSOPHY

The Prediction Of Kinematics And Injury Criteria Of Unbelted Occupants Under Autonomous Emergency Braking

Bastien, Christophe

Award date:
2014

Awarding institution:
Coventry University

The Prediction Of Kinematics And Injury Criteria Of Unbelted Occupants Under Autonomous Emergency Braking

By

Christophe Bastien

September 2014

A thesis submitted in partial fulfilment of the University's requirements for the Degree of Doctor of Philosophy

Department of Mechanical, Automotive and Manufacturing Engineering
Faculty of Engineering and Computing
Coventry University

In collaboration with
TASS International, Toyoda Gosei Europe NV,
and OK-Engineering GmbH

Abstract

This thesis comprises a programme of work investigating the use of active human computer models and the effects of forthcoming automotive safety features on vehicle occupants; more specifically, their unbelted kinematics and sustained injuries. Since Hybrid III anthropometric crash test dummies are unable to replicate human occupant kinematics under severe braking, the thesis highlighted the need to research the most appropriate occupant computer model to simulate active safety scenarios.

The first stage of the work focussed on occupant kinematics and developed unique human occupant reflex response target curves describing the head and torso relative angle change as a function of time, based on human volunteers' low deceleration sled tests. These biomechanics curves were, subsequently, used to validate an active human model, asserting its torso response, while confirming that further development in its neck response was necessary. The sled test computer validation proved that only an active human model was suitable to model a pre-braking phase.

The second stage of the work combined the occupant's kinematics of the pre-braking phase, followed by a subsequent frontal crash into a rigid barrier inducing an airbag deployment. The results suggested that, in a 1g frontal deceleration pre-braking phase, the kinematics of an unbelted occupant within the vehicle compartment was complex and in some cases extreme. With the parameters adopted within this unique study, it was observed that occupant motion and position relative to the airbag system varied depending on awareness level, seat friction, braking duration and posture. Additionally, it was observed that a driver holding the steering wheel with one hand could be out of the airbag deployment reach due to extreme Out-Of-Position (OOP). Results also concluded that the dynamic OOP scenario was intricate and would yield to higher occupant injuries. Future studies, into brake dive, seat geometry, seat stiffness and cabin packaging, are recommended to capture the vehicle configuration providing the highest dynamic OOP safety risk.

Finally, the investigations conducted, as part of this doctoral programme, led to the provision of new knowledge in the validation of active human models, a unique demonstration of the importance using human computer models, rather than crash test dummies, as well as the potential for the evaluation of future restraint systems in dynamics unbelted OOP, considering various posture scenarios.

Acknowledgements

I would like to thank my academic supervisors Professor Mike V. Blundell and Professor Clive Neal-Sturgess for their commitment to this project, expertise and kindness for which I will forever be grateful.

I would also like to express my gratitude to my industrial partners who have been instrumental to the completion of this work, especially Michael Freisinger (OK-Engineering GmbH), Robin van der Made (TASS), Riske Meijer (TNO), Prof Dr Joerg Hoffmann and Alex Diederich (Toyoda Gosei) for providing engineering support, software licenses, sled tests data, time and patience.

I would also like to thank my wife Athina and my children Lucas and Lydia who have been very supportive, loving and caring for me all along these years. Thank you for having brightened my life. I also thank my parents Philippe and Marie Martine Bastien who have invested all these years in my education.

I am also indebted to Ray Jones of Coventry University who has patiently reviewed my work and provided useful advice, as well as Jesper Christensen, Oliver Grimes and Deborah Stubbs for their moral support.

I would finally like to express my gratitude to the Faculty of Engineering of Coventry University who has kindly funded this research.

This thesis is dedicated to my grandfather

Joseph Garcia (known as "Pépito")

(1924 – 1996)

He taught me the value of hard work and perseverance.

I trust that he would have been proud of this achievement.

Table of Contents

List of Figures

List of Tables

List of Equations

Abbreviations

- ACR: Active Control Retractor
- AEB: Automatic Emergency Braking
- AHBM: Active Human Body Model
- ASsEt: Active Safety Assessment Environment
- ATD: Anthropometric Test Dummy
- BIW: Body In White
- DAB: Digital Audio Broadcasting
- DEKRA: German expert organisation in Automotive Engineering
- EPSF: Equivalent Plastic Strain at material failure
- EPSR: Equivalent Plastic Strain at material Rupture
- EuroNCAP: European New Car Assessment Programme
- FARS: Fatality Analysis Reporting System
- FMVSS: Federal Motor Vehicle Safety Standard
- FCW: Frontal Collision Warning
- GDP: Gross Domestic Product
- GHG: Greenhouse Gases
- GIDAS: German In-Depth Accident Study
- GPS: Global Positioning System
- GSM: Global SysteM for communication
- HMI: Human Machine Interface
- HS2: High Speed Railway 2
- JARI: Japanese Automotive Research Institute
- LDW: Lane Departure Warning

- LIDAR: remote sensing technology which measures the distance of an object by illuminating the target with a laser and analysing its reflection. LIDAR is a combination of the work Light and radar.
- HBM: Human Body Model
- HIC: Head Injury Criteria
- KE: Kinetic Energy
- MADYMO: Explicit Solver from TASS International
- NASS: National Automotive Sampling System Database
- NCAC: National Crash Analysis Center
- NHTSA: National Highway Traffic Safety Administration
- Nij: Neck Injury criteria which is considering Tension/Compression, Flexion and Extension
- ODI: Office of Defects and Investigation
- OEM: Original Equipment Manufacturer
- OM4IS:Occupant Model for Integrated Safety
- OOP: Out-of-Position
- OTS: 'On The Spot accident data collection study'. Collaboration between Loughborough University and TRL
- PBC: Peak Braking Coefficient
- PHBM: Passive Human Body Model
- PMHS: Post Mortem Human Subject
- PRISM: Proposed Reduction of car crash. Injuries through Improved SMart restraint development technologies. EU funded FP7 project
- RADAR: RAdio Detection And Ranging. Radar is an object detection system which uses radio waves to determine the range, altitude, direction, or speed of objects.
- STATS19: UK Department for Transport road accident dataset
- RAMSIS: Vehicle Cockpit Ergonomics Design and Simulation software

- SATNAV: SATellite Navigation system is a system of satellites which provide autonomous geo-spatial positioning with global coverage.
- THUMS: Total Human Model for Safety (Human computer model from Toyota Motor Company)
- TRL: Transport Research Laboratory
- vFSS: advanced Forward looking Safety System
- WLAN: Wireless Local Area Network

1.0 Introduction

Automotive vehicles have changed our lives by giving users improved freedom of movement by means of travel. There are so successful that their use has kept on increasing year on year (Figure 1.1) (Wilson, 2013).

Figure 1.1: Upward trend of total vehicles on the road in the U.S. since 1960 (Wilson 2013)

In 2013, it was reported that almost 2 million people died worldwide in automotive accidents, automotive accidents now being classed as the second biggest cause of death in the World after war (WHO 2013).

In spite of this statistic, since the first recorded vehicle automotive fatality occurred in 1889, vehicle safety has played a major role in reducing death on the road (American Iron and Steel Institute 2004), as manufacturers realised the need to demonstrate occupant protection before the public accepted the automobile as a viable and safe means of transportation.

1.1 Passive Safety: An Overview – Turn of the 20th Century until Now

The first level of protection was implemented through passive safety, whereby vehicles are able to mitigate accidents without any driver interventions. Three distinct, periods in the development history of automotive safety have been observed (American Iron and Steel Institute 2004).

The first period started from the turn of the century until 1935; developments to understand the extremely complex process of vehicle collisions, including the forces involved and the concept of energy absorbing capability of the vehicle structure were researched. This has led to the first crash test in the early 1930s. Nevertheless, only

basic automotive vehicle improvements were implemented and included the reduction of tyre blowouts to avoid loss of vehicle control, the self-starter to eliminate injuries with engine cranking, the incorporation of headlamps to provide night visibility, the installation of laminated glass to reduce facial lacerations and the adoption of an all-steel body structure for better protection (American Iron and Steel Institute 2004).

The second period spread from 1936 to 1965; then manufacturers introduced crash avoidance devices, including turn signals, dual windshield wipers and better headlamps. The safety of vehicle interior was improved by tests performed to simulate head impact into the instrument panel and engineering high penetration-resistant windshield glass. Means of restraining the occupants in the vehicles were believed to be important for occupant safety. In 1956 Swedish inventor Nils Bohlin working for Swedish manufacturer Volvo designed an effective three-point belt (Happian-Smith, 2002), having demonstrated from accident statistics that unbelted occupants sustained fatal injuries throughout the whole range of speed scale (up to 60mph). His invention was granted U.S. Patent 3,043,625 (USPTO 2013) and in 1959 seatbelts were fitted as standard equipment. More research by General Motors was performed on car-to-barrier frontal crash test, launching a vehicle into a retaining wall leading to observations of the crushed vehicle followed by interventions aimed at improving structural performance. The implementation of airbags started at the beginning of 1960s in order to address the poor seatbelt usage by implementing a safety device so that occupants did not need to take any action themselves (Happian-Smith 2002).

The third period spreads from 1966 until present. It started with the creation of the National Highway Traffic Safety Administration (NHTSA) in 1966. The Federal Motor Vehicle Safety Standards (FMVSS) was introduced to regulate several aspects of vehicle crashworthiness and crash avoidance performance. Hence the collective vehicle safety technologies, together with improvements to highways and better driver education, have contributed to a large drop in fatalities. To support the development of vehicle safety various computer codes were available, however their capabilities were still inadequate. In 1990, computer contact algorithm, strain rate dependant material models (Cowper-Symonds), improved contact algorithms (Figure 1.2) (NCAC 2013), as well as the first uniform pressure airbag model were made available

(LSTC 2012), providing a realistic set of tools to address predictive vehicle safety design improvements.

Figure 1.2: Example of standard CAE crash analysis: Rav4.0 NCAC crash model (US NCAP)

In 1994, Arbitrary Lagrangian and Eulerian (ALE) features, including jet models, were presented, which was the dawn of multiphysics applied to the field of vehicle safety (LSTC 2012). Arbitrary Lagrangian and Eurelian codes could allow the coupling of a CDF jet with a structural element, for example the modelling of gas pressure expelled from the pyrotechnic ignition against the airbag cloth, allowing modelling a more realistic airbag deployment. In 1995, airbag venting capabilities and improved airbag fabric materials became available. The coupling capabilities between fluid and structure (Figure 1.3) were however only implemented in 2000 by TASS with the "Gas Flow 1" product, as part of the MADYMO software (Mahangare 2007a; Mahangare 2007b).

Figure 1.3: Airbag deployment using Gas Flow 1 (grids in blue) (Mahangare 2006)

Many Original Equipment Manufacturers (OEM) made use of these computer tools to improve the safety of their vehicles. In 1988, at Mercedes-Benz, the maximum vehicle model size was 10,000 elements, 80,000 in 1994, 500,000 in 2000 (Du Bois 2010). Nowadays, OEMs run models of over 4,000,000 elements.

Thanks to all these engineering measures, since 1970, the fatality rate per 100 million miles travelled has dropped by 80% (International Transport Forum 2012).

Crash events can be separated in 3 distinct phases (Crandall 2012a; Campbell 2013):

- the vehicle impacting the barrier,
- the occupant impacting the restraint system and finally,
- the organs impacting the occupant internal body cavity.

As such, more intricate occupant models are now being considered to assess the safety of vehicles (Figure 1.4) to address organ injuries. Some research is now considering assessing vehicles using an omni-directional human computer model (Toyota 2011) which has already been used in injury trauma assessments (Evans 2013). Human pedestrian models have already been used by Daimler (Mayer 2013) to confirm the head impact contact time of a pedestrian struck by a vehicle fitted with a deployable bonnet. This new methodology using the Total Human Model for Safety (THUMS) human computer model has been accepted by the European New Car Assessment Programme (EuroNCAP 2013a), in few crash test scenarios, as a valid process to enhance the assessment of pedestrian deployable bonnets timing (Mayer 2013) before child and adult head impactors are performed to assess the vehicle pedestrian performance (EuroNCAP 2013b).

Figure 1.4: 50th percentile occupants: Hybrid III Anthropometric Test Dummy (left), THUMS4.0 (right) in Coventry University's Microcab lightweight EV vehicle interior (Evans 2013)

The advantage of such models is that they are more relevant when occupant safety is concerned: these models can evaluate human trauma injury while crash test dummies evaluate injury criteria. Even if the trauma parameters are still being debated by biomechanics experts (Crandall 2013), it is overall agreed that this is the future direction research should take to further improve safety, given that models could incorporate parameters relevant to the entire population, i.e. gender, age, percentile and stage of pregnancy (Kayvantash 2009; Crandall 2013).

These advanced CAE tools are still the main ones utilised in industry and are now meeting such new vehicle structural challenges, as the improvement of the safety crash compatibility of lightweight electrical vehicles against heavier vehicles and stiffer ones, where cabin space intrusion can be a major concern (Figure 5), reducing occupant survival space (Grimes 2013).

Figure 1.5: Frontal crash compatibility event between of lightweight electric vehicle Microcab and a Ford Fiesta (Grimes 2013)

Some earlier work has shown that the safety cell stability is currently difficult to achieve (Grimes 2013). This is due to un-optimised loadpath and the excessive use of glass fibre for the door opening panels (Figure 1.5), as a result of its lightweight properties and ease of manufacturing for low production volumes.

1.2 The Future Automotive Landscape

The landscape of the automotive industry, as we have known it for the last 40 years, is however going to change in the next two decades as the number of vehicles on our roads is steadily increasing (Wilson 2013).

A similar trend has been observed by the Department of Transport (Department of Transport 2011), with the growth in vehicles expected to increase from 250,000 in 2010 to 375,000 in 2035 (Figure 1.6). A similar conclusion was also drawn (Miles 2011) with an estimated increase of 25% from 2010 to 2035.

This trend is due to the increase in Gross Domestic Product (GDP) per capita, meaning that individuals will have more disposable income, increasing general demand for goods and services. Rising GDP impacts on car traffic growth as car ownership increases as well as people's 'value of time'. A car can take a user directly to the desired destination so may be preferable in terms of 'time cost' to a train or bus (Department of Transport 2013).

Figure 1.6: Forecast growth in Traffic by Vehicle Type, England (Department of Transports 2013)

Unfortunately, the transport network has not and is not following with growth at the same rate at the forecast number of vehicles. The total road length in Great Britain in 2012 was estimated to be 245.4 thousand miles, which is an increase of 2000 miles (0.8%) over 10 years (Department of Transports 2013). Minor roads made up 87% of total road length, with motorways and 'A' roads accounting for 1% and 12% respectively. Despite accounting for only 13% of road length in 2012, major roads (motorways and 'A' roads) accounted for 65% of road traffic (Department of Transports 2013).

New managed motorways have been commissioned to improve journeys' reliability (congestion) by controlling traffic flows more effectively through the use of new technologies, e.g. overhead gantries, lane specific signals and driver information signs (Highway Agency 2013). The variable speed limits keep traffic moving by controlling the flow of vehicles when the route is congested. A computer system is used to calculate the most appropriate speed limit based on the volume of traffic; when traffic builds up road users will be instructed to use the hard shoulder as an extra traffic lane, thus increasing the motorway's capacity, reducing congestion and keeping traffic moving. A review of these new motorway schemes has shown that by monitoring the flow, personal injury accidents have reduced by more than half (55.7%) and there have been to date zero fatalities (Highway Agency 2011). Casualties per billion vehicle miles travelled have reduced by just under two thirds (61%) since the introduction of managed motorways (Highway Agency 2011). These new motorway schemes (M1 J10– J13, M62 J25-30, M4 J19-20 and M5 J15-17, M6 J5-8 (Birmingham Box Phase 3), M25 Junctions 5–7 Managed Motorways, M25 Junctions 23–27 Managed Motorways) suggest to have a great potential, as they will support the economy by reducing the number of traditional widening schemes, creating a better return on investment and increasing safety at a national level. Nevertheless it is not currently clear if these schemes will address the 25% increase of vehicle traffic forecast in the future.

1.3 The Benefits of Autonomous Vehicles

Increasing the road network is a real political and financial challenge, and it must be done whilst simultaneously reducing accident rates, pollution and congestion (Miles 2011).

Figure 1.7: Traffic intensity. Use of autonomous vehicles (Miles 2011)

A concept of 'Intelligent Mobility' is now being discussed, which could in the future enable travellers to plan and execute their journeys seamlessly across the whole spectrum of available transport options whilst enabling more vehicles to flow more freely (Automotive Council UK 2011). As an example, in order to increase the flow of traffic, it was suggested that autonomous vehicles (which may be the same size as current or smaller) would be the able to share the same lane (Figure 1.7), as well as following the findings from the managed motorways where the speed is constantly monitored and adjusted to suit the driving conditions.

Figure 1.8: Workload on driver (de Warrd 1996)

However, it is not possible for a human driver to perform such task as there are too many parameters to control, extra effort required and as a result considerable stress on the driver (De Warrd 1996; Hansen 1986), as illustrated in Figure 1.8.

In built-up area, the Cabinet Office has investigated the cost of urban transport in Great Britain and has been shown that "*the challenges faced by transport in urban areas are broad, affecting not only the economy of cities but also people's health and well-being… for example, improving air quality and increasing levels of physical activity can help reduce the incidence of diseases which shorten life and exacerbate existing conditions such as asthma*" (Figure 1.9) (Cabinet Office Research Strategy 2009:2).

The cost of urban congestion reached £10.9bn in 2009.

Figure 1.9: Comparison of the wider cost of transport in English urban areas (£) (Cabinet Office Research Strategy 2009)

It has been documented that 89% of the congestion delays occur in urban areas (Miles, 2011). Means of controlling the flow of vehicles is necessary and lessons can be learnt again from the Managed Motorways (Highway Agency 2013).

Figure 1.10: Integrating systems inside and outside the vehicle (Vignau 2011)

Autonomous vehicles with self-parking features are being discussed for the future of automotive fleets. It is proposed, in order to improve traffic flow within the city, to plan the vehicle parking spot at destination prior to departure, and not at the last moment (Miles 2011). For this to happen, communication between vehicles is necessary and an important reliance on wireless technology is needed (Vignau 2011), as illustrated in Figure 1.10.

The huge challenge is to perform the integration between all vehicles in real-time, i.e. all vehicles must have the same time base; the signals must be reliable and robust. It is expected that high speed communications conducted through WLAN, Global SysteM for communication (GSM) for non-time critical information, and Global Positioning System (GPS) for navigation and radio via Digital Audio Broadcasting (DAB) (Vignau 2011). The "big challenge how to appreciate the value of the information from outside, and how to integrate it with the time triggered network inside the vehicle" as information coming from the outside of the vehicle are asynchronous, as GPS has a low update rate and is inaccurate, GSM has a limited range and can induce delays, WLAN has a limited range and road side cameras have a low update rate as well as limited accuracy (Vignau 2011). This is the future challenge the automotive industry will have to face, which will provide a vast amount of opportunities.

Looking at a subset of the integration of all vehicles, the project SARTRES (SARTRES 2011; SARTRES 2012) has investigated a concept road train

configuration including a manually driven lead truck, which is followed by one truck and three Volvo cars (S60, V60 and XC60), with all the following vehicles driven autonomously at speeds of up to 90 km/h, with a gap varying between 4m and 5m between the vehicles – thanks to a blend of existing and new technology (Figure 1.11), with the aim to develop systems facilitating the safe adoption of road trains on un-modified public highways in interaction with other traffic (SARTRES 2011; SARTRES 2012).

Drivers following the truck would be able to take their hands off the steering wheel and switch to other activities, like reading a book, browsing the internet, listening to music, etc…

Figure 1.11: Road train study (SARTRES 2011)

SARTRES has developed a new prototype Human-Machine Interface including a touch screen for displaying vital information and carrying out such requests as joining and leaving the road train as well as a prototype vehicle-to-vehicle communication unit that allows inter-vehicular communication.

As the vehicles travel closely together, additional safety benefits would ensue as the driver is taken out of the equation. This convoy setup could also offer significant aerodynamic benefits in terms of reduced drag, leading to an estimated 10% fuel saving.

Platooning could increase the stability of the traffic itself, resulting in less oscillation of traffic flow, hence using roads more effectively (PE 2011a). Whereas the concept has the potential to deliver huge benefits, it also faces some challenges, not just in

terms of engineering, but also in persuading motorists to trust the technology and take their hands off the steering wheel (PE 2011b). It is also suggested that a convoy could challenge the need of the High Speed Railway 2 project (HS2) for cost and consumer travel flexibility (PE 2013).

In spite of this promising prototype framework which has shown some great potential, it has been pointed out that the SARTRES system does not account for situations where a vehicle is brought to a sudden stop by an unusual event, for example, a mechanical failure of vehicle within the platoon (such as a tyre blow-out) or a collision between a manually driven vehicle and the platoon, given the close proximity between vehicles (PE 2013a). This case does not void the work derived from the SARTRES project, it just suggest that vehicles need to communicate with others, while they need to have their "say" and must be able to decide for themselves, e.g. to brake as emergency braking is activated if a danger is evaluated. Again, it can be observed that the platooning concepts have the potential to reduce congestion, environmental impact and improve safety, and that a protocol is needed to harmonise the future of autonomous vehicles (Vignau 2011). Considering the outlook of vehicle technology, the professional body of engineering (IMechE) has suggested that, based on SARTRES' success, fully autonomous vehicles will be part of the future, according to major automotive suppliers and OEMS (PE 2013b). The state of California has signed state legislation that will pave the way for driverless Google cars by 1st January 2015 (PE 2013b).

Nevertheless, it has been noted that the proposed legislation was introduced too quickly, as the technology is so new and that it lacked "any provision protecting an automaker whose car is converted to an autonomous operation vehicle without the consent or even knowledge of that auto manufacturer" (PE 2012).

Figure 1.12: BRAiVE's driverless journey in downtown Parma (Vislab 2013)

In July 2013, VisLab tested city centre driving in a real environment for the first time ever. BRAiVE, VisLab's (Vislab 2013) most advanced intelligent vehicle drove in the centre of Parma (Figure 1.12), negotiating two-way narrow rural roads, pedestrian crossings, traffic lights, artificial bumps, pedestrian areas, and tight roundabouts (VTC2013-Fall 2013).

Nissan has also released some information suggesting that this technology will also be included in their future vehicles (Richard 2013). The new Nissan LEAF, tested on Japanese roads, is capable of lane keeping, automatic exit, automatic lane change, automatic overtaking of slower or stopped vehicles, automatic deceleration behind congestion on freeways and automatic stopping at red lights. Nissan Executive Vice President for Research and Development, Mitsuhiko Yamashita, has publicised that: "*The realization of the Autonomous Drive system is one of our greatest goals, because Zero Fatalities stands alongside Zero Emissions as major objective of Nissan's R&D. Through public road testing, we will further develop the safety, efficiency and reliability of our technology*" (Richard 2013).

This is a clear suggestion that in the near future, driverless technology will be part of our lives.

In the short term, globally, active safety technology will be implemented from 2014 (EuroNCAP 2013c) which will start to take some subtle control over the driver's braking patterns in order to avoid and/or mitigate rear impact accidents.
This subtle control is classified as Autonomous Emergency Braking (AEB), which assists the vehicle in performing a complete stop, by initially warning the driver of the need to brake and then taking over the control of the vehicle if no action is detected.

Overall, this new "active safety" technology is the term used for collision, warning, avoidance and mitigation; the technologies adopted for active safety, to date, being (Kirkman 2014):

- Radar 24GHz (medium range) and 77GHz (long range)
- Ultrasonic sensor (parking aid)
- Camera
- Satellite Navigation Systems (SATNAV)

Vehicle safety is now split into primary safety and secondary safety (The AA 2011). Primary safety describes features designed to help avoiding a crash. Brakes and lights fall into this group as well as systems like electronic stability control or lane keeping support. Secondary safety features come into play once accident is unavoidable and are designed to reduce occupants' injuries. This covers seat belts and airbags, head restraints and the design of the body structure and vehicle interior.

A different terminology is also used for 'primary safety and secondary safety' which is 'integrated Safety', from the OM4IS research project aiming to characterise the occupant reactive behaviour in low load pre-crash phase (OM4IS 2011). Integrated Safety would include the active safety phase which will aim to avoid or mitigate the accident severity, the passive safety crash phase which will include deformable Body In white (BIW) structure and activation of the restraint system. It has to be observed that the Integrated Safety proposed by OM4IS does not include the concept of Post-Crash response technology which would, in the event of a severe crash, provide the ability to contact local emergency services in order to assist reaching the scene of the vehicle crash as quickly as possible (Ford 2013).

In the United States, NHTSA is also engaged in research to evaluate the effectiveness of automated braking systems in cases of accident avoidance and mitigation (NHTSA 2010). As part of this research, NHTSA is currently developing test procedures to evaluate active safety technologies to assess their benefits. In *« Preliminary Statement of Policy Concerning Automated Vehicles »* (NHTSA 2010), NHTSA has recommended that consumers should consider choosing vehicle models equipped with active safety technology recommended in the New Car Assessment Program (NCAP). Consequently, the AEB technology will be present in Europe and the United States.

The deployment of active safety is likely to be a first step to give confidence to the public that technology can indeed be beneficial to the driver; this may ease the introduction of the autonomous technology in some years to come. Nevertheless, research should also investigate the effect of such technology on driver behaviour.

1.4 Thesis Aim and Objectives

From the information gathered, it has been established that active control of the vehicle will take place (EuroNCAP 2013e), and will probably have an influence on the driver kinematics within the vehicle cabin and potentially on his/ her injuries should a subsequent accident occur. From January 2014, most new vehicles will be fitted with active safety technology (Traffic Technology International 2013) and in the next 20 years, drivers will be able to carry out any activities he/ she wishes in the driving vehicle (SARTRES 2011; SARTRES 2012). Consequently, this is likely to create a different safety scenario given that a standard crash test dummy is only calibrated in chosen directions of impact.

Research in the investigation in the comparison between Anthropometric Test Dummies (ATD) and human occupants (PRISM 2002) has shown that in a belted frontal low deceleration scenario (under 1g), motions are already different, as illustrated in Figure 1.13.

During pre-braking, the belted occupant is moving forward but is still central and far from the dashboard or steering wheel airbag system. As AEB systems will be implemented in Europe and the United States, their application may affect the occupant crash safety performance.

Figure 1.13: Comparison of ATD and human kinematics under extreme braking (PRISM 2002a)

EuroNCAP frontal crash scenario is testing a vehicle impacting a deformable honeycomb barrier at 64km/h using a belted occupant. Performing a crash test using pre-braking followed by a crash against EuroNCAP standards is suggesting that injuries to the driver are less severe (Berg 2012). On the other hand, NHTSA is performing 2 types of tests within the FMVSS208 legislative requirement for frontal structural and occupant safety assessment which relates to a vehicle impacting against a rigid barrier at 56km/h (35mph) with a belted occupant and a 40km/h (25mph) rigid barrier impact with an unbelted occupant (not considered in Europe). A pre-braking phase prior to the crash event would bring the occupant closer to the airbag before the accident. It has been documented that occupant proximity to an airbag leads to serious injuries (Morris 1998), consequently some concerns can be raised by the influence of such active safety systems on the occupant's posture and relative position to the airbag system during the braking phase.

Therefore, this doctoral investigation aims to ascertain the most appropriate occupant computer model to explore kinematics and potential injuries when new active safety features are introduced.

Consequently, as vehicles will perform active manoeuvres often unexpectedly, the hypothesis put forward and tested in this thesis is that it is important and necessary to use active human computer models to accurately simulate future active safety situations, i.e. occupant kinematics and injuries.

To objectively test this hypothesis, an Active Safety Assessment Environment (ASsEt) will be created to indicate the appropriate computer model for the future active safety assessments.

To meet the aim of this project the following key objectives will be addressed:

1. Create an Active Safety Assessment Environment (ASsEt) combining vehicle pre-braking phase followed by an accident scenario,
2. Validate an active human computer model against human volunteers low deceleration tests (1g maximum),
3. Incorporate the validated active human model into the ASsEt environment,
4. Conclude on the suitability of active human models in the ASsEt environment.

1.5 Structure of the thesis

The thesis will therefore contain the following sections (Figure 1.14):

- Chapter 1: An introduction chapter,
- Chapter 2: A literature review chapter, which lays the background and state of the art active safety future requirements,
- Chapter 3: A methodology chapter, which sets the ASsEt Environment which will be used to assess the hypothesis,
- Chapter 4: An application of a passive human model in passive Out-Of-Positions (OOP) chapter, which validates the stability and responses of state of the art human technology,

- Chapter 5: A validation of an Active Human model chapter, which validates kinematic responses between a new active human computer model and volunteer tests in a lap belt scenario,
- Chapter 6: A Kinematics and Injuries Of Unbelted Occupants Under Autonomous Emergency Braking chapter, which combines the proposed ASsEt environment and the newly validated active human model,
- Chapter 7: A Discussion chapter which reflects on the results obtained from the correlation and ASsEt environment studies,
- Chapter 8: A Conclusion chapter, which concludes on the outcome of the thesis,
- Chapter 9: A Future work chapter, which proposes follow-on studies.

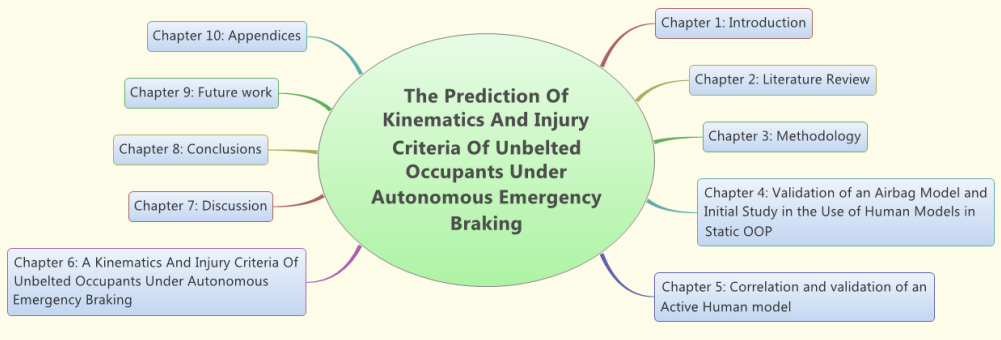

Figure 1.14: Thesis Structure

As a forewarning to the reader, the thesis will consider the worst case scenario, which is an unbelted loadcase subjected to an extreme frontal braking phase followed by a 40km/h (25mph) rigid wall accident. The list of published work from thesis is listed in Appendix A.

From the literature review (chapter 2), the thesis will focus on the potential effects of active safety on occupants' kinematics and injury criteria. The current human computer models have yet to be evaluated for emergency braking and other evasive safety manoeuvres. This work will use kinematics data from human volunteers, in a defined emergency braking scenario, to later address the gap in the body of knowledge which relates to the importance of using active human models in active safety scenario, especially in the cae of dynamic Out-of-Position (OOP).

1.6 Background of Collaborators in this work

This thesis was initiated thanks to the previous collaboration between Coventry University, Toyoda Gosei, Japanese airbag manufacturer, and TASS International, MADYMO software reseller, in project OoPSafe1 (2002 – 2006). OoPSafe1 looked into the modelling of OOP airbag deployments in static FMVSS208 scenario where a static small (5^{th} percentile) female anthropometric crash test dummy (ATD) was resting its chin and chest on a deploying airbag module. The work was researched by Manoj Mahangare (Mahangare 2007a; Mahangare 2007b) who looked into the importance of using computation gas flow modelling, representing the flow of gases travelling inside the unrolling airbag cloth, during deployment.

Following this initial work, a collaboration project code-named OoPSafe2, with the same partners, was initiated in January 2009 with the aim to investigate the effect of occupants' injuries during airbag in OOP using Manoj Mahangare's research in static OOP as a starting point and referenced in chapter 4 (Validation of An Airbag Model and Initial Study In the Use of Human Models in Static OOP). Contribution was provided by 2 MSc students in the early stages of OoPSafe2 in August 2010: Deborah Stubbs worked into the implementation of the airbag tether mechanical failure and Jhenu Kumar Subramanian investigated airbag permeability, while the author improved the computer modelling of the airbag plastic cover and researched on occupant kinematics and injuries using ATD and passive human models, also referenced in chapter 4. These models were used as a starting point in OoPSafe2 in order to study a dynamic OOP loadcase.

In 2011, Toyoda Gosei, as part of the OM4IS consortium, provided sled test data of 50^{th} percentile volunteers performed at the University of Graz, which were using a simple lapbelt restraint system. This data was pivotal to the work presented, as it led to the research in the application of human models with active muscle (reflex). This technology was at its infancy and a beta (development) model of an active human model was provided to the OoPSafe2 project. While this development version of the active human model was tested and improved within the work of this thesis, TNO kindly provided their technical support.

In 2012 a new partner joined the OoPSafe2 partnership, OK-Engineering GmbH, providing advice and expertise on active safety modelling scenario in MADYMO.

2.0 Literature Review

2.1 Accident statistics and passive safety

Motor vehicle safety on the roads has greatly improved in the past 40 years. Statistics have shown that the number of fatalities per billion kilometres travelled has reduced by around 80% since 1970 (Bureau of Transportation Statistics 2011; International Transport Forum 2013), as illustrated in Figure 2.1.

Figure 2.1: Fatalities per billion km travelled (1970 – 2010) (International Transport Forum 2013)

These improvements have been influenced by the introduction of better passive safety, whereby the vehicle structure coupled with the restraint system limit structural intrusions in the cabin area, as well as coupling the occupant to the seat which has the effect of enabling a better engagement with the airbag system (Stubbs 2010), as well as mitigating occupant ejection (Crandall 2013; Neal-Sturgess 2013; NHTSA 2013a). It is also suggested that speed management and effective drinking and driving policies reduced fatalities by nearly half between 2000 and 2010 (International Transport Forum 2012), as depicted in Figure 2.2.

Figure 2.2: Evolution in the number of fatalities amongst groups 2000-2011 (OECD & the International Transport Forum 2013)

All vehicles in Europe must pass legal safety requirements and have the Vehicle Certification Agency, VCA (VCA 2013) approval prior to the vehicles being sold. In the United States, vehicles can be sold on the trust that they meet legal requirements. NHTSA (NHTSA 2013b), part of "the Office of Defects Investigation (ODI) and as the U.S. Department of Transport National Highway Traffic Safety Administration", can "conduct defect investigations and administer safety recalls on everything from vehicles and equipment to tires and child safety seats" (NHTSA 2013b). It has to be noted that legal requirements between Europe and the USA, based on Federal Motor Vehicle Safety Standards (FMVSS), are different and that some vehicle tests can be more stringent, like interior head impact (FMVSS201 2013) and vehicle frontal impact with occupant unbelted (FMVSS208 2013). New talks have been opened between the European Union and the United States aiming to create "the world's largest free trade zone" (BBC 2013). Initial discussions have started on the requirements for vehicle brake lights, as car manufacturers from Ford to BMW want standardised safety regulations, so they "no longer have to manufacture separate parts to adhere to different safety standards" (BBC 2013). A lot more is needed to standardise the legislation and this will take many years. A major step in the harmonisation of safety testing is the introduction of Global Technical Regulations (GTR), where the specifications are aimed to be transposed into local legislations.

This is the case for pedestrian protection with GTR9, which has vastly harmonised the implementation of pedestrian safety testing all over the World (UNECE 2008).

Several consumer programs like European New Car Assessment Programme (EuroNCAP 2013c) also evaluate the safety level of new cars using laboratory crash tests. Others, like USNCAP, ANCAP, JNCAP, Insurance Institute for Highway Safety (IIHS 2013a) tests perform similar levels of assessments, which have generally similar safety assessment. Since 1996, EuroNCAP has become an important player in Europe and elsewhere in the improvement of vehicle safety. EuroNCAP has since its introduction and up to 2009 tested in excess of 300 of the bestselling car models in Europe (EuroNCAP 2012).

IIHS and EuroNCAP, as consumer test houses, will ensure that the vehicles will at least match the basic legal requirements, and in many cases set higher standards in order to push development at a faster pace than regulation. These safety testing programs raise consumer awareness, and put pressure on vehicle manufacturers to develop at a faster pace or to a higher standard, since there is concern that a poor or low rating will impact upon sales.

This trend can also be observed in the Swedish Folksam report (Folksam 2013) based on data both from real-life accidents and crash tests, including results are based on 105,000 car accidents that occurred between 1995 and 2008, involving 29,000 injured persons and using data from two-car collisions, hence the outcome of the collision is determined by the vehicle crashworthiness features and masses. Folksam's philosophy is that crash tests do not always correspond 100% with reality, as well as not taking into account cross-category accidents, e.g. SUV accidents against super-minis. Hence it is advocated that a vehicle "should be chosen a on basis of the results of real-life accidents, and secondly on the basis of crash test results" (Folksam 2013). It has been observed that "more modern cars usually have considerably higher safety standards and consequently fewer injured persons. A new small car may therefore be as safe as or safer than an old large car, but various makes and models differ considerably" (Folksam 2013).

These recommendations are important for the customer who would wish to purchase a vehicle, but not very useful for the vehicle manufacturer, as they need a metric to

design their vehicles, hence the legal requirements and the NCAP consumer tests, which are set and uniform across all Original Equipment Manufacturers (OEM).

Conveniently, some further research has suggested that, based there was a positive link between the safety rating of vehicles and their performance in real life accidents It was observed that "5-star rated Euro NCAP cars were found to have a lower risk of injury and fatalities compared to 2-star rated cars" (Kullgren 2010). This is confirming that OEMs are focusing their safety performance on serious crash outcomes, hence concluding that there is a "good concordance between Euro NCAP and Folksam real-world crash and injury ratings".

Considering the road fatality trend from 1970 - 2010 (Figure 2.1) and the latest results published in the latest Road Safety Annual Report 2013 (Figure 2.3) (International Transport Forum 2013), it can be observed that the number of fatalities overall is now level (average of around 5.6 road fatalities per billion vehicle-kilometre if ignoring Czech Republic and Korea).

Figure 2.3: Road fatalities per billion vehicles-kilometres in 2011 (International Road Transport Forum 2013)

The passive safety technology has reached full maturity and structural loadpath are very well understood (Grimes 2013), especially in the safety cell area (Christensen 2011; Christensen 2013). The challenge for the vehicle manufacturers is to balance the impact energy absorption and the vehicle mass. Considering, an Audi A2 which is best in class aluminium chassis, its EuroNCAP safety rating is only a 4 Star (EuroNCAP 2013d). The Body-in-White (BIW) of an Audi A2 weighs 20% of the total vehicle mass, hence increasing structural rigidity can only be performed as part of the main structure, which will have a direct repercussion on the vehicle mass, with

no obvious opportunity to remove vehicle mass elsewhere. The mass increase would lead to augmentation of Greenhouse Gases (GHG) emissions, hence increasing the challenge of passing the EU vehicle emission standard requirements Euro5 (Delphi 2012).

2.2 Active Safety: Opportunities and Future Assessment

Benefits of reducing the impact velocity

In order the reduce GHG emissions as well as the number of fatalities on the road further, the impact energy would need to be reduced. In a vehicle safety perspective, the accident has to be avoided, or if it cannot be avoided, then the impact energy needs to be as small as possible. As the energy stored in the vehicle is kinetic energy (KE), then reducing the vehicle velocity (v) before the impact would greatly reduce as KE is a power law describer in Equation 2.1.

$$KE = \frac{1}{2}mv^2$$

Equation 2.1: Standard Kinetic Energy equation (Berg 2012)

As an example, a vehicle weighting 2,100kg decelerating at 0.6g would reduce its impact energy by 75% after 2s pre-braking (Table 2.1 based from Berg 2012).

Table 2.1: Effect of impact energy when pre-braking is applied (Berg 2012)

As a consequence less energy is transmitted to the structure and hence to the occupant. In a case study relating to a BMW350d impacting an offset deformable barrier (ODB), reducing the impact velocity from 64km/h down to 40km/h has a major benefit for the driver, as injuries are reduced by at least 40%, as shown in Figure 2.4.

Figure 2.4: Difference in injuries when reducing impact speed (Berg 2012)

Observed driver responses

As a result, it is recommended that prior to a collision, in case of an accident, the vehicle speed should be reduced as much as possible (Berg 2012; Grover 2012). Some research was commissioned by the advanced Forward-looking Safety Systems working group (vFSS), led by DEKRA, which is promoting the market penetration of front protection systems designed to avoid accidents and to lessen the consequences of accidents into the volume-model segment and to further improve road safety. By evaluating the corresponding pre-crash braking behaviours, it was discovered that, based on the GIDAS database, in 24% of the 1,492 cases studied, the car drivers did not brake at all. This high number relates to the EuroNCAP research findings that 90% of road accidents are caused by drivers who are distracted or inattentive (EuroNCAP 2013e). In a further 23% (Figure 2.5) of cases the data contained no information on the braking behaviour. In all other cases the cars were braked before the impact. Of the latter, the deceleration was over 6 m/s² in 28% of the cases (Berg 2012). It can be observed that the tally of the percentages is 101% and not 100%, hence a small error in the data reporting occurred. Nevertheless the trends are very clear and this error is therefore not significant.

Figure 2.5: Frequency distribution of braking deceleration in the pre-crash phase (Berg 2012)

These statistics are showing clearly that the driver can have an important input in the collisions process. If 24% of the drivers have not braked, this could be classified as a driver error, as the collision has not been mitigated and could have been. It can also be concluded that there would be a potentially significant benefit to assist the driver in performing an emergency braking, and suggesting maybe that this could be made automatic. As a consequence, two (2) new systems could be introduced in future vehicles: Autonomous Emergency Braking (AEB) and Forward Collision Warning (FCW), which are very distinctive safety systems. If AEB performs an automated braking, FCW only warns the driver of a potential collision and pre-pressure the braking system, and will rely on the driver to take action (Thatcham 2012). Similar findings from the Highway Loss Data Institute (IIHS 2012a) have concluded that Forward collision avoidance systems, particularly those that can brake autonomously, along with adaptive headlights, which shift direction as the driver steers, show the biggest crash reductions.

IIHS has already reported some AEB technologies success stories in its literature, endorsing the benefits of active safety and even divulging the vehicle brand names, like the Volvo XC60, to incite other OEMs to follow suit (IIHS 2012b; IIHS 2013b).

Looking at collision types in the Fatality Analysis Reporting System database (FARS) it can be observed that most fatalities are involved in frontal impact, as depicted in Figure 2.6 (FARS 2013).

The GIDAS database also concurs with the FARS database, as about 50% of the seriously injured and about 40% of the killed vehicle occupants result from a frontal collision. In about 60% of cases the opponent in the accident was another vehicle (GIDAS) and of these cases a total of 40% were front-rear collisions. Considering this evidence, it can be suggested that frontal impact mitigation needs to be designed for in order of priority.

Figure 2.6: Passenger car fatalities by collision type (percentage) (FARS 2013)

More evidence has shown that in 8483 crashes used for analysing AEB effects, only 12% of the drivers performed a steering manoeuvre compared to 88% providing no steering input (Edwards 2013).

An FP7 project codenamed ASSESS (ASSESS 2012a) started in 2008 and completed in 2012, aimed to develop a relevant set of tests and assessment methods applicable to a wide range of integrated vehicle safety systems focusing in rear end collisions, considering driver behaviour, pre-crash system performance, crash performance evaluation and socio economic assessment (ASSESS 2012b). This European project has categorised a list of typical road traffic accidents which would benefit from active safety systems in rear collision scenarios (used later in the thesis).

Another report published by NHTSA, entitled "A Test Track Protocol For Assessing Forward Collision Warning Driver-Vehicle Interface Effectiveness", has revealed that a distracted driver takes 1.2s to 1.7s to react to a crash, while a 'warned' one could

react between 0.3s to 1.0s (NHTSA 2011), based on " the instant the driver returns their attention to the forward facing viewing position". The study has shown that FCW on its own was not sufficient to avoid the accident, as only 25.4% of possible accidents have been avoided using FCW alone. In the intent to identify which alert modalities most effectively assist distracted drivers in forward collision and lane departure crash scenarios, it was suggested that haptic seatbelts, based on 32 volunteers, offered better crash avoidance effectiveness than the other individual modalities (auditory, visual and combination of both).

Research in the AEB implementations

Some of this research has been pursued in the AEB Group, led by Thatcham Research, which has been created with the aim to design and implement test procedures reflecting real world data to encourage the development of autonomous braking technology, that can helping preventing or mitigating the effects of car-to-pedestrian and car-to-car crashes, and to ascertain any differences among systems that come to market. The Car-to-Car-Rear (CCR) crashes studied were defined as being a rear-end accident involving 2 vehicles travelling in the same direction, the struck vehicle should have at least 4 wheels, and the striking vehicle should be M1 (car or taxi) (Grover 2012).

Car-to-Car accidents have been analysed against STATS19 (Road Accident Dataset collected by UK Police) and On The Spot dataset (OTS) collected by Research teams at Loughborough University and the Transport Research Laboratory (TRL).

Table 2.2: Summary of STATS 19 clusters from UK accidentology study (Grover 2012)

The study considered accident severity, speed limit, junction detail, light conditions, weather condition ad vehicle manoeuvres. From this study, the 6 main relevant modes of collisions have been gathered in clusters, representing at least three quarters on the collisions. These clusters are listed in Table 2.2.

For practical requirements of a consumer/insurer test program, some clusters were either amalgamated or discounted as testing scenarios for two reasons:

- Low frequency of occurrence or
- Practical difficulties in test implementation.

Cluster 6 was difficult to interpret for a practical test as whether it should be at a roundabout or not at a junction at all, hence it was not selected as a test scenario. Cluster 5 is a low frequency so was discounted. The 'other' clusters 7 to 18 were also discounted since there were no features that were statistically over represented to help define the scenario detail (Grover 2012).

As a consequence, the following scenarios have been derived and proposed by Thatcham Research to EuroNCAP for active safety systems assessments (Figure 2.7).

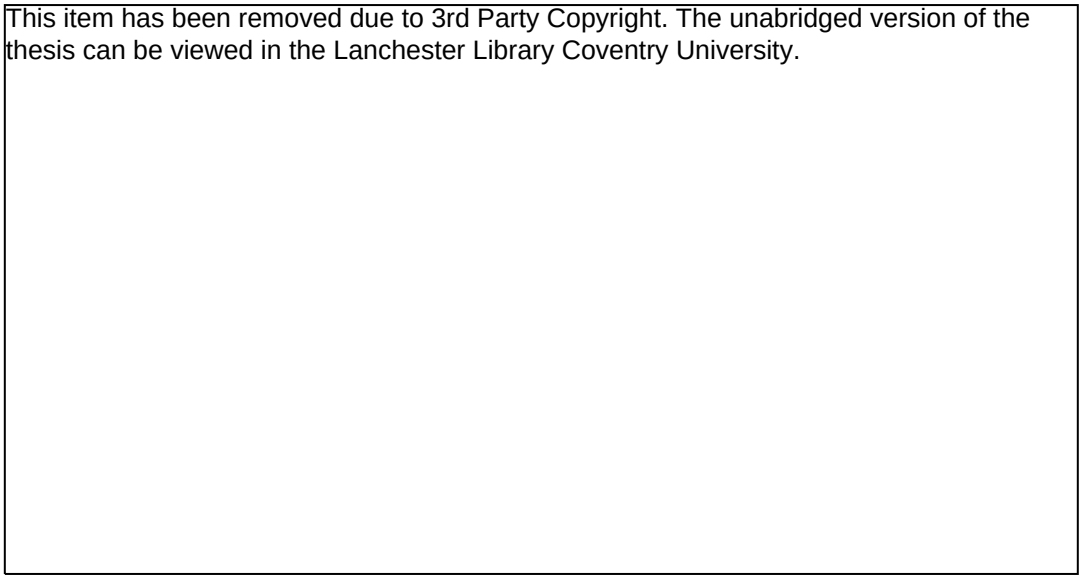

Figure 2.7: Thatcham EAB tests scenarios proposed to EuroNCAP (Grover 2012)

Thatcham Research has studied generic accident scenarios which would benefit from active safety (Thatcham 2014) and has estimated that active safety, and especially Autonomous Emergency Braking (AEB), could reduce annually in Europe:

- Within 3 years: save 60 lives and result in 760 fewer serious casualties
- Over 10 years: save 1,220 lives and nearly 136,000 serious casualties

In order to assess the efficiency of AEB systems, Thatcham Research has created a scoring system which will aim to evaluate the effectiveness of each AEB. The scoring system (Table 2.3) is weighted towards the low speed impact, as they reflect crash frequency, the risk of whiplash or personal injury claims (Thatcham 2013a).

The City tests do not take into account FCW in the calculations, but only AEB, as at low speeds there is little or no time for the driver to respond (Thatcham 2013a).

The rating is calculated using formula below (Equation 2.2):

$$AEB_{mitigation} = \text{Points}_{available} \times \frac{(\text{Test speed - Speed of Impact})}{\text{Test speed}}$$

Equation 2.2: AEB Mitigation Rating (Thatcham 2012)

Table 2.3: UK group rating points weighting as a function of approach speed (Thatcham 2013a)

The current active safety technologies utilise various means of impact avoidance and contain 4 main technologies, which are RADAR (use of radio waves), LIDAR (use of light and radar), Fusion (use of 1 lens) and stereo Cameras (use of 2 or more lenses) (Figure 2.8).

Figure 2.8: State of the art of AEB technology Avoidance Technology (Hulshof 2013)

- Based on 8 LIDAR sensing vehicles (Ford Focus, Mazda CX5, Fiat Panda, Mazda 6, Fiat 500L, VW up!, Volvo XC60, Volvo V40), it was shown that there was a lot a variability in the sensing trigger, as well as the braking rate.

These systems can avoid the accident up to 25km/h. It was found that at higher speeds, the accident was only mitigated and not avoided.

- One (1) test was performed using RADAR (Mitsubishi Outlander). The AEB stops from 30km/h, but no activation was detected for higher speeds.
- One (1) test involved a LIDAR, RADAR and Camera sensor fusion (optional fit), VOLVO V40. The stopping speed performance was 35km/h, which is better than of the tested RADAR system, and was also able to mitigate all speeds up to the maximum test speeds of 50km/h.
- One (1) test involved a Stereo Camera fusion system (Subaru Outback) performed the best as all speeds up-to 50km/h have come to a complete stop.

These tests have indeed proven that AEB system have potential to detect objects and prevent collisions, however they must be assessed as they do not perform with the same efficiency (Hulshof 2013).

Driver's acceptance of new AEB technology

One major issue which has been raised in publications and forums, is also the acceptance of such systems, as the customer knowledge and willingness to pay extra for these system is still limited (Langwieder 2012).

After confidential discussions with an OEM (Coventry University 2013), the implementation of active safety devices is very important to the automotive business, as it will inherently make the vehicles safer as well as further position the company competitively in vehicle safety engineering. As a consequence, the implementation of new technology must be incremental in order to foster the acceptance of such systems. These systems should be here to serve the driver as well as:

- "*support all types of driving styles*
- *enhance driving experiences*
- *enable customers to explore the capabilities of their vehicle with confidence*
- *be intuitive (switches itself ON when appropriate)*
- *be intelligent (only intervenes when needed)*
- *not patronise, annoy or overpower*" (Coventry University 2013).

A study was conducted aiming to understand the likely acceptance of active safety features in this vehicle OEM (Coventry University 2013). Thirty one (31) features were ranked in order of their safety benefit (1 to 10, 10 being the OEM's believed best active safety system), ranging from Intelligent Emergency Brakes (equivalent to AEB systems) up to night vision systems. Without this information, customers were asked to rank which active safety systems they believe should be installed in future vehicles (1 to 10, 10 being a "must have"). By multiplying these 2 quantifiers, a chart listing the relevance of active safety features, including safety benefits and customer wish, was derived (Figure 9).

Figure 2.9: Relevance of active safety features (including safety benefits and customer wish) (Coventry University 2013)

From Figure 2.9, it can be noted that "Intelligent Emergency Brake" scores the highest, meaning that the effectiveness of this system is also perceived as being important by the customers, as the rating was 54 out of a possible 100.

From this study, it can be concluded that AEB systems are likely to be more easily accepted by the customers than, rear view cameras, virtual co-pilot, hazard lights under heavy braking, driver monitoring and night vision score way under 20, which are seen as less beneficial. It must be noted that the sample size for the survey was not provided, nor the type of customers, hence it is not possible to generate an absolute rule from these results, but just a trend.

This can already be seen in 2013 models were AEB and FCW are becoming more available (Thatcham 2013a).

New implementation of AEB systems

EuroNCAP has since implemented new active safety requirements (Table 2.4), based on Thatcham Research's findings.

Table 2.4: EuroNCAP future test (2014) (EuroNCAP 2013f)

As a consequence, new star rating will be awarded (CARHS 2013), which will include AEB city, Lane Departure Warning (LDW) and AEB inter-urban (Figure 2.10).

Figure 2.10: Expected EuroNCAP roadmap (2014) (CARHS 2013)

AEB Inter-Urban systems are *"designed to work at speeds typical for driving outside of the city environment, for example on urban roads or highways"* (EuroNCAP 2013f). Inter-Urban and pedestrian systems include AEB function, Forward Collision Warning function and the Human Machine Interface (HMI), while the City system is primary AEB, as the time for collision warning is too short.

Since January 2014, EuroNCAP released the Safety Assist Test protocol (EuroNCAP 2013f), which will test AEB systems up to the speed of 80km/h, using an AEB mitigation rating method similar to the one derived by Thatcham Research, i.e. using Equation 2.2.

This protocol addresses the following accident scenarios:

- **Car-to-Car Rear Stationary (CCRs) –** a collision in which a vehicle travels forwards towards another stationary vehicle and the frontal structure of the vehicle strikes the rear structure of the other.
    - **Car-to-Car Rear Moving (CCRm)** – a collision in which a vehicle travels forwards towards another vehicle that is travelling at constant speed and the frontal structure of the vehicle strikes the rear structure of the other.
    - **Car-to-Car Rear Braking (CCRb)** – a collision in which a vehicle travels forwards towards another vehicle that is travelling at constant speed and then decelerates, and the frontal structure of the vehicle strikes the rear structure of the other.

The Safety Assist score is based on the weighted sum of the AEB, FCW and HMI (Human Machine Interface) totals and the scoring process is detailed in the EuroNCAP active safety protocol (EuroNCAP 2013f).
At this point in time (2014), all these AEB systems .are designed to consider protecting and mitigating accident/ collisions to other parties and the evidence to mitigate and avoid accidents is compelling. Nevertheless, the protocol which is being designed and enforced in 2014 also should also consider the occupants in vehicles fitted with AEB active safety systems.

2.3 Active Safety and Driver's response

Effect of driver postures on kinematics and injuries

The typical response to a crash event is to brace rearward into the seat and to straighten the arms against the steering wheel, or, to swerve to attempt to avoid the impacting vehicle (no pre-braking). While turning the steering wheel, the forearm can be directly positioned on the airbag module at time of crash which represents a potential injurious situation (Hault-Dubrulle 2010a; Hault-Dubrulle 2010b). From a

driving simulator study, it was shown that drivers observed 3 main postures prior to a crash. They either behave in a mitigating approach by bracing or moving their hand to the gear lever or an evasive action by swerving (Hault-Dubrulle 2010a). The consequence of turning the steering wheel can present a potential injurious situation as the arm is in front of the airbag module, which can cause serious head injury (Hault-Dubrulle 2010b), as displayed in Figure 2.11.

Figure 2.11: Potential injurious position due to driver posture (Hault-Dubrulle 2010b)

This example is showing the importance of OOP relative to a safety device. More research has also shown that severe injuries were observed for occupants positioned less than 250mm from a deploying airbag (Morris 1998). Consequently OOP occupants could be seriously injured by a deploying airbag.

Some research (Bose 2010) has also concluded that occupant posture to be the most significant parameter affecting the overall risk of injury in frontal collisions.
This research was based on a parametric study including a passive human MADYMO model in a 3 point belted environment subjected to a frontal crash. In this study, the human model was positioned in the vehicle "possible" postures during a pre-braking phase. Consequently the analysis does not include the modelling of the pre-braking event, just guessed outcome, followed by a 56km/h rigid wall impact pulse.

<u>This study raised however several major questions:</u>

1. Nine (9) initial positions were assumed during the pre-braking phase. No obvious literature was used to justify these positions,

2. The bracing of the human was included by tuning groups of muscles based on some volunteer test to replicate the hand grip and foot-pedal reaction forces. Nevertheless the kinematics of the bracing was not validated,
3. The study included a scaling of the 50th percentile human model to 95th percentile. Even if the MADYMO/Scaler (Rodarius 2007) allows scaling of human across percentiles, impact behaviour (injuries and kinematics) are not yet validated. Furthermore MADYMO /Scaler does not scale muscle activity levels across percentiles.

Bracing and reflex (defined later in this chapter) are important in the pre-braking phase. It seems that in the crash phase they are not as significant as the occupant's posture, as "results *of bracing simulations indicated that pre-collision muscle bracing produced marginal changes in the kinematics trajectories of the upper body and the lower extremities (less than 4 cm net displacement in the location of head centre of gravity*" (Bose 2010:8). Nevertheless the occupant posture and position in the cabin is a consequence of bracing and reflex.

Some field tests have been conducted to investigate the occupant kinematics of 17 volunteers under emergency braking (low deceleration under 1.0g), wearing a 3 point belt with a belt locking (after about 500ms) mechanism (Carlsson 2011), investigating the difference of kinematics of 5th percentile female, 50th percentile female, 50th percentile male, 95th percentile female and their respective HybridIII percentile Anthropometric Test Dummy (ATD) under various pre-braking levels and awareness. The study concluded that the overall head and chest motions were relatively small during braking (mean forward motions 55 ±26 mm for the chest and 97 ±47 mm for the head). In all cases when the seatbelt locking mechanism activated, the torso forward motion stopped and the head kept on moving.

Taller volunteers had a larger forward motion; females had a larger forward motion than males of the same sitting height. Passengers exhibited even larger motions than drivers for most of the volunteers (Figure 2.12).

Figure 2.12: The mean forward motion [mm] for the four volunteer groups, when exposed to the three levels of autonomous braking (-3, -4 and -5 m/s2). The ear marker's forward motion is illustrated according to the legend, and the corresponding thorax displacement (Carlson 2011)

A comparable series of tests have been undertaken (Kemper 2011) in a sled environment using a higher deceleration of 5.0g and has shown that the occupant kinematics was also different between relaxed and braced. It is shown that the tenser the occupant, the straighter the arms and the legs (Figure 2.13).

Figure 2.13: Representative comparison plot of relaxed and braced volunteer global trajectories (Kemper 2011)

Similar conclusions were drawn for pre-braking loads under 1.0g for male and female (Ejima 2007) and that this muscle activation was starting around 100ms – 130ms (Ejima 2008).

Interestingly, it was also discovered that a tensed occupant loaded the seatbelt less, but the feet, seat-pan and steering column more compared to a 'relaxed' occupant. This was also confirmed by the use of chest bands on each volunteer which were able to confirm the reduction of thoracic cage due to belt load (Beeman 2012).
It is widely accepted that vehicle occupants do not maintain exactly the same posture as crash ATDs during normal driving, nor under stressful conditions (vehicle pre-impact manoeuvres, emergency braking). Consequently, their posture at the time of impact may significantly differ from those used for restraint system development and evaluation (Hault-Dubrulle 2010a).

Assessment of ATD suitability in AEB scenario

Some research in the 'Proposed Reduction of car crash. Injuries through Improved SMart restraint development technologies' (PRISM) (PRISM 2002) has shown that the kinematics between belted (3 point) ATD and a human volunteer were very different. Considering evaluation pre-braking using ATD is not an option. An extreme braking has been applied on unaware volunteers and their kinematics compared to ATD (Figure 1.13).

The PRISM report made the following conclusions (PRISM 2002a):

- ATD torso has limited motion: buttocks remain very close to the start position and upper torso rotates forward slightly,
- Human torso has more motion: buttocks slides forward and upper body motion is exaggerated by more rotation about the diagonal belt,
- The ATD head flops forward, rotating head and neck downwards, hence the gap under the chin to chest decreases with forward motion,
- Human head is held upright, eyes remain level to retain forward vision, hence the gap under the chin to the chest increases with forward motion,
- Both the feet of the ATD and the human volunteers did not slide forward under braking, hence displaying a similar behaviour.

"*The thoracic spine of the Hybrid III ATD is a rigid steel component that is unable to bend or elongate as opposed to the human spine which has multiple segments that*

allow flexion, extension, and stretch" (Beeman 2012: 2). The neck from a HybridIII is unidirectional and is much stiffer than of a human (Paver 2010).
This is showing that the assessment of a belted occupant in a pre-braking phase can only be assessed using a tool representing human kinematics features.

Occupants' behaviour while driving

From the references listed previously, it is evident that the occupant posture can vary in the vehicle (Bose 2010) and that its relationship relative to the vehicle interior hard points and restraint system are likely to have an influence on the injury sustained by the occupants (Adam 2011).

This opinion is supported by the PRISM project (PRISM 2003b), which has investigated (N=40 subjects, 50% male, 50% female) drivers' posture in the vehicle (Table 2.8).

Interestingly, the survey was performed in November 2003, where the use of mobile phones was not as spread as nowadays. In 2011, it was estimated that there were "six billion mobile phone subscriptions in the world" (BBC 2012), hence a potential danger to monitor (WHO 2013).

In 2010, it was estimated that 50% of all Dutch drivers were using their mobile phone while driving at least once a week (International Transport Forum 2013). The United Nations have (WHO 2013) expressed concerns about the increase use of mobile phones while driving, as driving distracted is a "serious and growing threat to road safety". Nevertheless, it is agreed that "more work is needed to improve the systematic collection of data on mobile phone use in crashes to assess the extent and distribution of the problem" (WHO 2013).

Table 2.5: Activities performed while driving (PRISM 2003b)

The Dynamic OOP loadcase and unbelted occupants

Following active safety research some engineering solutions are now being proposed. When the AEB system is activated, the vehicle is decelerated and the occupant keeps on travelling at the same speed before the braking is applied. As a consequence, the occupant's head and thorax are moving closer to the airbag system. TRW have addressed this concern by engineering an Active Control Retractor (ACR) seatbelt technology to improve occupant position in relation to the vehicle's airbag restraint system (TRW 2011), as illustrated in Figure 2.15.

Figure 2.14: TRW ACR (Active Control Retractor) system illustration (TRW 2011)

ACR systems pretension the seat belt, hence removing seat belt slack to help to maintain the position of the occupant, avoiding any Out-of-Position (OOP) scenario should a secondary impact occur leading to an airbag deployment.

Another scenario to consider is the unbelted loadcase when pre-braking is engaged. If occupant Out-of-Position (OOP) is accessed via the FMVSS208 test protocol, using a 40km/h (25mph) unbelted occupant, as well as 2 static tests, OOP1 (chin on module) and OOP2 (chest on module), it is evident from Figure 14 that a pre-braking phase prior to a subsequent impact creates another OOP scenario which active safety system will now cause: a dynamic OOP loadcase.

Not wearing the seatbelt, in general, can be tragic, as recorded in the Global Status Report On Road Safety 2013 report (WHO 2013), where wearing a seat-belt reduces the risk of a fatal injury by 40–50% for drivers and front seat occupants. On Nebraska roadways, for example, 565 unbelted vehicle occupant fatalities were recorded during 2006-2010, which is an average of 113 fatalities per year. This accounts for 49% of all traffic fatalities during the five-year period and approximately 51% of all vehicle occupant fatalities 1,098 during the study period (Nebraska Strategic Highway Safety Plan, 2013).

In the UK, based on an AA Streetwise survey, 1 of every 20 drivers (5%) does not wear his seatbelt (BBC News 2011).

It has also well documented (NHTSA 2007) that the use of the seat belt at the time of the crash make a difference in the need for hospitalization, as people not wearing their seat belt at the time of the crash were more likely to be hospitalized compared to those wearing it (32% vs. 19%).

Considering the National Automotive Sampling System Database (NASS) (1997-2003) (NHTSA 2013c), it can also be suggested that, for unbelted cases, killed and seriously injuries represent 41% of all unbelted cases, for the front left row (driver side) as displayed in Table 2.9.

	Number of samples	Percentage	Percentage
Killed (AIS 6)	138	11.6%	41.0%
Seriously injured (AIS 3-5)	349	29.4%	
Moderately injured (AIS 1 -2)	596	50.2%	
No injuries	105	8.8%	
ALL	**1188**	**100.0%**	

Table 2.6: Unbelted cases from NASS databases

The discipline of wearing the seatbelt can be a cultural issue. Some early study was performed in PRISM (PRISM 2003b), which as a work-package studied the driver behaviour in 3 countries (UK, Spain and Austria).

The following 4784 samples have been collected:

- Austria City 17.20% (821 vehicles)
- Austria Motorway 23.04% (1100 vehicles)
- Spain Motorway 3.06% (146 vehicles)
- Spain Town 14.66% (700 vehicles)
- UK Motorway 38.29% (1828 vehicles)
- UK Village 3.75% (179 vehicles)

This led to the conclusion that 5% of all drivers in the study did not wear any seatbelts, and more worrying 26% of drivers in Spanish town were not wearing it (PRISM 2002b). Seatbelt wearing rates in Turkey are under 5% (WHO 2013), and its usage risen to 49% since a decree was made on March 2012.

During 2006-2010, reported safety belt usage in Nebraska ranged from a low of 79.0% in 2007 to a high of 85% in 2009. In 2010, safety belt usage was measured at 84.1% (Nebraska Strategic Highway Safety Plan 2013).

Figure 2.15: Seatbelt usable (front seat) (International Transport Forum 2013).

In some cases 3% of drivers in Ireland use their mobile phone, and amongst them 22% are not wearing seatbelts (International Transport Forum 2013). Looking at the Road Safety Annual Report (International Transport Forum 2013), it can be noted that in front seats, the wearing rate varies from 27% to 98%, but a large majority of countries have a wearing rate above 80%, as depicted in Figure 2.16. If comprehensive seat-belt laws covering all occupants are in place in 111 countries it does not mean that these are respected.

With the introduction of active safety, it is likely that new injuries due to AEB on unbelted occupants will emerge, as there is a misconception that driving slowly, example of 26% of driver in Spanish towns does not require the use of the seatbelt.

A vehicle is only capable of a certain maximum deceleration. This is dependent on the vehicle velocity, on the tyre, the road surface condition and the generation of the shear forces resulting from the elastic deformation of the tyre carcass and sliding behavior influenced by road friction (Blundell 2004). Road friction coefficients are very low on ice, around 0.6 on normal roads and in the order of 1.0 to 1.2 at the extreme end (MFES, 2010), as presented in Table 2.10.

Table 2.7: Road friction value as function of vehicle speed (MFES 2010),

The friction values obtained in Table 2.10 are consistently lower when the vehicle is driving faster; suggesting that, for the same vehicle, an AEB at lower speed would likely generate higher deceleration forces to the occupant than at higher speed.

2.4 Opportunities to Model the Occupant's kinematics under extreme braking

Volunteer kinematics testing

In order to obtain occupant kinematics information, tests on living humans were necessary as no relevant data would be extracted from a kinematic test using a cadaver. The volunteers involved in such tests were willing and healthy people who agreed to be part of a scientific experiment. The experiment had to be checked through an ethics committee in order to understand the necessity of such tests and to weigh potential physical and psychological risk to the volunteer. As an example, an ethics process was followed by Ejima in his sled test experiments where *"... Five healthy 23 year-old volunteers (3 males and 2 females) participated in the series of experiments. The protocol of the experiment was reviewed and approved by the Tsukuba University Ethics Committee, and all volunteers submitted their informed consent in a document according to the Helsinki Declaration"* (Ejima 2007).

Some literature on volunteer testing in low to medium deceleration scenarios was presented and illustrated in Figure 2.17 (Hüber 2013).

This review showed the current state of the art (including references) human volunteers in sled, vehicle, including the deceleration level and the direction where the deceleration is applied relative to the occupant. As such it can be noted that to date (2014): all tests are either frontal or lateral, not a combination of the two.

Figure 2.16: Summary of all volunteer tests (Hüber 2013)

Due to the fact that the risk on unbelted loadcase was higher than for a restrained occupant, an in depth search for unbelted tests was undertaken (Figure 2.18). The Occupant Model for Integrated Safety consortium (OM4IS) (OM4IS 2011) undertook the task using a pre-braking pulse in a simple lap-belt scenario. This decision was taken due to the risk of injuries: no 1g unbelted test have been undertaken as they are deemed too dangerous because of possible occupant ejection and contact against the interior of the cabin. The test has been very well documented as well as some methods of modelling muscle tension in LS-Dyna (Prüggler 2011a; Prüggler 2011b).

Figure 2.17: Comparison between the kinematics of an ATD and human volunteer (lap-belt only) (Hüber 2013)

The results from the OM4IS tests can be summarised by the fact, that, similarly to the 3 point belted case, the ATD kinematics differ greatly compared to the human volunteer, as displayed in Figure 19 (Hüber 2013).

Hüber had not recorded that the Japanese Automotive Research Institute (JARI) had also started to investigate occupant under low 'g' wearing a lap-belt (Ejima 2009). At first glance, the work look very similar to the OM4S sled tests, but differ greatly by the fact that JARI volunteers had to stay relaxed during the whole deceleration and not keep to a set posture (Figure 2.19).

Figure 2.18: JARI. Physical motions from the 3D motion capturing system (Male, 0.8G: Relaxed) (Ejima 2009)

The finding from this research was that occupants' muscle activity starts at around 100ms, while TNO's references pointed to an activation time between 10ms and 120ms (TNO 2012). The torso rotation is very large compared to the OM4IS tests, where the volunteers are requested to keep a small object (0.5kg) horizontal duration the sled motion, giving a straighter spine and arms response from the test (OM4IS sled tests will be discussed in detail in Chapter 4).

The same comments can be made as in Figure 14 (PRISM 2002a), except that the human volunteer's thorax is not restrained by the seatbelt, allowing larger rotations towards the dashboard and the airbag restraint system.

Human computer models.

The use of non-human surrogates allows experimentation to exceed ethical safety thresholds for humans and examine injurious or traumatic events. ATDs are mechanical surrogates designed to represent a particular demographic according to gender, size, and age. In addition, they are designed to exhibit a biofidelic response for specific loading conditions and thus may not produce biofidelic responses beyond their intended design specifications (Crandall 2013; Rubens 2013). However from the pre-braking tests performed, belted and unbelted, there is a clear mismatch in the occupant's kinematics in the active safety range when using ATD, hence one has to turn to human models computer tools to assess the behaviour of occupants under low deceleration.

Since 2005, 4 main human computer models were available:

- HUMOS2 (Vezin 2005; Kayvantash 2009)
- GHBMC (GHBMC 2013)
- THUMS4.0 (Toyota 2010)
- MADYMO Human Body Model (Lange 2005).

GHBMC, HUMOS2 and THUMS4.0 are based on cadaveric data and are not able to control the tension in their muscles. The clear advantage of these models is that they include skeleton details as well as internal organs for trauma assessment. Trauma indices for organs and body regions are still being researched (Crandall 2013), nevertheless this is a first step in creating tools to minimise further deaths on the road (Bose 2008; Crandall 2011). Since 2005, there does not seem to be a lot of development from HUMOS2 (Bulla 2013), and it is difficult to see this model continuing to exist, as very little development from 2005 has been published. Bulla has indicated that the future of human modelling is the GHBMC (Global Human Body Model Consortium), whose development started in 2008. This new human model is an FE model which is in direct competition with THUMS, and is being developed by Chrysler, General Motors, Honda, Hyundai, NHTSA, Nissan, Peugeot-Citroen, Renault, Takata and Toyota (GHBMC 2013). The latest update report from GHBMC is showing a level of development similar to the passive THUMS4.0. No clear development plans on muscle activity have been found in literature searches.

Initially, no muscle activation was available on THUMS4.0; however some later development suggested that FEA models would soon include levels of bracing/ reflex (Iwamoto 2012; Iwamoto 2013; Prüggler 2011a). These models are at the moment (2014) still under development, very heavy to compute and their positioning is a major task, as their joints are not simple kinematics joints, but proper articulations including tendons and muscles. The active THUMS is currently based on THUMS3 (THUMS4 with no internal organs) with the addition of 252 muscles (Iwamoto 2012; Iwamoto 2013), each of them modelled as a hybrid model of bar elements with active properties and solid elements with passive properties. This development model includes sliding interfaces of bones-to-muscles and muscles-to-muscles. The other model available is the MADYMO Human Model, which has been validated against cadaveric tests also (Lange 2005; TASS 2013) and is based on a multi-body architecture, which gives it the advantage of a very fast positioning without any considerable computer overhead. Some of the skeleton is based on ellipsoids, i.e. multi-body; some based on meshes connect with muscles. The multi-body controllers, which have been hard-coded, have been calibrated to allow this human model to balance itself under its own weight, thanks to a stabilising spine (Cappon 2006) and a stabilising neck (Nemirovsky 2010). Following the literature search, the human models' active features have been compared in Table 2.11.

Human Model	Available at the start of the research (2010)	Model type	Self-stabilising (head and neck)	Muscle activation model availability
HUMOS2	X	FE	No	No
GHBMC		FE	No	No
THUMS3.0	X	FE	No	No
THUMS4.0	X	FE	No	No
MADYMO Human Model	X	Multi-Body + FEA	Yes (Cappon, 2006 Nemirovsky, 2010)	Yes (planned in 2011)

Table 2.8: Comparison of Human models' active muscle features at the beginning of the research

Consequently, as the model must be fitted with active muscles, the MADYMO Human Model was chosen as the most adequate for this research.

MADYMO is the worldwide standard software for analysing and optimizing occupant safety designs. It contains an explicit solver which computes multi-body and finite element models. It is appropriate to resolve transient problems, i.e. time dependant, compared to steady state problems which primary use implicit solving methods. Explicit computation is very well suited for safety engineering and consequently, which makes it relevant to assess occupant injuries. A MADYMO standard input is explained in Appendix B.

The most advanced development model with muscle activation at the start of this thesis was the MADYMO Active Human Body Model (AHBM). Initially, the muscle activation features of this model were at their infancy and started to include very early reflex behaviour, but no bracing. The definition of these two terms is at this time very relevant to this thesis. In the Oxford English dictionary, "reflex" (Oxford English Dictionary 2013) is a noun which refers to an action which is "performed without conscious thought as a response to a stimulus", compared to "bracing" (adjective) from the verb 'brace' meaning to 'fasten tightly, clasp and give firmness to'. A reflex is then an unconscious action which tends to reposition the body to its initial posture when an un-expected force is applied on the person, using muscle activity after the person is beginning to move out of position/ balance. In contrast, a brace (or bracing) is creating a muscle activity before the OOP balance event occurs. The MADYMO AHBM contained reflex muscle activation levels, including neck, spine, hips and arms, and just one (1) level of co-contraction in the neck, allowing some level of bracing (TNO 2011). The leg muscle activation is controlled by the hip joint as no muscle activation is yet available in this model, which in reality should be controlled from the lower leg itself. Some work to characterise muscle activation was undertaken by IFSTTAR and could in the future be included in this model (Behr 2009).

2.5 Summary and current gaps in knowledge and understanding

Considering that new vehicles are now being fitted with active safety features, evidence gathered in this literature review suggests the necessity of investigating the influence of these new safety features using an un-restrained active human computer model. The reflex and bracing parameters are critical to assess the occupant's position and kinematics as well as potential subsequent injuries during a crash.

Following all this evidence, there is a need to model unbelted occupants' kinematics in a pre-braking scenario as well as injuries should the pre-braking lead only to accident mitigation. As current human computer models are unable to include the bracing of all the body limbs (except the neck co-contraction), the study will focus on the occupant's reflex behaviour, relating to a relaxed state of mind before the pre-braking starts. This is a first step towards investigating the effect of muscle activation as a consequence of forthcoming active safety requirements. This thesis will also investigate the usage and stability of an active human model using an Active Safety Assessment Environment (ASsEt), which is defined in detail in chapter 3, as part of the Methodology section.

3.0 Methodology

The aim of this chapter is to propose a methodology to test the hypothesis stating that it is important and necessary to use AHBM models to accurately simulate future active safety situations, i.e. kinematics and injuries.

This methodology will be focused around an Active Safety Assessment Environment (ASsEt) which will be derived in this section.

As such, this chapter will address the 4 main steps to build this environment:

1. The characterisation of the pre-braking phase, focusing on the parameters which could influence occupant's kinematics, i.e. position within the vehicle cabin,
2. The characterisation of the accident phase, subsequent to the pre-braking, defining the key parameters of the main occupant injuries,
3. The implementation of the ASsEt environment combining pre-braking and subsequent accident (Figure 3.1),
4. The derivation of the ASsEt environment performance, i.e. occupant's kinematics and injuries

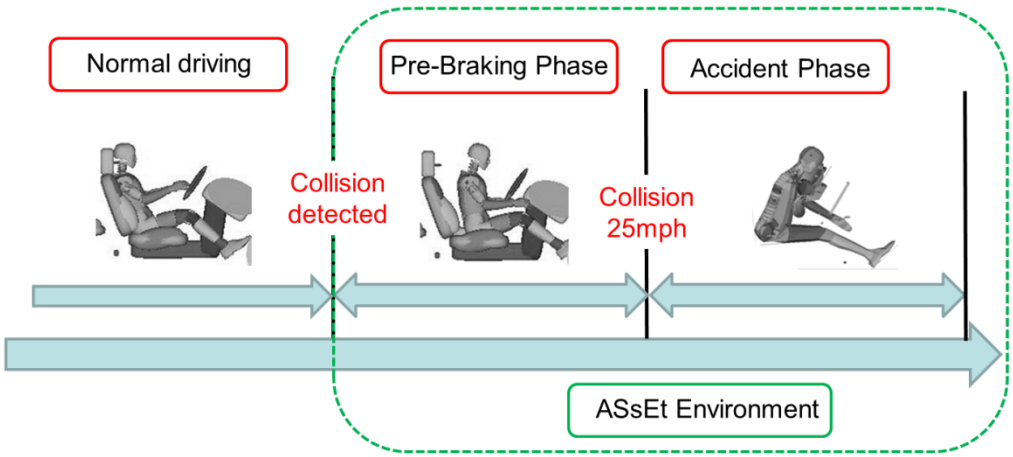

Figure 3.1: Underline of the ASsEt Framework

As the framework will consider a dynamic unbelted loadcase against a deploying airbag, it has been decided to relate and compare this new dynamic OOP loadcase to a legislative standard, FMVSS208 (FMVSS208 2012). Vehicles in the United States

must meet this requirement by law, i.e. 5th percentile female (Hybrid III) on the airbag module (OOP1 and OOP2) as well as 50th percentile unbelted at 40km/h (25mph) against rigid wall impact (Figure 3.2). The 5th percentile female occupant has been judged to be the worst occupant for 'on' airbag deployment (Figure 3.2) because of its proximity to the steering due to its size and its lower biomechanics tolerances, while the use of the 50th percentile ATD is to ensure that the airbag restraint system is still effective up to 40km/h (25mph) should the occupant be unbelted (FMSS208 2013).

Figure 3.2: FMVSS208 OOP1 (left) and OOP2 (right) tests setup (Mahangare 2007)

As such the proposed ASsEt environment will investigate and define the least favourable car to car rear accident which will be encountered at 40km/h (25mph). Consequently, in this ASsEt environment study, all final velocities computed during the pre-braking phase prior to the unavoidable accident will be 40km/h (25mph), as stipulated by FMVSS208.

3.1Characterisation of the pre-braking phase

During the pre-braking phase, an occupant's attitude will vary from one person to another, as well as change depending on the surrounding, such as distance to the steering wheel, starting posture, steering wheel grip strength, seat friction, deceleration rate and vehicle dive. These parameters are important in the determination of the occupant's position within the cabin during the braking phase and will be discussed in this section of the thesis.

3.1.1 Drivers' Positioning

Occupant's positioning a vehicle depend on many parameters, like amongst many the seat track position, the 'H' point (relative location of an occupant's hip joint), but also on the anthropometry, the percentile of the driver as well as the type of vehicle used. A position study using mannequins (Figure 3.3) is suggesting the challenge of defining the original driver's position as a function of percentile and vehicle category (Schneider 1979).

Figure 3.3: Generic distances between steering column and occupant (Schneider 1979)

It can be observed from Table 3.1 that the distance between the driver's sternum and the steering wheel centre varies across vehicle type even for the same percentile.

This study is suggesting that many variables are needed to position the occupant, and that to prove the application of the ASsEt environment, simplifications are needed.

The ASsEt environment must take into account any occupant models, however in order to validate the framework, a 50th percentile occupant will be used in a set seating position within a vehicle cabin. As such, the effect of the fore and aft seat travel will not be studied and the interior will focus initially on one vehicle which has been utilised in other research, which is a BMW325L (Advanced Simtech 2007), providing this research with a vehicle interior which has been validated for accident reconstruction purpose.

Future modifications can be made to capture exact seat track positions at a later stage.

It has been discussed in the literature review, ATD do not provide an accurate kinematics during the pre-braking stage, hence the framework will use a 50th percentile AHBM, centred about the average of the population and validated against cadaver data (Cappon 2006; TASS 2013). Few other reasons not to use the 5th and 95th percentile human models is because they are scaled from the 50th percentile and

yet not fully validated. The 5th percentile human female model has also not been developed, yet planned (GHBMC 2013).

Table 3.1: Generic occupant position relative to the steering wheel (Schneider 1979)

The occupant will be positioned in its seat using a gravity load, which will be applied all along the research. In order to keep the study to a manageable size and duration, all stances discussed later in this report will assume that, from the standard seating position, only the upper limbs are moved, not the feet and the pelvis.

3.1.2 Vehicle interior friction values

Having set the vehicle interior, right hand drive, (Advanced Simtech 2007), and the choice of occupant, a parameter which can have an effect on the occupant kinematics is the seat friction value. Tests were conducted to determine static and dynamic coefficients of friction between occupant clothing and automotive seat upholstery materials. Multiple materials were used for both the occupants clothing and the seat upholstery to examine friction variations with various material combinations (Cummings 2009), as "*seat friction is the only restraint for an unbelted occupant not otherwise restrained by other parts of the car such as doors, consoles, etc. Understanding the friction at the clothing-upholstery interface aids in the*

understanding and determining occupant kinematics and kinetics related to an accident" (Cummings 2009).

Table 3.2: Seat friction values (Cummings 2009)

The summary of the seat friction values can vary from a low 0.3, to a medium 0.5 and high 0.8 (Table 3.2). These parameters will be used as part of the framework as they will create a resistive force to the sliding motion which could generate different rates of limbs velocities.

3.1.3 Drivers' Posture

The PRISM European project (PRISM 2002), which was completed in 2003, studied the occupants' behaviours and postures whilst driving a vehicle. This study was conducted on 6 sites, 2 in the UK, 2 in Spain and 2 in Austria, recording information over 5000 vehicles (PRISM, 2002). Volunteers were tasked to follow a scheduled route in which they were filmed and photographed at different part of the set itinerary. The visuals were then inputted into a database and analysed. From this database, it was reported that 5% of all drivers did not wear a seatbelt (6% of all male drivers).
Most drivers were observed with both hands on the steering wheel in the FMVSS208 standard position (Figure 3.4) (PRISM 2003b). It was also observed that a large percentage of the participants adjusted the radio.

Figure 3.4: Volunteers preferred hand locations (PRISM, 2003)

It can be observed that stances vary and that a standard grip (10-2 o'clock) is the most frequent. Note that if at the time the study, 2002, was performed that mobile phones were not used as commonly as now. The framework has included a 1-hand grip stance (to replicate a typical mobile phone call scenario) as it has been considered as a future concern (WHO 2013).

As such 4 stances have been considered:

1. FMVSS208: standard test position,
2. Adjusting the radio (left hand): most frequent activity,
3. Mobile phone in left hand: as it is now illegal in most countries to use a hand-held phone,
4. Arm on armrest: activity leaving right hand free.

All other positions occurred less frequently, hence have not been included.
These positions were then modelled using the software MADYMO where the AHBM was positioned in the BMW325L interior model (Advanced Simtech 2007).

FMVSS208's hand positioning follows the legislative requirement, which has been also verified by the PRISM project findings (PRISM, 2003b) that 87.5% of the volunteers had a 3 and 10 o'clock right and left hand positioning (Figure 3.5).

Figure 3.5: FMVSS208 (2 hand grip) computer model setup (Bastien 2011)

Adjusting the radio's right hand positioning follows the PRISM's project finding (PRISM, 2003b) (Figure 3.6). The height of the left hand had been estimated in the computer model (Figure 3.7).

Figure 3.6: Right Hand position while adjusting radio (PRISM 2003b)

Figure 3.7: Right Hand position while adjusting radio (Bastien 2011)

The mobile phone in the left hand scenario (Figure 3.8) has shown that 67.5% of the volunteers who had reached their ear with the phone continued to hold it to their ear (Figure 3.9).

If no participant removed their right hand from the steering wheel during the event, some drivers used their right hand on the left side of the steering wheel to turn it in an attempt to swerve around vehicles (PRISM, 2003b).

Figure 3.8: Mobile phone adjustment computer model setup (PRISM 2003b)

Figure 3.9: Mobile phone computer model setup (Bastien 2011)

The right arm on the armrest scenario was chosen as a scenario considering the right hand not in contact with the steering wheel (Figure 3.10). It was noted that "82.5% kept their right arm on the rest and hand off the wheel" (PRISM 2003b), as is modelled in Figure 3.11.

Figure 3.10: Left Hand position while resting on armrest (PRISM 2003b)

Figure 3.11: Armrest computer model setup (Bastien 2011)

3.1.4 Drivers' grip modelling

To evaluate the occupant steering wheel gripping force, various researches have concluded that the power grip strength is approximately 300 N for women and 470 N for men (Bao 2000). These values are comparable with the information provided by NASA (NASA 1976), which is reporting a grip strength of 410N for male grip strength as a function of separation between grip element of 3.81cm (1.5in) which is roughly the diameter of the steering wheel rim. These values differ vastly from Bose (Bose 2010) who has extrapolated the hand forces from the steering column loads to a maximum of 151N, which is much lower than the 2 other references.

As a consequence, the maximum grip value of 400N was chosen, as the direct reading of the force value was judged more reliable than one obtained using an extrapolation method. The grip was modeled using a RESTRAINT_POINT between the AHBM's hands and the steering wheel body. This feature is a spring-damper element for which stiffness has been determined (Table 3.3) to simulate the hand releasing force (Meijer, 2007).

Table 3.3: RESTRAINT_POINT characteristic function (Bastien 2011)

The force level is monitored using a "SWITCH_SENSOR" command. Should the resulting force between the hand and the steering wheel body exceed 400N, the "STATE RESTRAINT_REMOVE" flag is activated, representing the effect of removing the hand from the steering wheel.

It has to be noted at this stage that the grip is modelled between 2 bodies, the hand and the steering wheel. As such, the grip is not defined by a grasp, i.e. the clenching of the driver's fingers around the steering wheel rim, but as a straight hand being 'glued' to the steering wheel rim, which is a limitation of the human model used in this study.

3.1.5 Typical pre-braking deceleration and duration until 40km/h (25mph)

Some occupant behaviour under extreme braking was conducted to understand their reaction (PRISM 2003a).

A vehicle test was performed to investigate unaware belted passenger occupants' behaviour while the vehicle, driven by a test pilot, was subjected to an extreme braking scenario. The braking was not autonomous, but exerted by the test pilot. Accelerometers at the centre of gravity of the vehicle outputted the vehicle linear deceleration (X direction), without taking the brake dive into account. A typical vehicle extreme braking curve from these tests is illustrated in Figure 3.12.

Figure 3.12: Straight line braking. Vehicle deceleration (PRISM 2003a)

From this deceleration pattern, it can be seen that the deceleration initially ramps up slowly during the first 0.3s and then abruptly to reach 0.9g after 1.0s (plateau).

This pulse is less severe than a constant step-function of 1.0g and shows that the longer the braking, the steeper the deceleration (Bastien 2010a). This pre-braking pulse suggests a more gradual deceleration for the 1st second of deceleration compared to a step-function constant pre-braking value.

In the near future, it will be possible to have a better representation of vehicle accident patterns (Edwards 2013), which could also include the deceleration phase by the introduction of telemetric data with recording devices in vehicles. A typical output (Figure 3.13) would include the vehicle speed as well as its deceleration. In the case presented in Figure 3.13, the vehicle deceleration rises at 3.8s very abruptly while the velocity sharply reduces, which therefore suggests that the vehicle did not brake before the impact.

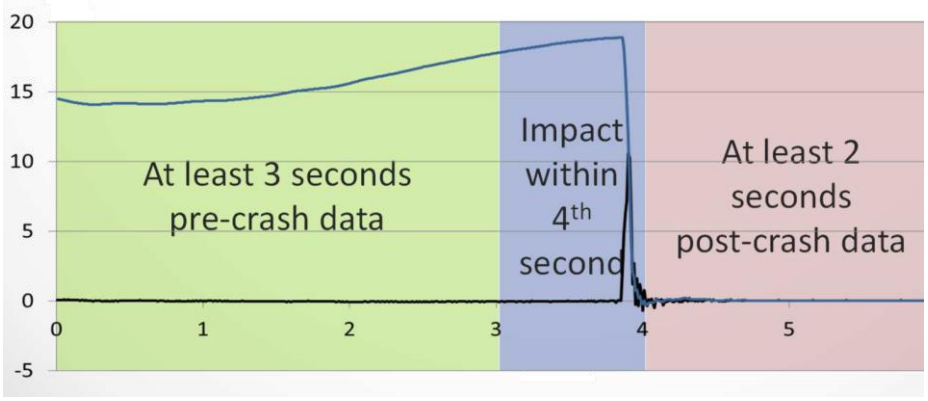

Figure 3.13: Telemetry output from a vehicle impacting an obstacle

As the framework assumes that the subsequent impact occurs at 40km/h (25mph), using the PRISM pre-braking pulse, it is possible to calculate the duration of the pre-braking of the vehicle (Bastien 2012a) to reach that critical impact speed. These curves were computed by setting initial velocities (60km/h, 80km/h and 100km/h) to a vehicle dynamics model (Advanced Simtech 2007) and applying the braking pulse illustrated in Figure 3.12. The vehicle velocity changes in the forward direction were extracted from the vehicle centre on gravity, as illustrated in Figure 3.13. The intercept of these velocities with the 40km/h (25mph) target velocity horizontal time axis provided the braking duration required for the study.

As a result, the time to reach 40km/h (25mph) was extracted from the MADYMO computation and listed in Table 3.4.

Figure 3.14: Critical braking duration to cross 40km/h (25mph) (Bastien 2012a)

Table 3.4: Braking durations to reach 40km/h (25mph) (Bastien 2012a)

In reality the AEB systems would apply a small amount of braking at a greater distance from the collision, allowing time for the driver to come back into the loop, and to steer or brake himself; i.e. the braking can act as a warning. The AEB systems would not apply immediate full braking, since this would be very unpleasant for the driver (Kirkman 2014), as it is better to give the driver and other occupants more time to brace before impact. There would then a greater level of braking force, ramping up, as the collision gets closer. Unfortunately latest AEB braking patterns had not been found by the author at the time this work was researched, consequently only the long braking durations were used in this study to investigate the most adequate human computer model to simulate kinematic and injury criteria response, which is the aim of this thesis.

These 3 braking durations derived in Table 3.4 will be used in the research to assess the effect of the braking period on occupant's kinematics.

3.1.6 Effect of brake dive

It is important at this stage to evaluate the relevance of the brake dive, as the unbelted driver will continue moving forward during the deceleration phase and the cockpit's velocity reduce, including a rotation of the cockpit due to the dive (measured with a laser from a target located in the front of the bonnet).

Considering some research undertake on brake dive (Ray 2006), it is suggested that for some vehicles, the brake dive can vary from -58.4mm (2005 Pontiac G6 and 1995 Mazda Protégé) to -109.2mm (2005 Chevrolet Impala and 1995 Ford Contour).

Even if the test values have been gathered for a start braking speed of 40mph (64km/h), it may be suggested that the 1995 Mazda Protégé could have no dive after 1.5s. while the 2005 Chevrolet Impala and 1995 Ford Contour could continue to have a 109.3mm dive at 1.7s and 100mm at 2.3 (Figure 3.14, value input by hand by the author from Ray 2006).

Figure 3.15: Vehicle brake dive values when starting speed is 40mph (Ray 2006)

It can be observed that the braking duration from 60km/h to reach 40km/h (25mph) (Table 3.4) is 1.1s; hence the brake dive variation would vary from -55.9mm to -109.3mm (almost double) between the vehicles listed in Figure 15. It can therefore be observed that the brake dive variation can be very large and maybe relevant; nevertheless it has been decided that this parameter should only be included in the framework in the future. The reason for this decision was based on the fact that exact vehicle dynamics information was needed and not available, including exact suspension definition, braking algorithms etc... This would have added too many variables at the early stage of the development of this ASsEt environment and would not have added any extra value to answer the hypothesis set in this thesis. Furthermore, should the brake dive be included in the early stage of generation the framework, then the vehicle dive attitude before the collisions would also have to be included in the ASsEt environment, which is adding unnecessary complexity at this point of the research.

Adding the brake dive variable into the project would not contribute to the overall aim of the thesis which is to ascertain the most adequate occupant computer model to simulate active safety scenarios.

3.2 Characterisation of the accident phase (subsequent to the pre-braking)

The accident phase, or crash phase, will involve defining the restraint system (here the airbag design) as well as the least favourable 40km/h (25mph) accident

Calibration of OOP airbag model to meeting FMVSS208

As the framework will consider an unbelted loadcase against a deploying airbag, it is first necessary for the 5th percentile female (ATD - Hybrid III) to meet the FMVSS208 OOP1 and OOP2 tests (FMSS208 2013). Injuries values will have to meet are listed in Table 3.5 (ISO/TR 10982 1998)

Table 3.5: FMVSS208 legal targets (FMVSS208 2013)

The head injury criteria (HIC) is an acceleration based injury criteria which is computed from the head centre of gravity. During the accident, the acceleration *a(t)* is extracted and the *HIC* calculated using Equation 3.1.

$$HIC = \max\left[(t_2 - t_1)\left(\frac{1}{t_2 - t_1} \int_{t_1}^{t_2} a(t)dt \right)^{2.5} \right]$$

Equation 3.1: HIC (Head Injury Criterion)

The neck injury criterion (N_{ij}) is considering the tension and compression forces in the neck (F_z) as well as the neck moments (M_{ocy}) which tend to cause flexion and extension. These forces and moments are normalised by dividing the neck force and

moments by a critical force (F_{zc}) and critical moment (M_{cy}) which are based on tolerance values provided in the FMVSS208 legislation (FMVSS208 2013).

The N_{ij} general form used in this thesis is listed in Equation 3.2.

$$N_{ij} = \frac{F_z}{F_{zc}} + \frac{M_{ocy}}{M_{yc}}$$

Equation 3.2: Nij (Neck Injury Criterion) general formulation

Determination of most severe crash pulse for the ASsEt environment.

In order to quantify the subsequent accident phase to complete the framework, typical vehicle collision types were chosen amongst from the ASSESS project (ASSESS 2012a) and are listed in Table 7. The minimum velocity of the subject vehicle for all urban scenarios is based on the speed limit of 50km/h (30mph), which is standard in most European cities (ASSESS 2012b).

Table 3.6: Real life accident assessment (ASSESS 2012b)

The ASSESS project separated 3 accidents categories listed in column 1 of Table 3.6:

- Rear collisions at constant speeds ('A1X' accident types):
- Rear collisions decelerating lead vehicle ('A2X' accident types)
- Rear collisions stopped lead vehicle ('A3X' accident types).

'X' represents a subset of a collision type where impacted vehicle speed, lead vehicle deceleration and impacting vehicle speed are different. As an example, scenario A1A is investigating a 100% overlap rear collision between 2 vehicles where the impacting vehicle is travelling at 50km/h while the impacted vehicle is travelling at 10km/h.

In order to compare the severity of the ASSESS accidents against a standard 56km/h (35mph) rigid wall impact; FEA was used to model the crash events. This comparison was set as NHTSA vehicle crash test database (NHTSA 2013d), which consider a 100% overlap impact against a rigid barrier. In cases A1A, A1B, A1C, A3A, A3B and A3C initial velocities were directly given for both vehicles computer model and positioned few millimeters apart at the start of the computer run in order to optimize computer runtime. For cases A2A, A2B, A2C, A2D, as the gap distance (δ_0) was 14m and 45m, a modified setup had to be implemented in order to reduce the computation time (ASSESS, 2012).
Vehicles were moved near to touching and the speed of the impacted vehicle (v*) of the impacting vehicle re-calculated to take into account the deceleration levels before impact using Equation 3.1 (v_0 being the original impacting vehicle velocity and 'a' the lead vehicle deceleration level):

Equation 3.3: Collision velocity (Bastien 2013a)

In Equation 3.3, the velocity of the impacted vehicle v^*, just before vehicle rear end is contacted, is computed by subtracting from its original driving speed (v_0) the change of speed caused by the constant pre-braking deceleration (a) within the gap distance (δ_0).

In the scenarios A3A, A3B and A3C it can be noted that the impacted vehicle initial velocity is set to zero. Following future EuroNCAP assessment strategies on AEB systems, Thatcham Research has proposed for such tests to have the handbrake from the impacted vehicle removed.

This work was implemented by performing computer simulations using LS-Dyna.

Table 3.7: Vehicle properties (NCAC) (*estimated from NCAC CAE model) (Bastien 2013a)

Considering ΔV being the relative velocity between impacting and impacted vehicles, it is suspected that A3A and A3C will be the worst loadcases.

In order to obtain accident crash pulses, the following vehicles have been chosen from the NCAC database (NCAC 2013), in which the dimensions and model properties are listed in Table 3.7. These LS-Dyna Finite Element Models have already been correlated against a 56km/h (35mph) rigid barrier models and will be used reproducing the ASSESS accidents. It can be noted that the mass of each vehicle is comparable. To compare the rear end collisions between the different sized vehicles various crash scenarios were chosen and the vehicle velocities were setup as in Table 3.6.

The Dodge Neon was chosen as the impacting vehicle for all scenarios and set as main investigation object, allowing the possibility to compare the crashworthiness of Neon against a smaller sized vehicle (Fiesta) and against a higher bumper height one (Rav4), all with a comparable mass (Figure 3.15 and Figure 3.16).

Figure 3.16: 'B' pillar deceleration representing a collision between a Dodge Neon (impacting vehicle) against a Ford Fiesta (Bastien 2013a)

From the assessment of the accidents recorded on Figure 3.15 and Figure 3.16, it can be noted that most of the accident crash pulses recorded on the B pillar do not exceed 25g in all cases, hence are less severe than a 56km/h (35mph) rigid wall impact. For the accident cases A1C and A3C (Figure 3.17), the ASSESS FP7 accident deceleration values are the highest, which is expect as ΔV between both vehicles in the highest, which was also suggested (Berg 2012).

Figure 3.17: 'B' pillar deceleration representing a collision between a Dodge Neon (impacting vehicle) against a Toyota Rav4 (Bastien 2013a)

It can also be noted that for ΔV values of 40km/h, which is the impact speed stipulated by FMVSS208 (impacts A1A) crash pulses recorded on the B pillar do not exceed 10g.

Figure 3.18: A1C impact between Neon (impacting vehicle) and Fiesta (impacted vehicles) vehicles (Bastien 2013a).

Looking at the National Crash Analysis Center (NCAC) report for the Dodge Neon (NCAC, 2013), it can noted that the seat cross member average acceleration against a full rigid wall at 56km/h (35mph) is around 34g (obtained at time 50ms). One can therefore conclude that within the limits of explicit finite element analysis, the accident patterns suggested by the ASSESS project are less severe than a full rigid

barrier test conducted at 56km/h (35mph) even if the impact velocity ΔV is 80km/h. This is to be expected as the main reason is that the impacting vehicle is colliding against a deformable structure.

From these analyses, designing vehicle structures for a 56km/h (35mph) impact to take into account all standard rear impact accidents against another vehicle seems a reasonable and safe approach.

Considering the ASsEt environment, it is important to understand the differences in impact severity in car to car and rigid wall impacts (both at 40km/h (25mph)) on an unbelted driver out-of-position after the AEB pre-braking has been applied (Figure 3.18).

Figure 3.19: Comparison of 'B' pillar decelerations between a Dodge Neon impacting various vehicles at 40km/h (25mph)- CFC180 [1]filter (Bastien 2013a)

Comparing the impacts, it is shown that the rigid barrier test displays the highest decelerations. Running the NCAC model, it is seen that at time 50ms, the pulse starts to rise and peak at around 62ms (Figure 3.18).

[1] 'CFC 180' is a standard Channel Frequency Class used to remove noise from a signal. The '180' channel frequency class is commonly used in vehicle safety applications, during the analysis of frontal crash data, to filter accelerometer signals (Stubbs 2013)

Figure 3.20: 40km/h (25mph) Neon rigid wall impact (Bastien 2013a)

The start of this rise occurs when the longitudinal members start to lock-up during the impact process leading to an increase of forces within the vehicle structure. It can be noted that the pulse is consistently higher than all the impacts on stationary vehicles (not hand braked) proposed in this study.

It can be seen that the rigid wall impact oscillates more as more components are being involved in the impact by resisting the load and then collapsing (Figure 3.18 and Figure 3.19).
The 3 other pulses are lower and are suggesting that the impacting vehicle is not engaging fully with the target.

Considering the impact with the Rav4, it can be observed that the Neon under-rides the Rav4, which has the effect of changing the load transfer through the vehicle longitudinal members (Figure 3.20). Looking at the differences in bumper height from Table 3.7, it can be calculated that the middle of the Neon's front bumper is 34mm above the Rav4's rear bumper, which does not seem to be enough to generate a direct impact.

This small bumper height difference coupled with vehicle differences in local stiffness, geometry, suspension settings vehicle seem to cause this under-ride phenomenon. As a consequence, the Neon loads the impacting vehicle structure lightly with a very shallow deceleration ramp increasing to about 10g at 60ms.

Figure 3.21: Neon under-rides Rav4 at 40km/h (25mph) (Bastien 2013a)

Similarly, in the "Neon against Neon" and "Neon against Fiesta" impacts, it can be clearly observed from Figure 3.21 and Figure 3.22 that the Neon suffers very small structural damage, compared to a 40km/h (25mph)rigid wall impact. However it can be also noted that the under-riding effect does not take place as with the Rav4.

Figure 3.22: Impact Neon (impacting vehicle) against Neon at 40km/h (25mph) (Bastien 2013a)

Figure 3.23: Impact Neon (impacting vehicle) against Fiesta at 40km/h (25mph) (Bastien 2013a)

Looking Figure 3.18, it can be noted that more load is generated at 20ms because the Neon's front and rear bumper heights to the ground are comparable, hence engage well, while the Fiesta's bumper, when struck by the Neon tends to be pushed downwards, resisting less. It may be suggested that this phenomenon is caused by the excessive difference in rear bumper height between these 2 vehicles (Table 3.7), estimated to be 119mm.

This part of the method is concluding that a typical secondary impact occurring at 40km/h is worst when the vehicle contacts a rigid wall, as the acceleration levels exceed car to car impact levels by a factor of 3.

This study has shown that regardless of the impacting bumper height, that the rigid wall crash pulse is consistently the worst loadcase (Bastien 2013a) and as such will be used from now on in the thesis.

3.3 The Active Safety Assessment Environment (ASsEt)

The active safety environment will now combine the pre-braking phase followed by the subsequent accident, as illustrated in Figure 3.1.

As such the two deceleration signals derived from the pre-braking (Figure 3.12) and 40km/h (25mph) rigid wall impact (Figure 3.18) can be combined together and reflect the braking duration before the accident occurs (Figure 3.24).

For the 1.1s configuration, the pre-braking pulse from Figure 3.12 is used up to the duration of 1.1s to reflect a 1.1s vehicle pre-braking. This pulse is then clipped at 1.1s to include subsequently the crash phase from Figure 3.18.

Figure 3.24: Example of combination of low 'g' pre-crash pulse with a high 'g' rigid wall impact (Bastien 2012a)

The same method is used for 1.7s and 2.3s configurations where the pre-braking signals are respectively clipped at 1.7s and 2.3s to then include the crash pulse from Figure 3.18.

It must observed that the crash pulse of the Neon has been scaled down from (Figure 3.23) by 0.685 to allow the calibration of the crash phase, as without pre-braking a 50^{th} percentile unbelted occupant must pass the 50^{th} percentile FMVSS208 occupant safety requirements.

The next chapter will also validate the airbag system against a 5^{th} percentile female against standard OOP1 and OOP2 requirements, which is part of the FMVSS208 directive (FMVSS208 2013). The value of 0.685 is specific to this framework, as the current framework has been setup with data available which are not from the same vehicle, i.e.:

- The airbag comes from an unidentified vehicle (not provided to the author) (Mahangare 2006),
- The pre-braking pulse comes from an unidentified vehicle (PRISM 2002),
- The interior package comes from a BW325L (Advanced Simtech 2007),
- The 40km/h (25mph) crash pulse comes from a Neon vehicle (Bastien 2013).

The ideal scenario would be to obtain all the information for the same vehicle to apply with the Active Safety Assessment Environment_(ASsEt). Nevertheless, the current setup has the merit to investigate the hypothesis set in this thesis. The proposed ASsEt environment will consider 3 different braking durations before the accident, as proposed in Figure 23.

The ASsEt environment is summarised in Figure 3.24, where more details are added from Figure 3.1, representing a dynamics OOP loadcase.

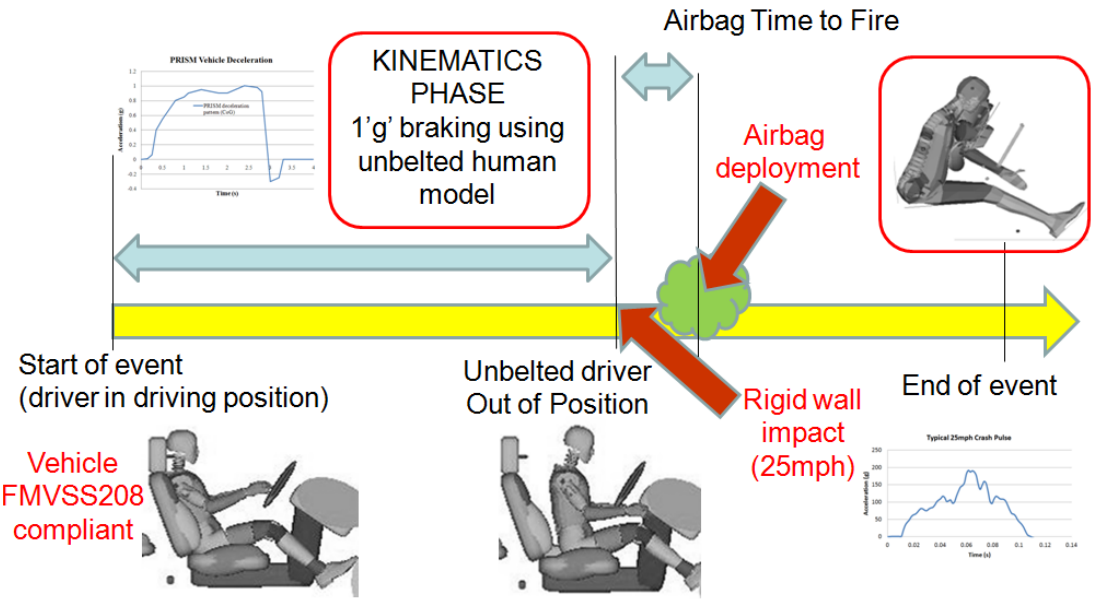

Figure 3.25: Proposed Active Safety Framework

The current implementation of this Active Safety Assessment Environment (ASsEt) includes variables and functions which have been setup from the information gathered in this chapter and summarised in Table 3.8. The current setup will allow a test environment to assess human computer models in active safety scenarios.

The ASsEt environment is not restricted and can be extended and modified, as suggested in Table 3.8, to assess future active safety systems, as described in Chapter 9 (Future Work and Opportunities), a well as considering real world accidents.

	Current ASsEt setup in the thesis and limitations	**Other implementations and future improvements**
Occupant model	Active Human Model	Active Human Model or future versions including different percentiles
Seat position	Set as constant value as BMW315L vehicle model provided	Can be a modified to suit other vehicle interior package
Seat friction	Set to 0.3; 0.5 and 0.8 as extremes	Can be a modified further if required

Seat geometry, stiffness and strength	**Set to straight planes with BMW325L seat stiffness parameters**	**Can include more detailed seat shape/ contour/ stiffness and strength**
Floor friction	Set to 0.8 (rubber shoes to carpet)	Can be a modified further if required
Seat stiffness	Set as BMW315L seat model stiffness function	Can be a modified to suit other seat designs and stiffness
Hand grip	Spring as hand grip release at 400N	Can be a modified further if required to meet occupant anthropometry, percentile and gender. Nevertheless, it is a multi-body limitation as the finger grip cannot be modelled
Occupant Stances	2 hand grip (FMVSS208), mobile phone, radio, armrest Feet positions	Can be a modified to suit any stances
Pre-braking pulse	Set as PRISM FP7 deceleration pattern	Can be a modified to suit vehicle performance
Brake dive	Not modelled in the thesis	Need vehicle dynamics input and vehicle dive included in the pre-braking motion
Braking Duration	1.1s, 1.7s and 2.3s	Can be modified to suit
Vehicle crash pulse	Based on Neon against rigid wall (40km/h (25mph))	Can be a modified to suit other vehicle architectures or accident scenarios (car to car for example)
Vehicle crash pulse as function of brake dive	Not modelled in the thesis	Can be a modified to suit other vehicle architectures
Airbag module	OOPSafe airbag model (from previous research)	Can be a replaced with dedicated airbag model
Airbag firing time	Set to 10ms in the model	Can be a modified to suit restraint performance

Collapsible steering column	None.	Can be added to suit restraint performance
Seatbelt	None. The study will address unbelted	Belt can be fitted if required with all pretentionners and load limiters

Table 3.8: Active Safety Assessment Environment current configuration and future opportunities

The current limitation is the omission of modelling the vehicle brake dive, due to fact that new evidence became apparent too late in the research (Thatcham 2011), where the author tested vehicles fitted with active safety features. The PRISM project neglected brake dive and only recorded vehicle X deceleration (PRISM 2003a). It is acknowledged that obtaining vehicle dynamics information is for the future important to improve the framework accuracy. Moreover, to make the framework complete, should brake dive be included, then the respective rigid wall impact crash pulse would need to be computed, in order to reflect a consistent approach.

No collapsible steering column was fitted because no data was provided about the vehicle provenance of the restraint system. As such, estimating its characteristic would have added some unnecessary complexity to the problem. This feature can be added in the future, as testing this framework on a full known vehicle would be again ideal.

The next step of the methodology is to assess the kinematics and the injury of the unbelted driver. The next section will address the output needed to perform this assessment.

3.4 Definition of the Active Safety System performance

Kinematics

During the pre-braking phase, it is possible, by using MADYMO, to monitor the position of the occupant via kinematics output (*.kin3 files), as illustrated in Figure 3.25 (Bastien 2012a)**.** Two points have been chosen on the occupant, which can be extracted from the mesh within the post-processor:

- **The solar plexus:** this point is located on the sternum and will be useful to monitor the distance from the thorax to the steering column

- **The top of the head:** this point has been chosen as it is related to head contact. The top of the head is less sensitive to head rotation; hence it is believed to be a better metric to measure distances from head to windscreen.

More output could be chosen and their number is not exhaustive.

Figure 3.26: Occupant kinematics during the pre-braking phase (Bastien 2012a)

It can be observed from Figure 3.25, that the occupant's stance can be setup in various configurations which can relate to Table 2.5. All the kinematics can be computed and tracked during the pre-braking phase.

A typical assessment of the ASsEt environment was performed using the full MADYMO official solver release 7.4 combined with a beta release of the Active Human model provided by TNO (Bastien 2012a). This beta release contained the full passive Human Model with the addition of control system loop (encrypted) which controlled the occupant's muscle activity depending on the forces applied. A typical MADYMO syntax can be found in Appendix B. In the scenario studied, the top of the occupant's head kinematics is plotted and analysed (Figure 3.26, Figure 3.27 and Figure 3.28) relative to the kinematics observed in Figure 3.25.

Figure 3.27: Top of the occupants' head X position (4 stances) (Bastien 2012a)

Figure 3.28: Top of the occupants' head Y position (4 stances) (Bastien 2012a)

Figure 3.29: Top of the occupants' head Z position (4 stances) (Bastien 2012a)

It can be noted that the X, Y and Z positions of the top of the occupant's head are similar for the FMVSS208 (standard 2 hand grip), radio and mobile phone stances, but are vastly different for the mobile phone stance where the head moves sideways (Y) by as much as 250mm and 300mm (at time 1.7s and 2.3s respectively).

The middle of the occupant's torso kinematics can also be plotted and analysed (Figure 3.29, Figure 3.30 and Figure 3.31).

Figure 3.30: Top of the occupants' head X position (4 stances) (Bastien 2012a)

Figure 3.31: Top of the occupants' solar plexus Y position (4 stances) (Bastien 2012a)

Figure 3.32: Top of the occupants' solar plexus Z position (4 stances) (Bastien 2012a)

It can be noted that the X, Y and Z positions of the occupant's middle torso are again similar for the FMVSS208 (standard 2 hand grip), radio and mobile phone stances, but are vastly different for the mobile phone stance where the head moves sideways (Y) by as much as 200mm and 400mm (at time 1.7s and 2.3s respectively).

The difference in kinematics between a mobile phone grip and an armrest grip is that in the later, the contact with the door tends to keep the occupant in line with the centre of the seat, while in the first instance, no means of restraint are present, hence the large motions. It is therefore proposed to compare the occupant's kinematics for the standard posture, FMVSS208 (standard 2 hand grip), and to compare it to the most

extreme which has been predicted from early MADYMO beta release models to be the mobile phone stance (Bastien 2012a).

Injuries

Occupant injury values will be calculated from the standard MADYMO output files (TNO 2011; TNO 2012) after the runs have been computed. All injuries will be computed against the injury requests from ***Table 3.9***.

This item has been removed due to 3rd Party Copyright. The unabridged version of the thesis can be viewed in the Lanchester Library Coventry University.

Table 3.9: Active Human Model injury files outputs (TNO 2012)

3.5 Methodology Summary and next steps in the thesis

The proposed Active Safety Assessment Environment can predict the kinematics and injuries of unbelted occupants under autonomous emergency braking. Using the scientific data drawn from this chapter, it is believed that this ASsEt environment is capable of objectively testing whether active human computer models should be the tool of choice for the future of active safety assessment.

This framework can capture the occupant's kinematics by plotting strategically its motion based on finite element nodes located on the surface of the human body, as well as subsequent accident injuries.

The proposed initial framework contains a large amount of variables and engineering features (Table 3.8), and looks to be a relevant safety tool for the future in spite of some necessary improvements in the modelling of the brake dive in the pre-crash and crash phases.

An early study (Bastien 2012), using a pre-release MADYMO AHBM with arms, neck, hips and spine muscle toning has shown that the mobile phone stance provided the most extreme kinematics as the occupant is moved away from the steering wheel centre line (Figure 3.25) and is at risk of contacting the steering wheel rim when the accident occurs. As such the standard 2 hand grip and the mobile phone stances will be the ones assessed in detail in this thesis.

Now that all the conditions are set, it is proposed to use this framework to assess the active human model in AEB scenario followed by a rigid wall impact.

The next chapter (chapter 4) will look at improvements and validation/ correlation of a smart airbag designed to meet FMVSS208 (Freisinger 2006), i.e. against a 5^{th} percentile female ATD, as this is necessary to calibrate the accident phase of framework. Kinematics and injury responses of a Passive Human Body Model (PHBM) as well as its stability against static deployment will be discussed before addressing in the following chapter a muscle activity validation and the application of the validated active human model in the proposed ASsEt environment.

4.0 Validation of an Airbag Model and Initial Study in the Use of Human Models in Static OOP

The aim of this chapter is to calibrate the Active Safety Assessment Environment, as discussed in Chapter 3, as part of the Methodology section. As the study considers unbelted occupants, the airbag system from the framework needs initially to comply with the FMVSS208 regulation in static position.

This chapter will discuss improvements and implementation of an OOP airbag based on previous research (Mahangare 2007a; Mahangare 2007b), followed by initial airbag deployment on passive human models in order to have an appreciation of the occupant's kinematics and injury values.

4.1 Introduction

Extensive studies have shown that the airbag deployment in OOP loadcases (based on FMVSS208 legislation) consists of two occupant loading phases: a punch-out effect where the airbag bursts out of its container with the airbag and airbag module cover accelerating towards the occupant, and a second loading phase during which the airbag is taking on its deployed shape and volume (membrane-loading effect). The loading associated with the airbag deployment creates injuries mainly in the head, neck and chest areas (Mahangare 2007a; Mahangare 2007b).

The mitigation of injuries associated with OOP scenarios have led to the low-risk development of "smart" airbags. Some advanced airbags contain multi-chambers and sacrificial tear seams in efforts to reduce the punch-out and membrane-loading effect (Mahangare, 2007; Blundell, 2006). Mathematical simulations of smart airbags use very complex techniques such as, fluid mechanics (Gas Flow) to describe the inflator gas flow (pressure gradient) and the initial airbag inflation, and improve the representation of the pressures within the airbag. For in-position scenarios, it is sufficient to represent the gas inside the airbag using a uniform pressure approach since the airbag is fully deployed when the occupant interacts during the crash. It has been shown that a driver slumped over the steering wheel and hence the driver airbag

module, increases the gas pressure inside the airbag leading to higher deployment forces (Blundell 2006), which creates a need to improve the accuracy of the airbag representation, in particular the airbag fabric material characteristics and its ability to accurately replicate the rupture of sacrificial tethers in order to simulate the airbag pressure characteristics.

The method used for simulating the sacrificial tear seam or "control chamber" failure presented in previous studies and thesis memoir (Mahangare 2007b) were not however successfully implemented, as the airbag straps failure could only be "released" using a time delay switch, as the control cloth failure mode was not properly captured. This technique has the disadvantage that the tether will fail at the same time regardless of the occupant mass and stiffness 'resting' on it, which will be shown later as an incorrect assumption. Should this airbag be used in AEB scenarios, the timing of the straps could be also dependant on the momentum of the occupant travelling towards the airbag, which will certainly change the airbag pressure pattern compared to a static deployment. In the previous work (Manhangare, 2007), a switch time was different for each loadcase OOP1 and OOP2, as well as different airbag cloth material behaviours, i.e. one for each loadcase. The model provided was nevertheless helpful as the airbag was pre-folded and re-folding it was beyond the scope of the author's thesis. It was assumed that the airbag folding was adequate, as well as the gas-flow and tank test inflation characteristics.

Another limitation of the previous work (Mahangare 2007b) was the modelling of the steering wheel airbag cover. The model provided, although meshed adequately for explicit finite element computation, had incorrect thicknesses and boundary conditions. The airbag cover had also constant thickness tear seam thickness which was also incorrect.

The airbag fabric permeability was also approximated by the previous author as the data was not available at that time.

This chapter will therefore include initially improvements to the previous airbag model by focussing on a mechanical failure (and not a time switch), airbag cover tear seam improvements, updating the airbag cloth permeability and conclude on the suitability of this updated OOP airbag model. This section will only address the key improvements to the model, based on a 5^{th} percentile ATD female. This initial section

will also prove that modelling a tether failure with a time switch is an incorrect assumption.

Once the updated airbag model is judged adequate, it is then possible to broaden the study by considering an average occupant and investigating the difference of responses between a 50th percentile ATD against a 50th percentile human model in static OOP situation.

4.2 Improvements to the original OOP airbag system

This section will focus on airbag modelling improvements from previous research in order to use it as the reference restraint system for the ASsEt environment.

4.2.1 Airbag Fabric material characterization

Initial improvements were needed in the airbag cloth material properties which needed more accurate representation.

The airbag fabric described in this report is uncoated, 350 decitex, for which the characteristics are obtained by performing tensile test and shear panel test.

Figure 4.1: Typical deployed airbag after the sacrificial tether failure (Bastien 2010)

Obtaining accurate airbag material characteristics is critical to the airbag deployment kinematics and determination of the exact tether rupture load (Figure 4.1).

Uni-axial tensile tests

To determine the characteristics of the airbag fabric material, a number of airbag fabric sample tensile tests were carried out. The test data used in this study was taken from material tests with 100 mm by 50 mm fabric samples, with tests conducted at

speeds of 100 mm/min and 1 m/s, with 100 mm/min representing the "static" load case and 1 m/s representing a "dynamic" load case.

In order to take into account the strain rate properties of the fabric material, MADYMO has the possibility to add a strain rate function to the material behaviour (TASS 2010). Two functions were investigated in this study: Cowper-Symonds and Johnson-Cook strain rate functions. Both functions relate the yield stress to the strain rate (c_1), and include a further amplification factor (c_2) which indicates how strongly the strain rate effect works on the yield stress hardening. A study showed that the Johnson Cook strain rate dependency function (Equation 4.1) provided the best level of correlation (Stubbs 2010) (Figure 4.2 and Figure 4.3).

$$g(\bar{\dot{\varepsilon}}) = 1 + c_2 \ln(\max(\frac{\dot{\varepsilon}}{c_1}, 1))$$

Equation 4.1: Johnson-Cook strain rate dependency function generalised formula (TASS 2013)

In MADYMO it is assumed that the yield stress is made up of two terms: a strain rate only term and a strain rate combined with the plastic strain term. If the amplification factor (c_2) is zero then the strain rate only affects the yield stress, whereas if the amplification factor is not zero (c_2), then the yield stress is scaled by a rate dependency function (c_1).

Figure 4.2: Correlation of airbag fabric warp stress-strain characteristics (Stubbs 2010)

Figure 4.3: Correlation of airbag fabric weft stress-strain characteristics (Stubbs 2010)

Further static tests were carried out on 100 mm by 50 mm fabric samples with a "perforation" across the width of the fabric at the mid length. The perforation is used to control the point at which the airbag fabric fails and to reduce the load at which it fails. A perforation could be implemented in the airbag "control chamber" to enable tuning of the airbag deployment (Figure 4.4 and Figure 4.5) (Stubbs 2010).

Figure 4.4: Computer correlation of cloth tearing (warp) (Stubbs 2010)

Figure 4.5: Computer correlation of cloth tearing (weft) (Stubbs 2010)

Using MADYMO MATERIAL.INTERFACE elements, it is possible to investigate the stress level for the sample to fail. This threshold is described as the ultimate normal traction force and is defined as the force per unit area, where the area of the tear seam is defined as the length of the tear seam multiplied by the element thickness (TASS 2010).

From the simulation optimisation, the Johnson-Cook function with c_1 = 1.0 and c_2 = 0.1 gave the best correlation of the simulation results to the physical dynamic test results. When the static tensile test simulations for perforated and un-perforated fabric were re-run with the same Johnson-Cook function, the models were stable and the correlation of the force vs. percentage strain was similar to the static results without the rate function, i.e. the correlation between the static tensile test simulation and physical test results was good. Consequently, the Johnson-Cook strain rate function representing the dynamic effects in the overall airbag fabric were implemented with the parameters c_1 = "1.0" and c_2 = "0.1" (Stubbs 2010).

Bi-axial tensile tests

A series of bi-axial tests, referred to picture frame tests, were used to investigate the shear stiffness of the airbag fabric. The shear stiffness is a function of shear stress against shear strain. The picture frame is essentially a pin jointed frame, clamped around the airbag fabric, fixed at the bottom corner and loaded at the top corner, as shown in below.

The airbag fabric is clamped in the frame so that the warp and weft run parallel with the sides of the frame. In this way, displacing the top corner of the picture frame applies a shear force to the fabric (Figure 4.6).

T

Figure 4.6: Picture frame test schematic and shear panel representation of the picture frame (Stubbs 2010)

The airbag fabric shear stress-shear strain characteristic, derived from the static picture frame tests is shown in Figure 4. The derived data (Equation 4. 1) (Bastien 2010b; Stubbs 2010) was therefore reflected to produce a symmetric function (Figure 4.7).

F = applied load
d = depth of shear panel
t = thickness of panel
Δl = length increase

Shear strain derived equation Shear stress derived equation

Equation 4. 2: Derived shear stress – strain equations (Bastien 2010b; Stubbs 2010)

The current computer models are using the MATERIAL.FABRIC_SHEAR MADYMO material model (TASS 2010). From the test result and computed correlation curve, it can be seen that these fabric models are non-linear.

Figure 4.7: Correlation of airbag fabric shear stress-shear strain characteristic (Stubbs 2010)

Looking closely to the picture frame test, the response is initially linear and then parabolic, which is due to fabric blockage/ locking effect at higher forces. The main airbag material characteristics are now defined and correlated (Stubbs 2010).

Fabric Dynamic Permeability

The airbag fabric is a woven material and permeable, causing a certain amount of pressure loss to occur during the airbag inflation process, which can be assessed via a permeability test machine (TEXTEST 2010).

The MADYMO PERMEABILITY.MODEL2 (TASS 2010) was used to represent the permeability characteristic determined using the FX3350 (TEXTEST 2010) airbag tester, in the airbag simulation with the newly correlated material characteristics (Subramanian 2010).

Figure 4.8: Cross section of Textest permeability correlation model showing a vector plot of cloth's displacements due to pressure and permeability (Subramanian 2010)

Based on a TESTEXT setup (Figure 4.8), the permeability curve function was computed (Subramanian 2010), as illustrated in Figure 4.9.

Figure 4.9: New airbag cloth permeability function updated from OoPSafe1 (Subramanian 2010)

The pressures calculated by the computer simulation of the Textest test match the pressures from the test, and the fabric bulge calculated is 10.07mm versus 10.26mm measured in the test. There is therefore a good level of correlation for the cloth permeability (Figure 4.10 and Figure 4.11).

Figure 4.10: Validation of new airbag permeability function against physical tests (pressure vs. time) (Subramanian 2010)

Figure 4.11: Validation of new airbag permeability function against physical tests (bulge vs. chamber pressure) (Subramanian 2010)

It can be noted that the approximation based on previous work (Manhangare 2007), was generally adequate as there is not a major difference in the permeability curves.

Airbag control cloth failure

Once the material properties and permeability have been set, it is now possible to model the mechanical failure of the airbag control cloth. The failure has been modelled using an INTERFACE element which was take tension load, like a membrane.

Using a simple spherical 60 litre airbag model and controlling the cross section force around the perimeter of the airbag and the cross section area, an estimate of the stress to failure was evaluated using the theoretical hoop stress of a sphere and comparing it against the section force divided by the cross section of the elements based around the circumference of this airbag (Stubbs 2010), as illustrated in Figure 4.12.

Unfortunately this failure method as well as other ones researched, using beam elements (Morris 1998), could not be transferred to another airbag design as most airbags are not spherical (Stubbs 2010). This was simply caused by the curvature change from the airbag tethers. The critical failure load had, consequently, to be tailored to meet the deployment timing.

Figure 4.12: Airbag mechanical control cloth failure modelling. Control cloth in yellow (left), control cloth failure elements (MATERIAL.INTERFACE elements) (right) (Stubbs 2010)

During the physical test, the control cloth ruptures. From the film data it believed that the control cloth breaks on one side, before the other, perhaps the first side failing between 30 and 45ms and the other side failing between 45 and 55ms. As such, the stress load in the INTERFACE has been computed to be 2.4E8N/m^2 to suit the deployment physical test.

Airbag model summary

Combining all the improvements discussed so far in this chapter, an updated and improved airbag model was derived with a key feature, which is a mechanical control cloth. The control cloth mechanically fails at a comparable timing from the physical tests (Figure 4.13) and is a key feature in the development of the ASsEt environment.

Figure 4.13: Airbag free deployment validation (Stubbs 2010)

Continuing the full correlation of this airbag in all the other impact modes (Manhangare 2007b) goes beyond the scope of this research, which will assume that the folding and other geometries are matching the physical airbag. The key feature being the mechanical failure of the control cloth is now embedded in the model.

4.2.2 Airbag cover correlation

The influence of the airbag module cover stiffness is extremely important in obtaining accurate injury predictions. This airbag pressure is caused by the bending of this cover, the ability of the tear seam to resist tearing as well as resisting the occupant's inertia.

The material characteristics used for this driver airbag cover model were initially derived from physical tests with speeds ranging from 100mm/min to 4m/s and have been validated during this study.

Some improvements were needed in the modelling of the cover from previous work (Manhangare 2007b), including incorrect cover thickness (Figure 4.14), inaccurate mesh boundary conditions, as well as erroneous tear seam definition (including geometry and the failure method).

Figure 4.14: Mesh definition of airbag module cover plastic reinforcement (left) with varying tear seam thickness (right). (Bastien 2010b)

Considering previous work (Manhangare 2007b), the pad cover was only restrained at the bolt fixings, but not at the 3 lips when the cover was located (Figure 4.15).

Figure 4.15: Updated boundary conditions for the pad cover (circled in green). (Bastien 2010b)

This problem was solved by selecting the missing nodes and applying a vertical boundary condition restraining their translations.

From previous work, the failure of the tear seams was performed using an INTERFACE element of constant thickness and orientation in the whole model. These assumptions were incorrect as the INTERFACE element will see some bending component in the deployment test which it is not tailored to resist to, but only tension and compression. Furthermore the INTERFACE elements cannot be triangular, which means that each corner of the tear seam had no elements at all, making this element type not physically representative.

The base material has been re-correlated, using prior work (Mahangare 2007b), but updating the Johnson-Cook parameters to match the material models. In this case c_1="35" and c_2="0.85" (Figure 4.16 and Figure 4.17).

Figure 4.16: Material property validation of the pad plastic cover (Bastien 2010b)

Figure 4.17: Modelling validation of the pad cover tear seam stiffness property (weakness line on 'B' surface) (Bastien 2010b)

The choice of a varying thickness tear seam, to simulate the tapered effect of the tear seam, with elemental strain deleted is used to simulate the tearing in the improved model. To achieve this the DAMAGE.STRAIN_PLASTIC (TASS 2010) model is used using an equivalent plastic strain at material failure (EPSF) to define initiation of material damage, where each integration point in the element fails independently if the corresponding equivalent plastic strain ε_p exceeds the failure strain ε_f specified by EPSF. This method has the benefit of enabling the failure to occur when a strain level (load) is exerted against the inner surface of the airbag module cover.

As a consequence, using the DAMAGE.STRAIN_PLASTIC function of MADYMO with suitable values of EPSF and Equivalent Plastic Strain at material Rupture (EPSR) around the tear seam line it is possible to obtain a better correlation (Figure 4.17).

Nevertheless, this is where the similarities end, as computed failure values generated form the test pictured in Figure 4.17 could not be used for a punch impact where bending loading is present. It was observed that by ignoring the bending component of the shells, the tear seams' response was too weak and breaking too early.

The tear seam geometry and modelling assumption is vastly different (Figure 4.18), hence it is not possible to capture the exact stress/ strain distribution in the tip area of the wedge (Christensen 2010).

Figure 4.18: Actual tear seam geometry and CAE discretisation (Christensen 2010)

From previous work (Ruff 2006) it is suggested that beam elements could also be used to model tear seams, because of their tension and bending properties. It was not clear however how the tear seam geometry can be transferred to beam section properties. A rigid punch test is therefore needed to validate the tear seam strength.
The technique used is therefore a reverse engineering approach, where the test is performed and then the tear seam strength tuned to suit.

A 4m/s punch-out test using a 100mm rigid sphere was carried out and from the correlation work undertaken, it can be seen that the opening of the cover is comparable to test, i.e. the visible opening and the acceleration levels correlate well (Figure 4.19). It was necessary to modify the strength of the tear seam locally to take into account that their thickness varies from around 0.85mm at the centre to 1.5mm at the edges.

Figure 4.19: Pad cover impact correlation visually at the moment of opening (left) and at acceleration correlation (right) (Bastien 2010b)

The airbag system is now ready for testing using an improved airbag, cover and permeability models.

4.2.3 Implementation of correlated airbag in OOP testing

Two OOP test set-ups are specified in FMVSS208 (Code of Federal Regulation, chapter 49, part 571, subpart 208, section S26), "procedure for low risk deployment tests of driver airbag": Driver position 1 (chin on module) a 5th percentile female driver represented using a 5th percentile Hybrid III ATD with chin on airbag module and Driver position 2 (chest on module) a 5th percentile female driver represented using a 5th percentile Hybrid III ATD with chest on airbag module.

The MADYMO simulations were improved to include the new airbag material characteristics, the airbag tether rupture model and the updated airbag cover created in this study (Bastien 2010b).

Airbag System Validation (OOP1)

Physical tests were conducted to assess the OOP1 impact scenario, chin on module. A comparison of the simulation and test kinematics are shown in Figure 4.20.

In both OOP1 tests, the control cloth ruptured at around 37ms. The rupture does not occur instantaneously and it is hardly possible to observe the duration of the rupture from the test data. In the simulation the rupture begins at 35ms and finishes around 52ms (Stubbs 2010).

Figure 4.20: OOP1 side view comparison of test and simulation for airbag module with the updated cover model (Stubbs 2010)

A comparison of the ATD output channel data for the simulation with the updated airbag cover model is shown in Figure 4.20. Looking at the injury traces, it has to be noted that the first 15ms are primary influenced by the airbag blast phase (punch-out phase) and that past 15ms by the airbag working pressure (membrane loading).

Figure 4.21: OOP1 occupant head X acceleration (Stubbs 2010)

Figure 4.22: OOP1 occupant neck F_Z force (Stubbs 2010)

Figure 4.23: OOP1 occupant chest X acceleration (Stubbs 2010)

Figure 4.24: OOP1 occupant chest deflection – sternum (Stubbs 2010)

Some injury curves are presented above in Figure 4.21, Figure 4.22, Figure 4.23 and Figure 4.24. In this OoP1 (chin on module), the head x acceleration and Upper neck Fz forces are at the beginning of the deployment heavily loaded in the punch out phase; the signal is flatter after 15ms. Chest deflection and chest x accelerations are loaded in a gradual manner after 17ms (Bastien 2010a).

The peak injury values for the 5th percentile in the OoP1 test and simulation are listed in Table 4.1.

Table 4.1: Comparison of 5th percentile occupant injuries in OOP1 for test and simulation (Stubbs 2010)

It can be observed that most injuries maximum values on the improved airbag assembly are closer to the test average.

Airbag System Validation (OOP2)

In the OOP2 tests, the control cloth ruptured at around 37ms. In the simulation the rupture begins at 35ms and finishes around 52ms (Stubbs 2010).

Comparisons between tests and simulations can be observed in Figure 4.25.

From the snapshots (Figure 4.25), it can be seen that the airbag module cover opens fully as in the test. The improvements in the airbag module cover computer model have yielded to improved injury predictions. It can be however noted that the airbag kinematics is different from 20ms, as it goes through the steering wheel rim.

Figure 4.25: OOP2 side view comparison of test and simulation for airbag module with the updated cover model (Stubbs 2010)

Physical tests have been conducted and simulated to assess the OOP2 scenario, chest on module (Hoffmann 2007) and it can be noted that the airbag kinematics already published is similar to the improved one (Figure 4.26).

Figure 4.26: OOP2 airbag deployment (Mahangare and Mahangare, 2007)

It has been explained that the friction between the airbag and the dummy could cause the differences compared to the test (Mahangare 2006), however to justify this, a parametric study of the friction parameter between the occupant and the steering wheel could have been undertaken to prove such a statement. It is a possibility that the airbag folding would need further investigation, as well as the airbag overall modelling assumptions. Overall, the modified airbag system is an improvement on the system injury predictions published in other thesis (Mahangare 2007b).

In such loadcase it maybe also proposed in the future to perform a convergence study on the gas flow Euler grid size in order to confirm whether the airbag unfolding is well captured.

Some injury curves are shown in Figure 4.27, Figure 4.28, Figure 4.29 and Figure 4.30 comparing the level of correlation between tests and simulations.

Figure 4.27: OOP2 occupant head X acceleration (Stubbs 2010)

Figure 4.28: OOP2 occupant neck Fz force (Stubbs 2010)

Figure 4.29: OOP2 occupant chest X acceleration (Stubbs 2010)

Figure 4.30: OOP2 occupant chest deflection – sternum (Stubbs, 2010)

In the OOP2 tests, the control cloth ruptured at around 35ms and 37ms. The rupture does not occur instantaneously and it is not possible to observe the duration of the rupture from the test data. In the simulation the rupture begins at 34ms and finishes around 45ms. The peak injury values for the 5th percentile in the OOP2 test and simulation are shown in Table 4.2.

Table 4.2: Comparison of 5th percentile occupant injuries in OoP2 for test and simulation (Stubbs 2010)

Comparing the OOP2 tests and simulation, it can be observed that the airbag module cover model is stiffer. The simulated cover does not open as far, preventing the airbag from deploying between the steering wheel hub and steering wheel rim and changing the position of the airbag against the occupant. The main effect of this is in the neck Fz component, in both magnitude and timing. Again, as for OOP1 test, the results with the improved airbag are closer to the OOP2 test average (Table 4.2).

Summary

The new airbag system model includes a mechanical control cloth which allows a deployment comparable with a standalone airbag physical test. When in OOP scenarios, the occupants' injuries and kinematics produce comparable responses to physical tests, as well as injury levels which are below the legal limit (based on the FMVSS208 test protocol). Consequently, the new airbag system can be used as a suitable tool for OOP assessment.

The following section will further justify the need of using a mechanical failure compared to a time switch based one.

4.3 Effect of ATD on airbag control cloth failure response

Using the improved airbag module model (folded cushion and cover) the 5th percentile dummy ATD model has been replaced by a 50th and 95th percentile ATD dummy in order to investigate the mechanical airbag tether failure effect. Airbag pressures and volumes have been plotted for each ATD for the two OOP scenarios (Figure 4.31 and Figure 4.32). The pressure graph shows clearly the burst pressure in the punch-out phase at the start of the inflation process and subsequently the airbag working pressure or "membrane loading phase" during the working time of the airbag. Each pressure phase creates loads on the occupant.

Figure 4.31: Airbag chamber internal pressures - OOP1 (Bastien 2010a)

Figure 4.32: Airbag chamber internal pressures – OOP2 (Bastien 2010a)

The burst pressure varies slightly in the first 20ms between the computer runs (Figure 28) depending on the ATD being impacted. As this even is very short in time, one may suggest that this pressure difference may mainly be due to the ATD's compliance and geometrical shape. The secondary pressure (membrane-loading) builds up and remains higher the heavier the occupant (inertia). The working pressure decays quicker for the 5th percentile female than for the 95th percentile male, starting from 45 to 50ms. This information concurs with the previous works (Horsch 1990) stating that heavier occupants slumped over the airbag increased the airbag pressure during deployment. It can be seen that the airbag volume increases in stages (Figure 4.33 and Figure 4.34), due to the gradual failure of the airbag control chamber.

The start of the tearing process is not always evident, however, the end of the tearing process can be observed by the sudden increase in airbag volume (Figure 4.33 and Figure 4.34).

Figure 4.33: Airbag chambers internal volumes – OOP1 (Bastien 2010a)

Figure 4.34: Airbag chambers internal volumes – OOP2 (Bastien 2010a)

Considering the tether rupture timing results from Figure 4.32, it can be noted that the tether failure starts at approximately time 0.34, but ends at a different time for each deployment study (Figure 4.33).

Figure 4.35: Tether rupture time vs. ATD (Bastien 2010a)

Figure 4.36: Airbag losses by permeability (Bastien 2010a)

The permeability plot (Figure 4.34) suggests that the losses due to permeability are comparable for the first 0.4 units of time for the different ATD sizes investigated. Nevertheless, the permeability losses increase the heavier ATD, as more pressure is applied to the airbag, leading to airbag volume reduction.

This proves that the improved mechanical tether failure is better suitable for this application compared to e.g. a time switch derived from 5th percentile dummy ATD OOP tests.

4.4 Application of the 50th percentile MADYMO Human Body Model (HBM) in FMVSS208 Scenarios

Using the validated computer model, it is possible to investigate the injury levels sustained by various occupants' sizes and compare airbag response levels. This study will compare the 50th percentile passive HBM and 5th, 50th and 95th percentile ATD model in static stance against airbag responses.

MADYMO contains a huge database of crash test dummies, as well as human body models (TASS 2010) developed to simulate living human beings. Human volunteer, for low severity tests, as well as Post Mortem Human Subjects (PMHS), for high severity test, were used to validate the kinematics and dynamic of such occupant computer model. The disadvantage of ATD models is that they are not

multidirectional, which limits possibilities for their application, as opposed to the multidirectional HBMs.

The 50th percentile male facet occupant model, or facetted HBM, was chosen because of its excellent computational stability and computation speed and its ability to measure injuries (Lange 2005; TASS 2013). The HBM is based on a multi-body architecture comprising of joints where the human limbs are represented by bodies (ellipsoids) and complex curves (case of the HBM skin) based on meshes which are defined as facets. These facets' stiffness and compliance are given by the joint stiffness it is connected to, as well as facets force/ displacement characteristics.

This model has been directly derived from the anthropometry database RAMSIS, making the model as representative as possible to a mid-size male occupant. All the components of the HBM use a multi-body approach, which provides a quick runtime compared to similar finite element HBM models, like the HUMOS (Kayvantash 2009), which are slower, but contain more definition of human vital organs. To improve the contact between the airbag and the HBM facets models the contact option FACE_TYPE ="FRONT" (TASS 2010) was used to prevent nodes of the airbag to be trapped in the HBM model, which would change the dummy's kinematics and injury predictions.

Comparing the airbag performance across all the occupants tested (Figure 4.31 and Figure 4.32); the 50th percentile HBM has a similar response as the 50th percentile ATD model in the airbag blast phase (punch out effect, time < 0.15). The differences are more pronounced in the airbag working phase (membrane loading phase, time > 0.15), where differences in the pressure, volume and permeability losses are more evident.

Looking at the airbag pressure plots (Figure 4.37 and Figure 4.38), it can be seen that the airbag working pressure in the case of a 50th percentile HBM and a 95th percentile ATD model is very similar in magnitude and shape, in both OOP1 and OOP2 loadcases.

Figure 4.37: Overall comparison of airbag pressure between the 5th, 50th, 95th ATD model and the 50th HBM – OOP1 (Bastien 2010a)

Figure 4.38: Overall comparison of airbag pressure between the 5th, 50th, 95th ATD model and the 50th HBM – OOP2 (Bastien 2010a)

The airbag volume plots (Figure 4.39 and Figure 4.40) and permeability losses (Figure 4.41 are showing that for OOP1, the airbag volume and losses in both 95th percentile ATD model and 50th HBM are identical. The sudden jump in airbag pressure indicates the end of the sacrificial tether rupture, indicating an identical timing failure for both 95th percentile ATD model and 50th HBM.

For the OOP2 loadcase (Figure 4.42) , the events follow the same trend as for OOP1, but more differences are visible in the sacrificial tether rupture time (later in the 50th percentile HBM) and higher gas losses by permeability (higher in the case of the 50th percentile HBM).

Figure 4.39: Overall comparison of airbag volumes between 5th, 50th, 95th ATD model and 50th HBM - OOP1 (Bastien 2010a)

Figure 4.40: Overall comparison of airbag volumes between 5th, 50th, 95th ATD model and 50th HBM - OOP2 (Bastien 2010a)

Figure 4.41: Overall comparison of airbag permeability losses between 5th, 50th, 95th ATD model and 50th HBM - OOP1 (Bastien 2010a)

Figure 4.42: Overall comparison of airbag permeability losses between 5th, 50th, 95th ATD model and 50th HBM - OOP2 (Bastien 2010a)

Injury levels between a 50^{th} percentile anthropometric dummy model (ATD) and a 50^{th} percentile HBM are listed in Table 4.3.

Looking more closely to the 50^{th} percentile ATD model and HBM, it can be observed from Figure 4.38, that both occupants have the same timing response and almost the same compliance during the punch out phase (between time 0 and 0.15).

Table 4.3: Comparison between 50th Percentile ATD model and 50th percentile facetted HBM in both FMVSS208 OOP scenarios (Bastien 2010a)

Figure 4.43: Comparison of airbag pressure between 50th ATD model and 50th HBM (Bastien 2010a)

Figure 4.44: Comparison of airbag volume between 50th ATD model and 50th HBM (Bastien 2010a)

Comparing again the 50th percentile ATD model and to HBM (Figure 4.38), it can be noted that differences can be found in the membrane loading phase (t > 0.15).

The airbag pressure in combination with the HBM is constantly increasing, reaching pressure values greater than in combination with the ATD model from time 0.5s onwards. This is confirmed by the volume plots (Figure 4.39) where in OOP1 and OOP2 scenarios, in the case of the HBM occupant, the volume at time 0.5 starts to reduce (compared to the 50th percentile ATD model), which leads to the airbag pressure increase.

The OOP1 kinematics can be clearly seen in Figure 4.40, were the HBM stays longer in contact with the deploying airbag from 50ms (Bastien 2010a).

This item has been removed due to 3rd Party Copyright. The unabridged version of the thesis can be viewed in the Lanchester Library Coventry University.

Figure 4.45: OOP1. Kinematics comparison between 50th percentile ATD model (left) and 50th percentile HBM (right) (Bastien 2010a)

In the OOP2 loadcase, it can be observed from the animations (Figure 4.41) that, like in reality, the HBM's spine is more flexible than the 50th percentile ATD model.

Looking at the neck and head area, it can be seen that the neck is more compliant from t=50ms, which allows the head to push down against the airbag and restricts airbag deployment, creating extra airbag pressure.

Figure 4.46: OOP2. Kinematics comparison between 50th percentile ATD model (left) and 50th percentile HBM (right) (Bastien 2010a)

From the obtained airbag pressure results from Figure 4.38 (Bastien 2010a), it can be concluded that the original punch-out effect is primarily caused by the inflator characteristics and the occupant's compliance. The second phase is characterised by an increased airbag working pressure caused by the occupant's mass transfer. As the HBM is rolling more on the airbag (Figure 4.40 and Figure 4.41), it results in a higher airbag pressure than the ATD model from time 0.5 onwards (Figure 4.38).

The HBM with the same stature as an ATD model showed small differences in the kinematics in frontal airbag impact. The largest differences were seen in the in the membrane loading phase. The difference in kinematics is caused by the limbs and joints of the HBM being more flexible than that of the ATD model, causing differences in loading of the airbag. All above mentioned differences between HBM and ATD model are likely to be the causes of the different in the injury levels.

The MADYMO HBM's (Lange 2005) early response in the OOP2 loadcase (before time 0.5) is a good fit to the MADYMO 50th percentile ATD model in static FMVSS208 scenarios with respect to the airbag pressure and volume levels (Figure 4.38 and Figure 4.39).

In the OOP1 loadcase it appears that the local compliance of both occupants in the neck area is different as the values of the peak and trough before time 0.15 are different (Figure 4.38). For the ATD model the airbag pressure are 0.71 and 0.34 at its peak and trough, respectively, compared to 0.67 and 0.29 for the HBM model. The main difference in kinematics between these two models appears clearly after time 0.5, in both OOP1 and OOP2 loadcases, mainly caused by the difference of the spine compliance, where the HBM's spine is more compliant than that of the ATD model (Figure 4.40 and Figure 4.41).

4.5 Summary of the preliminary study

This early study investigated the effect of airbag deployment in OOP scenarios and has looked into the behaviour of an airbag when restraining occupants of various masses and statures. It has shown that airbag punch-out effect and injury peaks have been modelled correctly using the MADYMO Gas Flow tool.

Extensive correlation work with the airbag module components (chambered cushion and cover) has been performed to simulate the OOP tests, with noticeable improvements in injury predictions. It has been shown that the control chamber rupture does not occur at the same time for all applications, which was made evident with the implementation of a mechanical control cloth failure model. The airbag model with improved mechanical tether failure predicts adequately the major injury values measured in real static FMVSS208 OOP tests and enables the representation of airbag deployment behaviour in any OOP scenario, including dynamic OOP.

The study concludes that the MADYMO 50th percentile HBM's kinematic motion differs from that of a 50th percentile ATD model especially in the membrane loading phase, where the HBM's spine response causes the occupant to roll over the airbag, and therefore increasing the airbag's internal pressure, hence changing the airbag tether's failure time. In addition, the base analysis of the OOP injury values between a 50th percentile ATD and 50th percentile HBM suggests that the HBM model is a very stable model and that it provides a comparable response in the same range as the 50th percentile ATD occupant, as well as with other different occupant ATD sizes (5th and 95th).

The next section of the thesis will focus on the validation on an active human model which is based on the PMHS model architecture used in this chapter.

5.0 Validation of an Active Human Model Restrained by a Lap Belt in Emergency Braking Scenario

This chapter cover the correlation and validation of an AHBM restrained by a lapbelt in a frontal linear emergency braking scenario. Due to the danger of unbelted tests for the volunteers, a minimum of occupants restraints is needed (Ejima 2009).

The method used in this section is to initially derive the target human motion curves based from volunteer tests, and then replicate the same test numerically before performing the correlation and validation to the target curves originally derived.

5.1 Muscle Activation Target Curves Derivation

The study presented was based on the information gathered from the OM4IS consortium, which had undertaken sled tests under low 'g' deceleration conditions (Prüggler, 2011). The tests involved a number of volunteers, from whom 7 complete data sets were extracted, examining volunteers' joint kinematics extracted from an 8-camera Vicon motion-tracking system (Vicon 2012).

Experimental Testing

The OM4IS tests undertaken with 7 male volunteers (Prüggler 2011a), corresponding to a 50th percentile human population range (average height 179cm (+/-5cm) and mass 74kg (+/-4kg)), focused on frontal and lateral sled tests. The sled test manoeuvres represented typical lane change swerving manoeuvres and emergency braking scenarios (PRISM 2003a) and were converted into average displacement/time functions, as per Figure 5.1 (maximum acceleration level of 0.90 g in frontal and 0.55g in lateral load directions).

The data provided by Prüggler to the author for the correlation of the AHBM detailed in this chapter were based on 4 volunteers with 3 or 4 repeat tests each. This data was judged by Prüggler to have the most representative response of a reflex scenario.

For the purpose of the study, only the frontal validation was performed, as part of the ASsEt environment.

Figure 5.1: Sled deceleration - time function (frontal and lateral) (Bastien 2012a)

The sled model was composed of linearly guided frame on which a seat could be rotated 90 degrees to modify the loading condition on the occupant from lateral to frontal. The lateral test setup is presented in Figure 5.2.

Figure 5.2: Sled test (lateral setup) (Prüggler 2011a)

The tests were setup as follows:

- The occupants are attached to a rigid seat using a standard lap-belt,
- The occupants are sitting straight, with their legs positioned on an adjustable foot rest such that their leg angle can be adjusted to a constant 130 degrees for each volunteer,
- The occupants are given a small object to be held steadily when the sled is in motion,
- The volunteers are not supposed to be aware of the start of the sled motion.

A typical volunteer posture is illustrated in Figure 5.3.

Figure 5.3: Typical posture setup for OM4IS sled tests (Prüggler 2011a)

This test varies greatly from previous research (Ejima 2009), as the occupant had to stay relaxed during the whole duration of the emergency braking. It has also to be noted that Ejima only performed 1 test on 5 different persons, which only gives an indication of the kinematics and not an absolute. As this chapter will show, occupant's kinematics varies greatly even within the same percentile.

In this test setup proposed in this test (OM4IS 2011), the occupant is asked to keep his posture performing a reflex, as the subject should not be aware of the sled start time, hence limiting a bracing behaviour.

Each test recorded 70 location points, generating a large amount of information.

Data Extraction and data quality

Before extracting and choosing the data, it is important to remember that the overall aim of the study was to compare a human body computer model to real world volunteer tests. Following original results obtained from the OM4IS sled test research, it was documented that there was a large inter-subject differences, not only in the amplitudes, but also in the characteristics of the entire movement, indicating large test variability amongst the volunteers (Prüggler 2011a).

If each marker's motion had to be correlated to tests, then the task would be impractical, beyond computational reach (CPU and data storage), as too many variables would be involved.

The number of study points had therefore to be reduced to a manageable size, whilst keeping the relevant reflex event features for computer correlation. To further facilitate the reduction of the number points, it was assumed that the occupant's head and torso do not deform during a 1g deceleration, i.e. the head's skull stays intact, same for the upper thoracic cage which does not crush during the event, although it is

understood that there may be some spinal movement. Therefore, any change of angle from any member will be reflected by all the points belonging to this member, meaning each, head and torso, form a rigid body. One of the other clear advantages of this method is that angle calculations do not depend on the position of the travelling sled; hence no correction factors are needed in the (X) direction of motion.

The points on the head and torso are listed in Table 5.1 with the point locations displayed in Figure 5.4.

Table 5.1: Relevant Markers on Subjects On Head And Torso (Bastien 2012a)

Figure 5.4: Location of key Vicon points on the occupant head and torso (Bastien, 2012)

The information from the relevant marker from OM4IS test has been processed and their coordinates have been plotted against time (Figure 5.5 to Figure 5.12).

Figure 5.5: X Coordinates of RBHD (Right Back of Head) as function of time (Bastien 2012a)

Figure 5.6: Z Coordinates of RBHD (Right Back of Head) as function of time (Bastien 2012a)

Figure 5.7: X Coordinates of RFHD (Right Front of Head) as function of time (Bastien 2012a)

Figure 5.8: Z Coordinates of RFHD (Right Front of Head) as function of time (Bastien 2012a)

This item has been removed due to 3rd Party Copyright. The unabridged version of the thesis can be viewed in the Lanchester Library Coventry University.

Figure 5.9: X Coordinates of RPEC (Right Pectoral) as function of time (Bastien 2012a)

This item has been removed due to 3rd Party Copyright. The unabridged version of the thesis can be viewed in the Lanchester Library Coventry University.

Figure 5.10: Z Coordinates of RPEC (Right Pectoral) as function of time (Bastien 2012a)

This item has been removed due to 3rd Party Copyright. The unabridged version of the thesis can be viewed in the Lanchester Library Coventry University.

Figure 5.11: X Coordinates of RBAK (Right Back) as function of time (Bastien 2012a)

Figure 5.12: Z Coordinates of RBAK (Right Back) as function of time (Bastien 2012a)

It can be noticed and already documented; there is noticeable kinematics variability within the same percentile (Prüggler, 2011a). As such it may already be suggested that the conditions for each volunteer may not have been equal, for example pulse, belt forces and friction parameters may have been different. Maybe the physiological state of each volunteer was different, i.e. maybe they were stresses or maybe relaxed.

Figure 5.13: Target markers for OM4IS tests (Prüggler 2011a)

Some markers have been selected such that their location on the volunteers (Figure 5.13 and Figure 5.15) was comparable and listed in Table 5.2.

Table 5.2: Marker position comparison between OM4IS and Ejima (2009)

A typical start and maximum posture position represent the type of kinematics recorded in the OM4IS tests (Figure 5.14).

Figure 5.14: A typical OM4IS frontal sled test

These OM4IS test results can be compared to the results obtained in previous research (Ejima, 2009), as illustrated in Figure 5.15.

Figure 5.15: Physical motions from the 3D motion capturing system (Male, 0.8G: Relaxed) (Ejima 2009)

It can be observed that in both tests (OM4IS and Ejima) the seat is rigid and does not provide any cushioning. This is important as a rigid seat provides a constant test setup as well as controlling the friction between the occupant and the seat. Any cushioning would mould to the occupant's thighs and would consequently add a friction force which would be impossible to determine accurately, hence adding an unknown to the validation process.

From the kinematics plots extracted from these 2 independent series of tests (Figure 5.16, Figure 5.17 and Figure 5.18) it can be noted that the response trend tends to be comparable, except that in the OM4IS test, the volunteer's motion is less pronounced. It has to be noted that the Ejima's sled test pulse was not provided in the literature, hence some differences may be present between the 2 series of test, assuming the Ejima's pulse to be representative of an typical emergency braking scenario and comparable to the OM4IS' one.

This is suggesting that the data from OM4IS are credible, as they genuinely compare to the Ejima's work. The Ejima's results values were evaluated graphically (Figure 5.15) and offset in Z and X to align with the OM4IS test data as the reference of each test was different.

In the Ejima tests, the occupant is more in a crouched position at 600ms (Figure 5.15) whereas in the OM4IS the volunteer is still very much straight (Figure 5.14), in spite the fact that in both tests only a lap-belt is used.

This is clearly showing that the 2 test conditions are very different, relaxed against keeping a determined posture, and predict different outcomes, as if the start motion is comparable, the Ejima tests present an exaggerated motion (Figure 5.16, Figure 5.17 and Figure 5.18).

Figure 5.16: Comparison between Ejima (2009) and OM4IS head motions

Figure 5.17: Comparison between Ejima (2009) and OM4IS base of neck motions

Figure 5.18: Comparison between Ejima (2009) and OM4IS shoulders motion

Using the comparison graphs (Figure 16, Figure 17 and Figure 18), it can be noted that each volunteer's kinematics tends to stay within a defined envelope, i.e. there is

little scatter of kinematics for the same volunteer tested, which reinforces that human being do not behave the same, occupants' kinematics being colour coded.

Comparing some occupant passenger behaviour in pre-braking scenario (PRISM 2003a) have shown that their posture and reaction (Figure 5.19) was more aligned with the OM4IS setup than the research performed by JARI (Ejima 2009). As a conclusion, it is suggested that the OM4IS tests are a better metric to validate a vehicle occupant active human model.

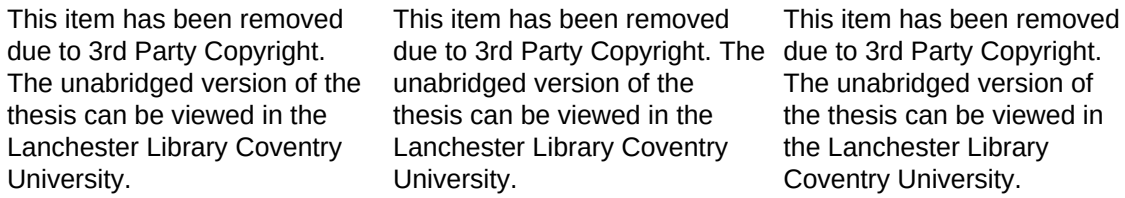

Figure 5.19: Pictures of passengers holding objects and subjected to pre-braking (Left: cup; middle: CRABI ATD, Right: HIII 3 year old) (PRISM 2003a)

Creating muscle tensioning target curves is a challenge as there can be a scatter between the coordinates of each marker on the volunteers' body and the 50th percentile AHBM. As such, matching the coordinates of each marker and perform comparisons will be problematic, as these markers locations need to match exactly between volunteers, as well as the node position on the Finite Element Model.

The approach undertaken is to consider a relative change of the head and the torso angles as a more universal measure of generating target curves. Indeed, the markers' coordinates are volunteer specific, but the relative head and torso angle target curves are not. As such, nodes on computer model can used as markers as close as the markers positioned on the volunteers. This approach is suitable, because the occupant is attached to the sled about the pelvis, which suggests that the torso will rotate about the hip and that the position of the feet and legs will remain unchanged during the low 'g' test event. Had the volunteer been unbelted (fully unrestrained), this approach would not have been adequate.

Derivation of Target Curves

As discussed, the methodology used is to extract relative marker angles.

The general method of capturing the torso and the head angle change is to calculate the angle based on the torso and head plane normals once the human has rotated, as displayed in Figure 5.20.

This can be performed by simply finding the centre (O) (Equation 5.1) between 4 marker points, 2 of them being the mirror, based on Figure 20.

$$E\begin{pmatrix}\frac{x_a+x_b}{2}\\ \frac{y_a+y_b}{2}\\ \frac{z_a+z_b}{2}\end{pmatrix};F\begin{pmatrix}\frac{x_c+x_d}{2}\\ \frac{y_c+y_d}{2}\\ \frac{z_c+z_d}{2}\end{pmatrix};O\begin{pmatrix}\frac{x_e+x_f}{2}\\ \frac{y_e+y_f}{2}\\ \frac{z_e+z_f}{2}\end{pmatrix}$$

Equation 5.1: Extraction of 3D angle from the occupant's head (Bastien 2012a)

This item has been removed due to 3rd Party Copyright. The unabridged version of the thesis can be viewed in the Lanchester Library Coventry University.

Figure 5.20: Extraction of 3D angle from the occupant's head (Bastien 2012a)

Once the centre is calculated, 2 vectors are computed in the plane where the 4 markers lie (Equation 5.2).

$$O\vec{A}=\begin{pmatrix}x_a-x_o\\ y_a-y_o\\ z_a-z_o\end{pmatrix};O\vec{B}=\begin{pmatrix}x_b-x_o\\ y_b-y_o\\ z_b-z_o\end{pmatrix}$$

Equation 5.2: Definition of 2 non-collinear vector passing through the plane centre (O) (Bastien 2012a)

The normal of this plane is computed using a cross-product, which is described and expanded in Equation 5.3.

$$\vec{n}=O\vec{A}\wedge O\vec{B} \qquad \vec{n}=\begin{pmatrix}(y_a-y_o)(z_b-z_o)-(y_b-y_o)(z_a-z_o)\\ (z_a-z_o)(x_b-x_o)-(z_b-z_o)(x_a-x_o)\\ (x_a-x_o)(y_b-y_o)-(x_b-x_o)(y_a-y_o)\end{pmatrix}$$

Equation 5.3: Calculation of normal to the plane passing through (O) (Bastien 2012a)

The angle θ is the angle between vector k (vertical) and the normal of the plane (AOB) based on the Vicon points and is calculated in Equation 5.4.

$$\theta = arc\cos\left(\frac{\vec{n}.\vec{k}}{\|\vec{n}\|.\|\vec{k}\|}\right)$$

Equation 5.4: Calculation of the head angle θ from the vertical (Bastien 2012a)

This method, as mathematically rigorous, brings however some fundamental difficulties:

- Once a 3D angle is calculated, it is very difficult to visually verify its value, which would make the overall interpretation very complex and maybe suggestive,
- For small angles close to the horizontal, the *arcos(x)* function will return the same value, even if the angles are of different signs, which may be a problem to create the target curves,
- Outputting such function is complex using a FEA post-processor.

In order to overcome these fundamental difficulties, some simplifications had to be performed and these came by looking at the test setup and volunteer motions.
It was noticed that the sled motion was aligned with the volunteers' sagittal plane, where biomechanics extension and flexion motions occur. Using the sagittal plane's geometrical properties, it is suggested that either side of this plane would provide a similar kinematics response, hence that the projection of the markers from 1 side of the volunteer (left OR right) onto the sagittal plane would be representative of the motion of both sides of the volunteer.
Assuming the travelling motion being in X and the Z axis being vertical, then all the motions will be taking place in the XZ plane. Therefore the general method of capturing angle can be simplified to reflect the statements above.

The relative angular change from the projected point on the sagittal plane can be therefore defined more robust and simpler way.

Considering the side view, 4 points are considered to generate the head and torso relative angle target curves: RBHD, RFHD, BAK and RPEC (Figure 5.21).

Figure 5.21: Markers for frontal load case relative angle calculation (Bastien 2012a)

RBHD, RFHD, BAK and RPEC's y coordinate is assumed to be 0 (projection) and the relative angle change is computed from Equation 5.5.

$$\theta_{frt}^{\circ}(t) = \tan^{-1}\left(\frac{\Delta z(t)}{\Delta x(t)}\right) \times \frac{180}{\pi} - \theta_{frt}^{\circ}(0)$$

Equation 5.5: Derivation of frontal angle calculation as a function of time (Bastien 2012a)

Equation 5.5 calculates the relative frontal angle calculation as a function of time (t) and is used in his thesis in the derivation of both head and torsion relative angles.

The same validation process as for the lateral case has been performed to ensure the quality of the projection of the Vicon points on the XZ plane.

Using MADYMO and post-processing the markers' output in HyperView, it has been possible to verify the accuracy of the projection of the Vicon points in the XZ plane (Figure 5.22), proven here on an arbitrary lateral motion setup.

Figure 5.22: Correlation of computation simulation and Equation 5.5, using the XZ projection of RFHD, RBHD, RPEC and RBAK (Bastien 2012a)

Using this methodology on the markers located in Figure 4 using the frontal test information from the OM4IS tests, a set of responses curves were calculated as well as the target curve was computed using the median value of the tests (Figure 5.23 and Figure 5.24) (Bastien 2012a).

Figure 5.23: Head frontal motion relative angle for all 13 tests (Bastien 2012a)

Figure 5.24: Torso frontal motion relative angle for all 13 tests (Bastien 2012a)

From Figure 5.23 and Figure 5.24, it can be observed that there is a very large spread of responses amongst the 4 volunteers (Proband1 to Proband4), where "Head Fxx" and "Torso Fxx" relate respectively to a test number 'xx' with head and torso motions outputs.

Some early work has shown that calculating a trend for the motions of the head and the torso via a median curve across all the data was possible but led to a poor level of agreement between the MADYMO model and the median target curves (Bastien 2012a), suggesting more investigation in the test data analysis. Instead of generating a

global response, a new approach based on clustering volunteer responses (Crandall 2012b; Lesley 2004) was sought.

Investigating the results plotted on Figure 5.23 and Figure 5.24, it can be noted that:

- 3 or 4 tests have been conducted on each volunteer. The responses in head and torso relative angle change suggest that the volunteers "Proband 1, 3 and 4" were not pre-disposed as the responses are scattered and not following a decreasing angle response due to an anticipated/ learned behaviour of repeated tests. Only "Proband 2" is showing a learned behaviour, as each conducted test shows a decreasing head and torso angle change.
- A large displacement of the head in "Proband3 Head F02" and has a large head rotation for a torso rotation close to the median target, which looks very different that all the other 12 tests conducted. Maybe the test was conducted before the volunteer was fully ready, or this is showing a great level of variability in bracing
- "Proband 1" and "Proband 4" tests have similar levels of head rotation, but the torso relative angle variations of "Proband 4" are higher (around 15 degrees) than in "Proband 1" (4 degrees). This confirms that volunteers' responses are not consistent and not predictable and that the resistance to motion (reflex or bracing) level between volunteers of the same percentile, here 50^{th} percentile, can vary both head and torso or just in head angular rotation.
- The volunteer "Proband 2" is showing consistently the weakest resistance to the frontal sled motion in head and torso relative angle changes.
- The volunteers of "Proband 1" and "Proband 3" (rejecting sample "Proband3 Head F02" and its associated torso response "Proband3 Torso F02") are presenting the strongest motion resistance to the frontal sled motion in head and torso relative angle changes.

As a consequence it is proposed to build 3 head and torso motion target curves:

1. The median of all the curves, will give the typical overall human motion level (Bastien 2012a),

2. As "Proband 2" displayed consistent weak motion resistance behaviour, this volunteer response can be chosen to describe this reflex response. The median of all the "Proband 2" tests will provide a typical weak resistance to motion trend (based on 1 volunteer providing 3 tests). This median will be assumed to represent more a reflex behaviour as the resistance is the weakest and will be used later on to validate the active human model,

3. The median of all the "Proband 1" and "Proband 3" (rejecting sample "Proband3 Head F02" and its associated torso response "Proband3 Torso F02" due to excessive head rotation), will give an a typical strong resistance which is more a bracing behaviour (based on 6 tests from 2 volunteers).

As volunteer responses may have been influenced by the conditioning of earlier experiences, i.e. repeat test, this suggests that the test results distribution is skewed. It was therefore necessary to use the tests median value to define the target curves. This target method was preferred to the standard deviation technique as the later leads to undesired corridors which could relate to non-physical regions.

From the findings of the OM4IS consortium, the test tolerance corridor window was set between 37.8% and 62.5% as it provided with the best physical reasonable window.

The clustered responses are shown in Figure 5.25 and Figure 5.26 (Bastien 2013b).

Figure 5.25: Head Relative Angles motion targets (Bastien 2013b)

Figure 5.26: Torso Relative Angles motion targets (Bastien 2013b)

These clustered responses shown in Figure 5.25 and Figure 5.26 will now be used to assess the kinematics behaviour of the latest AHBM model.

5.2 Setting up the Active Human Model in a vehicle or sled

MADYMO Active Human Model Architecture

The MADYMO AHBM is a very complex model which aims to capture an occupant reflex behaviour, which is responding to a motion, unaware (Figure 5.27).

Figure 5.27: MADYMO Active Human Architecture (TNO 2011)

The architecture contains the following features:

- It understands the original reference occupant posture before a motion is applied
- It includes a reaction time delay, which represents the time it takes for the occupant to sense that he/ she has moved from the initial position. The MADYMO user manual refers from 10ms to 120ms (TNO, 2012) and Ejima (Ejima 2009), from his test of 100ms for his lap belted occupants
- It includes the brain processing time and transfer of information to the muscle for activation. These values are hard coded in MADYMO and are:
    - Neck controller delay: 40ms,
    - Spine controller delay: 70ms,
    - Arms controller delay: 70ms,
    - Legs controller delay: 100ms.

- Include an active behaviour switch which allows then the muscle to perform an action. The activation can be turned OFF, i.e. '0', (cadaver state) or ON, i.e. '1' (reflex state). These switches influence the controller speed.

It has to be noted that this model should only accept the values of '0' or '1'. Nevertheless, to represent a weaker response of the muscles in some body regions, it is possible to input intermediate values. Intermediate values would suggest a weaker muscle response or slower than needed, i.e. the controller and/or the muscle would need to be further developed to address this.

Positioning of the Active MADYMO Human Model

This item has been removed due to 3rd Party Copyright. The unabridged version of the thesis can be viewed in the Lanchester Library Coventry University.

This item has been removed due to 3rd Party Copyright. The unabridged version of the thesis can be viewed in the Lanchester Library Coventry University.

Figure 5.28: Definition of joint rotations of the facet human model, in its reference position (TNO 2011)

In order to position the human model, the INITIAL.JOINT_POS elements have to be used (Figure 5.28).

All joints that are needed for positioning the human model are defined in the INITIAL.JOINT_POS elements in the human model user-file. Positions of all other joints are defined in the human model include-file, and these should not be edited by the user.

A human model is by default positioned relative to the (global) reference space coordinate system. However, the human model can be positioned relative to a body of another system. This can be done in the CRDSYS_OBJECT '*Human_Attachment'* and the associated ORIENTATION *'Human_Attachment_ori'*.

The human attachment element *'Human_Attachment'* is comparable to the dummy attachment element *'Dummy_attachment'* in a dummy model, which is located at the H-point.

In order to position the active human model, the Joint Positioning Tool in XMagic (Figure 5.29), has been used to move each joint to the required position and within their bio-mechanical reach (TASS 2010). Once the file is saved, only the joint properties (Degrees of Freedom) are updated with no alteration to the human system model file. In Figure 5.29, some joint modifications are performed in the left window, with the changes reflected 'live' in the right window.

Figure 5.29: Joint Positioning in XMagic (RHS) – Joint values (LHS) (Bastien 2012a)

Because of the flexibility of the spine and neck of the facet human model, it is a bit more complex to position this model in a seat than a dummy model. Consequently, in order to position the AHM model in a perfect equilibrium state, a pre-simulation is needed.

Positioning of the facet human model is done in three steps:

1. The complete human model is positioned and orientated correctly with respect to its environment by initialising the position and orientation of the human joint (Human_jnt) or the Human attachment. Vertebrae can be orientated in order to put the spine in a seating position. The human model can best be positioned just above the seat with its pelvis at the correct horizontal position. In a relaxed seating position the human spine is curved differently than in a standing position or a straight seating position. To model a relaxed seating position the vertebral joints of the facet human model can be rotated in the user-file. The extremities are orientated with respect to the parent component by changing the orientation of the joints in the positioning elements (INITIAL.JOINT_POS). The human model can

for example be placed in a driving position. This can be achieved, if needed, by using the Joint Positioning tool in XMAgic.

2. A pre-simulation is performed in which the facet human model is put into the seat by a gravitational field only (acceleration field of -9.81 m/s^2 in the Z direction). The run time for positioning the facet human model needs to be large enough for the model to find its equilibrium (typically about 0.5s) in which all active behaviour should be switched on (all active switches in the DEFINE variables set to '1'). The joint position degrees of freedom (JOINT_DOF) of all joints in the user-file must be defined in the output (OUTPUT.JOINT_DOF) so they can be re-mapped after the pre-simulation. The main MADYMO commands are listed in Appendix B.

   It has been noticed that it is important to add contact friction between the AHBM and the seat, as the lack of friction prevents, in some cases, the AHBM to find equilibrium. Depending on the application, also the joints in the arm (from Glenohumeral until wrist joints) could be also locked to keep the arms in the desired position. It could also be required to add some point restraints for certain directions to keep the human model at the desired position in the seat or holding the steering wheel.

   In the pre-simulation stage, it has been found advantageous to start routing the seatbelt on the AHBM. For the lap belt, it was discovered that setting the following joints to 0 was necessary (Table 5.3) and as illustrated in Figure 5.30.

Joints	R1
Glenohumeral-L Jnt	0
Glenohumeral-R Jnt	0
ElbowL_jnt	0
ElbowR_jnt	0

Table 5.3: Joint setup prior to lap belt fitting in XMagic

Using the XMagic Belt Fitting Wizard (F10) was found to be particularly useful.

Figure 5.30: AHBM joint positions to facilitate lap belt fitting (Bastien 2012a)

When the pre-simulation is complete, the belt slack can be removed still by using the 'Straighten lap belt' switch from the Belt Fitting Wizard (Figure 5.31) and tightened.

Figure 5.31: Removing belt slack by straightening the belt (Bastien 2012a)

It should be checked that the belt is not too tightly pulled at the beginning of the simulation and should not exceed a value of 100N (TNO 2012).

At this stage, the pre-simulation can be executed. It is important to verify however that the AHBM is in equilibrium. To check that it is so, it is necessary to include output switches from the MADYMO solver to request occupant to headrest, seat and

floor contact forces. It is good practice to separate contacts so that the equilibrium can be explained.

The request for contact output is OUTPUT_CONTACT where all relevant contacts are listed.

This request is executed in conjunction with the CONTROL_OUTPUT where:

- TIME_STEP must be filled in, describing the frequency of the output requests,
- TIME_HISTORY_CONTACT which list the contact to output.

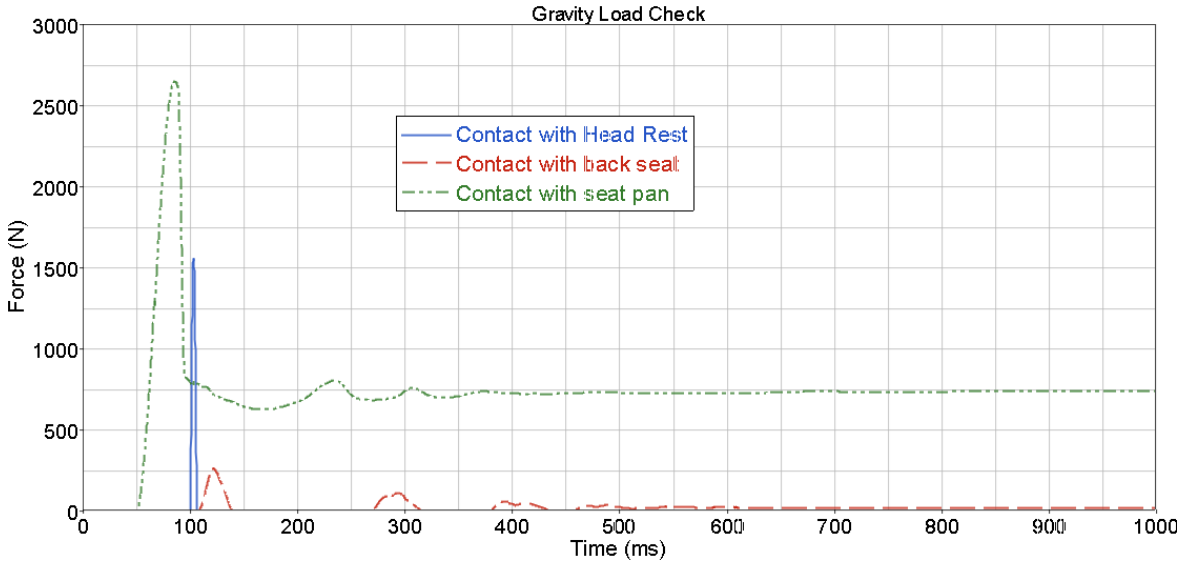

Figure 5.32: Typical AHBM gravity load contact force check

The following output from Figure 5.32 is describing the transfer of forces between the AHBM and the seating structure. It can be noted that after 500ms the AHBM is in equilibrium. Note that in this case, most of the load goes in the seat pan.

3. In order to re-map the kinematics outcome of the gravity load phase, the output from the last time step in the JNTPOS file of the pre-simulation should be copied to the positioning elements (INITIAL.JOINT_POS) of the impact simulation file.

   The request for Joint Position output is OUTPUT_JOINT_DOF where the SIGNAL TYPE must be set to 'POS'.

   This request is executed in conjunction with the CONTROL_OUTPUT where:

   - TIME_STEP must be filled in, describing the frequency of the JOINT position requests,

- JOINT_DOF_OUTPUT_LIST (select ALL), lists the joints positions to output.

Using the XMAgic "Initial Joint Positioning" Tool, the end time (or relevant time) of the simulation can be chosen and the joint positioned re-mapped by selecting the *.jps (joint position) file created from the gravity pre-simulation. In Figure 5.33 it can be noted that the gap between the driver's buttocks and legs against the seat pan has been closed.

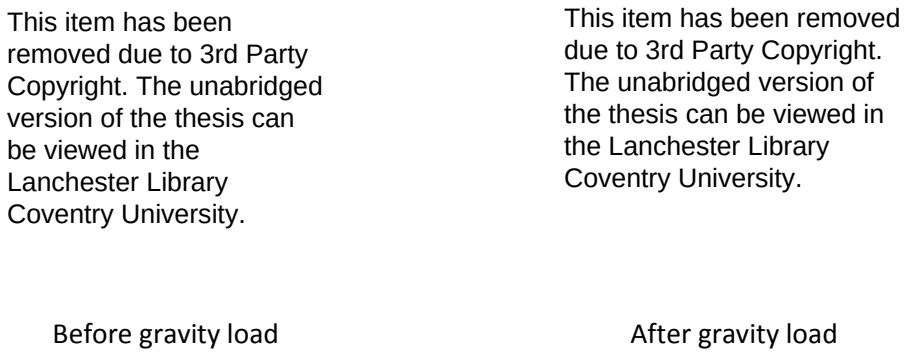

Figure 5.33: Typical re-mapping of AHBM joints after gravity loading (Bastien 2012a)

In the impact simulation, the joints and bodies that were locked/ rigid for the settling should be set to free/deformable again, and possible added point restraints should be removed.

Contacts

The main human model contact commands are already embedded within the computer model include-file. These are contacts of the head and arms with the rest of the body, contacts between the legs, feet and shoes, and some contacts internally in the neck.
The user has to define the external contact interactions between the human model and its environment. To facilitate this, the human model has predefined contact groups that can be used directly in the external contact interactions. All these groups include both the skin and the underlying bones. Besides the groups for external contacts, also some groups are present used for internal contacts only. The contact groups available for external contacts are listed in Table 5.4.
It is recommended to define contact only if it is really needed, in order to avoid an unnecessary increase in calculation time. As a start for a simulation, the most proper

way is to define contact only where it is expected. Thereafter, the contact assumptions should be checked, and necessary corrections and/or refinements can be made.

Table 5.4: List of Contact Groups included in the AHBM study (TNO 2012)

There are two different types of contact entities which can be used with an AHBM, planes composed of Multi-Bodies (MB) and Finite Element (FEA) facets.

AHBM and MB contacts (MB interior)

If the AHBM is positioned on a MB (Multi-Body) entity which is much stiffer, like for example a non-deformable hard seat with no foam (or contact to a dashboard for example in the scenario of a hard contact in the unbelted loadcase), then the contact is calculated from the deformation of the human flesh.

As good modelling practice (Du Bois, 2010), the 'rigid and non-deformable' surface should be set as master segments. A generic contact definition below explains a typical contact between an AHBM and a rigid surface.

The main MADYMO contact commands between the AHBM and Multi-Body components are listed in Appendix B.

Figure 5.34: Plane (MB) normals (Bastien 2012a)

It must also be ensured that the planes normals point towards the AHBM, as the opposite would generate an infinite force on the occupant (Figure 5.34).

AHBM and FEA contacts (FEA seat and airbags)

These contacts are more complex to treat as there can be some vast differences in contact stiffness and thicknesses. No obvious difficulties were encountered which using the AHBM.

One precaution, in order to improve the contact and making it more robust, in some minor cases is to specify the **FACE_TYPE='FRONT'** to make the element normals consistent and avoid some elements passing through others and not being released by the contact (Appendix B)

The switch **FACE_TYPE="FRONT"** is making sure that the element normals are facing the same direction. This is equivalent to the LS-Dyna command AUTOMATIC_SURFACE_TO_SURFACE (LSTC, 2012), in which the "AUTOMATIC" switch fulfils the exact same purpose.

Active Human Model Outputs

Some key bio-mechanical marker positions on the AHBM can be output in a CSV (Comma Separated Variable) file, as coded in Appendix A. These flags could be used for further analysis if required.

Some strategic markers point outputs are listed in Table 5.5 and the full process summarised in Figure 5.35.

Point on AHBM	Point Description	Output name	Node allocated
CHIN	Chin	chin_node_out	16011
RSHO	Right Shoulder	RSHO_node_out	31014
LSHO	Left Shoulder	LSHO_node_out	21003
RCLA	Right Clavicle	RCLA_node_out	13341
LCLA	Left Clavicle	LCLA_node_out	13333
RPEC	Right Pectoral	RPEC_node_out	13249
LPEC	Left pectoral	LPEC_node_out	13248
THEA	Top of Head	THEA_node_out	16090
RBHD	Right Back of Head	RBHD_node_out	16147
LBHD	Left Back of Head	LBHD_node_out	16070
RFHD	Right Front of Head	RFHD_node_out	16144
LFHD	Left Front of Head	LFHD_node_out	16067
RBAK	Right Back (Shoulder plate)	RBAK_node_out	13103
LBAK	Left Back (Shoulder plate)	LBAK_node_out	13101

Table 5.5: List of Contact Groups included in the AHBM

Figure 5.35: Global Flow chart of the AHBM pre-simulation for occupant positioning (Bastien, 2012)

5.3 Correlation of Active Human Model to Tests

Model setup

The model used is an Active Human Body Model (AHBM) provided by TNO (TNO 2012), which is based on cadaver testing and includes a stabilised spine, allowing the AHBM to stand straight and balance its own weight (Cappon 2006; TASS 2013). The model provided a simple method to scale the muscle activity from passive behaviour (cadaver, switch set to '0') to active behaviour (switch set to '1') for which the model has been validated for these two states. As such, with muscle activity turned on, the model will try to maintain its initial position under the influences of external disturbances. Conveniently, any muscle activity set between '0' and '1' can be used to simulate a state between sleeping and awake or reduced muscle strength. These muscle activity features are based on biomechanical data which are included in the muscle parameters and in the neural delay coded in the model (TNO 2012).

The controller parameters available for adjustments were the neck, the spine, the arms and the hips. After strategic computations, it was discovered that the controller scalars were in the region ranging from '0' (cadaver state) to '2' (meaning that a person acts twice as fast but has the same level of muscle force). The scalar value of '2' was investigated as it was not possible to modify the encrypted controller values, hence modifying the controller scalar above the allowable range was considered as a potential tuning parameter, which could have provided some information about the model's behaviour. Scalars exceeding '2' provided an unstable torso response after 1s.

A new feature, like neck co-contraction was also available (ranging from '0' to'1'), as well as a delayed response switch, which could include the occupant state of awareness before the sled motion takes place.
In this study:

- the delay was set to its lowest value from literature of 10ms for the correlation as it is believed that the volunteers were not anticipating the sled start time,
- co-contraction was not activated for the weak and median correlation as only some small evidence on head resistance to rotation can be seen for the very strong head bracing in the first 200ms (Figure 5.25).

The OM4IS sled test has been modelled using MADYMO utilizing planes for the seat and the floor and ellipsoids for the upper structure (Figure 5.36).

Figure 5.36: OM4IS sled modelled in MADYMO (Bastien 2012a)

The 0.5kg mass of the object the volunteer had to hold still during the experiment (repeatability purpose, arm equilibrium) was restrained to the occupant's hands.

The lap belt was modelled by common belt characteristics and had a width of 50mm and a 1mm thickness (Figure 5.37). A coefficient of friction of 0.3 was applied between the lap belt and the occupant's thorax and thighs.

Figure 5.37: Lap belt positioning (Bastien 2012a)

Friction values between the occupant and the seat and occupant to the floor have been respectively estimated to be 0.5 and 0.8 (Cummings 2009).

Correlation method

In order to investigate the effect of each controller scalar parameter on the AHBM kinematics and its robustness and stability, computer runs needed to be performed involving a frontal and a lateral investigation, using 4 variables from Table 5.6. To obtain a better definition of the problem, it has been decided to use 3 levels per

variable, i.e. each variable can take the value '0', '1' or '2', so that any level of non-linearity would be captured. The value of '2' only makes the controllers work twice as fast at a controller value set to '1'. This approach has been used since the AHBM control parameters were tuned on other volunteer tests. As these controller values are encrypted in the model provided, it was proposed to use this scalar to perform changes in the activation parameter.

The value of 3 levels has been selected as the number of runs would be greatly amplified should the levels be increased any further (Bastien 2012b).

Table 5.6: Variable Names and Activity Levels (Bastien 2012a)

In order to compute the controllers' activity levels factors, response surfaces were generated by 3 series of runs including frontal and lateral scenarios:

- The first Design of Experiment (DOE) was a full factorial analysis which also coupled the controller scalar values between the frontal and lateral runs. This inherently created 3^4 = 81 computer permutations which then defined the boundary values of the design space.
- 30 Hammersley runs were executed to capture the centre of the response surface.

For each DOE run, the computer model response 'errors' (or discrepancies) to the target curves (Figure 5.25 and Figure 5.26) have been computed using the square of their difference. This difference was plotted as a response surface, with the aim to minimise this difference during the whole time duration of the event.

Following these runs, it was discovered that the definition of the response surfaces was not adequate to converge to a solution, i.e. the surfaces were not smooth enough, especially for the Kriging surface interpolation which was based on the exact definition of the response points, to allow a robust optimisation (Figure 5.38).

Using this data, another response surface using a second order 'Moving Least Squares' (MLS) function (not passing directly through the response points) was built (Figure 5.39). However this second order function was also deemed unsuitable for robust optimisation as the residuals were too large. For these reasons an additional 60 Hammersley runs were executed in order to improve the response surface definitions, i.e. defining more gradual curvature permitting enhanced optimisation stability.
These extra 60 Hammersley points allowed the MLS approximation to become a cubic.

In this study, a total 171 controller variable permutations were evaluated (81 + 30 + 60). The examples below illustrate the effect of occupant head relative angle change for the frontal sled tests (at time 0.61s), against Elbow_activation_parameter and Hip_activation_parameter (Figure 5.38), representing the time when maximum frontal relative head rotation would take place.

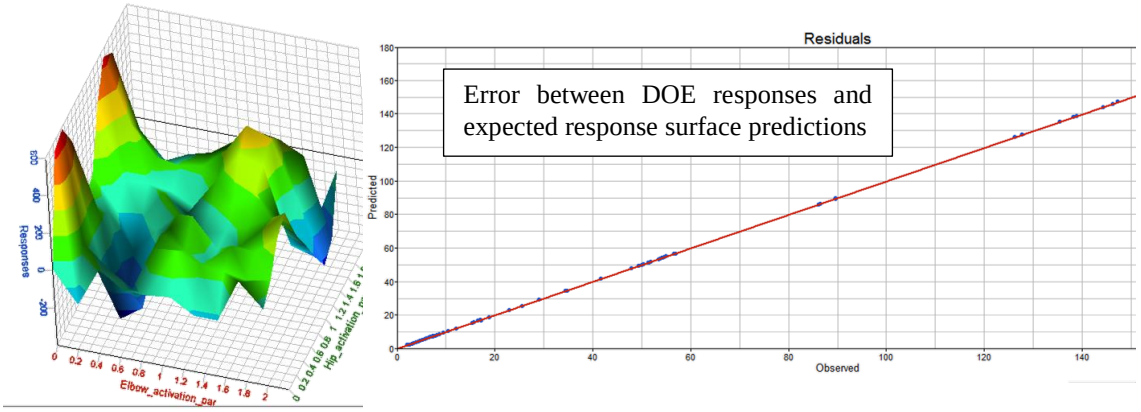

Figure 5.38: Kriging interpolation for Frontal Head relative angle for time 0.61s (3D response and residuals)

In Figure 5.38, using a Kriging approximation, the response surface went through all the response points (see graph on the right), as the observed values (computed by MADYMO) were exactly the same as the predicted ones (extracted from the responses surface). Nevertheless, the approximation appeared very jagged, which was a problem with respect to optimisation convergence.

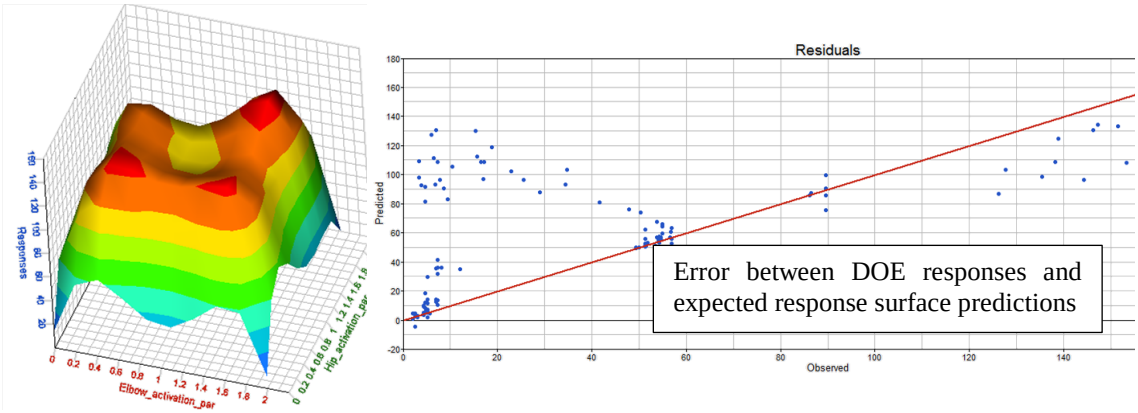

Figure 5.39: Moving Least Square interpolation for Frontal Head relative angle for time 0.49s (3D response and residuals)

In Figure 5.39, using MLS approximation, the response surface did not pass through all the response points (see graph on the right), as the observed values (computed by MADYMO) were very different from the predicted ones (extracted from the responses surface). It did nevertheless look smooth, which was a better condition to find optimisation convergence. However the response surface is far from what is happening in reality, hence it could not realistically be used.

Following the numerous DOE computations, it has not been possible to converge numerically and obtain the most suited scalar combination to match the relative angle target curves extracted from the OM4IS tests.

The interpolation either goes through the DOE points and creates a Kriging interpolation surface unsuitable for stable optimisation, as it was not smooth enough, or used a smooth MLS one for which the approximation predictions were very far from the target response values generated from the DOE. Neither approximation can converge towards the ideal solution. This could mean that having only 1 parameter to alter the stiffness of a range muscle (e.g. the spine) did not give any time control on the 'details' of the muscle activity event. The scalar was directly activated at time 0 and could not be tuned with respect to time and intensity (Bastien 2012a).

As a consequence, it was decided to undertake a more methodical approach to compute the controllers' calibration. The first instance was to obtain the best torso rotation fit to the target curves, then to adjust the neck parameters to obtain subsequently the required head angular motion. This method was carried out all along the computer iterations in this study.

The torso response was met using the default active switch of '1', while the best fit for the head rotation was the estimated using a neck scalar to be 0.6 with a co-contraction value of 0, as this phenomenon is not visible for the first 200ms as shown in (Figure 5.25).

As a consequence the controller scalar would need to be reduced from '1' to '0.6', as listed in Table 5.7.

Motion level	Run number	Settings					Reaction time (ms)	Neural delay (on/off)
		Spine	neck	arms	Hip	Co-contractions		
Standard AHBM	TNO	1	1	1	1	0	10	on
Reflex	23	1	0.6	1	1	0	10	on
'strong configuration ' Bracing	25	2	2	2	2	0	10	on

Table 5.7: Proposed new controller scalar values needed to simulate human frontal low 'g' deceleration motion (weak and strong).

The human head and torso motion correlation plots are shown in Figure 5.40 and Figure 5.41 present a good envelope of motion behaviour, weak and stronger

It can be seen that the torso response is square shaped and gives a very good match to experimental data especially in a weak motion response. The respective head response is comparable to test until 0.7s, then the head relative angle reduces instead of being constant and keeping the head at the same relative orientation.

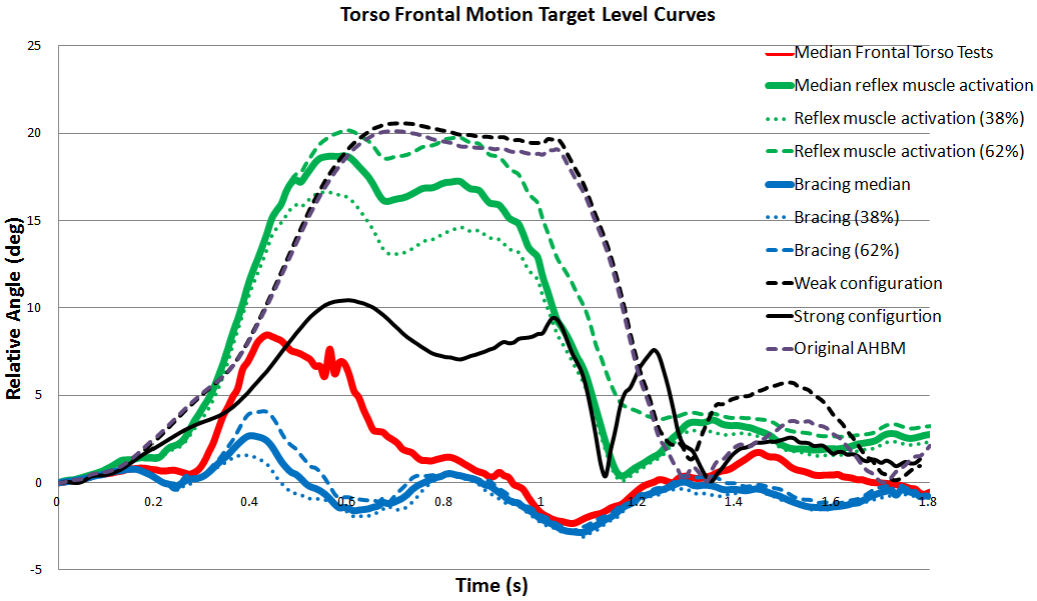

Figure 5.40: Torso frontal correlation of weak and medium/strong motion responses.

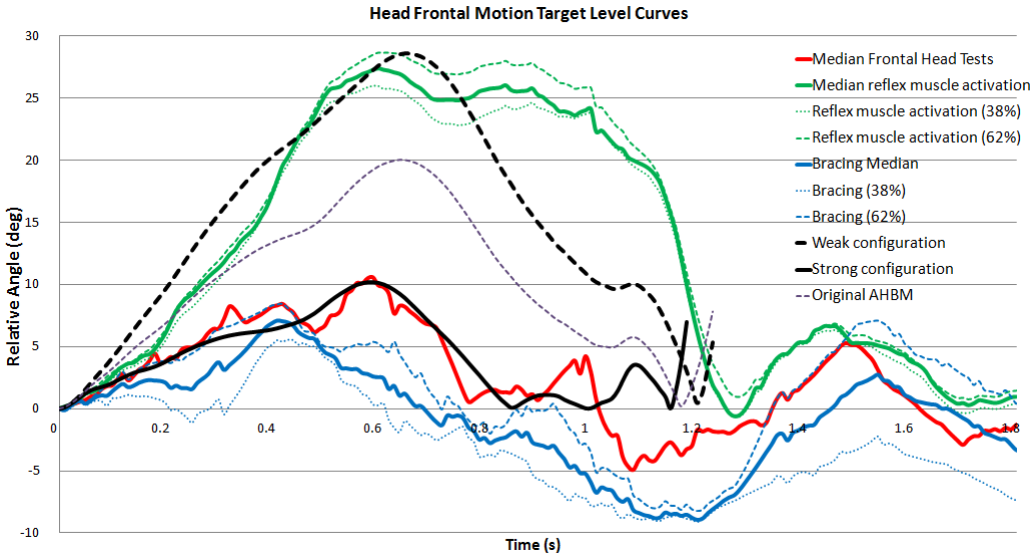

Figure 5.41: Head frontal correlation of weak and medium/strong motion responses

The head frontal motion is suggesting that the muscle in the MADYMO model are weaker from time 0.7s than in the tests in this 1'g' loading regime with a lap belt.

One possible hypothesis may be that the head model motion is not calibrated for large torso frontal motion caused by a 1'g' frontal with lap belt restraint.

Extra torso motion will tend to rotate the head forward which may cause the generation of extra bending moment in the neck due to head gravity forces compared to when the torso stays straighter, hence causing the neck muscles to weaken. A partial confirmation of this hypothesis can be found in previous work based on a 3 point-belts volunteer setup, which has shown comparable volunteer tests and

correlation curve shapes between the MADYMO 7.4.1 active human model, in spite of the fact that the maximum chest and neck displacements were less than 20% smaller than the average maximum respective responses from the volunteers (Meijer 2012).

It is however necessary to be aware that the metric between the 3 point belt correlation (Meijer 2012) (displacements) and this study (relative angle changes) is different, hence it can be concluded, assuming all volunteers being the same in both experiments, that their difference of motion has to come from the restraint system, the lap belt allowing more body rotation than a 3 point seatbelt, hence causing neck muscles to weaken in this low 'g' frontal scenario.

The stronger motion correlation using muscle controller values of '2' provides a good fit for head motions for the first 1.0s and reasonable torso motions for the first 0.6s of the test. It has however to be noted that muscle scalar values above '1' are not validated in this model. This muscle scalar only relates to the speed the human reacts and not to an increase of muscle strength, which is here being suggested, as the overall human motion is reduced.

It can therefore be suggested that this extra force seen in the tests could be caused by the volunteer expecting the sled motion or 'seeing' the start of the sled motion, hence bracing. Sadly, no test videos were available to assess whether the volunteers were bracing in each test.

Most head and torso motion curves are showing a strong resistance (3 curves for weak motion vs. 10 for stronger motion resistance), which could have been caused by the fact that volunteers were in line with the sled motion, hence may have had a cognitive input. It would have been beneficial to have blindfolded the volunteers to remove this potential cognitive input and take away (or reduce further) the bracing component. Maybe the start of the sled motion could have been sensed by the volunteers, like a sound or a vibration in the seat. More investigation may be needed to be determined whether the volunteers were pre-disposed.

MADYMO 7.4.1 human model with a muscle scalar of '2' is correlating for the wrong reasons, as some bracing is likely to be taking place and this model is not yet suited for it.

It has to be noted that the current model controls the hips relative to their original position, but does include active knees. Maybe some previous research findings on knee muscle tension (Behr 2009) could be considered for implementation.

Considering Figure 5.40, it can be noted that are strong similarities between the shape of the torso relative angle response and the median test curve. The magnitude difference is also relatively small, as the test target is 18deg. while the computer response is 20deg. which is marginal. It can be therefore concluded that, within the small sample of test volunteers, the modeling of the torso response, using an active switch of '1', under pre-braking scenario, is adequate.

Considering Figure 5.41, it can be noted that the head relative angle ramp-up which uses the modified controllers at 0.6 follows closely the test target curve and reaches a comparable maximum (26 deg.) at 0.7s. The original controller curve of '1' departs from the target curve from 0.3s and peaks at 0.7s with the value of 20deg. which 6deg. off the test value. From 0.7s, the shape of the neck response curve diverges from the shape of target curve and drops almost straight away while the test curve remains 'square' and start dropping at around 1.2s. These findings have been provided to TNO as a pointer for future low 'g' neck biomechanics considerations, especially in the shape of the neck response (Meijer 2013a; Meijer 2013b; Meijer 2013c).
It is now possible to confirm the correlation of this new Active Human Model (neck controller at '0.6') and the Original model (neck controller at '1') by overlaying the response from the computer models to the OM4IS test data previously extracted. All the computer results fall within the test, which is proving that the correlated AHBM's kinematic response is believable.

It can be observed is that in spite of the neck discrepancies to the tests, the Original MADYMO model still provides overall a believable response, as listed in Figure 5.42 to Figure 5.49.

The difference between the 2 computer models happens in RFHD, where the X and Z values differ mostly at time 0.68s (Table 5.8).

	X coordinate (mm)	Z coordinate (mm)
Original Model	204.9	921.7
Optimized Model	222.5	898.4
Difference (mm)	17.6	22.6
Discrepancy (%)	8	3

Table 5.8: Discrepancies between optimized and original model

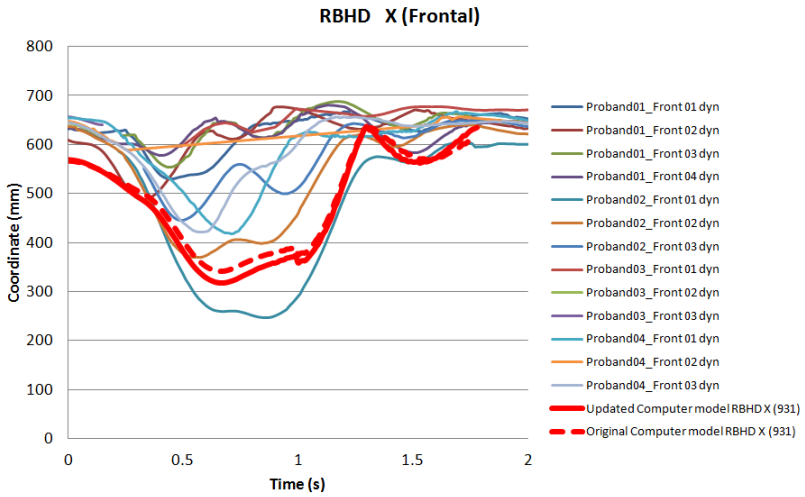

Figure 5.42: Correlation of occupant back of head (RBHD) 'X' component to OM4IS tests

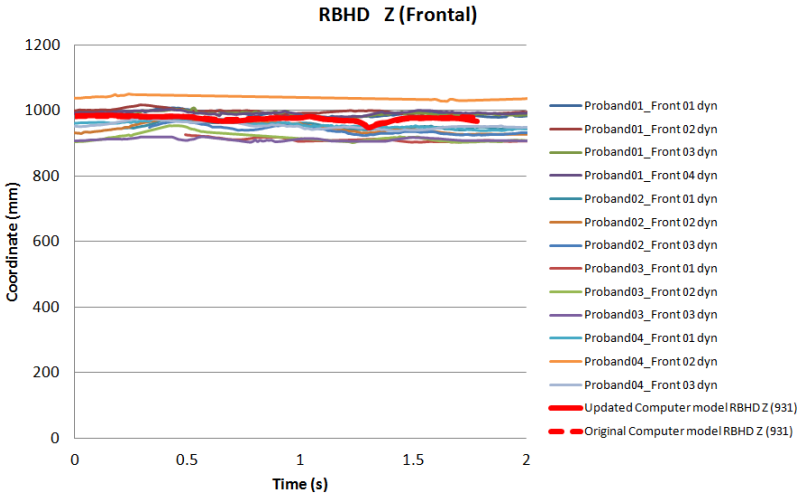

Figure 5.43: Correlation of occupant back of head (RBHD) 'Z' component to OM4IS tests

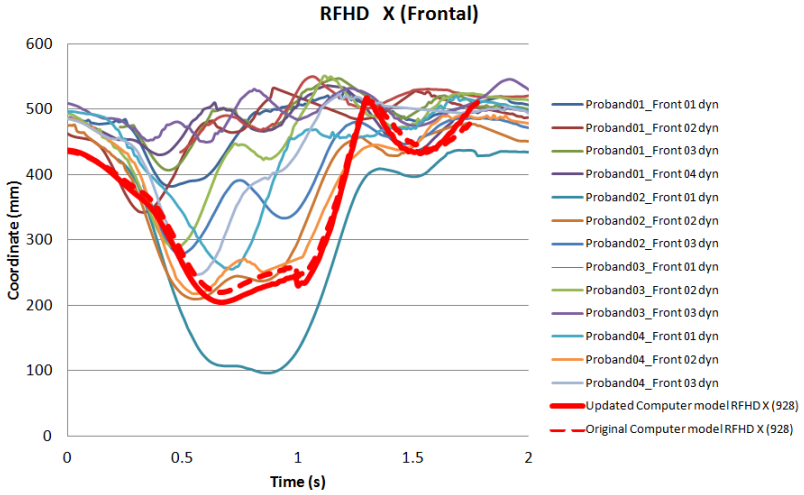

Figure 5.44: Correlation of occupant front of head (RFHD) 'X' component to OM4IS test

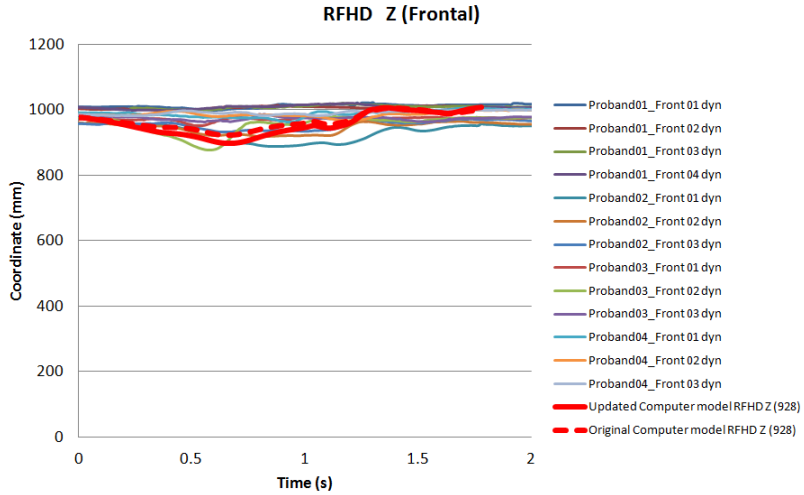

Figure 5.45: Correlation of occupant rear of head (RFHD) 'Z' component to OM4IS tests

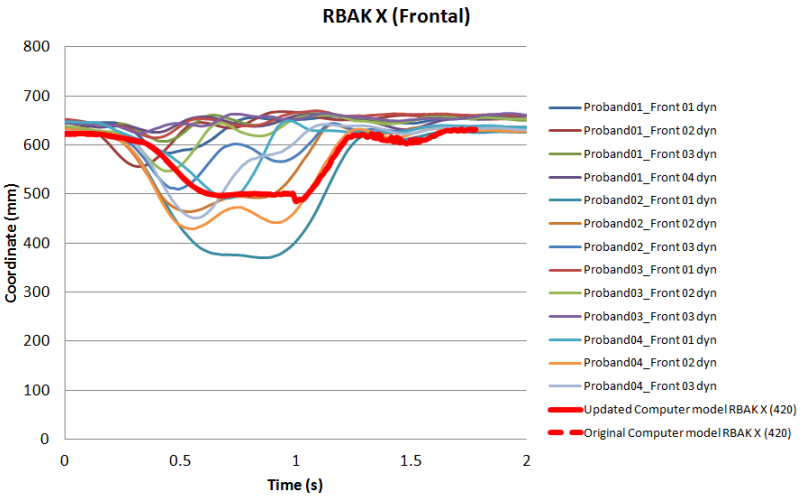

Figure 5.46: Correlation of occupant rear torso (RBAK) 'X' component to OM4IS tests

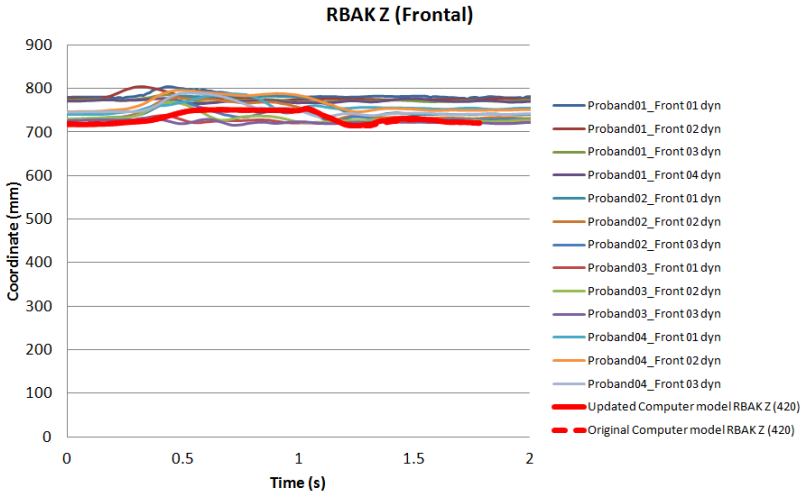

Figure 5.47: Correlation of occupant rear torso (RBAK) 'Z' component to OM4IS tests

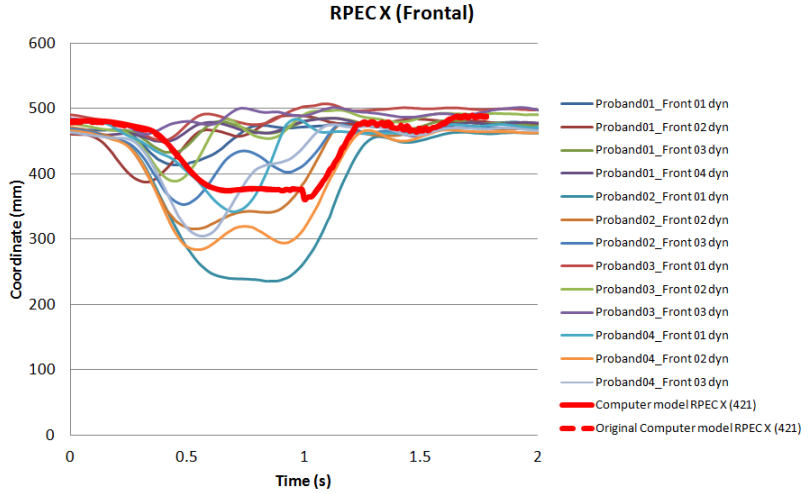

Figure 5.48: Correlation of occupant front torso (RPEC) 'X' component to OM4IS tests

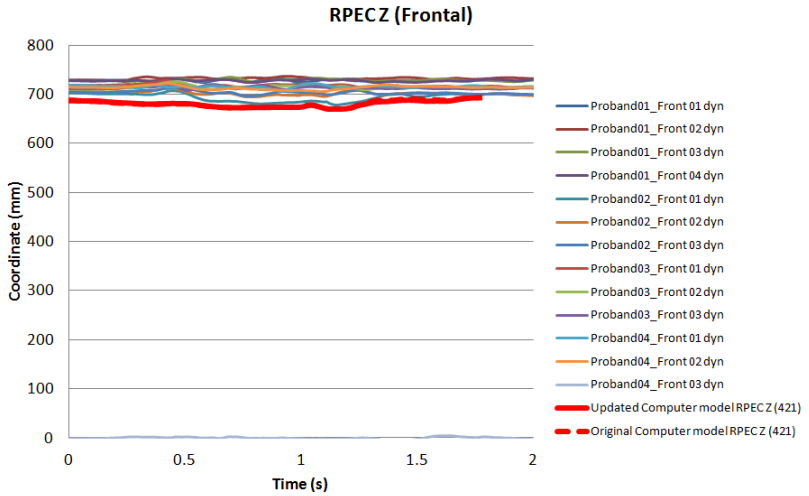

Figure 5.49: Correlation of occupant front torso (RPEC) 'Z' component to OM4IS tests

The main difference is in the direction where the 2 models' head position will differ by 8%, which is small for effective deceleration duration of 0.5s; nevertheless the shape of the neck response would need to be investigated for further improvements.

A new MADYMO Active Human Model is being modified and will include a more detailed neck model, including 233 muscles which are now been 'routed' inside the neck (Figure 5.50), compared fewer muscles routed outside (Figure 4) and routed outside the neck envelope. These muscles "have been extracted from PMHS data of Delft University of Technology (TUD) and have been validated successfully using volunteer posterior-anterior frequency perturbation tests of TUD" (Meijer 2013a).

Figure 5.50: New Active Human Model Neck development (Meijer 2013a)

This development model still needs low 'g' frontal validation against OM4IS tests, presented in this thesis, as well as the lap-belt, low 'g' and fully relaxed volunteer tests (Ejima 2009).

These kinematics prove that performing the optimisation based on head and torso target curves meet the OM4IS tests and that this method is successful to validate controller values to match relate to test data.

Since the model validation is complete, it is possible to compare the kinematics of the original MADYMO model, the optimized controller one and a passive model, still based on the original active model architecture, but with all the muscle activation values turned OFF (Figure 5.51).

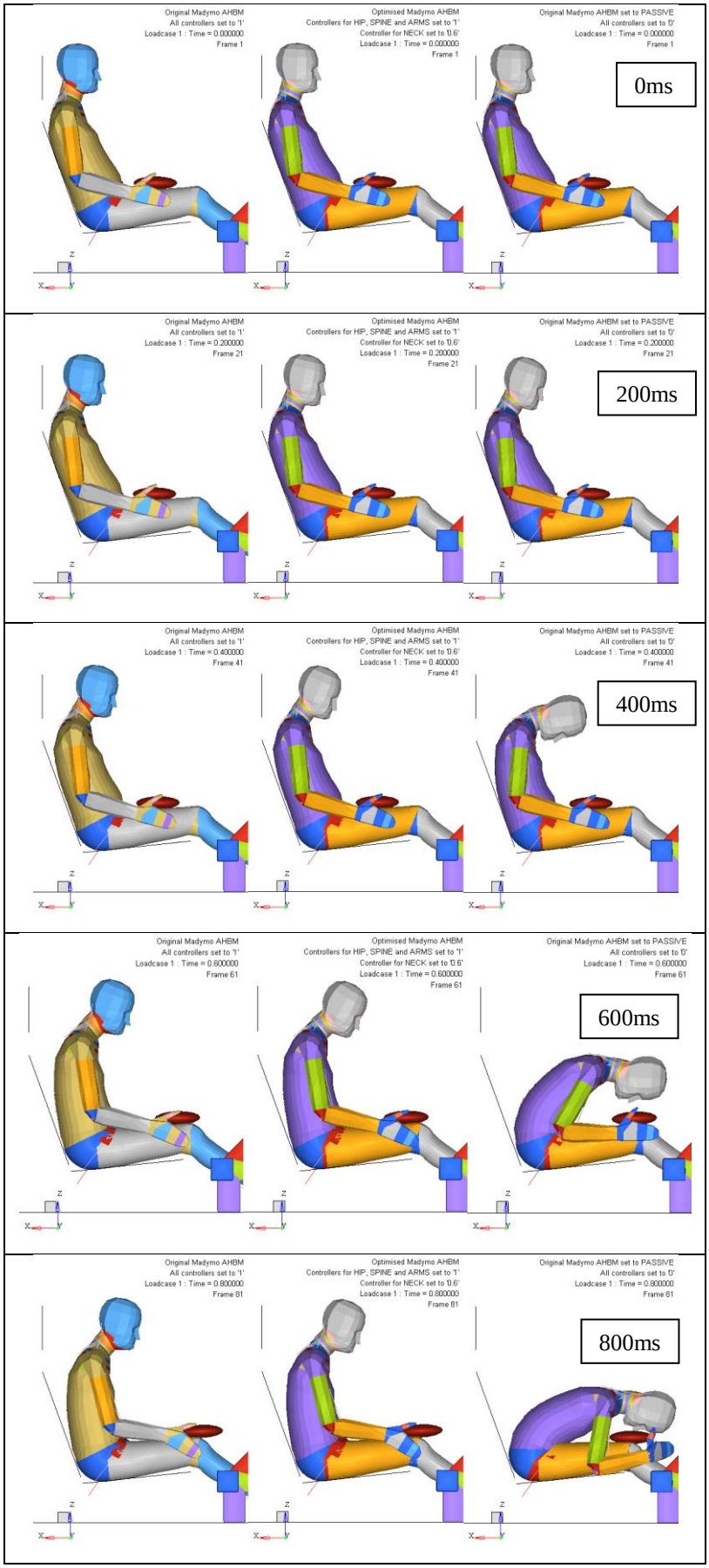

Figure 5.51: Comparison of kinematics (1g): Original AHBM (left), Optimised (middle), passive (right)

It can visually be seen that the torso's motion is very similar between the original and optimised Active Human Models, whilst there is visually a small difference in the head rotation, and this in all stages of the pre-braking (Figure 5.51).

The passive human model has very different kinematics and this before 200ms (Figure 5.52 and Figure 5.53).

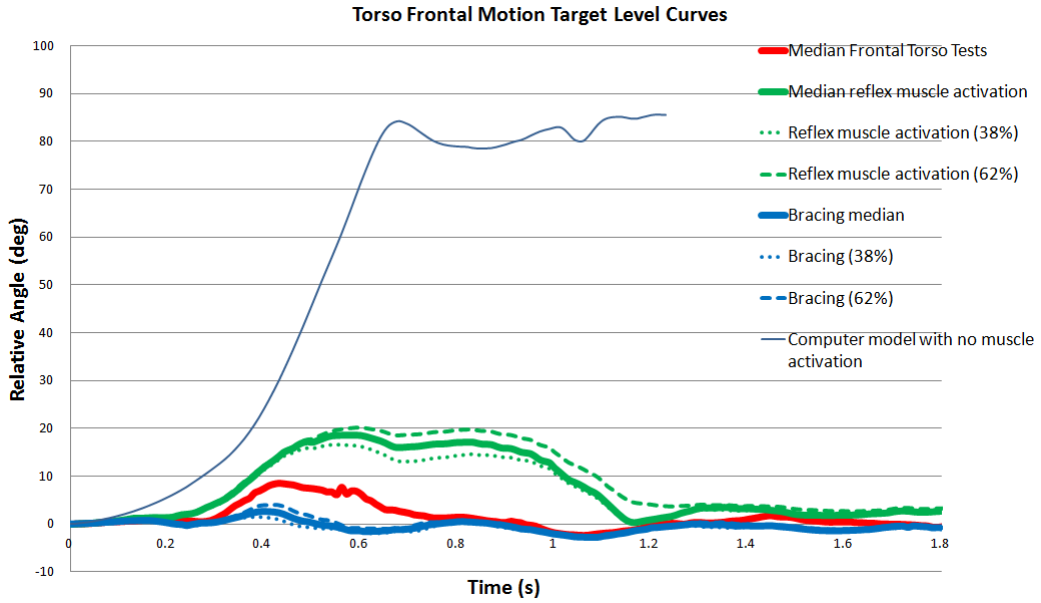

Figure 5.52: Comparison between a passive human model response against reflex target curves (Torso)

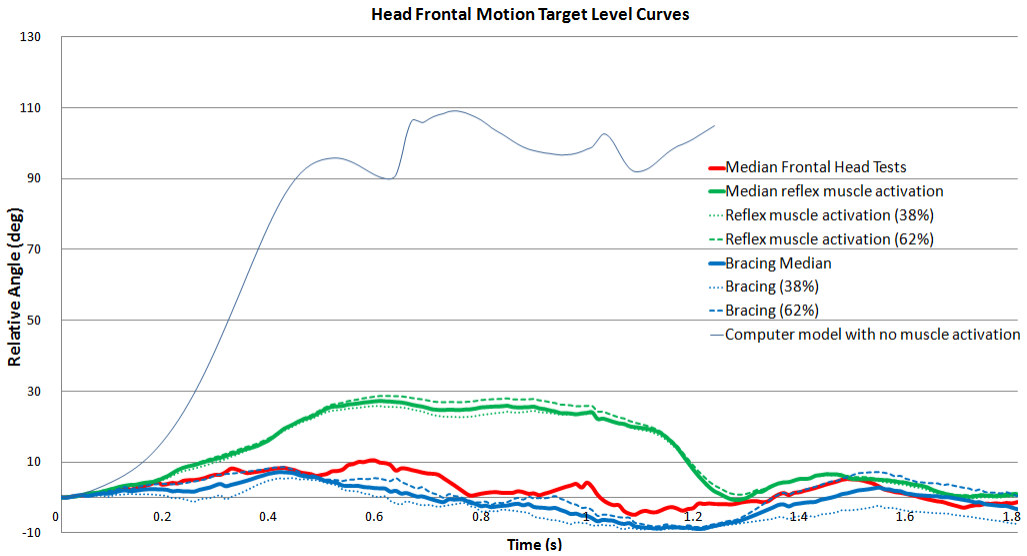

Figure 5.53: Comparison between a passive human model response against reflex target curves (Head)

These graphs confirm that the kinematics does not match the target reflex curves at any time during the deceleration event.

5.4 Summary of the Active Human Model Correlation

The work from this chapter has compared the kinematics of a passive human and an active human model. Both models share the same biomechanics properties and geometries, based on anthropometric data (bones and muscles) as well as being validated against cadaver test data (Cappon 2006). Their main difference lies in the muscle activation feature, where the active human model is capable of a reflex and bracing behaviour while the passive model displays an inert behaviour.

This chapter has analysed Vicon data from the OM4IS consortium and has proposed an efficient way to generate biomechanics targets which consider relative head and torso angles based on volunteer tests.

Based on these tests, a clustering method was undertaken to generate a reflex and bracing head and thorax motion behaviour for which target curves have been generated. It has to be noted that the reflex target curves (head and thorax) have been generated with 3 samples which presented no bracing or pre-disposed behaviours, while a bracing target was based on the remaining 10 volunteers, which is understood to be a small sample to derive absolute claims.

Neverthless, using past experience, a methodical method was used to perform the correlation of this active human model restrained by a lap belt in frontal manoeuvring conditions by first validating the thorax motion before tuning the head rotations.

It was found that the default controller from the active human model were in general adequate to model the reflex behaviour of an occupant in a lap belt restraint configuration, except for the head motion which would require a smaller controller value due to the effect of increased thorax rotation (compared to the validation performed using a 3 point belt). A good correlation against head and torso relative angles was achieved, as well as against kinematics test raw data from the OM4IS tests, using the smaller scalar. Correlating against head and torso relative target angles was successful.

It could also be suggested that stronger motions resistance may be a combination of bracing and muscle activity. Even if the model correlates reasonnably well with a muscle scalar value of '2', it would not be realistic to use it for such a purpose, as the bracing feature is not present in the coding, nor the knee muscle tensionning. It is suggested that more research is needed to define these parameters, which could be validated against the motions curves generated in this paper.

A comparison between active and passive models has been performed, and it has been observed that under a lap-belt environment, and asking volunteer to keep to a set posture, the active human model's kinematics are believable when compared to test data and one video evidence. It has also been observed that a passive human model was totally inadequate to model a low 'g' event. It is therefore understood that should a subsequent impact occur (accident) that injuries based on the passive human model will not be representative, as the original posture, i.e. boundary condition, would be incorrect.

The work performed in this chapter shows that the latest MADYMO 7.4.1 active human model can represent a lap-belted human behavior in frontal pre-crash braking using various levels of muscle activity. The next chapter will address the integration of such active model in the Active Safety Assessment Environment proposed and also investigate the performance of a passive model in vehicle environment for comparison.

6.0 Safety Assessment of Autonomous Emergency Braking Systems on Unbelted Occupants Using a Fully Active Human Model

The final chapter of this thesis focuses on the suitability of the correlated 50th percentile AHBM from chapter 5.0, to assess the safety benefits of a typical Autonomous Emergency Braking System (AEB) followed by a subsequent 40km/h (25mph) rigid wall impact. This final study will investigate the occupant's kinematics as a function of various postures and states of awareness to determine the degree of out-of-position from the standard FMVSS208 sitting position and their respective chest, neck and head injuries. This study is significant as it has been reported that occupants could undergo serious airbag injuries when positioned too close to the airbag module (Morris 1998) or when the airbag was not present, disabled or out of reach (Happian-Smith 2002).

Investigations in improving the computation runtime will also be addressed.

6.1 Drivers' Kinematics Study

6.1.1 Study setup

The aim of this section is to evaluate the kinematics of an occupant under an unexpected emergency braking in different states of awareness, in a generic vehicle environment (based on Figure 3.12). The framework defined in chapter 3 will be used and will assume a 50th percentile human model is a fixed vehicle interior based on a BMW325L, i.e. define seat stiffness and floor friction value. No bracing is applied prior to the braking event taking place.

The parameters which will be considered in this study are the seat friction parameter and the state of awareness of the occupant. Seat friction accounts for the evaluation of tendencies in lower extremities load paths, i.e. footrest and pelvis.

The seat friction coefficient in vehicles is of the order of 0.8 (Cummings 2009). Nevertheless, values utilised for the correlation 0.5 and lower (0.3) were studied to evaluate the spread of kinematics response to this variable. The seat model was constructed from planes with a stiffness characteristics extracted from an accident reconstruction technical report (Advanced Simtech 2007). In all instances, it was assumed that the friction between the feet and the floor to be 0.85 representing rubber sole shoes to carpet resistance value.

The awareness level can vary greatly. A "very aware" person has a reflex response time of 10ms; an "aware" occupant of 120ms, which can be modelled as a 'motor reflex delay' in the human model (TNO 2012). During the sled correlation section, a reflex delay of 10ms was used, because the occupant was 'primed' for a sled test. It the scenario analysed, this reflex delay was slightly increased arbitrary to 30ms to reflect that the occupant has his/ her mind more on the road.

The hand is attached to the steering wheel using a RESTRAINT.POINT command in MADYMO with a maximum grip force level of 400N (Bao 2000; NASA 1976), to simulate a possible hand release.

The lists of normal awareness computer runs are listed in Table 6.1 (Bastien 2013b).

Table 6.1: Normal awareness computer setups (Bastien 2013b)

Prior to performing the kinematics study, the occupant was positioned in the vehicle using a 1g vertical 'Z' for the duration on 1.5s to balance the occupant with its environment (TNO 2011), as discussed in Chapter 5.0. During the 1g emergency braking, the 1g vertical gravity field was maintained.

The frontal braking pulse, as described in chapter 3, was applied on the human model as a reverse pulse with the cabin and airbag system set as static.

6.1.2 Results of the occupant kinematics' study of 2-hand grip stance ("very aware" or "aware")

The first results concerning the seat with very low friction indicated that the driver's pelvis was sliding forward until the leg contacted the dashboard, as shown in Figure 6.1. The pelvis is sliding because of the lowest resistance provided by the seat relative to the direct loading through the arms.

The torso (solar plexus) almost stayed still (+0.05m forward motion from original position, +X in Figure 3) due to the resistance of the arms, which consequently moved the head away from the airbag (-0.05m rearward motion from initial position, -X in Figure 6.2).

Figure 6.1: Scenario with seat with friction set at 0.3 (30ms and 120ms awareness displayed Left to Right) at time 0s (top) and 2.5s (bottom) (Bastien 2013b)

It was noted that for a very low seat friction, the occupant kinematics was very similar for a "very aware" and "aware" person, especially after 0.5s for the top of the head as

well as the solar plexus, as can be noted in Figure 2 and Figure 3, where the displacement curves mostly overlap during the duration of the event (Bastien 2013b).

Figure 6.2: Summary of displacement of top of occupant's head (Bastien 2013b)

It can be noted in Figure 6.2 that the head has a flexion motion due to the 1g braking pulse which is greater for a motor reflex delay of 120ms than 30ms, as the neck muscles are activated later. When a slower reflex occurs, it takes 500ms to match the head motions of an occupant with a faster reflex.

Figure 6.3: Summary of displacement of occupant's solar plexus (Bastien 2013b)

It can be noted in Figure 6.3 that, for the same seat friction value, the solar plexus has a greater linear motion the longer the motor reflex delay.

6.1.3 Discussions and conclusions on the occupant kinematics' study of standard grip stance ("very aware" or "aware")

Increasing the seat friction parameter increases the sliding force responsible for the occupants' motion. As illustrated in Figure 6.4, increasing the friction from 0.5 to 0.8 increases the resistive force to motion from 500N to 650N.

Figure 6.4: Occupant force on pelvis a function of seat friction and awareness (Bastien 2013b)

Figure 6.5: Comparison of occupant kinematics for seat friction 0.5 (30ms and 120ms awareness displayed in blue and green respectively). Pre-braking duration of 2.3s (Bastien 2013b)

Figure 6.6: Comparison of occupant kinematics for seat friction 0.8 (30ms and 120ms awareness displayed in blue and green respectively). Pre-braking duration of 2.3s (Bastien 2013b)

Figure 6.4 also suggests that a motor reflex delay less than 120ms does not have an influence on the seat force due to friction. The human model used has a stabilising spine which will naturally keep the occupant seating straight and hence transfer the load onto the seat. The mass transfer looks very noisy early in the seat force readings (Figure 6.4), which may be caused by the repositioning of the human model from the initial gravity positioning as well as the early muscle activity which affects the heads' forward motion (flexion). Looking at scenarios with greater seat frictions, i.e. 0.5 and 0.8, it can be observed that the kinematics are different initially due to the fact that the seat friction resists the pelvis motion and obliges the torso to rotate towards the steering column. This is clearly illustrated in Figure 6.5 and Figure 6.6 (Bastien 2013b).

This suggests that the higher the seat friction the greater the torso rotation as the relative speed between the pelvis and the torso increases.

Looking at the reflex levels, Figure 6.5 and Figure 6.6 suggest that a slower reflex leads to a closer thorax position relative to the steering column, because the arms are reacting later.

Indeed, with a slower reflex, the velocity of the torso (measured at the solar plexus) is higher from approximately 1.2s (Figure 6.7), as the muscle activity in the human model is lagging. With increased velocity, the momentum is increased.

Figure 6.7: Velocity of human model's solar plexus (Bastien 2013b)

As the hands are restrained on the steering wheel by a RESTRAINT.POINT command, the arms rotate at the steering wheel attachment to compensate for the momentum. As a consequence, the distance between the driver and the steering wheel has to reduce.

Figure 6.8: Occupant's arm angle change (deg) (Bastien 2013b)

Figure 6.9: Hand force on the steering wheel (N) – 2hand grip (Bastien 2013b)

As illustrated in Figure 6.8, the occupant's arm's angle starts to reduce from run_11b ("very aware") to run_21b ("aware") at time 1.5s. The force exerted on the steering wheel is reduced (Figure 6.9) and the occupant is therefore closer to the steering wheel, as illustrated in Figure 6.6. Considering the 2 hand grip scenario discussed in this section, it can be noted that the active human model's kinematic response can clearly be explained through the analysis of Figure 6.7, Figure 6.8 and Figure 6.9, hence it can be concluded that this model is suitable to model a pre-braking phase for an unbelted occupant.

6.1.4 Comparison of Active and Passive human models under pre-braking in a vehicle interior in 2-hand grip stance

Using the same setup, it is possible to analyse the kinematics response of a fully passive human model by comparing it with a 2 hand grip with 30ms (green) and 120ms (blue) configuration (Figure 6.10). It can be observed that a passive human is totally inadequate.

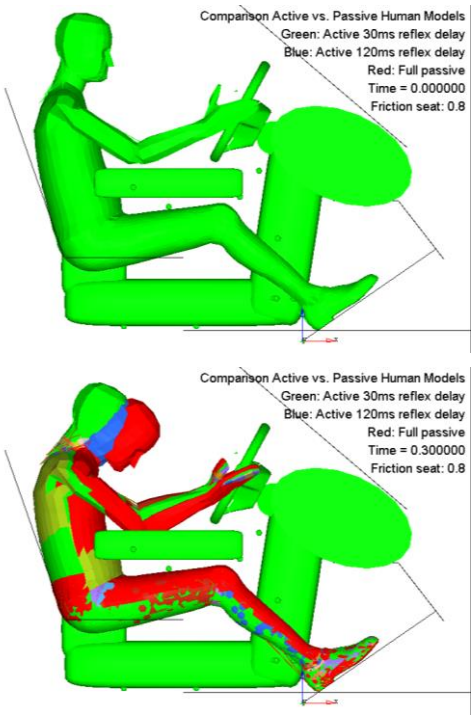

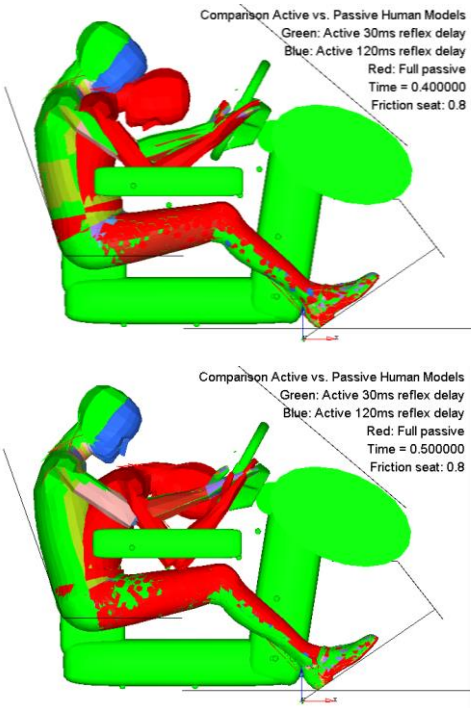

Figure 6.10: Differences of kinematics between an alert, less alert and passive occupant model

Kinematics is showing that the top of the head of a passive model displaces in X on average in excess of 0.48m while the active models do not reach a maximum of 0.17m (Figure 6.11). The torso for a fully passive human moves forward very rapidly to reach 0.17m while the active ones do not exceed 0.05m (Figure 6.12).

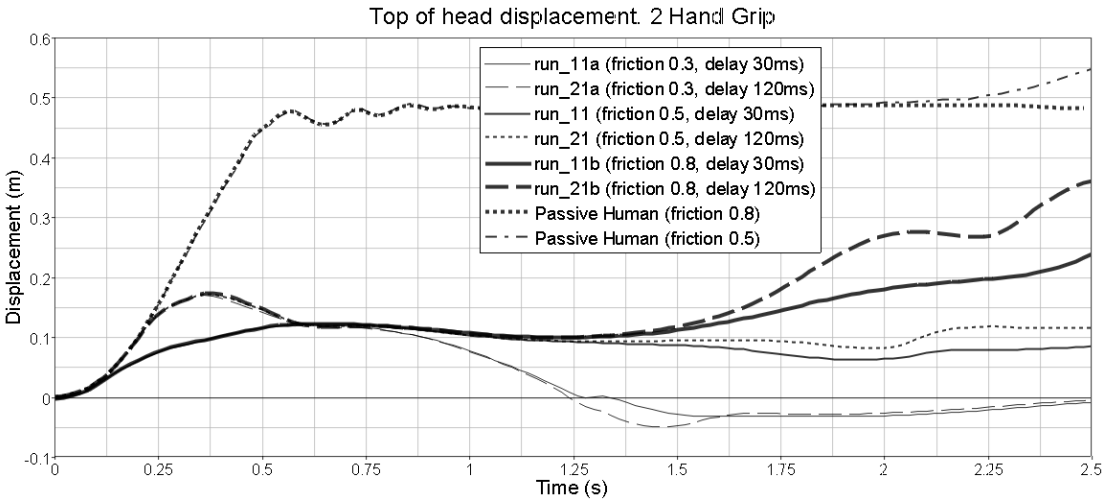

Figure 6.11: Comparison of top of the head displacement between active and fully passive human models

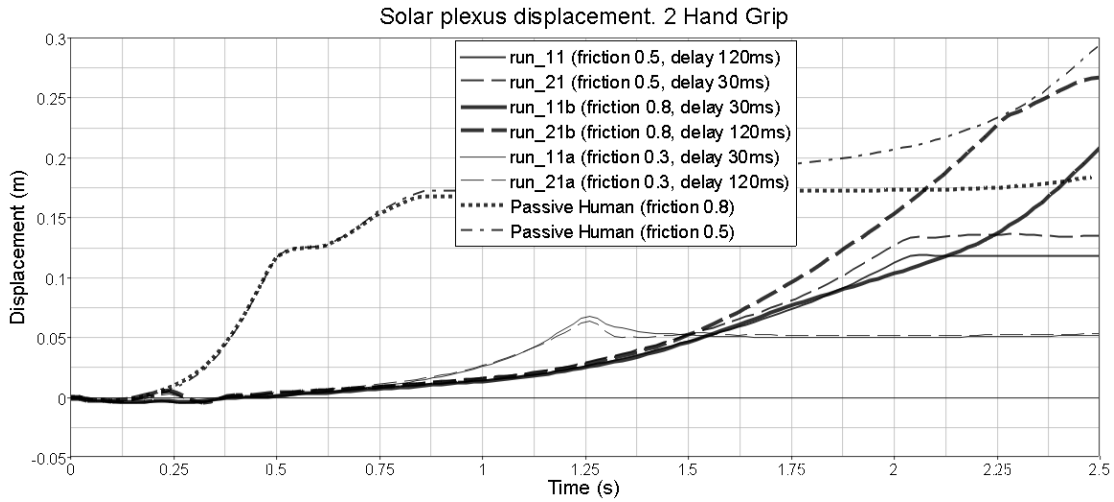

Figure 6.12: Comparison of torso displacement between active and fully passive human models

This study has confirmed that in all cases a fully passive model is inadequate. Using such model for unbelted scenario, in a vehicle cabin including a steering wheel, will not provide the correct kinematics, leading to an erroneous position relative to the restraint system, which will yield to incorrect injury values.

6.1.5 Results of the occupant kinematics' study of 1-hand grip stance ("very aware" or "aware")

In order to investigate the safety concerns of drivers using mobile phones while driving (WHO 2013), the following study has considered modelling a driver holding the steering wheel with one hand (closest to the door) and raise the other hand up to the ear, as such mimicking the typical use of mobile phone at the wheel.

Using the same model setup as the 2 hand grip, removing the left hand from the steering wheel and raising it to the ear level, it has been shown that the coefficient of friction had a great importance in the position of the occupant using a mobile phone (Bastien 2013b). To ensure that the hand would remain close to the ear, the shoulder and elbow joints were locked during the whole computation. The computer runs are listed in Table 6.2.

Table 6.2: 1-hand grip computer setup (Bastien 2013b)

From the kinematics observed in Figure 6.13, Figure 6.14, Figure 6.15 and Figure 6.16, it can be observed that:

- The greater the friction, the closer the occupant is situated to the seat centreline (Y direction in Figure 6.15 and Figure 6.16),
- The faster the motor delay, the closer the occupant is situated to the seat centreline (Y direction Figure 6.13, Figure 6.14 and Figure 6.15).

Figure 6.13: Kinematics results of mobile phone stance friction 0.3. "Very aware" (top), "aware" bottom. Time: 1.1s (Bastien 2013b)

Figure 6.14: Kinematics results of mobile phone stance friction 0.5. "Very aware" (top), "aware" bottom. Time: 1.1s (Bastien 2013b)

Figure 6.15: Kinematics results of mobile phone stance friction 0.8. "Very aware" (top), "aware" bottom. Time: 1.1s (Bastien 2013b)

Should the braking duration exceed 1.1s, for lower seat frictions, the occupant can find itself seriously OOP and totally out of the reach of the airbag deployment zone (Figure 6.16).

Figure 6.16: Effect of seat friction value on occupant kinematics – 1 hand grip (mobile phone). Time: 1.775s (Bastien 2013b)

In all cases, the right hand still holds the steering wheel, which can be seen in Figure 6.17, as the grip value is under 400N.

Figure 6.17: Hand force on the steering wheel (N) – 1 hand grip (mobile phone) (Bastien 2013b)

As expected, the longer reflex delay means that the occupant has a higher momentum; hence more restoring force in the hand is needed.

At time 1.4s, the occupant slides sideways considerably, causing the hands to react more, hence the peak starting at 1.4s. At 1.5s the knees contact the knee-bolster which has for effect to restrain the occupant from moving any further; hence the forces in the hands reduce.

Using this latest MADYMO human body model, it was possible to re-confirm that a braking duration in excess of 1.1s positions the occupant out-of the airbag zone of influence, as previously reported (Bastien 2012a). Hence considering the vehicle modelling assumptions, the study will disregard braking duration values above 1.1s, as the vehicle's stiffness definition outside the steering wheel and airbag system areas are unknown.

6.1.6 Comparison of Active and Passive human models under pre-braking in a vehicle interior in 1-hand grip stance

As performed for a 2-hand grip, the top of the head and the solar plexus' displacement have been plotted (Figure 6.18 and Figure 6.19), to show that the passive human does not resist the deceleration and moves quicker towards the steering column from 0.6s. At that time, the head displacement remains constant as it is in continuous contact with the steering wheel. This can also be observed in the kinematics depicted in Figure 6.20.

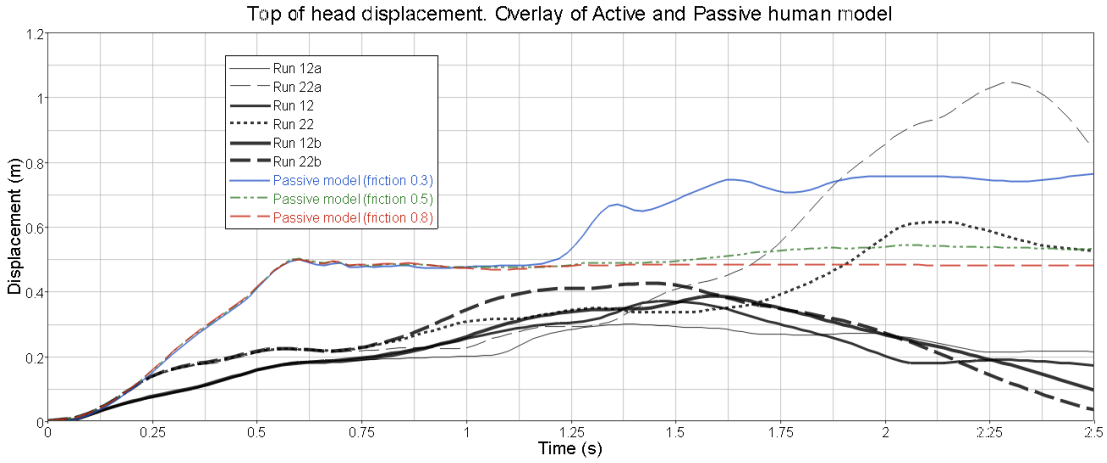

Figure 6.18: Comparison of top of the head displacement between active and fully passive human models

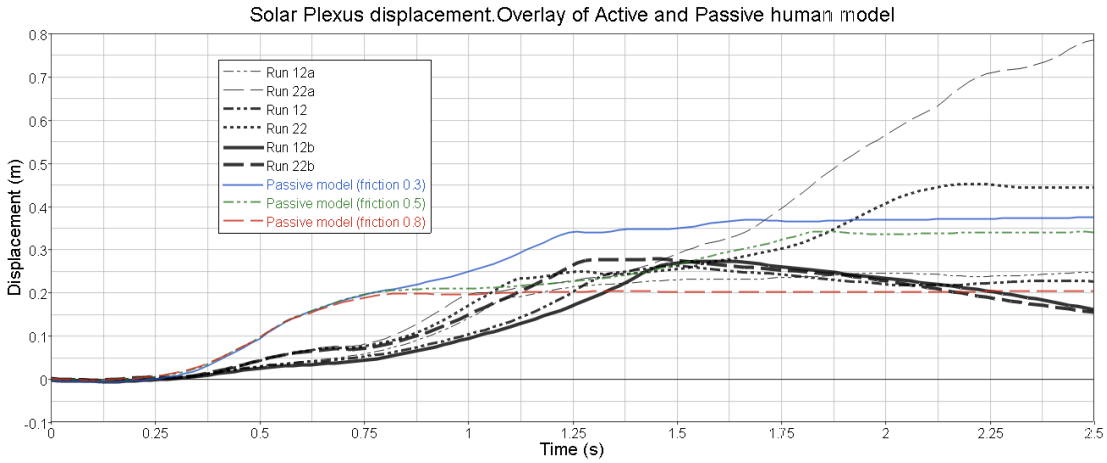

Figure 6.19: Comparison of thorax displacement between active and fully passive human models

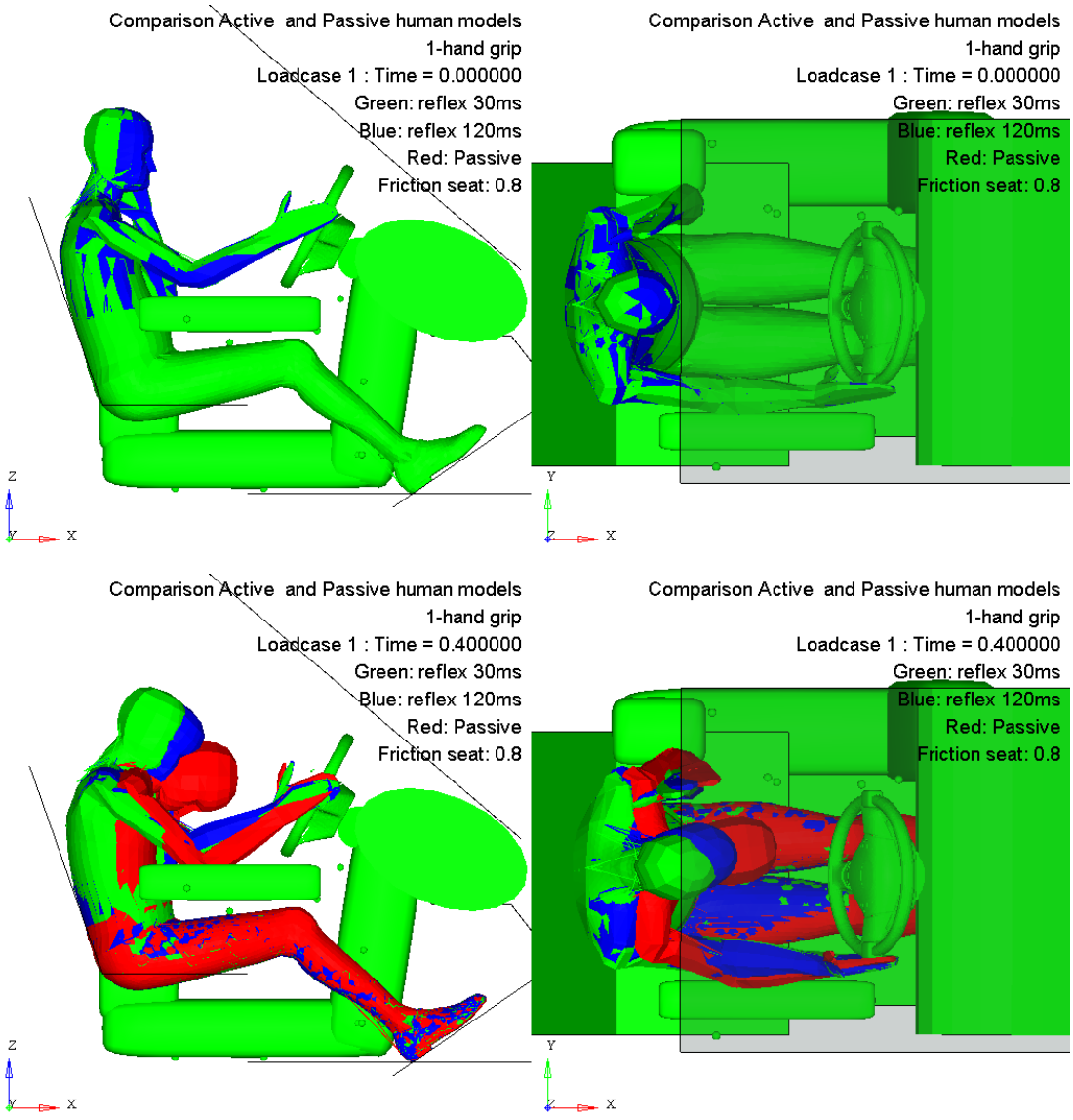

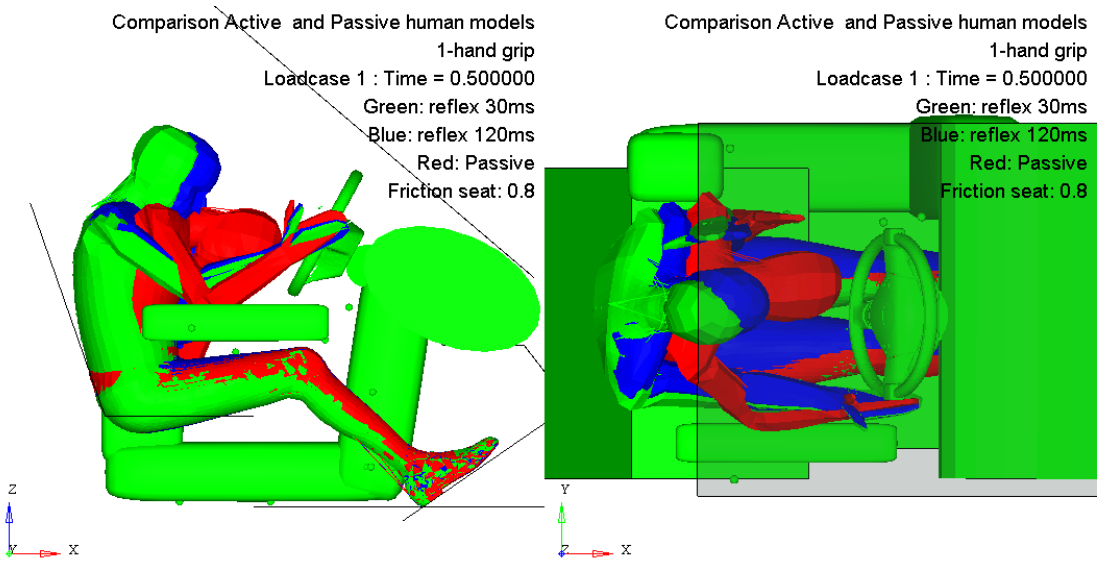
Comparison Active and Passive human models
1-hand grip
Loadcase 1 : Time = 0.500000
Green: reflex 30ms
Blue: reflex 120ms
Red: Passive
Friction seat: 0.8
Comparison Active and Passive human models
1-hand grip
Loadcase 1 : Time = 0.500000
Green: reflex 30ms
Blue: reflex 120ms
Red: Passive
Friction seat: 0.8

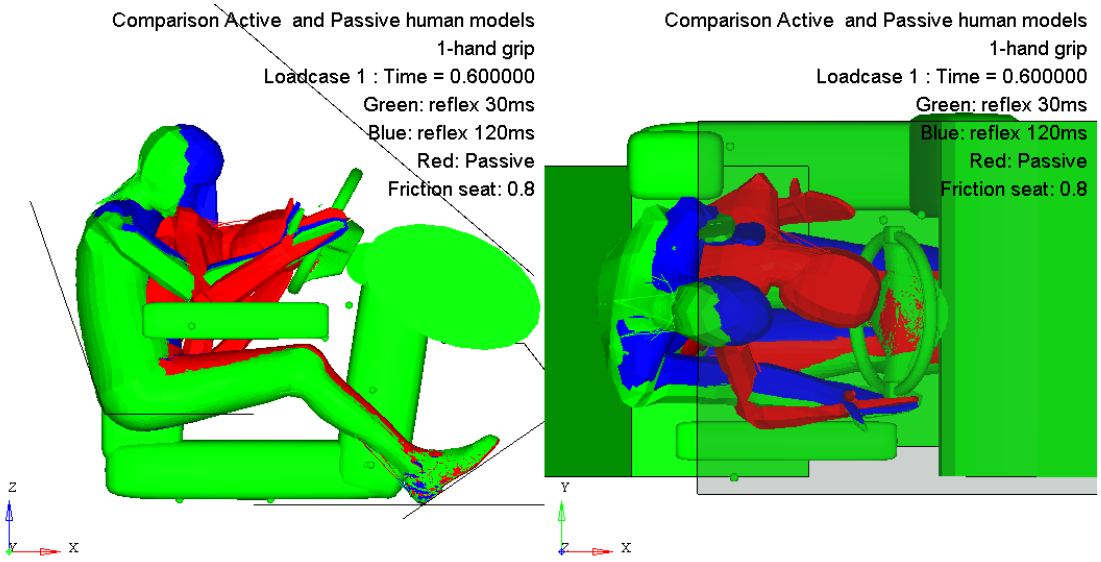
Comparison Active and Passive human models
1-hand grip
Loadcase 1 : Time = 0.600000
Green: reflex 30ms
Blue: reflex 120ms
Red: Passive
Friction seat: 0.8
Comparison Active and Passive human models
1-hand grip
Loadcase 1 : Time = 0.600000
Green: reflex 30ms
Blue: reflex 120ms
Red: Passive
Friction seat: 0.8

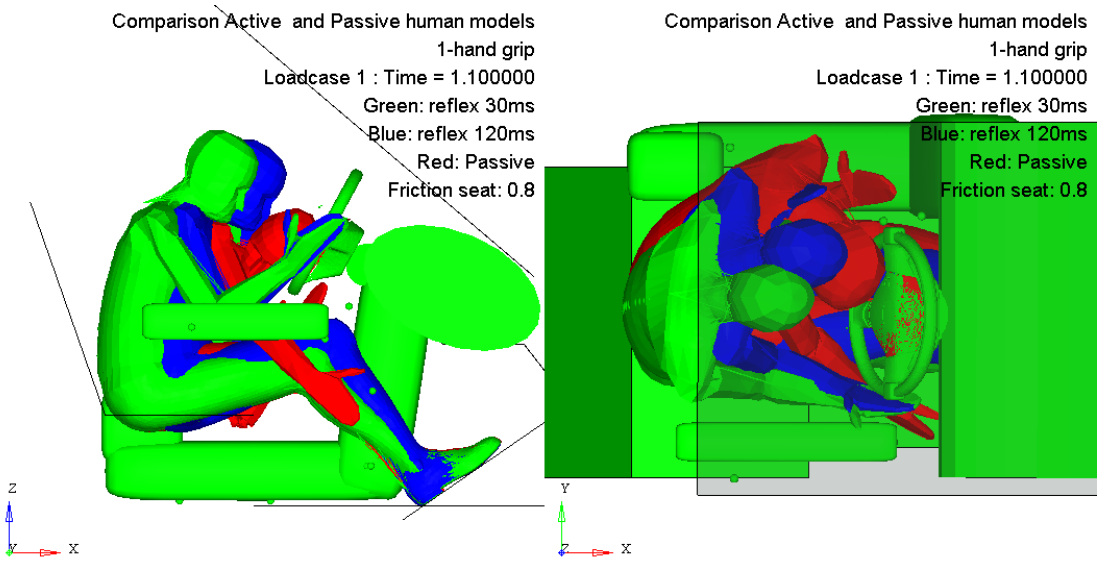
Comparison Active and Passive human models
1-hand grip
Loadcase 1 : Time = 1.100000
Green: reflex 30ms
Blue: reflex 120ms
Red: Passive
Friction seat: 0.8
Comparison Active and Passive human models
1-hand grip
Loadcase 1 : Time = 1.100000
Green: reflex 30ms
Blue: reflex 120ms
Red: Passive
Friction seat: 0.8

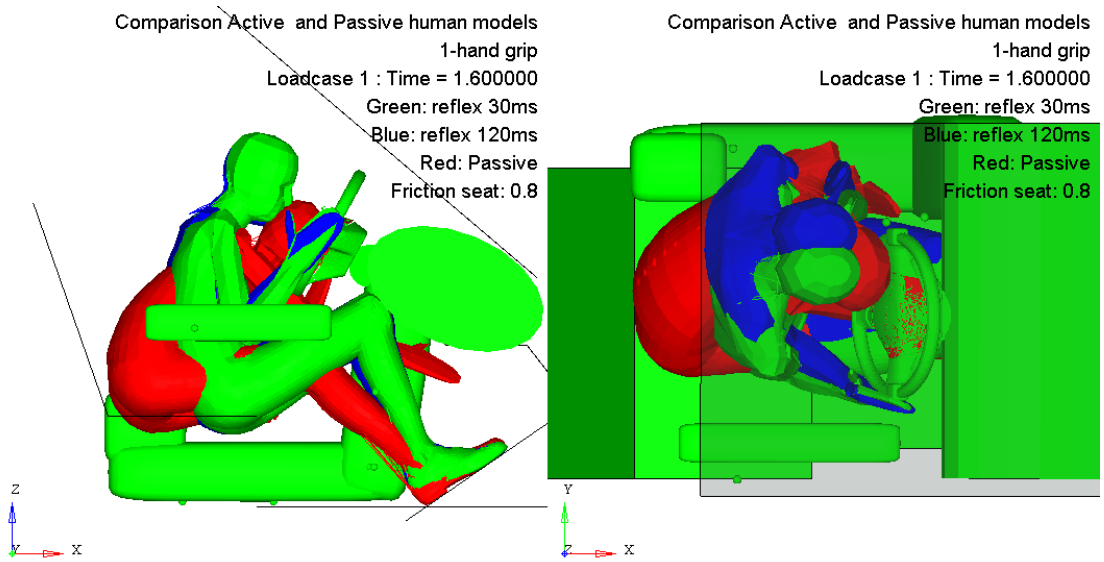

Figure 6.20: 1-hand grip. Comparison between active and passive human models (Left: Side view, Right: Top view) as function of time

It can be noticed that the active human has larger kinematics than the passive model, which is contradictory to the 2-hand grip stance and this for low seat friction.

The reason for this is that, as discussed in the 2-hand grip, should the seat friction be lower, then the occupant is more out-of-position, as less friction force keep it on the seat. As a consequence, when muscle tension is activated, the occupant's arms remain straighter than a passive model (Figure 6.20), which amplifies the rotation about the hands allowing the occupant to rotate more than the passive model which slouches against the steering wheel.

Figure 6.21: Effect of lower seat friction on 1-hand occupant stance kinematics (Bastien 2013b)

This rotation causes the occupant to reach extreme positions, as depicted in Figure 6.21.

6.1.7 Summary of the driver kinematics study

From the computation performed and analysis of the results, it has been confirmed that, in spite of its biofidelity (Lange 2005; Cappon 2006) and anthropometry, a passive human model is not suitable to study active safety pre-braking scenarios. The inertial and muscular properties of a passive human model are not sufficient to represent realistic resistance to pre-braking forces.

In a 2-hand grip, the occupant's kinematics is not believable and too different from an active human behaviour to make the later part of the study regarding injuries relevant.
In a 1-hand grip, the occupant's kinematics is also not believable and too different from an active human behaviour. The head contacts the steering wheel too early, the head is rotating too early by a large angle and the spine has slouched too much to be realistic.
This concludes that only an active human model is to be used for such scenario investigation.

The driver kinematics suggest that, within the computer setup investigated, the occupant needed to have a good level of awareness (motor reflex delay < 120ms) to resist an unexpected AEB with no Frontal Collision Warning (FCW).
Considering the computer assumption used in the framework, an occupant using a mobile phone will be in the airbag envelope up to 1.1s of AEB braking duration with no FCW. Should the duration last longer and should an impact occur, then the occupant will not be protected by any restraint systems.
In all standard grip starting positions, i.e. with the 2 hands on the steering wheel, the study shows that the human model will resist the deceleration up to a braking duration of 2.5s (computed for all runs) even though it will move closer to the steering wheel. No hand loads has exceeded the 400N threshold level.
All the kinematics runs are overlaid in Figure 6.22 and Figure 6.23 for comparison (Bastien, 2013b).

Figure 6.22: Summary of Solar Plexus displacement (all runs) (Bastien 2013b)

Figure 6.23: Summary of Top Head displacement (all runs) (Bastien 2013b)

Following the study it can be concluded that the first component of the occupant motion is the seat friction (based on Figure 6.4), which controls the first 1.0s of the motion. The second part of the motion is due to the motion of the arms which is a result of the own increased kinetic energy as well as possibly the torso's kinetic energy (Bastien 2013b).

Higher friction leads to higher relative velocities from the pelvis to the thorax, hence greater energy of rotation of the thorax relative to the pelvis, leading to increased rotation of the arms, reduction of grip force and consequently closer proximity to the steering wheel.

Considering Figure 6.22 and Figure 6.23, the change of energy transfer comparing 2 occupants having different motor reflex delay, i.e. awareness, is difficult to pinpoint accurately. As such a 'transition zone' has been evaluated from the graphs which bands the possible starts of the increase in kinetic energy from the torso. This zone starts around 1.0s and finishes at 1.5s.

As a summary, considering all the variables in this posture study (seat friction, reflex delay and braking duration), it can be concluded that the active human model's kinematics can, in both hand grip scenarios, be logically explained. As such it is concluded that the AHBM's response in the pre-braking phase is leading to reasonable and believable kinematics.

6.2 Drivers' Injury Study

6.2.1 Background and study setup

The aim of this section is to investigate the effects of a vehicle accident following a pre-braking phase on unbelted occupants' injuries. It is assumed that the occupant will have a reflex behaviour and not a bracing one as the braking event is assumed sudden and unforeseen, meaning that the driver is unaware and unresponsive to the impending collision.

This study will compare the occupant protection level based on a standard FMVSS208 rigid wall crash test (40km/h (25mph)) against a 1g vehicle deceleration until the vehicle reach 40km/h (25mph), then followed by a rigid wall impact.

Figure 6.24: Severe braking scenario followed by rigid wall impact (airbag fire time set to 10ms) (Bastien 2013b)

As described in this chapter, the pre-braking phase will cause the occupant to be out-of-position before the impact takes place, as illustrated in Figure 6.24.

Following the kinematics study, injuries have been extracted for chosen scenarios following the framework discussed in the Methodology section. The scenarios with the friction parameter of 0.3 have not been further analysed as the occupant's head has moved away from the airbag (Figure 6.1). Cases where head and thorax positions lie within the airbag envelope were favoured.

Performing a pre-braking followed by a gas flow airbag deployment can be performed; doing so would be very computationally expensive, as in explicit finite elements, the element time step is based on the lowest stress wave propagation value of the model. The model will have to iterate at a time step value until the runtime duration is reached, here up to 2.3s. To mitigate lengthy computation, the most utilised method in MADYMO is to rigidise any finite element meshes which are not contributing to the injury event until absolutely necessary. In our case, any airbag finite element components are not needed until the airbag is expected to deploy, i.e. when the accident occurs. As a consequence, all unnecessary finite element meshes during the pre-braking phase are set to RIGID until the accident occurs, requesting then the airbag deployment. When the airbag time to deploy is reached, the time step will then drop accordingly, the gas flow grid be activated and will sub-cycle 17 times for each finite element time step (Blundell 2006).

A model with rigidised elements should compute more rapidly, nevertheless MADYMO will have to perform many sub-cycles to scan the RIGID element state using a logical switch, which is a lengthy process, as well as storing the inertia tensors, slowing the computation further down. During the pre-braking phase (without airbag deployment), it has been observed that the occupant thorax's velocity was not zero, as displayed in Figure 6.7, nevertheless low (0.35m/s).

The remark above allows the following question to be raised: due to the fact that the solar plexus velocity is low, as illustrated in Figure 6.7, can it be assumed that the occupant is in a state of equilibrium relative to the steering wheel and not moving before the accident event starts?
Should the answer to this question be positive, then it would mean that the occupant kinematics could be computed once and for all during the pre-braking phase, then the

final occupant kinematics' position be remapped in an OOP crash position to injury assessment. A split run or 2-step run would be therefore much faster.

In order to validate whether these assumptions are true, a split-run strategy will be investigated and final occupant' injuries compared to a 1-step pre-braking/ crash computation run. As a 1-step run contains all the actual physical event of the pre-braking phenomenon, hence it is assumed to be more representative than a 2-step method. To validate the 2-step method, its injury results should match the 1-step method.

The scenarios with the friction parameters of 0.5 and 0.8 were selected (Table 6.1 and Table 6.2), considering 3 braking durations aiming to reduce the vehicle from its original cruising speed down to 40km/h (25mph) (Bastien 2013b), as listed in Table 6.3 and Table 6.4.

Table 6.3: 2-Step computation setup (full pre-braking simulation with injury based on re-mapped occupant kinematics (Bastien 2013b)

Run Name	Starting speed (km/h)	Braking Duration (s)	Seat Friction	Awareness (ms)
Run 40_switch	60	1.1	0.5	120
Run 41_switch	60	1.1	0.8	120
Run 42_switch	80	1.7	0.5	120
Run 43_switch	80	1.7	0.8	120
Run 44_switch	100	2.3	0.5	120
Run 45_switch	100	2.3	0.8	120
Run 50_switch	60	1.1	0.5	30
Run 51_switch	60	1.1	0.8	30
Run 52_switch	80	1.7	0.5	30
Run 53_switch	80	1.7	0.8	30
Run 54_switch	100	2.3	0.5	30
Run 55_switch	100	2.3	0.8	30

Table 6.4: 1-Step computation setup (specific pre-braking simulation and accident simulated together, using a Rigid Switch)

The vehicle crash pulse information utilised has been obtained from previous research (Bastien 2013b) and braking durations of 1.1s, 1.7s and 2.3s as derived in the Methodology section (chapter 3).

As it is not currently possible to re-map the full joint velocity (feature not developed yet by TASS, programmer of MADYMO), the repositioning in the 2-stage configuration only involves the final posture without the final velocity of all the human joints. This is very important information at this point in time.

6.2.2 Calibration of restraint system under 40km/h (25mph) unbelted 50th percentile occupant

As described in the "Preliminary study" chapter, the airbag model used has been improved and meet OOP1 an OOP2 5th percentile female static tests, as derived in chapter 4. In order to use the proposed framework, the airbag system must also meet 40km/h (25mph) unbelted 50th percentile occupant. To allow a qualitative comparison between the injuries, it has been necessary to scale the magnitude of the input crash pulse by 65% in order to generate a safe vehicle under FMVSS208 unbelted injuries for a 50th percentile AHBM, as explained in Chapter 3.

By doing, so the FMVSS208 reference injury levels prior to applying the framework can be extracted and presented in Table 6.5. These injuries meet all the legal requirements.

Reference FMVSS208 unbelted loadcase (run 31c), unbelted occupant (40km/h (25mph)rigid wall pulse)		
HIC		168
Chest acceleration (g)		54
Neck force	Tension (N)	1308
	Compression (N)	785
Neck Moments	Flexion (N.m)	11
	Extension (N.m)	13
Neck Injury Criteria	N_{ij} TE	0.1
	N_{ij} TF	0.2
	N_{ij} CE	0.2
	N_{ij} CF	0.1
Femur	Axial load - compression(N)	5968

Table 6.5: Injury reference values (unbelted 50th percentile occupant with 40km/h (25mph)crash pulse

The injury traces of the reference scenario are displayed in Figure 6.25, Figure 6.26, Figure 6.27 and Figure 6.28 and reflect the values extracted from Table 6.5.

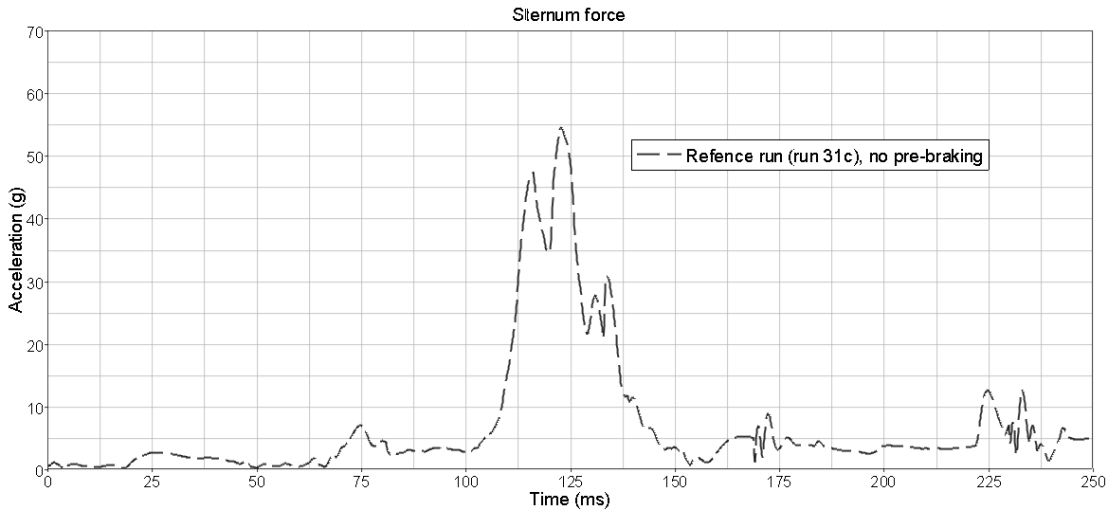

Figure 6.25: Reference scenario. Sternum acceleration.

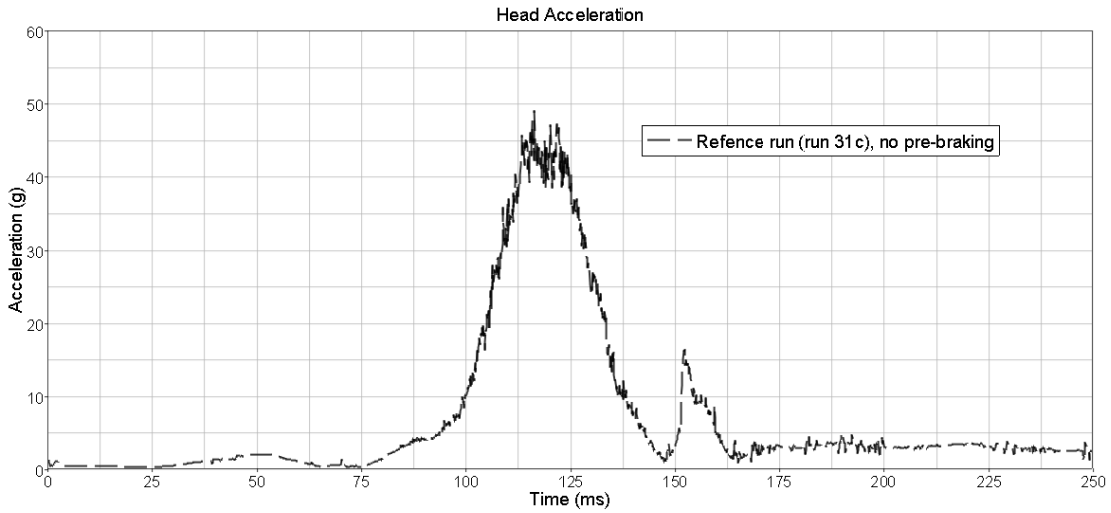

Figure 6.26: Reference scenario. Head acceleration

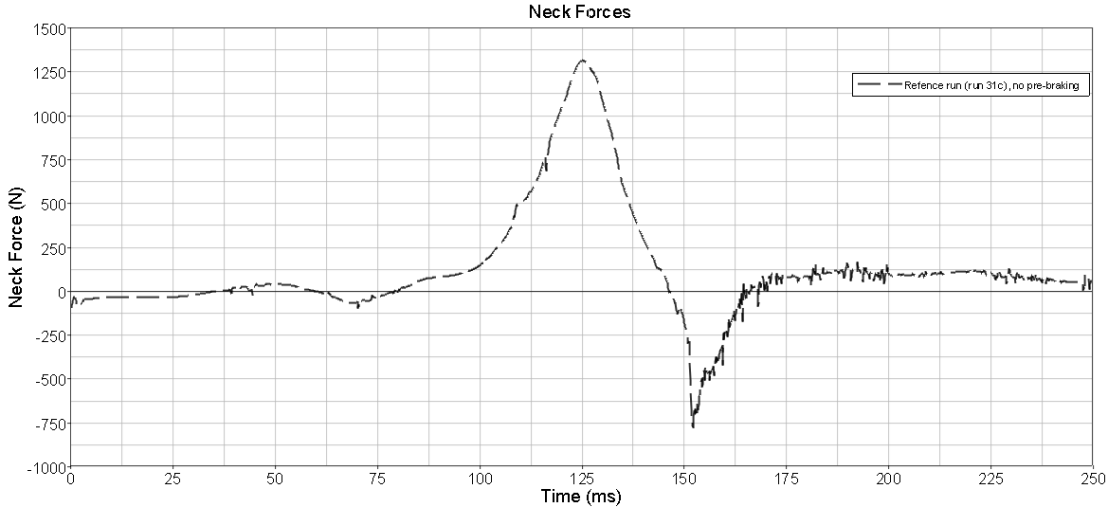

Figure 6.27: Reference scenario. Neck Force

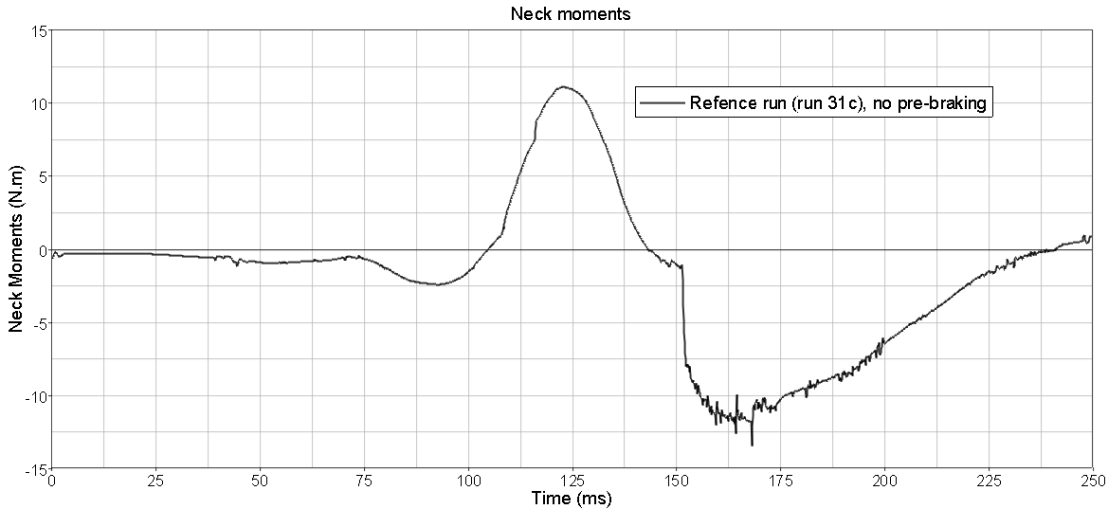

Figure 6.28: Reference scenario. Neck moments

One clear event which can be captured through a cutting plane (Figure 6.29), is the start of the sternum force, which begins around 110ms (Figure 6.25). This event is caused by the sternum contacting the steering wheel (Figure 6.29).

Figure 6.29: Cross section through scenario at time 112ms (Bastien 2013b)

It must also be noted that in the model, the steering wheel is mounted to a rigid bracket, with no steering column compliance and collapse possible. Consequently, the chest acceleration values quoted in this study are comparative values and not absolute ones.

The full occupant impact kinematics is captured in Figure 6.30.

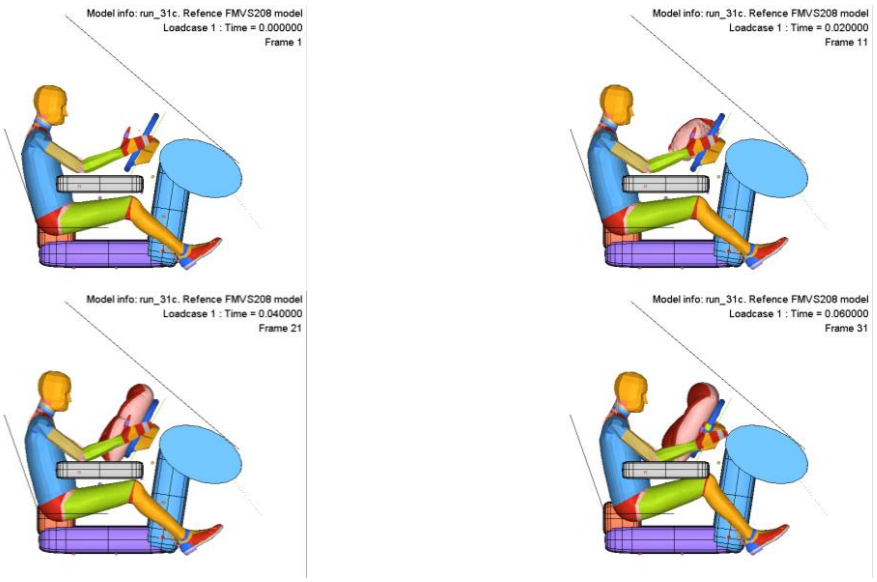

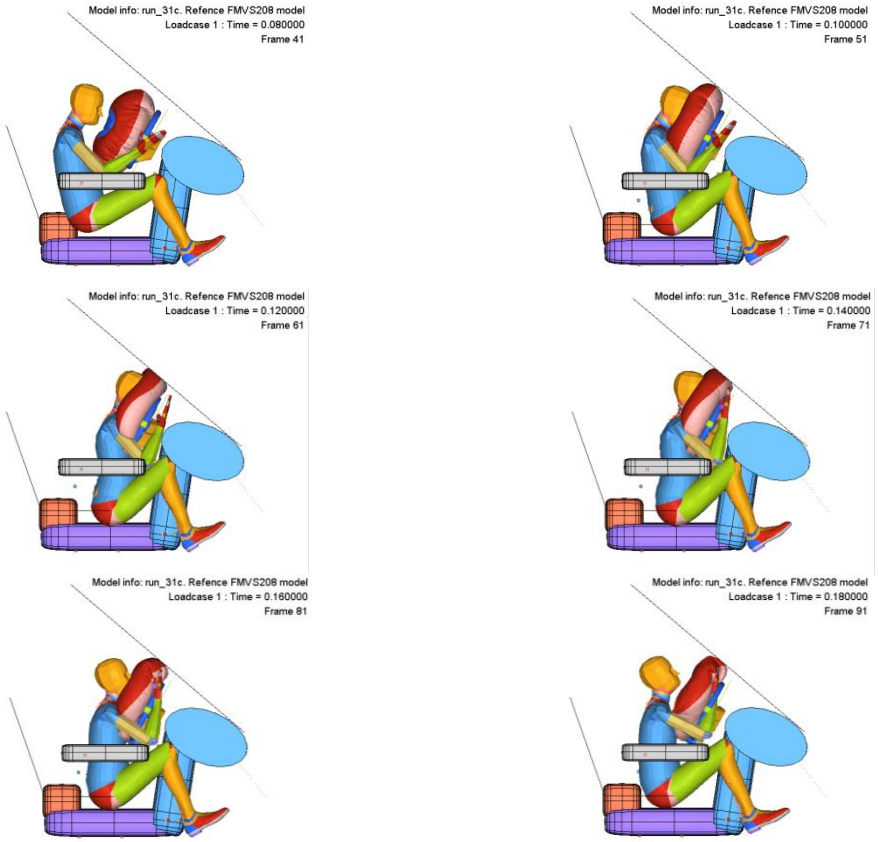

Figure 6.30: Reference scenario impact occupant kinematics

From the computer animations, it is possible to output the forward (X) velocities of the occupant top of the head and solar plexus (Figure 6.31). The impact velocity is around 6.0m/s to 6.5m/s prior to contact with the restraint system.

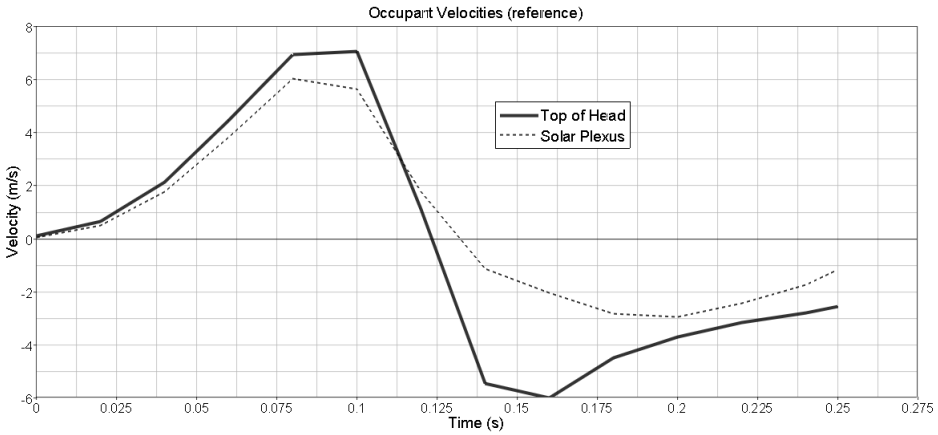

Figure 6.31: Occupant top of the head and solar plexus forward velocity(X)

This value will be compared later on with occupant forward velocities during the pre-braking stage.

6.2.3 Results for the standard 2 hand grip

RUNTIMES COMPARISION BETWEEN THE 2 METHODS

The 2-Step split method involves performing the following evens sequentially:

- Performing a full pre-braking event of 2.3s, in order to capture the full braking duration explained in the Methodology section,
- Reposition the occupant in the vehicle at 1.1s, 1.7s and 2.3s
- Subject the occupant to a 40km/h (25mph) accident.

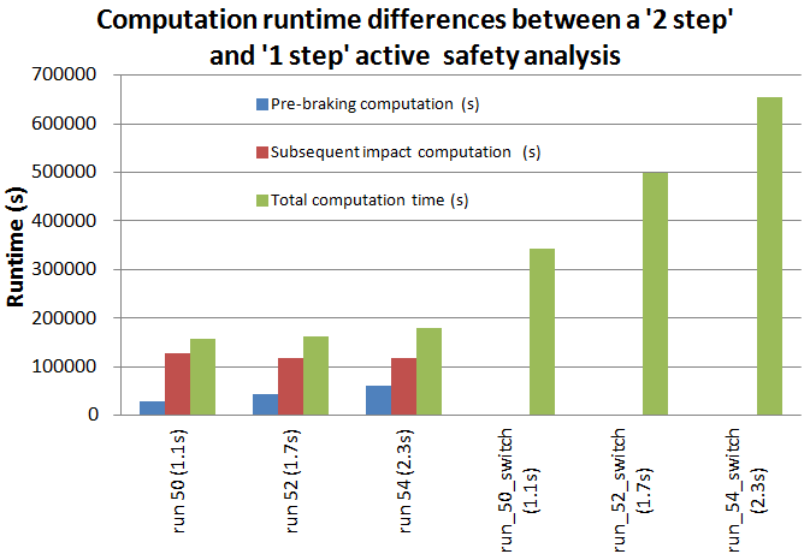

Figure 6.32: Runtime differences between 1-Step and 2-Step approach

The comparison has been performed by running all this study on one 2.4GHz node, with 12 cores. Looking at results in Figure 6.32**,** it can be observed that the 2-step split method is much faster than the 1-step one by a factor of 2.3 and 4.3 for a pre-braking duration of 1.1s and 2.3s respectively.

Because the 1-Step method includes all the framework parameters, it is judged that this method is the more accurate of the two, as it includes all the occupant pre-braking momentum events.

The following section will comment on the level of accuracy of the 2-Step method by comparing its injuries against the 1-Step method.

INJURY CURVES

From Figure 6.2 and Figure 6.3, it can be observed that the head and solar plexus displacements are very similar at time 1.1s. This suggests that the position of the occupant in each pre-braking loadcase is comparable at time 1.1s, just before the accident takes place.

Also, it can be noted that the occupant contact velocity against the restraint system is much lower in the pre-braking phase (Figure 6.33 and Figure 6.34) than in a 40km/h (25mph) FMVSS208 unbelted scenario (Figure 6.31). Nevertheless, occupant velocities in the pre-braking do not exceed 0.025m/s for the head and -0.025m/s for the torso for a braking duration of 1.1s.

Figure 6.33: Torso velocities (X) (Bastien 2013b)

Figure 6.34: Top of the head velocities (X) (Bastien 2013b)

Considering the 2-steps run_40, run_41, run_50 and run_51, it can be observed that the injury traces extracted for the repositioning are comparable for a re-mapping position describing a pre-braking lasting 1.1s (Figure 6.35**,** Figure 6.36**,** Figure 6.37 and Figure 6.38*)*, which is as expected.

The fact that the injury curves do not overlay 100% means that small differences in positioning are present which are caused by different seat friction and occupants' awareness level values.

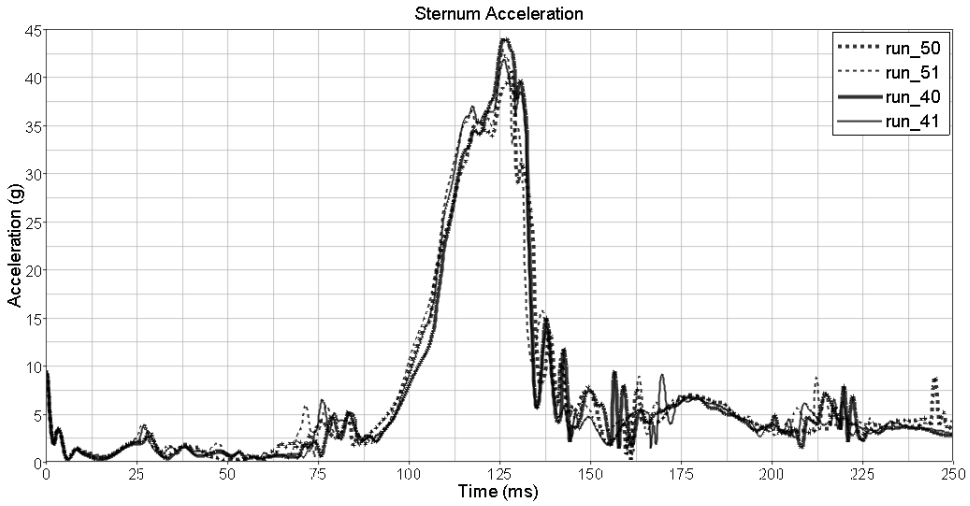

Figure 6.35: Sternum acceleration for all re-mapped cases at time 1.1s (2-step analysis)

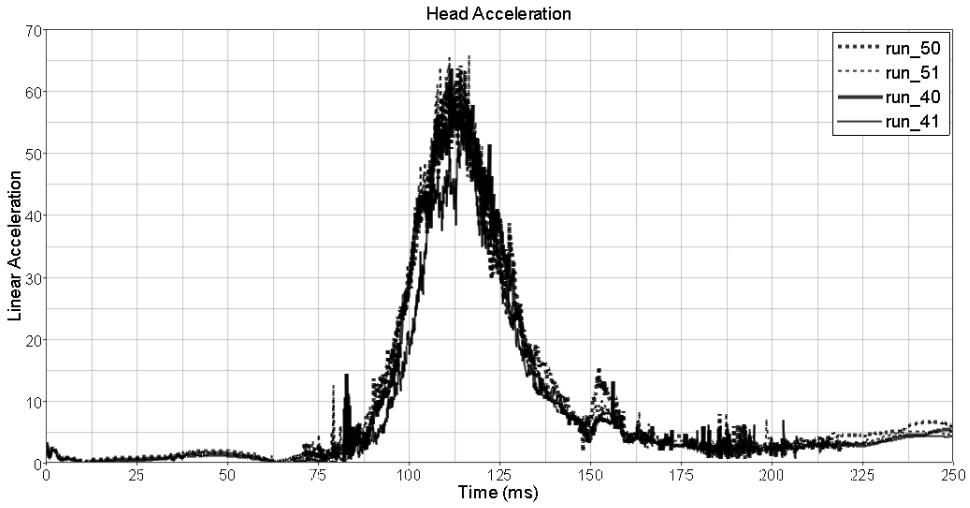

Figure 6.36: Head acceleration for all re-mapped cases at time 1.1s (2-step analysis)

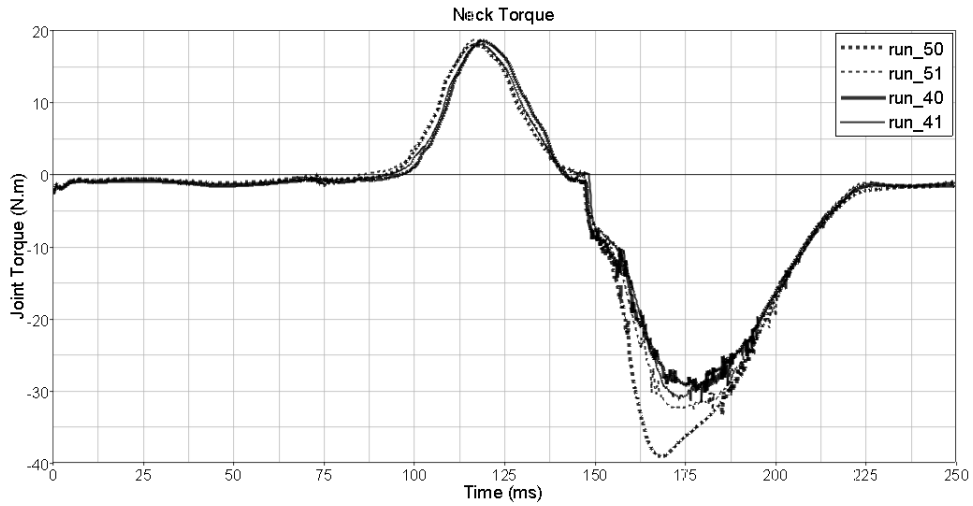

Figure 6.37: Neck torque for all re-mapped cases at time 1.1s (2-step analysis)

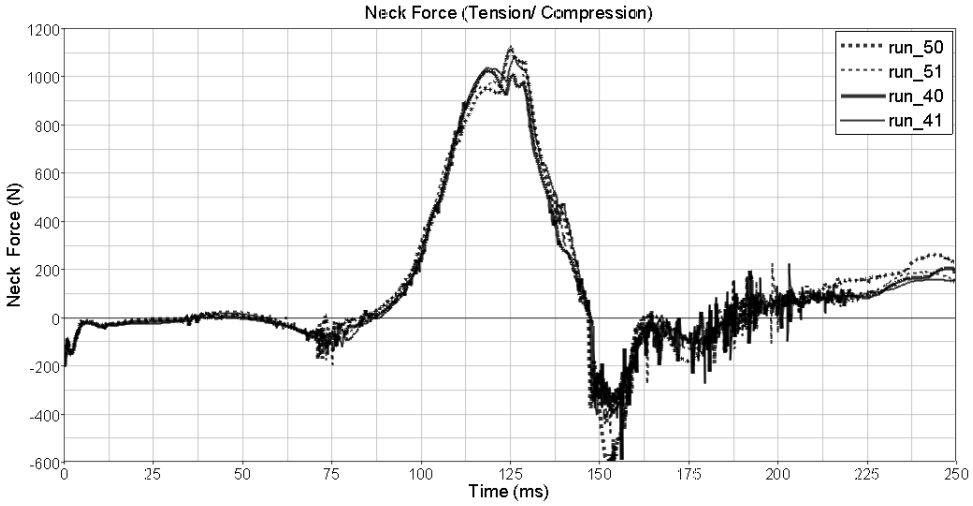

Figure 6.38: Neck forces for all re-mapped cases at time 1.1s (2-step analysis)

Comparing run_40, run_41, run_50 and run_51 to their 1-Step counterparts' run_40_switch, run_41_switch, run_50_switch and run_5_switch, it can be noticed that the injury values are in general higher (Figure 6.39**,** Figure 6.40**,** Figure 6.41 and Figure 6.42)**.**

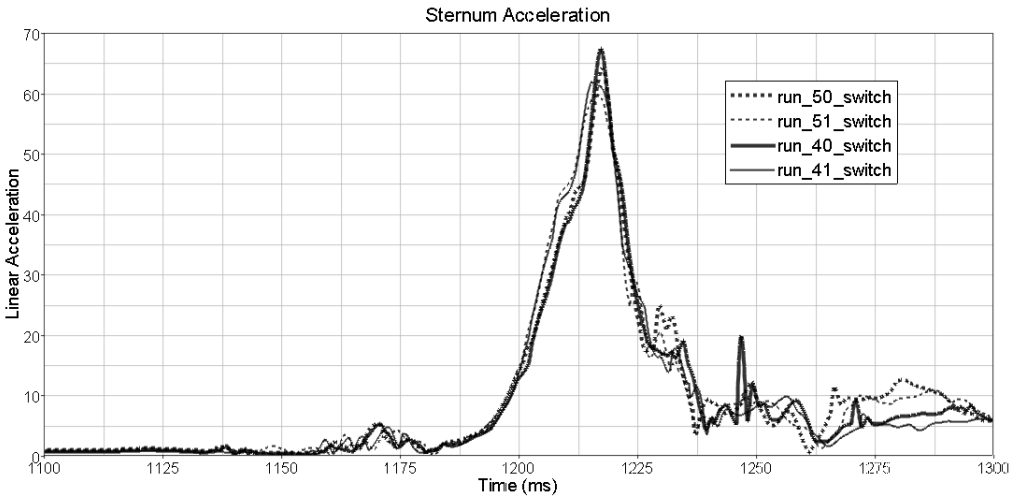

Figure 6.39: Sternum acceleration (1-step analysis) for pre-braking lasting 1.1s (1-step analysis)

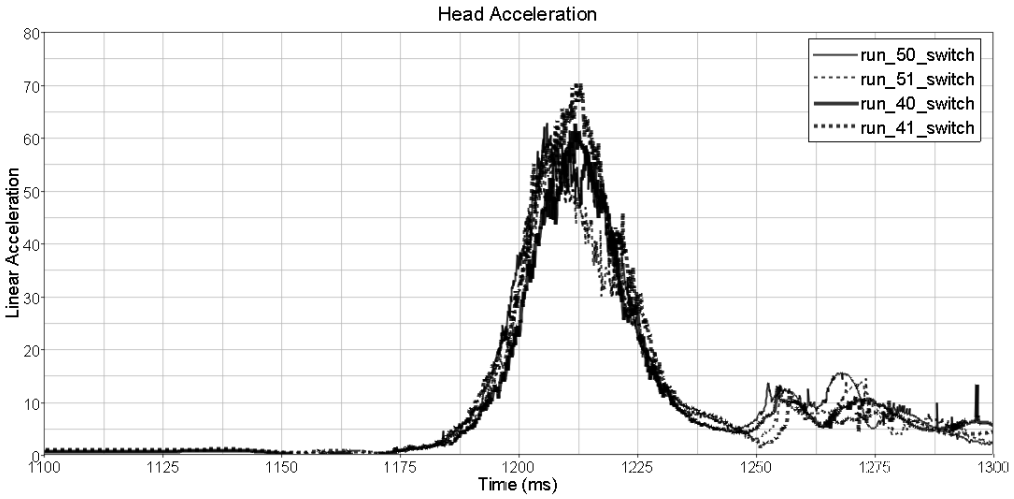

Figure 6.40: Head acceleration (1-step analysis) for pre-braking lasting 1.1s (1-step analysis

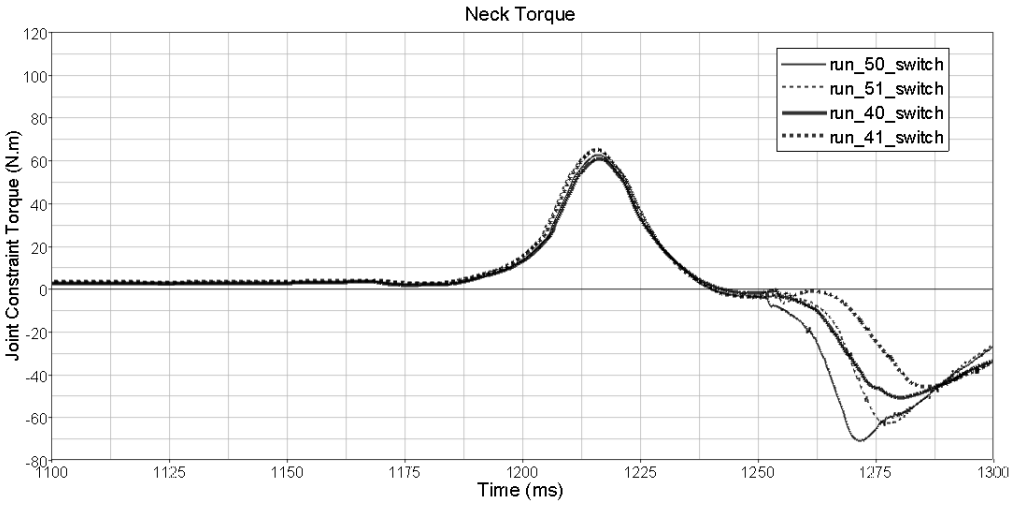

Figure 6.41: Neck torque (1-step analysis) for pre-braking lasting 1.1s (1-step analysis)

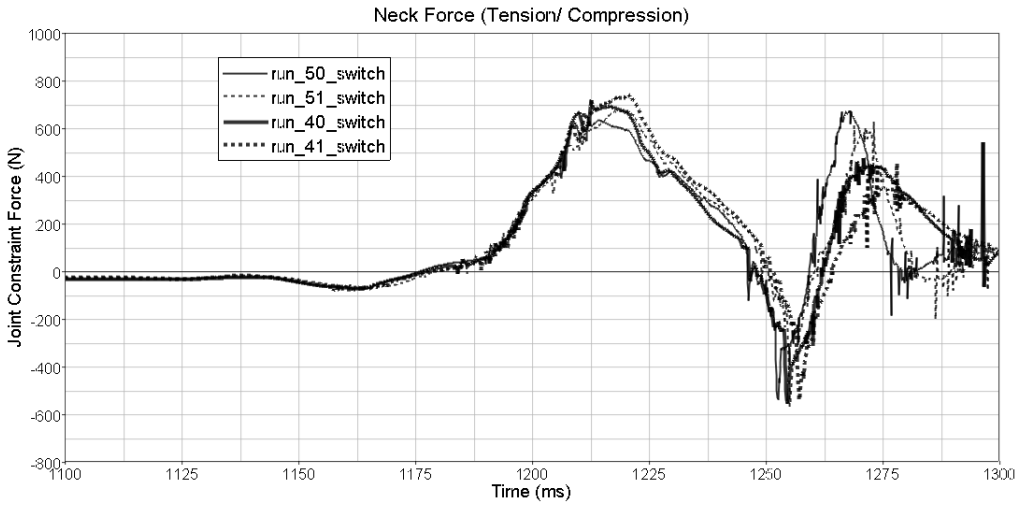

Figure 6.42: Neck force (1-step analysis) for pre-braking lasting 1.1s (1-step analysis)

It can be concluded that omitting the occupant initial velocity, even small, by only re-mapping the position induces differences in injury values. As a consequence, it can be postulated that even if the occupant initial velocity is small (Figure 6.33 and Figure 6.34), the effect generated by the momentum before a subsequent accident is non-negligible. As a consequence, at this point of the study, even for a pre-braking duration of 1.1s, only a 1-step analysis will provide realistic boundary conditions for occupant injury assessment.

At this point in time, it was recommended to TASS to program a routine which would automatically re-map joint and mesh velocities, in the same manner they can re-map joint-positions, as it is believed that this tool would have the great benefit to reduce greatly the computation time of the proposed framework (Figure 6.32).

Pursuing the study, more analyses were undertaken with braking duration of 1.7s and 2.3s. These runs have been overlaid to compare their shapes and magnitudes (Figure 6.43**,** Figure 6.44**,** Figure 6.45 and Figure 6.46).

All the impact events starting at 0s are re-mapped positions while the others reflect the braking duration, i.e. 1.1s (black), 1.7s (purple) and 2.3s (blue).

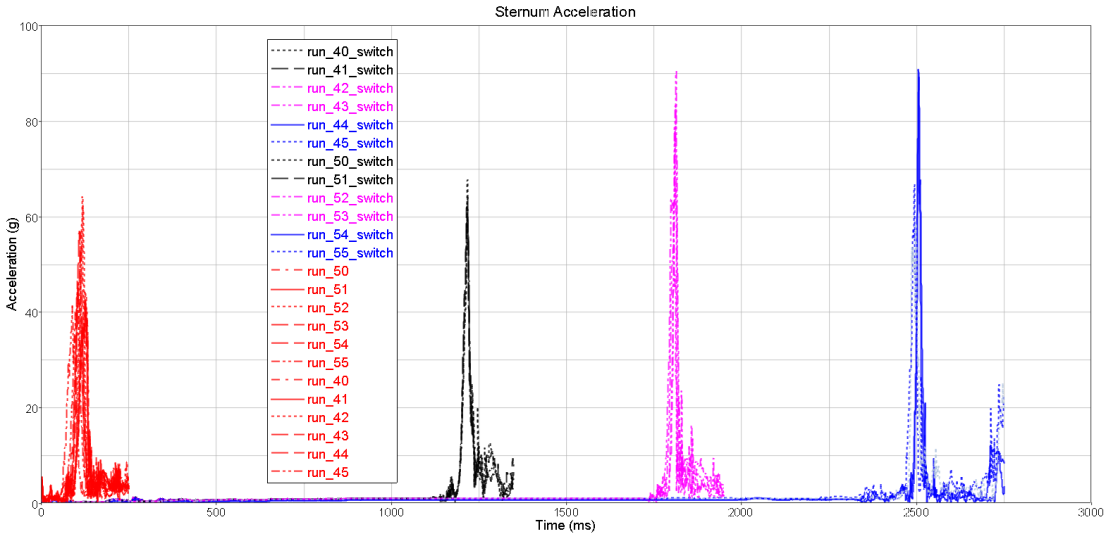

Figure 6.43: Overlay of all sternum accelerations (1-step and 2-steps)

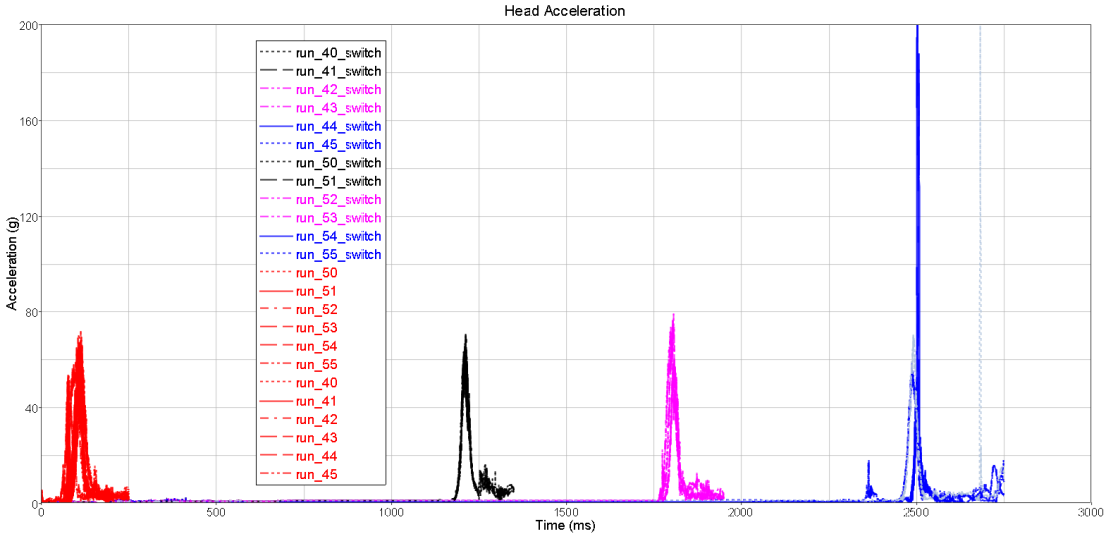

Figure 6.44: Overlay of all head accelerations (1-step and 2-steps)

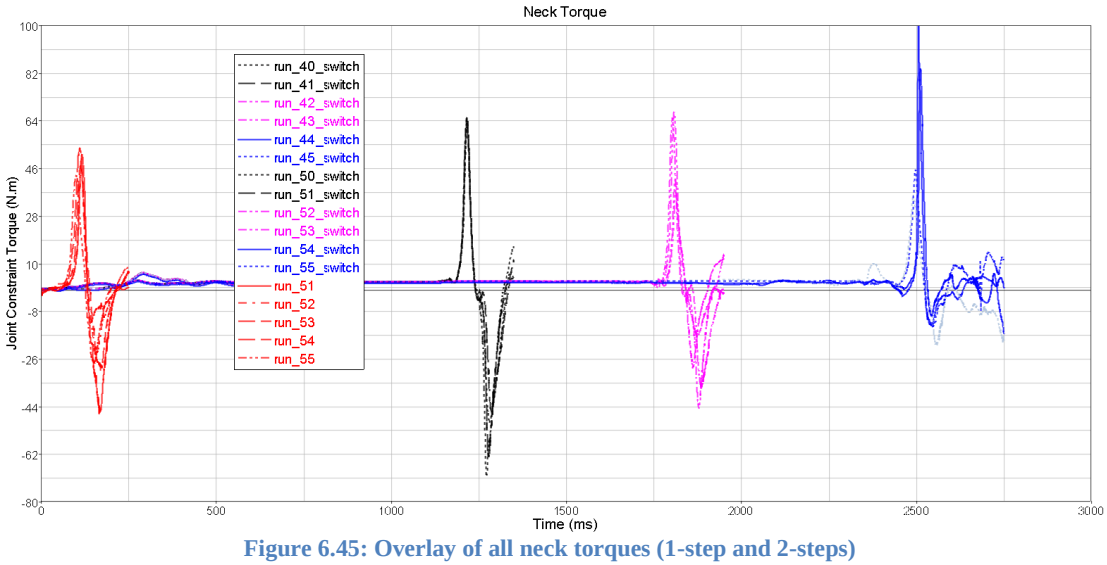

Figure 6.45: Overlay of all neck torques (1-step and 2-steps)

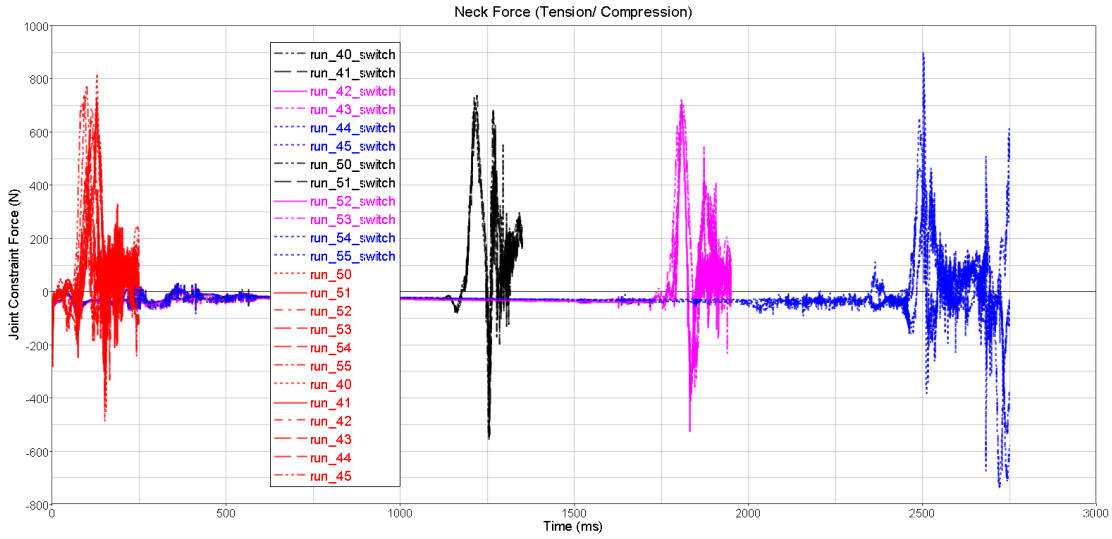

Figure 6.46: Overlay of all neck forces (1-step and 2-steps)

It can be noticed that, in general, the longer the braking duration, the higher the injury peak values.

MAXIMUM INJURY VALUES COMPARISONS

Injury values can be compared between the 2 methods and the reference model (Figure 6.47 and Figure 6.48).

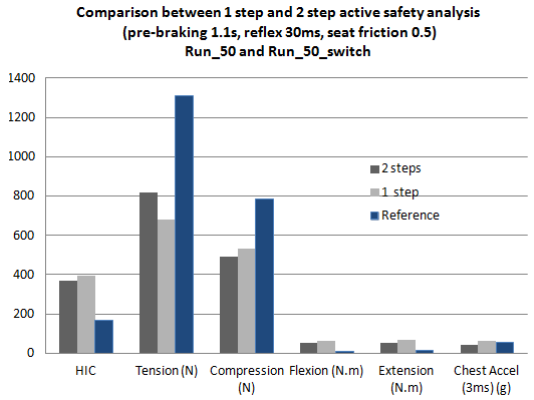

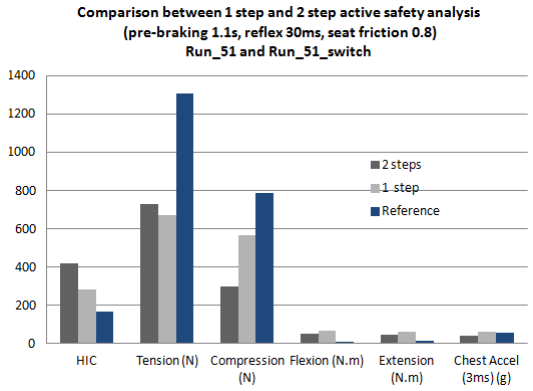

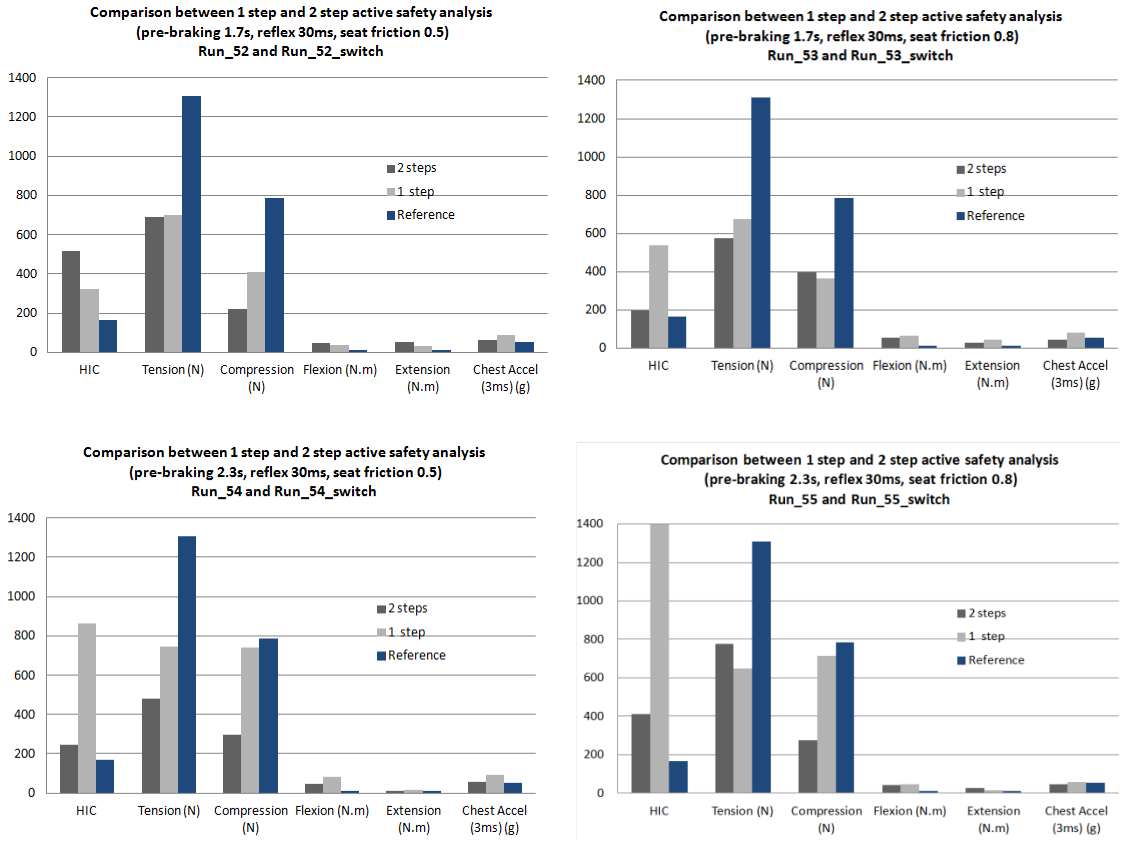

Figure 6.47: Summary of injury values (30ms reflex)

It can be noted that the 2-Step method is not adequate, as it does not give the same values as a 1-Step method. As such, this method will not be recommended, unless joint and mesh initial velocities can be remapped after the kinematics run. Comparing the injuries between a 1-Step method and the Reference model, it can be observed that except in the case of neck forces (Tension and Compression, all the values, the pre-braking scenario is worse in all counts for a 30ms and 120ms reflex delay (Figure 6.47 and Figure 6.48).

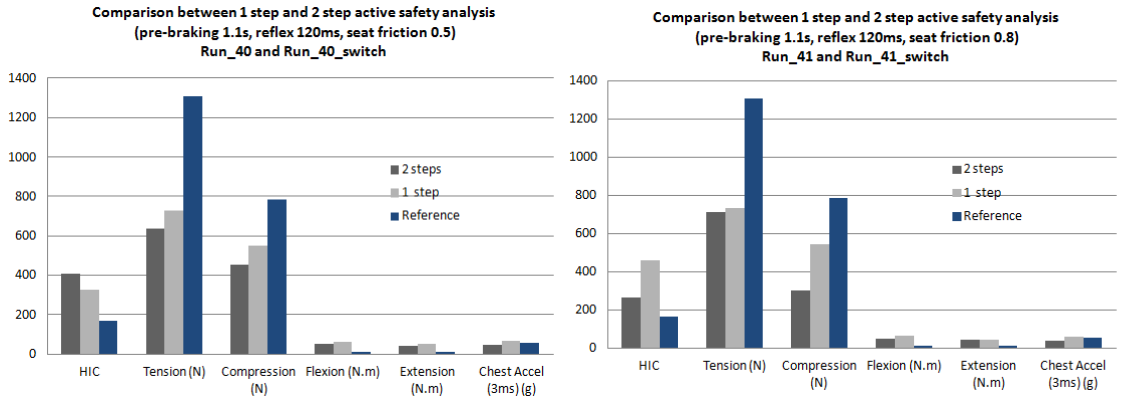

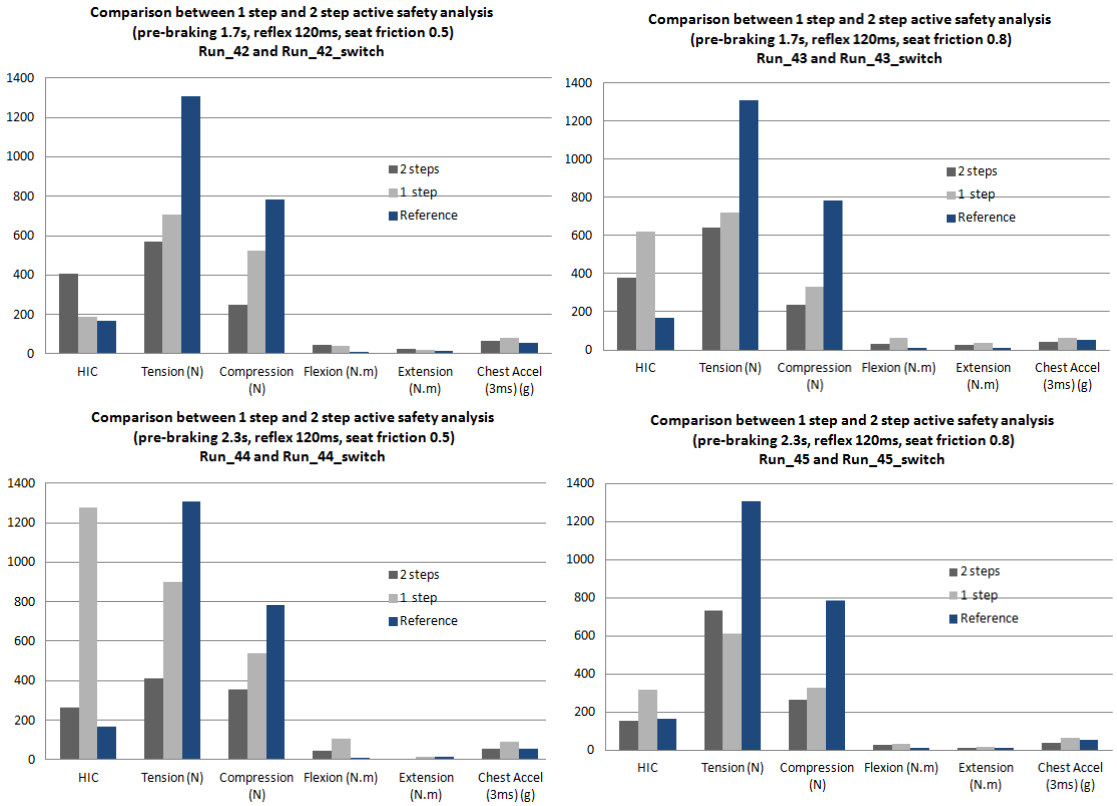

Figure 6.48: Summary of injury values (120ms reflex)

The neck tension and compression values are consistently higher for the reference model, which is indicating that there is a difference in the neck/ head area between a direct 40km/h (25mph) crash and a pre-braking followed by a subsequent accident.

Looking at a kinematics overlay between the reference model and a typical 1-Step model, it can be noted that during the pre-braking phase, the occupant's head is tilted more forward because of the force caused by the pre-braking deceleration (Figure 6.49) and this already at time 1.1s.

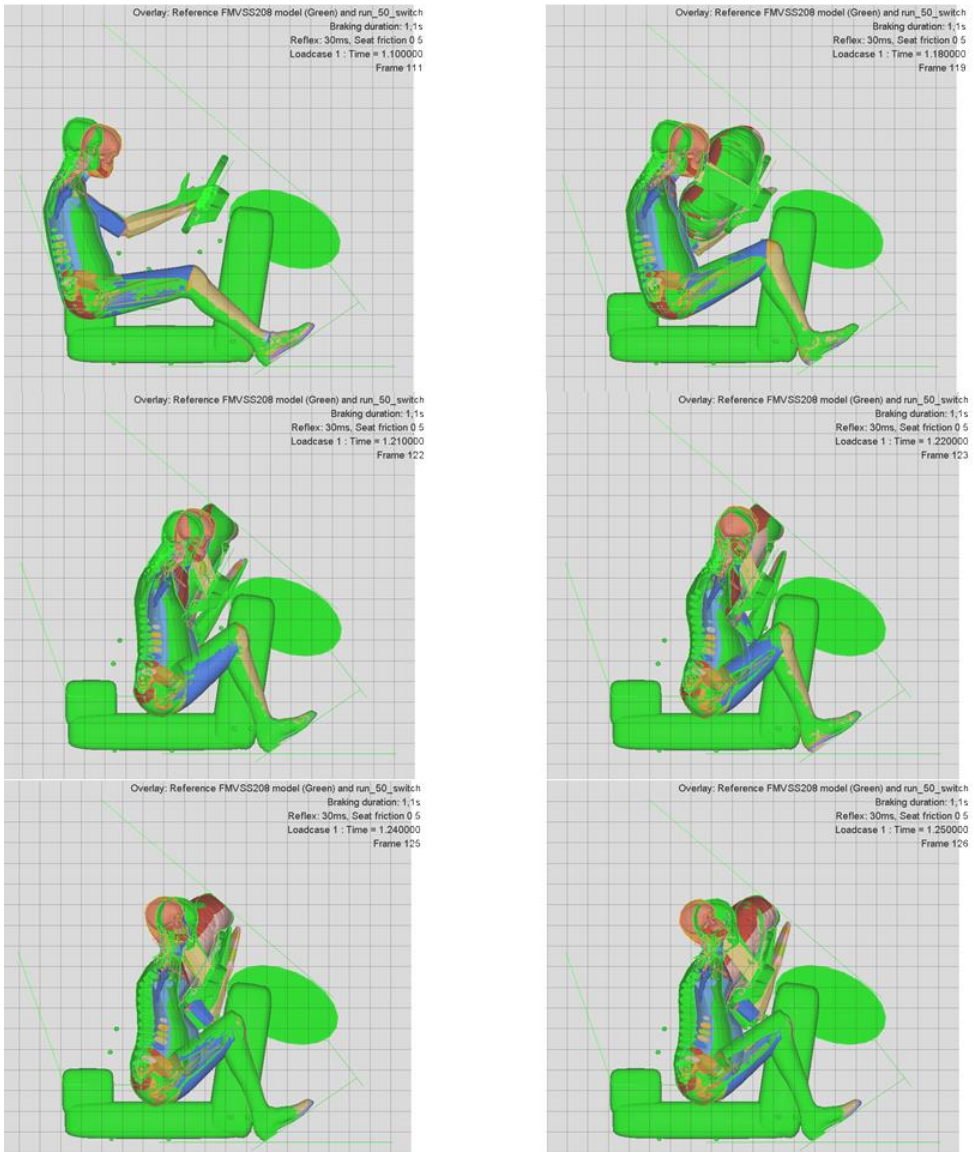

Figure 6.49: Overlay cross section between the Reference model and a typical pre-braking followed by a subsequent accident

In Figure 6.49, it can be observed that the head of the pre-braking model contacts the airbag first and that the neck of the reference model is straighter, which means that it takes more tension/ compression. It can be observed from Figure 6.47 and Figure 6.48 that contacting the airbag earlier does not generally increase the occupant's injury levels.

Comparing the start position of the occupant in Figure 6.49, and the end position of the occupant in the braking phase (Figure 6.5 and Figure 6.6), it can be also observed that the occupant's knees relative to the knee bolster are different. In Figure 6.5 and Figure 6.6, the knees are closer, which will imply that the kinematics during the

accident phase will be different. Furthermore the impact velocity of a standard FMVSS208 occupant has been estimated to be 6.5m/s (Figure 6.31), compared to 0.4m/s during a braking phase involving muscle tension (Figure 6.33 and Figure 6.34).

As a consequence, in the standard FMVSS208 test, more momentum will be generated and transferred into the airbag/ steering wheel assembly. This can be observed by monitoring the femur loads extracted from the computations, as displayed in Figure 6.50 and Figure 6.51.

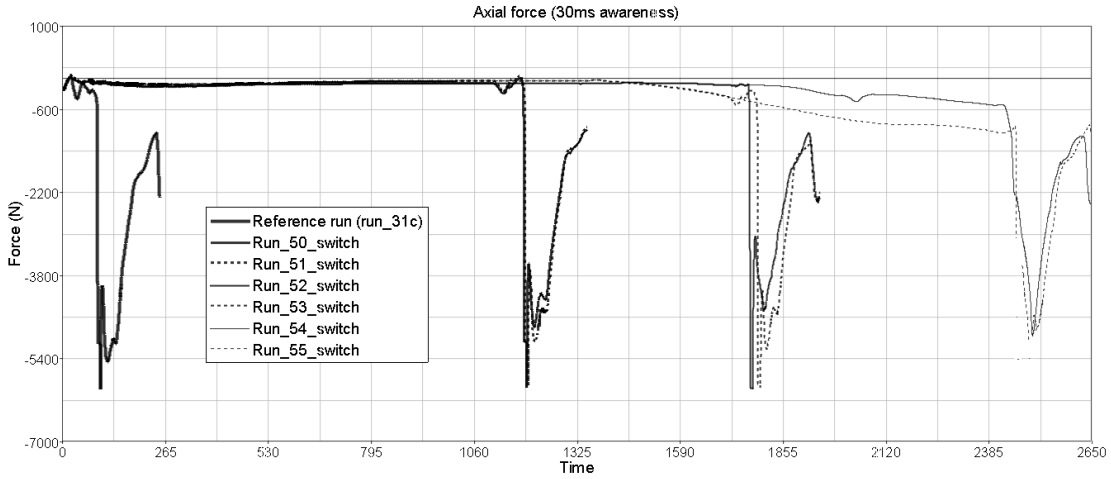

Figure 6.50: Femur loads (1 step) for occupant with 30ms awareness level

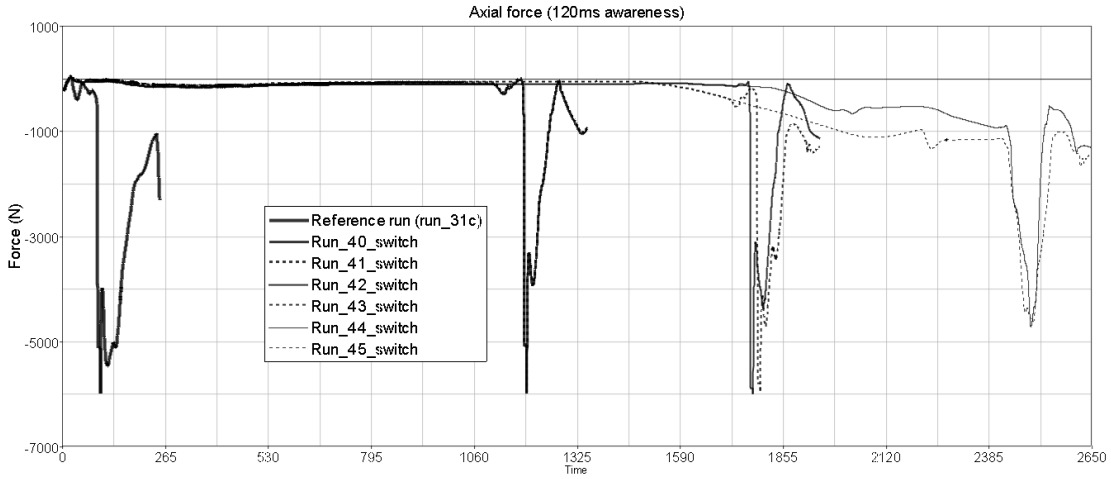

Figure 6.51: Femur loads (1 step) for occupant with 120ms awareness level

It can be observed from Figure 6.50 and Figure 6.51 that the longer the braking duration, the lesser the load on the femur. This is caused by the fact the femur is closer to the knee bolster prior to the crash event, as in the pre-braking duration of 2.3s studies in the ASsEt environment. As such less momentum is generated and

consequently less axial force is applied on the femur. The difference in initial velocity and position due to the occupant tensioning its muscles in the pre-braking phase seem to have a noticeable influence on the femur injury traces from Figure 6.50 and Figure 6.51 and are consistently lower than the reference loadcase. If the occupant is less aware, then more momentum is generated, leading to higher femur loads, as observed in Figure 6.50 and Figure 6.51. Increased friction on the occupant creates resistance to movement, hence more load is transferred to the femur from the foot and the tibia. As such, with increased resistance, the load in the femur increases until the knee joint starts to rotate. When this happens, the load in the femur decreases. When later the femur contacts against the knee bolster the compressive load picks-up again and is further amplified when the accident takes place. It can be noted that within the pre-braking phase only of the ASsEt environment, the axial force in the femur is around 1000N, which is less than the legal limit of 6800N. Nevertheless this is a considerable load in the occupant's knee joint for a typical pre-braking phase. If an accident is then taking place, the femur axial load can increase in the order of 6000N (Figure 6.50 and Figure 6.51), which is, within the ASsEt environment parameter used, close to the legal limit. The braking duration is influencing the occupant's kinematics in the subsequent crash scenario. A longer braking duration (2.3s) would mainly cause a rotational torso momentum in the crash phase because the knees are already in contact with the knee bolster at the time of impact. A shorter braking duration (1.1s and 1.7s) would allow a legs and torso translation followed by a rotation. As a consequence, the pre-braking phase will have an influence the restraint system ride down performance (Figure 5.52 and Figure 5.53

By dividing the reference injury obtained in Table 6.5 by the injury scenario studied (i.e. including the pre-braking phase), it is possible to calculate whether the occupant's injuries have increased or decreased. A ratio of '1' would mean that no change is observed, while a value greater than '1' would suggest an increase (direction highlighted by the arrow in Figure 5.52 and Figure 5.53).

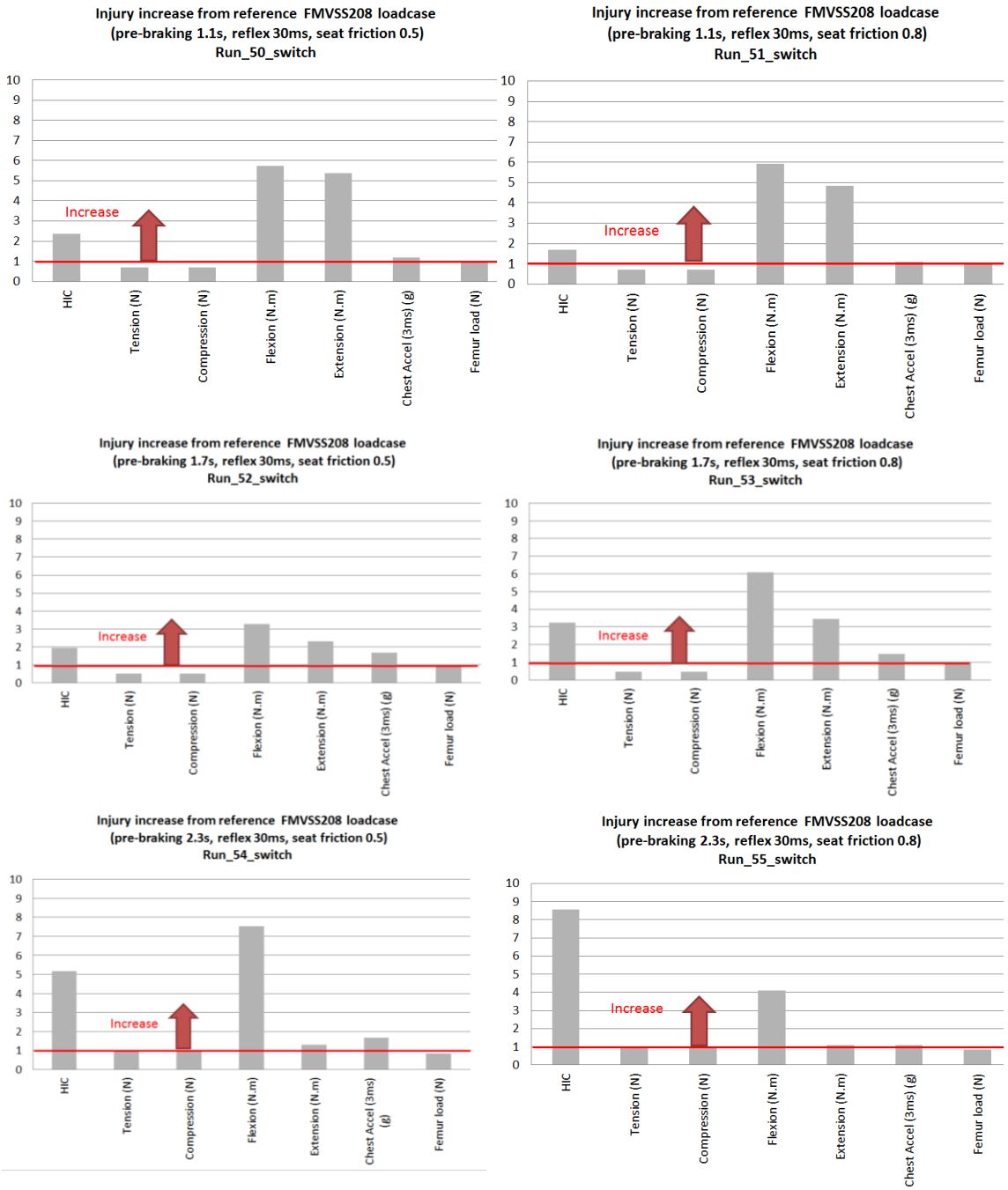

Figure 6.52: Injury increase from reference loadcase, Reflex 30ms

Comparing also the occupant's momentum in the Reference loadcase and a pre-braking scenario, it can be noted that the impact velocity of the occupant against the restraint system is around 6.5m/s in a 40km/h (25mph) rigid wall impact (Figure 6.31) compared to a maximum of 0.3m/s for the torso (Figure 6.33) and 0.4m/s for the head (Figure 6.34). This suggests that proximity to the airbag as well as the occupant's momentum have both an influence on the injury criteria. As a consequence, a sweep of braking duration would be necessary to assess the worst scenario giving the highest injury value.

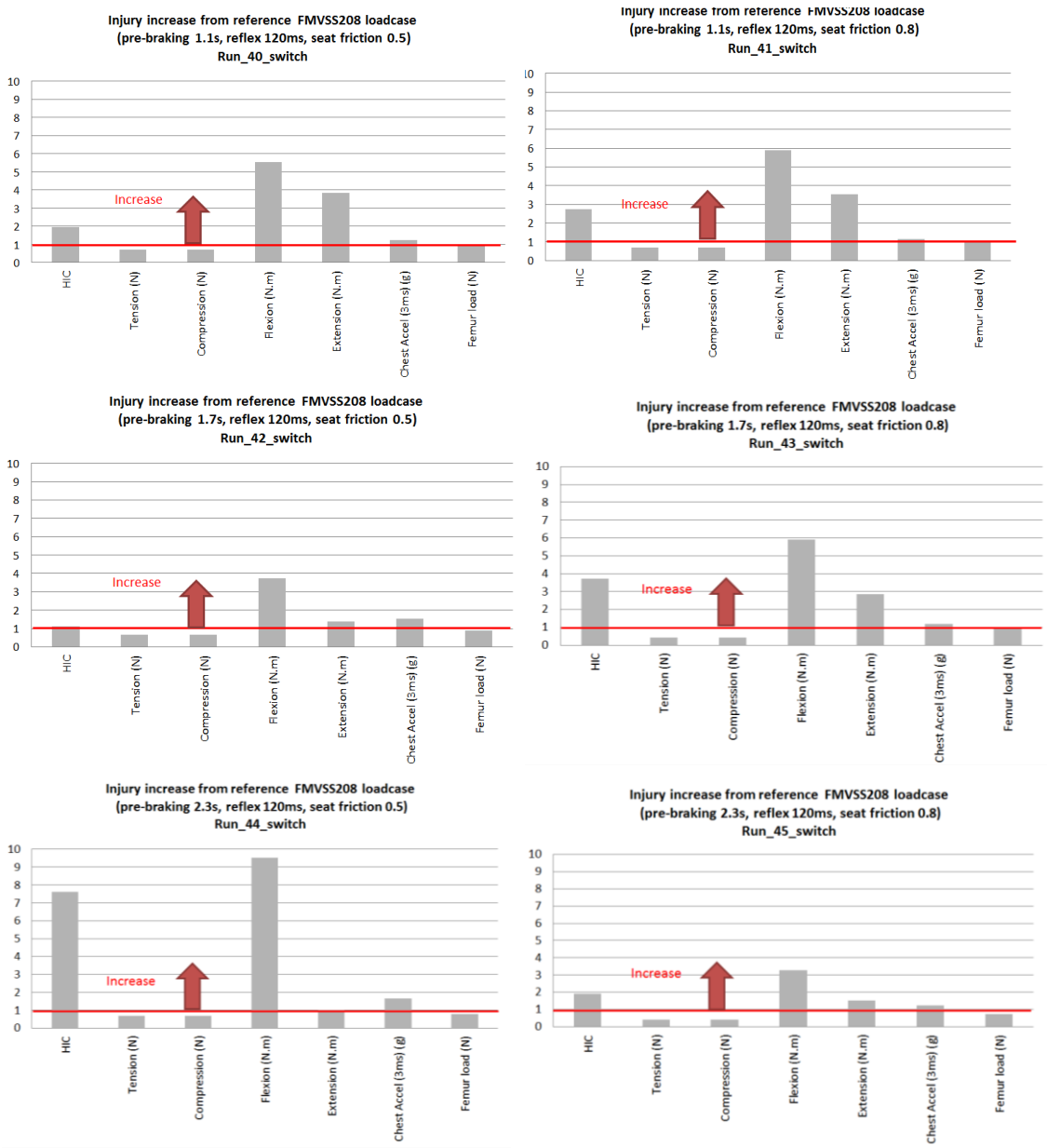

Figure 6.53: Injury increase from reference loadcase, Reflex 120ms

6.2.4 Results for the 1 hand grip (Mobile Phone)

As discussed in the previous section, it has been observed that the occupant using a 1 hand grip was away from the airbag zone of influence after 1.1s. As a consequence, it is assumed that a braking duration longer than 1.1s is not desirable with the parameters chosen within the current framework. As a result, only injuries up to 1.1s will be investigated, as the current computer model does not have the full vehicle interior geometry and stiffness characteristics to objectively provide a fair injury comparison compared to the 2-hand grip scenario previously studied in this chapter.

Furthermore, based on the findings from this chapter, only a 1step analysis method will be used.

Consequently only 4 computations have been performed and summarised in Table 6.6.

Run Name	Braking Duration (s)	Seat Friction	Awareness (ms)
Run 46_switch	1.1	0.5	120
Run 47_switch	1.1	0.8	120
Run 56_switch	1.1	0.5	30
Run 57_switch	1.1	0.8	30

Table 6.6: 1-hand grip CAE models considered

During the impact, it can be observed that the head deceleration contains various sharp peaks, as displayed in Figure 6.52, especially for run_46_switch and run_47_switch where the reflex delay is longer, i.e. 120ms vs. 30ms.

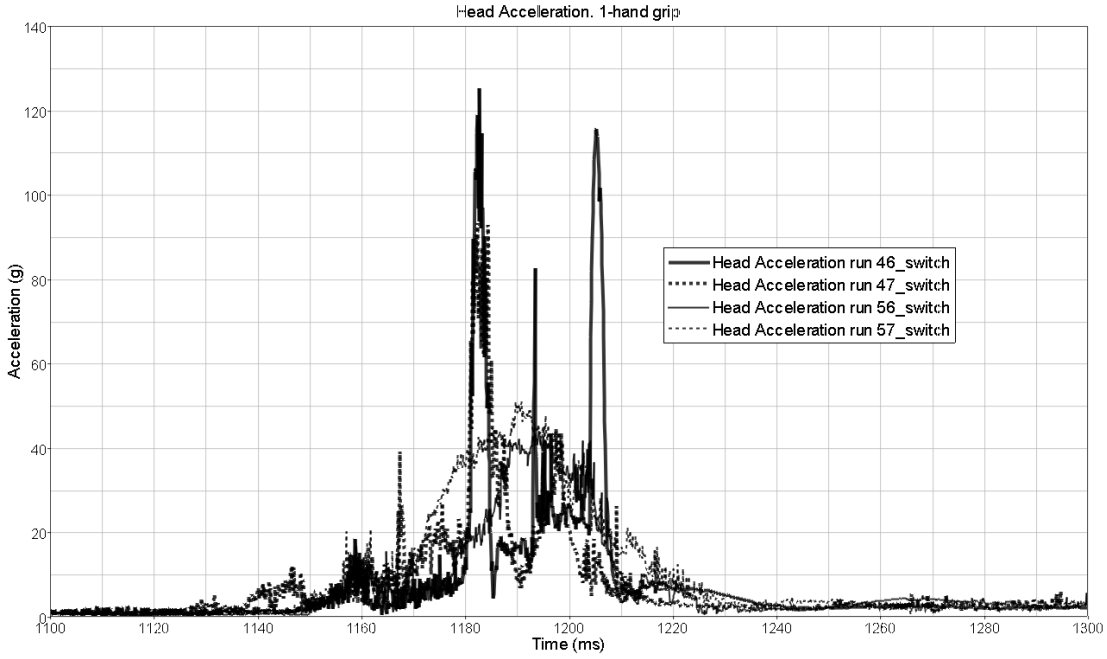

Figure 6.54: Head acceleration. 1-hand grip

The reason for these peaks is that the head overlaps less the airbag that the 2 other cases, as the reflex delay moves the occupant more outboard, as is depicted in Figure 6.53.

There is a perfect correlation between the timing of the head deceleration and the head contact against the steering wheel.

.

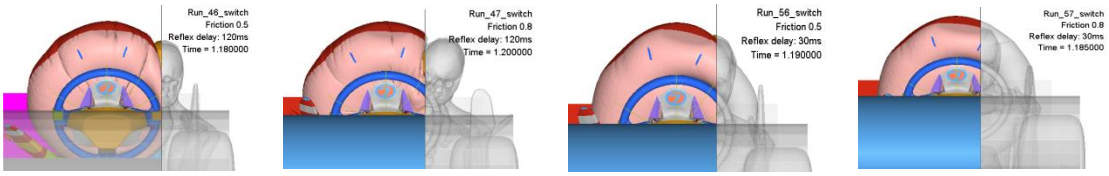

Figure 6.55: Head to steering wheel interaction

Considering torso impact force against the steering wheel (Figure 6.54), it can be observed that in all cases the chest decelerations is higher for the most outboard occupant positions, i.e. for run_46_switch and run_47_switch for which the reflex delay is longer, i.e. 120ms vs. 30ms (Figure 6.55).

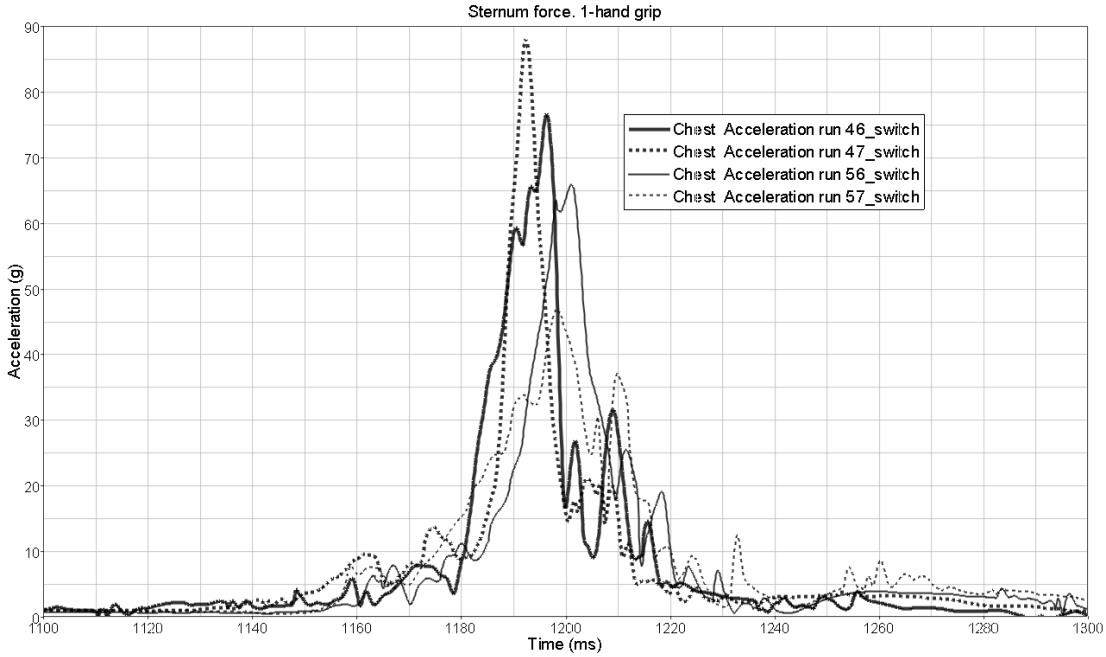

Figure 6.56: Torso acceleration. 1-hand grip

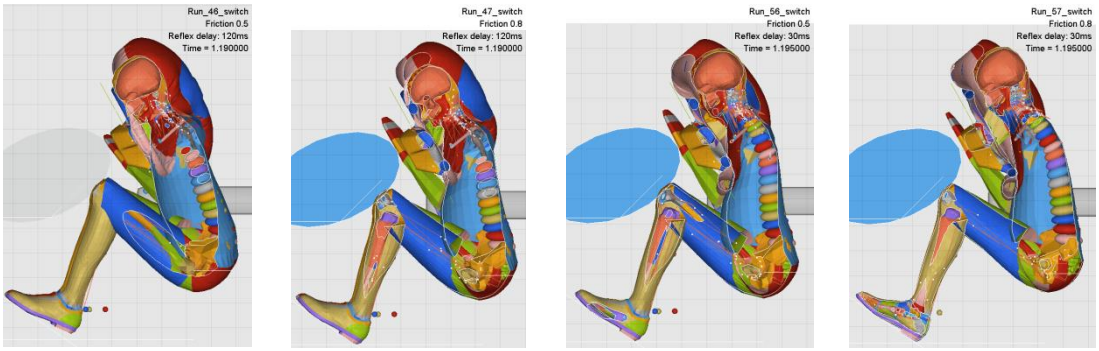

Figure 6.57: Chest to steering wheel interaction

This is caused by the fact that the airbag is not protecting the occupant as well as it is designed for. In Figure 6.55, it can be observed that in run_46_switch and

run_47_switch, the head and torso are contacting the steering wheel while in run_56_switch and run_57_switch the airbag is creating a safety buffer.

The trends in neck force and neck moments, depicted in Figure 6.56 and Figure 6.57, match the contact time of the head against the steering wheel, which is asymptotic at 1.180s, which is aligned with the start of the hard contact of the torso against the steering wheel rim.

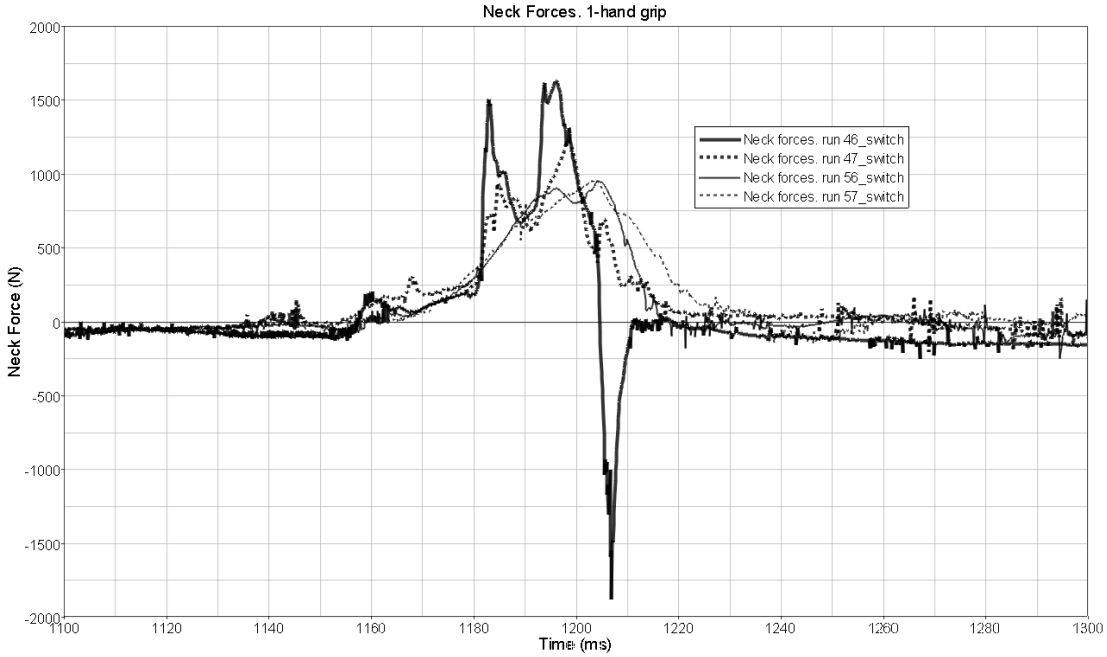

Figure 6.58: Neck forces. 1-hand grip

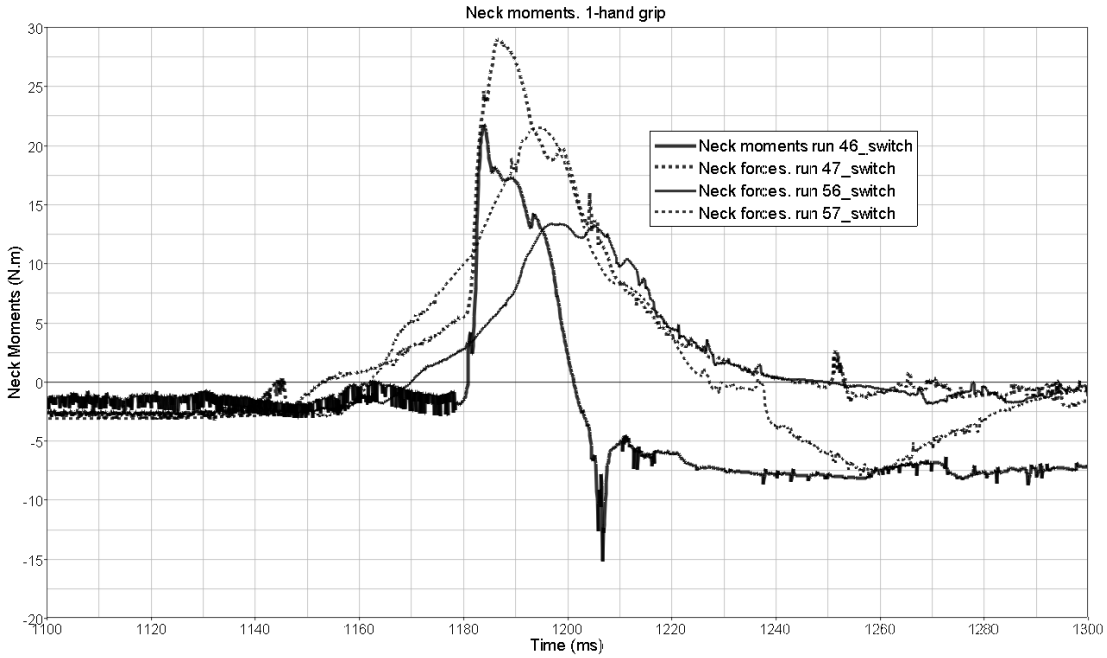

Figure 6.59: Neck moments. 1-hand grip

For braking durations higher than 1.1s, no restraint systems will be present to protect the occupant, as such it is expected that the generated injuries are likely to be much worse.

MAXIMUM INJURY VALUE EXTRACTION

Injury values can be compared between the 1-hand grip and the reference model (Figure 6.58), for a pre-braking duration of 1.1s.

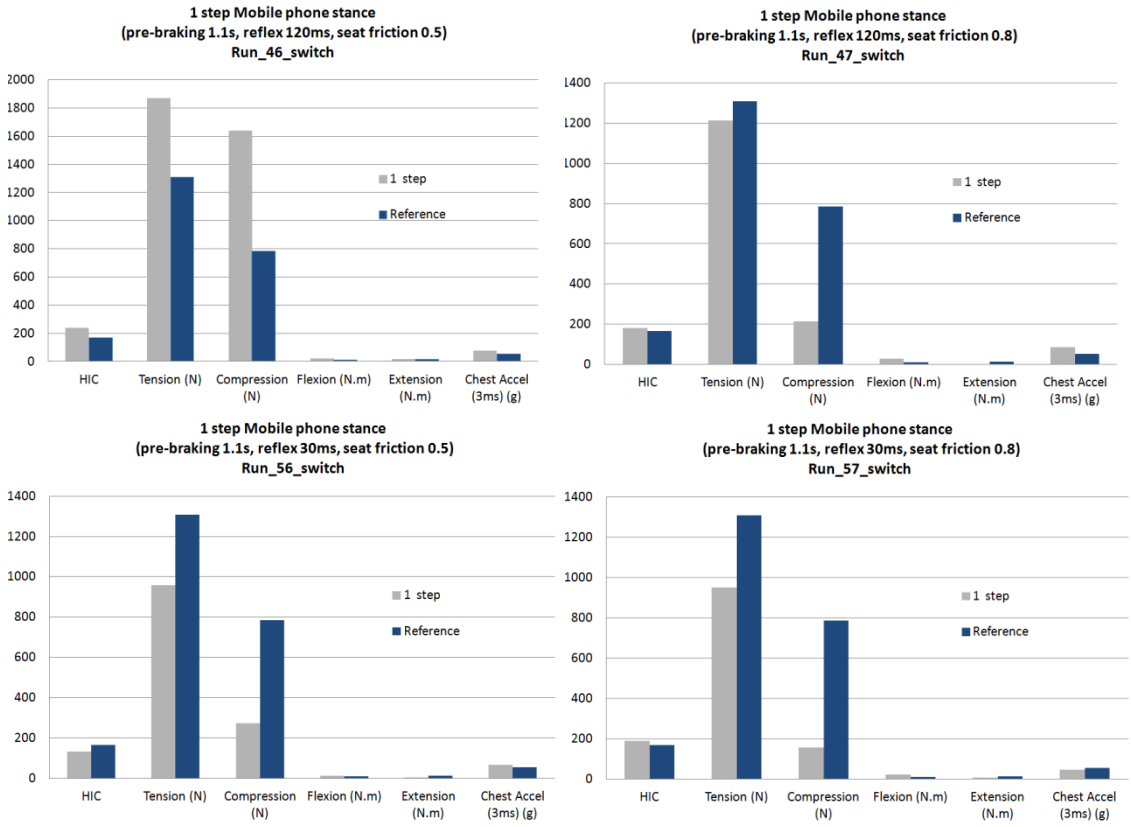

Figure 6.60: Comparison between the 1-hand grip stance and reference model for braking duration of 1.1s

It can be observed that occupants who are less alert will undergo higher injury values than the ones the restraint system would provide for a standard 2-hand grip, i.e. reference loadcase (Figure 6.59).

It is suggested in Figure 6.59, that in general alert occupants would withstand in general lower levels of injuries than a reference FMVSS208 loadcase. This may be because of the smart airbag used in this study which tends to inflate initially with a

bigger volume outboard than in its centre. Consequently, more cushioning would be available for the occupant early in the crash event.

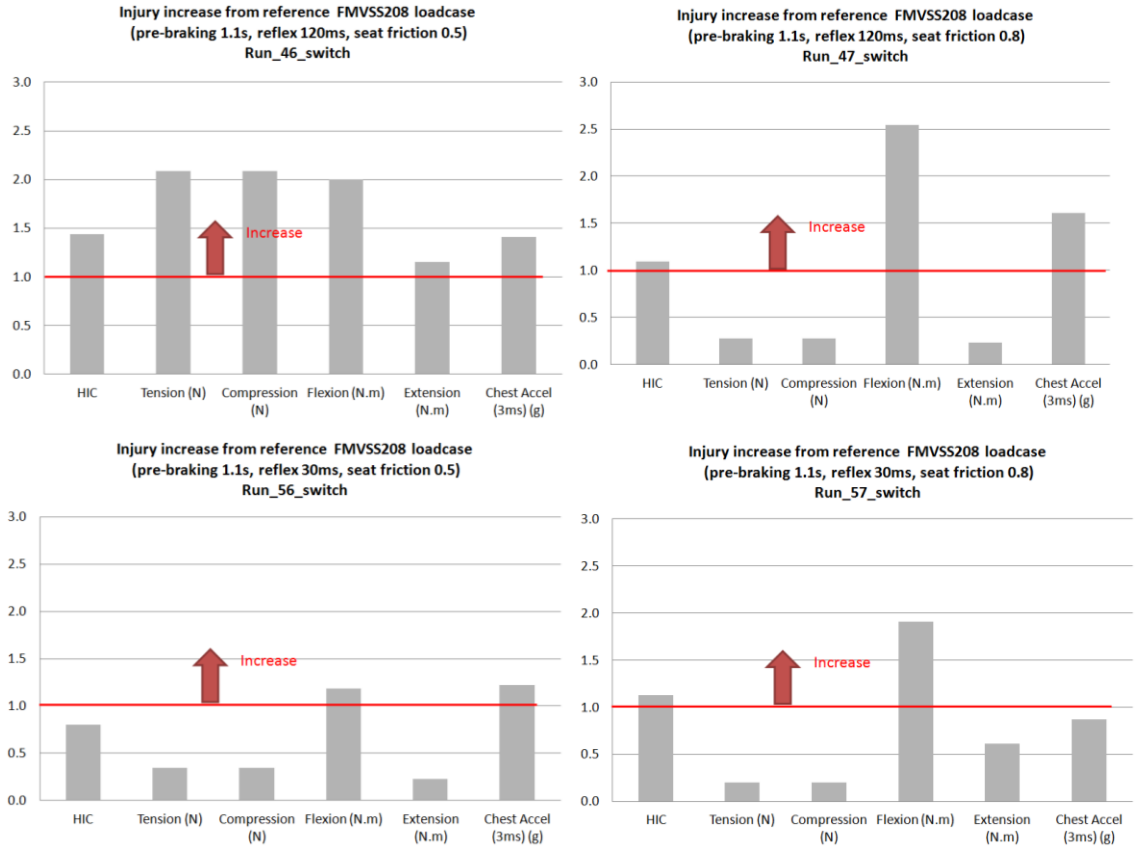

Figure 6.61: Injury increase from reference loadcase (pre-braking duration 1.1s)

The 1-hand loadcase has been analysed for a pre-braking of 1.1s, which positions the occupant still closer to the restraint system. It is suspected that a longer braking duration will not be favourable to the occupant as the benefit of the airbag system will not be there and that the only means of restraining the unbelted occupant is the dashboard.

6.3 Summary of the kinematic and injury assessment of the Active Human Model

The study concludes that the MADYMO AHBM is suited to model active safety scenarios and that the generated kinematics and injuries provided could be logically explained and plausible.

The study has established that, within the active safety scenario investigated, the occupant's kinematics depend on the seat friction coefficient, arms' kinematics and the level of awareness.

Two methods were investigated in order to investigate the opportunity to improve the speed of the ASsEt environment injury computation. It has been concluded that, failing to re-map the pre-braking initial velocity, it was not possible to reduce the framework computation runtime. As a consequence, only a 1-step run including pre-braking followed by a subsequent accident was a meaning full method for the ASsEt environment.

It has been noticed that injury values varied between a standard FMVSS208 50^{th} percentile unbelted occupant and its injuries sustained through the ASsEt environment. The mechanics of dynamic OOP suggest to be a very complex phenomenon and that momentum and proximity to the airbag are both certainly 2 important parameters for injury causation. It was noticed that in the FMVSS208 test, the occupant is far from the airbag, but its throw away velocity is higher than an aware person using muscle activation who is closer to the airbag, hence having a lesser airbag contact momentum.

It was not possible to conclude on the definition of the worst loadcase for a 2-hand grip 'aware' occupant within the ASsEt environment, nevertheless dynamic OOP suggested injury values are generally higher than injuries assessed through standard FMVSS208 test configuration. It is however possible to reiterate, based on the study undertaken in Chapter 6 and the findings in Table 2.6 from the Literature Review chapter, the safety benefits of using a seatbelt in case of accidents. Concerns from the WHO (WHO 2013) about the use of mobile phones seem to be substantiated from the analysis performed, reinforcing the fact that using a mobile phone whilst driving is not recommended.

It would be therefore recommended that various braking durations are investigated to verify the overall safety performance of such active safety systems.

It has been observed that a 1-hand stance generated large rotations of the occupant in the cabin, which leads to an offset across the cabin having for effect to move away from the restraint system zone of influence. In the study presented, for a set of framework parameters, it has been observed that the occupant would start to be vulnerable from a pre-braking duration of 1.1s. This offset seems to be more important for lower seat friction values and lower awareness levels.

Overall, the study concludes that the MADYMO AHBM used in this research provides believable kinematics and injury response behaviours. This model is very stable and has responded in a plausible manner when numerous variables, like seat friction, reflex delay and braking duration, were introduced.

7.0 Discussion

The study undertaken has investigated the prediction of the kinematics and injuries of unbelted occupants under Autonomous Emergency Braking.

Systematic testing (as detailed in chapter 5) has shown that in an unbelted loadcase, the torso is not restrained by a 3 point seatbelt; therefore its motion is expected to display more pronounced rotations. Moreover, the seat friction will reduce the occupant's forward motion during the pre-braking phase; consequently, considering also the statement about the torso increased rotations, it is reasonable to suggest that an unbelted passenger's motion under a pre-braking loadcase would respond in a similar way as a passenger wearing a lapbelt. Therefore, the volunteer tests conducted were based on a sled model with a lapbelt restraint configuration.

In the first step, the active human computer model's kinematics, using a lapbelt, has been successfully validated against a data set of 3 volunteers encompassing head and torso displacements under 1g frontal deceleration. A lapbelt was used in this study because it would have been too dangerous to perform tests on volunteers in an unbelted configuration, given the potential of ejection and body contacts against the sled interior. This configuration was judged the most adequate to evaluate relevant human volunteers reflex kinematics properties with a certain relevance to an unbelted loadcase (OM4IS, 2010 and Ejima, 2009).

The correlation in chapter 5 ("Correlation of an Active Human Model Restrained by a Lap Belt in Frontal Manoeuvring Conditions") was executed by generating head and torso motion target curves based of the median of 13 volunteers tests, performed by the OM4IS consortium (OM4IS 2011) at the University of Graz (Hüber 2011a) (Hüber 2011b), utilising 6 markers on each human (2 on the head, 2 on the torso and 2 on the back). It is acknowledged by the author that the number of volunteers displaying a clear 'reflex' behaviour was small; also, it is not known whether the volunteers were anticipating the sled's starting motion, hence generating some bracing behaviour.

This said, the active human model in its original configuration presented a slightly stiffer neck response than the one that emerged from the tests. This may be caused by the fact that the current active human model was correlated against volunteers wearing a 3-point seatbelt, preventing any excessive thorax rotation, which would inherently lead to a greater head rotation amplitude. Nevertheless, after weakening the

neck's response (i.e. making its muscles weaker), the validated active human model's overall kinematics have been overlaid against all of the 13 volunteer tests and presented a believable motion behaviour of a 'tensed'/'active' occupant, as the responses laid within the observed OM4IS data samples. Therefore, this correlated model can predict scenarios where the torso's rotation is excessive, e.g. where the seatbelt is not restraining its motion. It was noted that a passive human model could not replicate any of the active kinematics from the sled tests; hence, the muscle activation is a necessary feature to model low deceleration frontal braking scenarios (under 1.0g). A new MADYMO active human model will be shortly released in MADYMO 7.5.0 and its kinematics should be re-evaluated against the OM4IS test and target curves generated to ensure that the new modifications in the neck area are acceptable.

The thesis has shown that the setup of the MADYMO active human computer model has major setup advantages compared to a full finite element model one, such as the THUMS4.0. This is due to the fact that the MADYMO active human model is a hybrid of multi-body and reduced finite element shell models. During the setup, the limb joints can be independently moved, carrying directly the finite element mesh at the same time, limiting mesh geometrical distortions hence limiting the risk of computation instabilities. Setting up the contacts within the model is now straightforward, once the MADYMO switch on the FACE_TYPE orientation was applied (see Appendix A). Some unpublished work by the author in the positioning of the THUM4.0 finite element model (Evans 2013) has highlighted the need of using prescribed motions transformations to the rigid bones in order to place hands and feet in the proper position and location in the vehicle cabin. For instance, the re-mapping of the flesh strain values caused by the contact of the buttocks against the seat for example prior to performing a crash simulation was necessary, making a full finite element model very cumbersome to use. It is noteworthy, however, that the MADYMO active human model is only capable of outputting injury criteria and not trauma values, as no internal organs are present in the model. Consequently, each model can answer a different research question and could be regarded as "fit for purpose" should be used in specific applications.

The thesis has shown that the MADYMO active human model is suited to model the occupant kinematics in a full 2.3s pre-braking duration event. This model computes rapidly and is very stable. Having proven that the reflex behaviour was believable, this active human model is a very useful and effective industrial tool to model the occupant's motion within the cabin.

The thesis has also highlighted in detail the modelling of the second phase of the ASsEt environment, i.e. the accident phase. It has been proven that a 1-step simulation was the only method currently suitable to simulate the proposed ASsEt environment, i.e. encompassing a continuous computation of the pre-braking and the crash event.

This conclusion also makes sense, in a physical sense, as the occupant in the pre-braking stage has an initial velocity, hence, possesses more momentum than an occupant static with a re-mapped joint positions (setup from a 2-step analysis). This velocity, which is in the order of 0.3m/s, has major consequences on the magnitude of change in the injuries. In general, looking at the 2-hand grip results, the 1-step simulation predicts generally higher injuries than a 2-step simulation. The drawback of a 1-step simulation, nevertheless, is its computational cost; hence, a method to remap the human velocities from the pre-braking phase would yield to a very important computational improvement.

Considering the validity of the active human model in an unbelted scenario, it can be noted that its correlation was performed with a lapbelt. Consequently, it can be argued that this model may not be suitable in an un-restrained environment, as the boundary conditions appear to be very different. In section 5.4, it was proven that during the first part of the pre-braking phase the seat friction was the key contributor to the occupant's motion, justifying that this model is appropriate for unbelted scenario.

Consequently, the effect of the friction has in principle in the early phase of the pre-braking (less than 1.0s) the same function as the lapbelt (Cummings, 2009). Because the lapbelt is physically overlapping the occupant's lap and is fully secured to the vehicle structure, it will restrain the occupant more than seat friction past a 1s braking duration. Nevertheless, the first phase is to resist pelvis motion (translation and rotation) and load the arms which will either resist the second phase of the pre-braking or flex. As such, the modes of restraint are comparable between the 2 examples.

In order to justify the suitability of this model, an ASsEt environment has been created to replicate a frontal active safety scenario in order to assess the computer model's response. Considering a 2-hand grip, it has been observed that the occupant kinematics, i.e. postures, could be logically explained, by the means of pelvis to seat forces, steering wheel hand grip forces and arm angles. The more aware the occupant, the further his/her posture from the steering column, as its muscle activation, hence resistance, is faster compared to a distracted person or unaware. The less aware occupant has increased body momentum which is reacted late by the arms, leading to an elbow flex, i.e. change of arm angle relative to the steering wheel. Similarly, the higher the seat friction, the further the occupant is from the steering wheel, which is an expected outcome. Consequently, the occupant's reflex kinematics can be logically explained. As it has been documented that it would be too dangerous to perform the OM4IS and Ejima volunteer tests unbelted (Ejima 2009), this validated active human model is the most advanced model to simulate such an extreme 1g frontal braking loadcase.

During the pre-braking phase, within the ASsEt environment's variables used and for a braking duration of up to 2.3s, no hard contacts of the head and thorax against the vehicle interior were observed. This suggests that, within the parameter values selected in this thesis, the pre-braking phase on its own of an unbelted occupant is not life threatening. It has been observed, however, that the knees were contacting the knee bolster when excessive pre-braking durations were in place. In this instance, the recorded axial compression loads on the femurs were computed at 943N (during the pre-braking phase, prior to the accident), which is below the legal value of 6800N. Nevertheless, this appears to be a considerable load on the occupant's knee joint and as such, maybe a more detailed study of the patella injuries would need to be considered using possibly a Finite Element Model to investigate the potential permanent damage (Crandall, 2013).

As humans may be considered as symmetrical about the sagittal plane, the muscle activity is also symmetrical for a frontal deceleration. It can be observed in the thesis that the driver's feet were in all pre-braking scenarios side by side which may be representing a typical stance using an autonomous vehicle or using a cruise control. This posture uses the property of the sagittal plane, comparable to the OM4IS test setup for which the model has been validated against, and has the advantage to

remove 1 variable in the study which is the feet positioning in the foot well. Usually drivers have their right foot on the accelerator and their left foot on the foot rest, hence it would be beneficial to further validate this active human model in a more common vehicle driving standard and record for example the magnitude and timing of feet forces on a rigid force plate against the same OM4IS test setup. Such a test could have been relevant as it would have broken the symmetry in the loading and would have confirmed whether both sides of the active human model work well and detect whether the muscle coupling between the left hand side and right hand side of the human model is validated. In the current test configuration, it is not 100% certain that this model's cross interactions have been properly validated as the tests are symmetrical about the sagittal plane. It is expected that more detailed work in this area of validation is needed from the software vendors. It is believed that the feet position would be more relevant for the stance in which the occupant is holding the steering wheel with 1-hand and not with a 2-hand grip, as excessive upper body rotations in a 1-hand grip has already been recorded in this thesis.

As the 1-hand grip involves a body rotation which is taking place laterally, it can be questioned whether the model's lateral motion amplitude is accurate, even if the motion response can be generally explained. Indeed, this model is not yet validated for 1.0g lateral loadcase or lateral motion. Some work has been performed (Ejima, 2012) (Bastien, 2012), nevertheless in the first case only 3 volunteers datasets were extracted and in the later a huge scatter was observed. The latest MADYMO Active Human Model 7.5.0 (TNO, 2013), still does not have any lateral correlation under 1.0g. Consequently, should the 1-hand grip lateral motion be logical, its amplitude and magnitude are not guaranteed. It is not certain if the pre-braking was to happen in a cornering scenario, as the centrifugal force would exert a lateral load for which the correlation level is not documented.

As discussed in the Methodology section, it is believed that the vehicle brake dive, not modelled in this thesis, may also have an influence on the occupant's kinematics within the cabin and the injuries. In the Literature Review section of this thesis, it has been observed that the brake dive, recorded from the front of the vehicle, was in the order of 100mm (Ray 2006). This may not affect a belted occupant as the lapbelt component of the 3 point belt secures the occupant in the vertical direction. Consequently, if the vehicle dives, the cabin dives with the seat and the occupant's relationship with the airbag remain constant. In the case of an unbelted human

occupant model (or a less aware active human), when the vehicle brakes suddenly and dives, the occupant keeps on travelling forward while the front of the vehicle moves downwards changing the cabin's relationship between the driver and the restraint system. This has for effect of positioning the airbag system lower than its intended position set by occupant, having adjusted the steering column height and angle before driving the vehicle. This may be cause for concern as the occupant's sternum relative position to the airbag system will be unknown. As a result, the outcome of such scenario would need further investigation. Consequently, modelling this brake dive feature (Ray 2006) and considering the driver's level of awareness must be a relevant future research topic (section 3.5). Preliminary studies (Bastien 2012a) have shown that holding a mobile phone against the ear closest to the car door was causing reduced body lateral motions away from the seat centre line due to the presence of the door. In the case where the occupant is holding the mobile phone to the ear closest to the centreline of the vehicle, no means of restraining the motion is available. As such, within the modelling assumptions in the ASsEt environment, it has been suggested that a braking duration above 1.1s would position the occupant away from the airbag's deployment zone. This offset is more important for lower seat friction values and lower awareness levels (section 6.3). As such it is being proposed that the kinematics may also be influenced by the feet positions and the type of vehicle hand-drive. It is suggested that the angle of the tibia to the floor is relevant as more load can be transmitted the more stretched the leg is, causing more resistance to the motion (section 6.2.3). Hence for a stretched leg with the foot pressing the accelerometer, a left hand drive vehicle may lead to lesser lateral occupant motion than for a right hand drive vehicle as the angle of the foot relative to the floor will provide less counter force.

During the accident phase, all injuries could be explained as well as the trend from the framework which suggests that most upper body injuries increased during a pre-braking followed by a 40km/h (25mph) rigid wall impact compared to a direct 40km/h (25mph) rigid wall impact. In contrast, the femur, classified as a lower body member, is seeing lesser compressive axial load (943N) the longer the pre-braking phase, as a longer event positions the femur closer to the knee bolster as well as a smaller initial velocity which leads to less momentum than a standard FMVSS208 40km/h (25mph) unbelted test. It has been observed that, compared to a standard FMVSS208 test, a pre-braking duration, even lasting up to 1.1s, has recorded different

neck forces, i.e. neck tension and neck compression (section 6.2.3), as it has been observed that if the overall body was not moving, the head was rotating during this early period of pre-braking. Consequently, the head position between these 2 conditions was slightly different, hence causing the difference in injury. This example shows that the computer modelling of the pre-braking phase should in future consider in the design of the restraint system should the vehicle be fitted with AEB systems. In the case of a 2-hand grip, for a long braking duration, it has been observed that femur loads decreased compared to shorter pre-braking durations or no pre-braking at all. Consequently, consideration should be given to not deploying the knee airbag as the femur forces would be expected to be smaller due to reduced momentum before the accident. In the potential case of a brake dive, the airbag deployment may adjust its opening direction as a function of the occupant posture and the severity of the brake dive.

In the case of a 1-hand grip, it can be observed that the injuries are in one scenario consistently higher and in other scenarios not conclusive either way (Figure 6.63).

The inconclusive scenarios may be attributed to the innovative deployment method of the OOP airbag utilised in this study which inflates initially more outboards to reduce the OOP1 and OOP2 loadcases. Therefore, it may be suggested that thanks to the 'smart' airbag deployment shape used in this study there may be more cushioning in the steering wheel rim area than with a standard airbag. It was observed that occupants' injuries were less severe than a standard FMVSS208 test for braking durations less than 1.1s, thanks to its outwards deployment technology (section 6.2.4). A more detailed study involving changing airbag shape and inflation parameters would be required to validate this observation.

On the other hand, for longer braking duration, it was observed that for the 1 hand grip the occupant will be completely OOP and will not be protected during the accident phase. What is certain is that after 1.1s, the occupant is out-of the airbag deployment reach which is not a desirable scenario.

As a result of this study (chapter 5 and 6), it emerges that active human computer models are the tools of the future to model active safety scenarios, and will be needed to engineer forthcoming restraints systems including a similar dynamics OOP loadcase.

The real challenge for the future designers would be to locate the vehicle configuration which will generate the highest unbelted occupant injuries using this

dynamics OOP scenario, so that the restraint systems and vehicle interior could be designed to reduce these levels. A proposed methodology would involve the creation of a multi-objective optimisation to include all injuries met within a set of design parameters; this could be part of a design space based on the vehicle design. Section 6.3.2 has shown that injury values varied between a standard FMVSS208 50^{th} percentile unbelted occupant and its injuries sustained through the ASsEt environment. The mechanics of dynamic OOP suggest a very complex phenomenon and that momentum and proximity to the airbag are both certainly two important parameters for injury causation. It was noticed that in the FMVSS208 test, the occupant is far from the airbag, but its throw away velocity is higher than an aware person using muscle activation who is closer to the airbag, hence having a lesser airbag contact momentum. It was not possible to define the worst loadcase for a 2-hand grip 'aware' occupant within the ASsEt environment, nevertheless dynamic OOP suggested injury values are generally higher than the injuries assessed through standard FMVSS208 test configuration. It is therefore recommended that various braking durations and pattern are investigated to verify the overall safety performance of such active safety systems.

In Europe, it is illegal to drive without wearing a seatbelt, while it is permitted in some states in the US, hence reflected in the need of the FMVSS208 unbelted test. For the majority of the belted cases, studies on AEB system have shown clear safety benefits, which have led to the recommendation of such safety features by EuroNCAP, NCAP and IIHS.

In the unbelted loadcase, it has been shown in the study that the awareness level was very important in influencing the occupant's position relative to the airbag system during the pre-braking phase. Consequently, it can be proposed that means of proactively bring the driver back into the braking loop be favoured in order to avoid the crash. As an example, the braking pattern may include a sharp initial braking so it can be sensed by the driver to help him to refocus. Another method would be to use haptic seatbelts which would vibrate or seatbelts using a reversible pre-tensioner (TRW 2011) and hence raise the level of awareness of the driver.

The study has also shown that the use of mobile phones should be discouraged. Hands-free mobile phones would still reduce the level of the driver's awareness, which is not recommended from the results obtained within the parameters set in the

ASsEt environment. These hand-free mobile phones would still be better than hands-held ones as these, in addition of the reduced awareness, cause occupant body rotation away from the seat centreline, away from the restraint system. From the results obtained from this thesis, it may be suggested that means of controlling the use of mobile phones in an unbelted environment would be safety critical. Maybe some means of disabling such devices would be needed should the vehicle automatically detect that an occupant is not buckled up.

After confidential discussions with an OEM of premium, it is not known that any AEB system fitted a vehicle engineered and sold only in European markets would be disabled should the occupant be unbelted (Coventry University 2014). The reasons are that the restraint system in a European market is not tuned for the FMVSS208 unbelted loadcase and that it is also illegal to drive without a seatbelt. In order to remind the driver, the majority of vehicles sold in Europe have a belt minder, which projects a constant audible warning in case of non-compliance.

With early radar AEB systems that primarily provided collision mitigation (not full avoidance) for moving and stationary targets (the later only if a target was already in the sensors' detection range) some automotive manufacturers initially deemed that only 0.4g deceleration would be applied for unbelted occupants within CAE computer simulations of FMVSS208 unbelted tests. Consequently, simulations (with and without pre-impact braking) suggested that the occupant displacement due to pre-impact braking (down to approximately 28.8km/h (18mph)) was not sufficient to cause injuries above their original 40km/h (25mph) test (Coventry University 2014). With more recent AEB systems engineered against Euro NCAP's latest test protocol and sold worldwide, vehicles should be avoiding collisions with stationary targets up-to 56km/h (35mph). Consequently a 40km/h (25mph) FMVSS208 unbelted crash test would be in the real-world avoided regardless of the wearing of the seatbelt (Coventry University 2014).

This scenario is however different from the one researched in this thesis. The study sets the impact collision at 40km/h (25mph) regardless of the braking duration, while the OEM, using a HybridIII ATD and not a human computer model, starts the scenario at 40km/h (25mph) and then activates the brakes, which would likely lead to a more favourable outcome for the occupant. The complexity of the scenario is evident and would require a more in-depth study using the ASsEt environment with

the parameters of Table 3.8 to investigate occupant protection in real-life events and the influence of such systems in the US in an unbelted transport environment.
A legal representative has informed the OEM that law suits in the US involving unbelted drivers were not successful anymore, which is suggesting that people will have to change their attitude and buckle-up (Coventry University 2014). The OEM advises customers via the hand book that the wearing of a seat belt is recommended in all markets.

Overall, in this study, it has been observed that the driver level of awareness was an important parameter which influences the occupant's proximity level of the airbag as well as its pre-braking momentum. This thesis has shown also that more alert drivers were more centrally aligned to their seat, which is beneficial as they are in the zone of influence of the restraint system. It is suggested that monitoring the driver's awareness would be an important feature in the design of future restraint systems, as this would lead the maximum efficiency of the braking system and a reduced influence of OOP dynamics. A new active system monitoring awareness is being studied (Honeywill 2013) correlating the driver's facial features, the road ahead and the driver's hand gesture. These systems are expected to play a major role in the future of safety on unbelted occupant in vehicles fitted with AEB. It may be proposed to reduce the severity of the pre-braking to 0.4g (Coventry University 2014), should an unbelted driver be distracted, in order to bring back the driver in the loop, and optimise his position within the cabin for the restraint system to work best. This proposal would, however, result in an increased braking distance, which in some cases may not be a suitable option. Consequently, a trade-off between avoiding the accident all together, with the risk of inducing injuries for an unbelted occupant, and allowing the accident to happen by mitigating the impact collision speed, which would lead to a better outcome for the occupant, may have to be evaluated in real-time. Some proposals to generate such real time crash scenario algorithm have already been discussed (Bose 2010) based on potential AIS outcomes and may be the solution to such a technological challenge.

8.0 Conclusions

This thesis has answered the research question posed in section 1.4 (Thesis Aims and Objectives) which was to investigate which occupant computer model was the most appropriate to interrogate occupants kinematics and potential injuries when new active safety features are activated. In order to do so, a hypothesis stating that it was necessary to use active human computer models to accurately simulate future active safety situations, i.e. occupant kinematics and injuries, was set and tested against a newly created Active Safety Assessment Environment (ASsEt).

The study has met all its objectives. It originally investigated human occupants' kinematics in low deceleration scenarios and concluded that humans and HybridIII crash test dummies had a different set of kinematics. This important discovery has led to the preference of human computer models over crash test dummies with the incorporation reflexes in order to include occupant posture control, especially needed in an unbelted loadcase. The objective of defining an ASsEt environment to replicate pre-braking followed by an un-avoidable accident was met, including detailed studies of car to car vehicle accidents.

An AHBM reflex behaviour was correlated against lap-belted sled test data. This correlated scenario is the closest test to an unbelted loadcase which can be performed safely on volunteers. Unique reflex motion target curves for the head and torso relative angular motions were derived from the work presented. The correlation has suggested some modification to the original MADYMO model by weakening the muscles' strength in the neck area. The new validated AHBM model's position accuracy (at maximum head displacement) was improved by 8% compared to the original MADYMO AHBM model provided at the beginning of this study and has voided the use of passive human models for unbelted low deceleration events altogether.

As part of the objectives set, an Active Safety Assessment Environment (ASsEt), which included a pre-braking phase (1g) followed by a 40km/h (25mph) accident, was proposed to investigate the kinematics and injuries of the correlated unbelted human occupant computer model. This framework has overall highlighted that the newly

correlated AHBM's kinematics could be scientifically explained as well as its respective injuries.

The research investigated a 2 hand grip and a 1 hand grip (hand closest to the door holding the steering wheel). In all the cases studied, the unbelted occupant's kinematics could be scientifically explained, re-enforcing the fact that this model has believable kinematics outcomes.

The 2-hand grip study suggested that, within the framework parameters chosen, higher seat friction values and greater awareness were beneficial to the occupant remaining in-line with the steering wheel and the airbag restraint system. On the other hand, smaller seat friction values and lesser level of awareness would position the occupant closer to the steering wheel before the accident occurs.

In the case of a 2-hand grip, long braking durations (2.3s in the ASsEt environment) caused a higher femur axial load during the braking phase, than shorter braking durations.

The 1-hand grip study also concluded that, within the framework parameters chosen, higher seat friction values and greater awareness were beneficial to the occupant remaining in-line with the steering wheel and the airbag restraint system. However, it was also observed that for braking durations above 1.1s, the occupant was out of the airbag deployment reach, suggesting that should the subsequent accident occur after that time, then no current safety system would be present to mitigate occupant injuries. It was observed that, regardless of the grip configuration, the awareness level was an important factor in the occupant's position relative to the restraint system. It was suggested that future active safety systems should consider monitoring the occupant's state of alertness within vehicle cabin so that occupant's forward motion during pre-braking phase could be minimised, especially should the occupant be unbelted.

Overall, it has been observed that injuries of an unbelted occupant were higher in a pre-braking phase followed by a 40km/h (25mph) crash (ASsEt environment) compared to a standard 40km/h (25mph) direct impact. Results also concluded that the dynamic OOP scenario was intricate and that more details in a future study, for example brake dive, seat design, seat stiffness and cabin packaging, would be needed to capture the vehicle configuration providing the highest dynamic OOP safety risk.

Based on the research undertaken in Chapter 6 and the findings summarised in Table 2.6 of the Literature Review chapter, it is suggested that wearing seatbelts results in a clear benefit for occupant safety. Concerns about the use of mobile phones (WHO 2013) seem to be substantiated from the analysis performed, reinforcing the fact that using a mobile phone whilst driving is not recommended.
The implementation of active safety suggests that drivers not wearing their seatbelt would sustain higher level of injuries should a secondary impact follow an emergency braking phase.

It has to be noted that the conclusions stated in this thesis refer to the set of parameters chosen for the ASsEt environment, which is a very specific set of circumstances, with the conditions set in Table 3.8. In order to make a more general claim on the effect of AEB on the safety of unbelted occupants, a statistical study, such as a Monte-Carlo analysis, would be needed in order to capture the least favourable accident with the respective vehicle interior conditions for the unbelted occupant.

The computer runtime of this ASsEt environment was also investigated, leading to the conclusion that, at this point in time and with the technology available, the computation of the pre-braking phase and the accident could not be split at the cost of under-estimating occupant's injuries.

This thesis has highlighted the importance and the necessity of using AHBM models to accurately predict the kinematics and injuries of unbelted occupants under AEB. Based on the proposed ASsEt environment, active safety emergency braking has an effect on unbelted occupants' position within the cabin. The MADYMO AHBM computer model seems, to date, to be the most suited computer model to simulate active safety frontal pre-braking frontal scenarios, as it is validated for impact, 1g pre-braking (based on work from this thesis) and provides believable responses in variable hand grip postures and occupant awareness level.

9.0 Future Work and Opportunities

This thesis has addressed the simulation of the kinematics and injuries of unbelted occupants in an emergency pre-braking phase followed by a subsequent accident using an AHBM which has been correlated to a frontal volunteer sled tests.

Some further work and opportunities can follow this study. These are organised in 3 categories:

1. AHBM algorithmic improvements and validation
2. Framework algorithmic improvements
3. Application of the framework in a vehicle design cycle

9.1 AHM algorithmic improvements and validation

Neck model improvements

The study has shown that the shape of the head motion response varied from the target curve computed in this thesis. Some new work has emerged suggesting an updated AHBM with updated neck and arms (Meijer 2013a). This model will be made available in MADYMO 7.5.0, not yet released, and should be re-assessed against the OM4IS tests to prove its validity.

Investigation of the new AHBM which includes bracing against bracing test target curves

From literature, the new MADYMO 7.5.0 AHBM (Meijer 2013b; Meijer 2013c) should also be capable of bracing; hence its response could also be assessed against the motion curves displaying anticipated behaviours

Validation of the AHBM against OM4IS vehicle data (frontal) and accident reconstruction cases

The author has only been provided with a partial set of the OM4IS sled test data and not the tests performed with volunteers within a vehicle. It would be beneficial to obtain all this vehicle test data, including vehicle geometry (including suspensions) and cabin geometry to replicate the vehicle test and compare the motions between the AHBM from the sled and the vehicle model. This study could validate the AHBM's kinematics response when brake dive is

present. Once completed, this study could be extended and applied in the case of accident reconstruction cases where a pre-braking phase has been identified and injuries from a subsequent impact recorded.

Initial Joint velocity extraction from the pre-braking phase

The current ASsEt environment would benefit from the generation of algorithms allowing the re-mapping of the MADYMO AHBM nodes and joint velocities from a pre-braking phase onto itself, advocating a 2-phase analysis method. By doing so, the ASsEt environment would run more rapidly as current runtimes could be reduced by a factor of 4.

An extension of such algorithm could be beneficial to other human models which may not be active, like the THUMSv4.0, whose kinematics are not current adequate (Iwamoto 2013) to simulate occupant position under extreme vehicle braking. The proposed work would utilise the MADYMO AHBM during the pre-braking phase to then re-map the full positions and velocities on a full/ partial passive Finite Element model which has the capabilities of investigating trauma on internal organs, which the current Active Human Model cannot do. The new proposed method would be beneficial for accident reconstruction cases, for example, where multi trauma investigation is need, hence requiring a full Finite Element model for trauma injury assessment. Other methods have already been used to 'graft' localised Finite Elements (Jiang 2010) of the injurious trauma areas to passive multi-body human models. Nevertheless, when muscle activation is present, this method is challenging, as this 'hybrid' model would need to re-attach the Active Human Model and be fully recalibrated before use.

9.2 Environment algorithmic improvements

Implementation of the brake dive in the current framework and steering column collapse characteristics

As indicated in the Methodology section, the brake dive may need to be included as video evidence and literature reviews have suggested that this phenomenon was evident. Currently, the vehicle is fixed and the acceleration force fields applied. A method to capture the brake dive and apply the associated crash pulse, i.e. 40km/h (25mph) rigid wall impact with a vehicle in nose dive attitude, would be needed to

assess the change to steering column angle and collapse stiffness relative to the occupant's torso and their effect on injuries.

9.3 Application of the ASsEt environment in a vehicle design cycle

The design process

It is proposed to implement the framework alongside the development of the FMVSS208 legislative requirement of a vehicle as displayed in Figure 9.1.

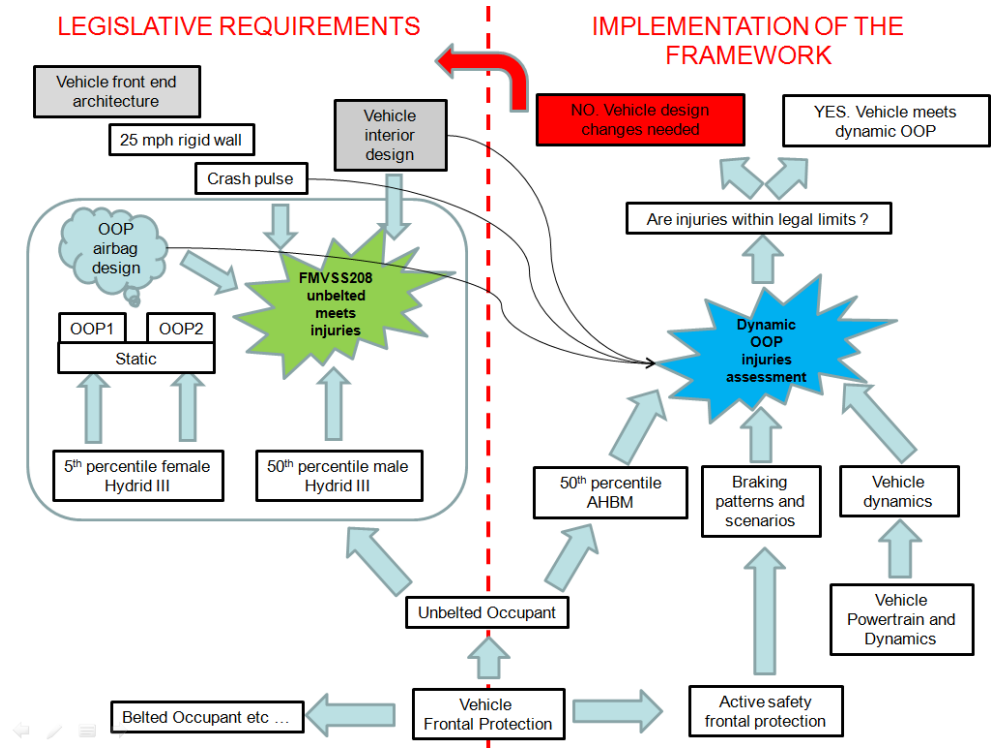

Figure 9.1: Typical implementation of the Active Safety Assessment Environment with the design process

The automotive manufacturer would firstly design to meet the passive and 40km/h (25mph) FMSS208 legal requirements and then feed the airbag design, the vehicle crash pulse and the vehicle interior design (including the steering column mechanical properties) to the Active Safety Assessment Environment which would embed also the vehicle dynamics and active safety features acting upon the vehicle pattern and braking scenarios. Should injury levels be above legal values then structural and interior vehicle design changes will have to be implemented, which might involve the airbag design, steering column ride down characteristic, seat stiffness etc...

Designing for Dynamic OOP guidelines

As explained in the thesis, the ASsEt environment parameters chosen have been taken from the literature and are not part of a single vehicle.

It might be therefore beneficial to re-run the framework with a consistent set of input from one vehicle and create some design guidelines in order to generate best practise to consider the dynamic OOP unbelted loadcase. In order to generate such guidelines, it may be able to consider performing a DOE and extract injury response surfaces as function of vehicle interior, vehicle architecture, active safety measure parameters, including ranges. By doing so, a database of response surfaces could be stored and provided to the designer to find the best set of design parameters in order to consider Dynamic OOP requirements early in the vehicle interior design phase

Analysis of real world crashes

Using the conclusions of the thesis it would be proposed to demonstrate the effect of active safety on actual injury cases, using accident databases such as OTS, GIDAS, FARS etc…. The study could look at the cases of death and serious injury in frontal impacts and focus on the cases involving a lack of belt use. The study could then investigate the level of injury of such occupants should AEB been present and conclude whether an unbelted occupant would be better off with a vehicle with no AEB or with a vehicle with an AEB effect assumed.

The seat design process

The seat loading in belted and unbelted is different, as the unbelted loads the end of the seat pan more vertically than in a belted loadcase. As such, during a pre-braking phase, the position of the human occupant will be different from a 50th percentile HybridIII crash test dummy in standard FMVSS208 40km/h (25mph) loadcase, leading to a potential different seat pan load direction in a subsequent impact. This might be critical for the design of the seat pan local stiffness.

Driver posture analysis and awareness level

As explained in the thesis, driver posture and awareness levels are very important, especially during the pre-braking phase. The next work would need to consider

whether an airbag system would be able to still protect an occupant in extreme OOP, like observed in a 1 hand grip or if the occupant is distracted.

As observed in this thesis, active safety, and particularly AEB, has some great potential to reduce fatalities on the road. This work has opened the door to other safety challenges linked with this merging technology which should now address the safety of vehicle occupants.

10.0 References

Adam, T., Untaroiu, C., (2011) 'Identification of occupant posture using a Bayesian classification methodology to reduce the risk of injury in a collision'. Transportation Research Part C: Emerging Technologies, 19 (6), 1078-1094

Advanced Simtech. (2007) '07.OF.UK.03287/MB, 2007'. Accident investigation report

American Iron and Steel Institute. (2004) 'Vehicle Crashworthiness and Occupant Protection'. Technical report [online] available from < www.autosteel.org> [5 July 2013]

ASSESS. (2012a) 'Assessment of Vehicle Safety Systems'. FP7 project [online] available from <www.assess-project.eu> [01 January 2013]

ASSESS. (2012b) 'ASSESS D4.1b - FINAL - Action plan pre_crash evalution-PUBLIC-2010-03.01'. Technical Report [online] available from <www.assess-project.eu/downloadables/Public%20Deliverables/ASSESS%20D4.1b%20-%20FINAL%20-%20Action%20plan%20pre_crash%20evalution-PUBLIC-2010-03.01.pdf > [1 July 2013]

Automotive Council UK. (2011) 'Intelligent Mobility: A National Need'. Technical Report [online] available from <www.automotivecouncil.co.uk/wp-content/uploads/2011/12/ITS_Report_15_11_11.pdf> [25 July 2013]

Bao, S. (2000) 'Grip strength and hand force estimation'. SHARP. Tech. Rep. 65-1-2000, Department of Labour and Industries, Olympia

Bastien, C., et al. (2010a) 'Investigation into Injuries of Out-Of-Position (Oop) Posture Occupants and Their Implications in Active Safety Measures'. ICRASH2010 International Crashworthiness conference proceedings. Held 20-21 September 2010 at Washington DC

Bastien, C., Blundell, M. V., Stubbs, D., Hoffmann, J., Freisinger, M., Van Der Made, R. (2010b) 'Correlation of Airbag Fabric Material Mechanical Failure Characteristic for Out of Position Applications'. ISMA2010 international conference proceedings. Held 16-17 September 2010 at Leuven, Belgium

Bastien, C., Blundell, M., Hoffmann, J., Freisinger, M., Van der Made, R., Neal-Sturgess, C. (2011) 'Investigation Of Pre-Braking On Unbelted Occupant Position And Injuries Using An Active Human Body Model (AHBM)'. ESV 2011 international conference [online] available from <www-nrd.nhtsa.dot.gov/pdf/esv/esv22/22ESV-000296.pdf>. held 20-21 June 2011 at Washington DC [20 June 2011]

Bastien, C., Diederich, A., Freisinger, M., Hoffmann, J., Van Der Made, R., Blundell, M. V., Neal-Sturgess, C., Huber, P., Prueggler, A. (2012a) 'Influence of Human Bracing on Occupant's Neck, Head and Thorax Injuries in Emergency Braking Combined With An FMVSS208 Impact Scenario'. ICRASH2012, international crashworthiness conference proceedings. Held 14-15 July 2012 at Milano

Bastien, C., Christensen, J. (2012b) 'Lightweight Body in White Design Using Topology-, Shape and Size Optimisation'. EVS26 international conference proceedings. Held on 5-6 May 2013 at Los Angeles, California

Bastien, C., Blundell, M., Neal-Sturgess, C. (2013a) 'Influence of Vehicle Secondary Impact Following an Emergency Braking on an Unbelted Occupant's Neck, Head and Thorax Injuries'. International Journal of Crashworthiness 18 (3), 215-224

Bastien, C., Blundell, M. V., Neal-Sturgess, C., Hoffmann, J., Diederich, A., Van Der Made, R., Freisinger, M. (2013b) 'Safety Assessment of Autonomous Emergency Braking Systems on Unbelted Occupants Using a Fully Active Human Model'. ESV2013 International Conference [online] available from <www-nrd.nhtsa.dot.gov/pdf/esv/esv23/23ESV-000006.PDF>. Held 27-30 June 2013 at Seoul, Korea [27 June 2013]

BBC News. (2011) 'One in 20 drivers not belting up, survey suggests'. Article [online] available from <www.bbc.co.uk/news/uk-13775695> [1 July 2013]BBC. (2012) 'UN: Six billion mobile phone subscriptions in the World'. Article [online] available from < www.bbc.co.uk/news/technology-19925506 > [1 July 2013]

BBC. (2013) 'Transatlantic Trade Talks Open Amid Tensions'. Article [online] available from <www.bbc.co.uk/news/business-23221503> [1 July 2013]

Beeman, S., Kemper, A., Madigan, M., Franck, C., Loftus, S. (2012) 'Occupant kinematics in low-speed frontal sled tests: Human volunteers, Hybrid III ATD, and PMHS'. Journal of Accident Analysis and Prevention (47), 128-139

Behr, M., Poumarat, G., Serre, T., Arnoux, P.J., Thollon, L., Brunet, C. (2009) 'Posture and muscular behaviour in emergency braking: An experimental approach'. Accident Analysis and Prevention (42), 797–801

Berg, A., Rucker, P. (2012) 'Crash Test Using a Car with Automatic Pre-Crash Braking'. ICRASH2012, international crashworthiness conference proceedings. Held 14-15 July 2012 at Milano

Blundell, M., Harty, D. (2004) *The Multibody Systems Approach to Vehicle Dynamics*. Elsevier, ISBN 0 7506 5112 1

Blundell, M., Mahangare, M. (2006) 'Investigation of an Advanced Driver Airbag Out-of-Position (OoP) Injury Prediction with MADYMO Gasflow Simulations'. MADYMO User Meeting proceedings. Held 8-9 November 2006 at Delft.

Bose, D., Crandall, J.R. (2008) 'Influence of active muscle contribution on the injury response of restrained car occupants'. Annals of Advances in Automotive Medicine. (52), 61–72

Bose, D., Crandall, J.R., Untaroiu, C.D., Maslen, E.H. (2010) 'Influence of pre-collision occupant parameters on injury outcome in a frontal collision'. Journal of Accident analysis and Prevention (42), 1398–1407

Bulla, M. (2013) 'Human Body Model Evaluation Crashworthiness Applications'. CARHS Human Modelling and Simulation in Automotive Engineering conference proceedings. Held 6-7 June 2013 at Aschaffenburg, Germany

Bureau of Transportation Statistics. (2011) 'National Transportation Statistics'. Technical Report [online] available from <www.rita.dot.gov/bts/sites/rita.dot.gov.bts/files/publications/national_transportation_statistics/index.html> [01 July 2013]

Cabinet Office Research Strategy. (2009) 'The wider costs of transport in English urban areas in 2009'. Technical Report [online] available from <webarchive.nationalarchives.gov.uk/20100428141142/http://cabinetoffice.gov.uk/media/307739/wider-costs-transport.pdf> [30 May 2011]

Campbell D. (2013) 'Impact! A Horizon Guide to Car Crashes'. BBC4 [24 October 2013, 23:00]

Cappon, H., Mordaka, J., Van Rooij, L. (2006) 'A Computational Human Model with Stabilizing Spine: A Step Towards Active Safety', SAE Technical Paper 2007-07-1171, Society of Automotive Engineers

CARHS. (2013) 'EuroNCAP 2013-2016 Desktop Roadmap'. Technical Report [online] available from <www.carhs.de/etc-doc/EuroNCAP_Desktop_Roadmap_2013-2016.pdf> [4 July 2013]

Carlsson, S., Davidsson, J. (2011) 'Volunteer occupant kinematics during driver initiated and autonomous braking when driving in real traffic environments'. IRCOBI International Conference [online] available at <www.ircobi.org>. Held 14-16 September 2011 at Krakow, Poland

Christensen J. (2010) 'Modelling Of Airbag Pad Cover By Plate Theory'. Unpublished MSc dissertation. Coventry University

Christensen, J., Bastien, C. (2011) 'Lightweight Hybrid Electric Vehicle Structural Optimisation Investigation Focusing on Crashworthiness'. International Journal of Vehicles Structures and Systems, 3 (2), 113-122

Christensen, J., Bastien, C. (2013) 'Buckling Considerations and Cross-Sectional Geometry Development for Topology Optimised Body In White'. International Journal of Crashworthiness Journal 18 (4), 319-330

Coventry University. (2013) Confidential discussions with an OEM of premium vehicles [05 June 2012]

Coventry University. (2014) Confidential discussions with an OEM of premium vehicles [25 June 2014]

Crandall, J.R., Bose, D., Forman, J., Untaroiu, C.D., Arregui-Dalmases, C., Shaw, C.G., Kerrigan, J.R. (2011) 'Human Surrogates for Injury Biomechanics Research'. Journal of Clinical Anatomy 24 (3), 362–371.

Crandall, J.R. (2012a) 'Simulating The Road Forward: The Role Of Computational Modelling In Realizing Future Opportunities In Traffic Safety'. IRCOBI 2012 International Conference [online] available at <www.ircobi.org>. Held in September at Trinity College Dublin, Ireland.

Crandall J. (2012b) Private Correspondence on confidential matter [20 July 2012]

Crandall, J.R. (2013) 'International Advanced Course on Injury Biomechanics'. Course notes. Held 11-15 March 2013 at Barcelona, Spain

Cummings, J., Osterholt, G. (2009) 'Occupant Friction Coefficients on Various Combinations of Seat and Clothing'. SAE International Journal, paper 2009-01-1672 [online] available from <papers.sae.org/2009-01-1672>, Society of Automotive Engineers [1 June 2013]

Delphi. (2012) 'Worldwide Emission Standards - Passenger Cars and Light Duty Vehicles'. Technical Report [online] available from <delphi.com/pdf/emissions/Delphi-Passenger-Car-Light-Duty-Truck-Emissions-Brochure-2011-2012.pdf> [05 July 2013]

Department of Transport. (2011) 'Road Transport Forecasts 2011, Results from the Department for Transport's National Transport Model'. Technical Report [online] available from <assets.dft.gov.uk/publications/road-transport-forecasts-2011/road-transport-forecasts-2011-results.pdf> [25 July 2013]

Department of Transport. (2013) 'Road lengths in Great Britain: 2012'. Technical Report [online] available from <www.gov.uk/government/uploads/system/uploads/attachment_data/file/208692/road-lengths-in-great-britain-2012.pdf> [25 July 2013]

De Waard D. (1996) 'The Measurement of Drivers' Mental Workload'. PhD Thesis [online] available from <sunburst.usd.edu/~schieber/pdf/deWaard-Thesis.pdf> [1 July 2013]

Du Bois P. (2010) 'Crashworthiness and Impact Engineering with LS-Dyna'. Engineering Course Notes, California, Livermore Software Technology Corporation

Edwards, A., Grover, C., Amendolagine, M., Ferro, M. (2013) 'Telematics; how can this data be used for safety analysis?'. IRCOBI International Conference [online] available at <www.ircobi.org>. Held 11-13 September 2013 at Gothenburg, Sweden

Ejima, S., Ono, K., Holcombe, S. (2007) 'A study on Occupant Kinematics Behaviour and Muscle Activities during Pre-Impact Braking Based on Volunteer Tests'. IRCOBI International Conference [online] available at <www.ircobi.org>. Held 12-13 September 2007 at Maastricht, Netherlands.

Ejima, S., Ono, K., Holcombe, S. (2008) 'Prediction of the Physical Motion of the Human Body based on Muscle Activity during Pre-Impact Braking'. IRCOBI International Conference [online] available at <www.ircobi.org>. Held 17-19 September 2008 at Bern, Switzerland.

Ejima, S., Ono, K., Holcombe, S. (2009) 'Prediction of Pre-Impact Occupant Kinematics Behaviour Based on the muscle activity during Frontal Collision'. IRCOBI International Conference [online] available at <www.ircobi.org>. Held 9-11 September 2009 at York, UK

EuroNCAP. (2012) "EuroNCAP Rating Review. Report from the Rating Groups'. Technical Report [online] available from < www.euroncap.com> [1 July 2013]

EuroNCAP. (2013a) 'Pedestrian CAE Models and Codes'. Technical Bulletin [online] available from < www.euroncap.com/files/TB-013---Pedestrian-CAE-Models-v1.2---0-5d5ac737-4089-494a-be87-14c1f44763c4.pdf > [14 June 2014]

EuroNCAP. (2013b) 'Pedestrian Testing Protocol'. Technical Report [online] available from < www.euroncap.com/files/Euro-NCAP-Pedestrian-Protocol-v7.1.1---0-c573c763-8670-44fb-86ae-c43f19641b2f.pdf> [14 June 2014]

EuroNCAP. (2013c). Website: www.euroncap.com [3 July 2013]

EuroNCAP. (2013d) 'Audi 2 safety rating, Pre-2009 Test Protocol'. Technical Report [online] available from <www.euroncap.com/results/audi/a2.aspx> [16 July 2013]

EuroNCAP. (2013e) 'Automatic Emergency Braking – AEB'. Article [online] available from < www.euroncap.com/results/aeb.aspx> [3 July 2013]

EuroNCAP. (2013f) 'Assessment Protocol – Safety Assist'. Technical Document [online] available from <www.euroncap.com/files/Euro-NCAP-Assessment-Protocol---SA---v6.0---0-03d1ee92-316f-4c23-918d-76c7496ba833.pdf > [16 July 2013]

Evans, R.J. (2013) 'Injury Prevention Within A Car, Focusing On The Inclusion Of Seatbelt And How Best To Model The Steering Column'. Unpublished MSc thesis. Coventry University

FARS. (2013) 'Fatality Analysis Reporting System'. Technical database [online] available from <www.nhtsa.gov/FARS> [1 July 2013]

FMVSS201. (2013) 'Head Impact Protection'. Federal Legislation [online] available from <www.nhtsa.gov/cars/rules/rulings/headprot/pubnprm.html> [3 July 2013]

FMVSS208. (2013), Occupant Crash Protection'. Federal Legislation [online] available from <www.nhtsa.gov/cars/rules/rulings/headprot/pubnprm.html> [3 July 2013]

Folksam. (2013), 'How Safe is your Car?'. Technical Report [online] available from <www.folksam.se/polopoly_fs/1.11226!/webbversioneng_R6546.pdf> [3 July 2013]

Ford (2013) 'Post-Crash response technologies'. Press announcement [online] available from <corporate.ford.com/microsites/sustainability-report-2012-13/vehicle-technologies-response> [16 May 2014]

Freisinger, M., Hoffmann, J. (2006) 'Investigation of an Advanced Driver Airbag Out-of-Position (OOP) Injury Prediction with MADYMO Gasflow Simulations', MADYMO user Meeting conference proceedings. Held 6 November 2006 at Dearborn

GHBMC. (2013) 'Global Human Body Model Consortium'. Technical Information [online] available from < www.ghbmc.com> [16 July 2013]

Grimes, O., Christensen, J., Bastien, C. (2013) 'Lightweighting of a Hydrogen Fuel Cell Vehicle whilst Meeting Urban Accident Criteria'. EVS27 international symposium conference proceedings. Held 17-20 November 2013 at Barcelona, Spain

Grover, C., Weekes, A.M. (2012) 'Selection of test scenarios for Autonomous Emergency Braking (AEB) test procedures'. ICRASH2012 international conference proceedings. Held 18-20 July 2012 at Milano, Italy

Hansen P. (1986) *The Joy of Stress*. New York, Pan Macmillan

Happian-Smith J. (2002) *An Introduction to Modern Vehicle Design*. Oxford, Butterworth Heinemann

Hault-Dubrulle, A., Robache, F., Pacaux, M.P., Morvan, H. (2010a) 'Determination of Pre-Impact Occupant Postures and Analysis of Consequences on Injury Outcome. Part I: A Driving Simulator Study'. Journal of Accident Analysis and Prevention 43 (1), 66-74

Hault-Dubrulle, A., Robache, F., Drazetic, P., Guillemot, H., Morvan H. (2010b) 'Determination of Pre-Impact Occupant Postures and Analysis of Consequences on Injury Outcome. Part II: Biomechanical Study'. Journal of Accident Analysis and Prevention 43 (1), 75-81

Highway Agency. (2011) 'M42MM Monitoring and Evaluation. Three Year Safety Review'. Technical Report [online] available from <assets.highways.gov.uk/specialist-information/knowledge-compendium/2009-11-knowledge-programme/HCG-HRG_264763_001b_V2__2_.doc.pdf> [25 July 2013]

Highway Agency. (2013) 'Smart Motorways'. Article [online] available from <www.highways.gov.uk/our-road-network/managing-our-roads/managed-motorways/> [25 July 2013]

Hoffman, J., Freisinger, M., Blundell, M., Mahangare, M., Ritmeijer, P. (2007) 'Investigation Into The Effectiveness Of Advanced Driver Airbag Modules Designed For OOP Injury Mitigation'. ESV2007 International Conference [online] available from <www-nrd.nhtsa.dot.gov/pdf/esv/esv20/07-0319-O.pdf>. Held 18-21 June 2007 at Lyon, France [12 January 2013]

Horsch, J., Lau, I., Andrzejak, D., Viano, D. et al. (1990) 'Assessment of Air Bag Deployment Loads'. SAE Technical Paper 902324, Society of Automotive Engineers

Honeywill, T. (2013) 'How Cameras Can Monitor Driver Distraction And The Road Ahead'. Article [online] available from <www.carsafetyrules.com/cameras-can-monitor-driver-distraction-road-ahead/1115/> [2 December 2013]

Hüber, P., Prüggler, A., Kirschbichler, S., Steidl, T., Rieser, A., Wolfgang Sinz, W. (2013) 'Occupant Model for Integrated Safety: Challenges in Testing and Simulation'. CARHS Human Modelling and Simulation in Automotive Engineering Symposium proceedings. Held 13-14 May 2013 at Aschaffenburg, Germany

Hulshof. W., Knight, I., et al. (2013) 'Autonomous Emergency Braking Test Results'. ESV2013 International Conference [online] available from <www.euroncap.com/files/AEB-Test-Results-ESV-2013---0-a837f165-3a9c-4a94-aefb-1171fbf21213.pdf>. Held 27-30 June 2013 at Seoul, Korea [20 June 2013]

IIHS. (2012a) 'They're working. Special issue: Crash Avoidance'. Status Report 47 (5) [online] available from <www.iihs.org/externaldata/srdata/docs/sr4705.pdf> [3 July 2013]

IIHS. (2012b) 'They're working: Insurance claims data show which new technologies are preventing crashes. Status Report 47 (5) [online] available from < http://www.iihs.org/iihs/sr/statusreport/article/47/5/1> [26 June 2014]

IIHS. (2013a) 'Insurance Institute for Highway Safety'. Insurance Testing [online] available from <www.iihs.org/> [3 July 2013]

IIHS. (2013b) 'More good news about crash avoidance: Volvo City Safet reduces crashes'. Status report [online] available from < www.iihs.org/iihs/sr/statusreport/article/48/3/1> [26 June 2014]

International Transport Forum. (2013) 'Road Safety Annual Report 2013'. Technical Report [online] available from <www.internationaltransportforum.orr/Pub/pdg/13IrtadReport.pdf> [17 March 2013]

ISO/TR 10982. (1998) 'Road Vehicles – Test Procedures for Evaluating Out-Of-Position Vehicle Out-Of-Position Vehicle Occupants Interactions with Deploying Airbags'. Technical Report, First edition 1998-03-15 [online] available from www.iso.org/iso/catalogue_detail.htm?csnumber=63781 [1 March 2012]

Iwamoto, M., Nakahira, Y., Kimpara, H., Sugiyama, T. (2012) 'Development of a Human Body Finite Element with multiple muscles and their controller for estimating Occupant Motions and Impact responses on Frontal Crash Situations'. Stapp Car Crash Journal, 56, 231-268

Iwamoto, M., Nakahira, Y., Kimpara, H., Sugiyama, T. (2013) 'Development of A Human FE Model with Multiple Muscles and Their Controller for Estimation of Occupant Motions In Pre- and Post-Crashes'. CARHS Human Modelling and Simulation in Automotive Engineering Symposium proceedings. Held 13-14 May 2013 at Aschaffenburg, Germany

Jiang, C., Sturgess, C.E.N., et al. (2010) 'Kinematics simulation and head injury analysis for rollovers using MADYMO'. International Journal of Crashworthiness 15 (5), 505-515

Kayvantash, K., Bidal, S., Delcroix, F. (2009) 'HUMOS - An FE Model for Advanced Safety and Comfort Assessments'. Technical Paper [online] available from <www.altairhyperworks.co.uk/technology/files/papers/2009/ altair_uk_humos_vt_kayvantash_14052009_format.pdf> [1 March 2012]

Kemper, A., Beeman, S., Madigan, M., Franck, C., Duma, S. (2011) 'Effects of Bracing on Human Kinematics in Low-Speed Frontal Sled Tests'. Annals of Biomedical Engineering 39 (12), 2998–3010

Kirkman, P. (2014) 'Active Safety'. Lecture notes for module 331MAE Vehicle Structures and Safety. Held 3rd February 2014 at Coventry University, UK

Kullgren, A., Lie, A., Tingvall, C. (2010) 'Comparison between Euro NCAP Test Results and Real-World Crash Data'. Journal of Traffic Injury Prevention, 11 (6), 587-593

Lange, R., van Rooij, L., Mooi, H., Wismans, J. (2005) 'Objective Biofidelity Rating of a Numerical Human Occupant Model in Frontal to Lateral Impact'. Stapp Car Crash Journal 49, 457-479

Langwieder, K., Bengler, P., Maier, F. (2012) 'Effectiveness of driver Assistance Systems and the need for promotion regarding the Aim Vision Zero'. ICRASH2012 International Conference Proceedings. Held 18-20 July 2012 at Milano, Italy

Lessley, D., Crandall, J., Shaw, G., Kent, R., Funk, J. (2004) 'Normalization Technique for Developing Corridors from Individual Subject Responses'. SAE International. Paper 2004-01-0288, Society of Automotive Engineers

LSTC. (2012), 'LS-Dyna. Keyword User's Manual. Volume 1'. Technical Manual [online] available from <ftp.lstc.com/anonymous/outgoing/trent001/manuals/LS-DYNA_manual_Vol_I_R6.1.0.pdf> [12 March 2012]

Mahangare, M., et al. (2007a) 'Investigation Into The Effectiveness Of Advanced Driver Airbag Modules Designed for OOP Injury Mitigation'. ESV2007 international conference [online] available from <www-nrd.nhtsa.dot.gov/pdf/esv/esv20/07-0319-O.pdf>. Held 18-21 June 2007 at Lyon, France [12 January 2012]

Mahangare M. (2007b) 'To Model an Airbag for Out-Of-Position Occupants in Frontal Impacts'. PhD Thesis, Coventry University

Mayer, C. (2013) 'Application of Numerical Human Body Models within Automotive Development Aspects of Model Verification And Validation'. 9th ARUP European Conference Proceedings. Held 2-4 June 2013 at Manchester

Meijer, R., Rodarius, C., Adamec, J., Nunen, E., Rooij, L. (2008) 'A First Step In Computer Modelling Of The Active Human Response In A Far Side Impact'. International Journal of Crashworthiness 13 (6), 643–652

Meijer, R., van Hassel, E. (2012) 'Development of a Multi-Body Human Model that Predicts Active and Passive Human Behaviour'. IRCOBI international conference [online] available at <www.ircobi.org>. Held 12-14 September 2012 at Dublin, Ireland.

Meijer R., Hassel E., Elforai H., Broos J., Van der Made R. (2013a) 'The MADYMO Active Model, Validations an Applications'. CARHS Human Modelling and Simulation in Automotive Engineering conference. Held 6-7 June 2013 at Aschaffenburg, Germany

Meijer, R., Broos, J., Elforai, H., de Bruijn, E., Forbes, P., Happee R. (2013b) 'Modelling of Bracing in a Multi-Body Active Human Model'. IRCOBI international conference [online] available at <www.ircobi.org>. Held 11-13 September 2013 at Gothenburg, Sweden

Meijer, R., van Hassel, E. (2013c) 'Evaluation of an Active Multi-Body Human Model for Braking and Frontal Crash Events'. IRCOBI international conference [online] available at <www.ircobi.org>. Held 11-13 September 2013 at Gothenburg, Sweden

MFES. (2010) 'Skidding Friction: A Review of Recent Research'. Technical Report [online] available from <mfes.com/friction.html> [1 August 2010]

Miles J. (2011) 'Intelligent Mobility: the future'. ARUP LS-Dyna user conference proceedings. Held 15 January 2011 at Solihull, UK

Morris, C.R. (1998) 'Measuring Airbag Injury Risk To Out-Of-Position Occupants', SAE International Paper, 986098, Society of Automotive Engineers

NASA. (1976) 'Male Grip Strength as a Function of the Separation between Grip Elements'. Technical Report [online] available from < msis.jsc.nasa.gov/sections/section04.htm#_4.9_STRENGTH> [6 April 2013]

NCAC. (2013) 'Finite Element Model Archive'. Computer Models Database [online] available from <www.ncac.gwu.edu/vml/models.html> [1 July 2012]

Neal-Sturgess, C. (2013) 'Injury Causation & Rollover 2013'. Unpublished Course Notes, Coventry University

Nebraska Strategic Highway Safety Plan. (2013) 'Fatal Crashed Involving Unbelted Vehicle Occupants'. Technical Report [online] available from < www.transportation.nebraska.gov/safe/tysummit/2012/presentations/1-Fatal-Crashes-Unbelted.pdf> [8 July 2013]

Nemirovsky, N., Van Rooij, L. (2010) 'A New Methodology for Biofidelic Head-Neck Postural Control'. IRCOBI International Conference [online] available at <www.ircobi.org>. Held 14-16 September 2011 at Krakow, Poland

NHTSA. (2007) '2007 Motor Vehicle Occupant Safety Survey'. Technical Report (Volume 4 Crash Injury and Emergency Medical Services Report) [online] available from < www.nhtsa.gov/Driving+Safety/Research+&+Evaluation/2007 +Motor+Vehicle+Occupant+Safety+Survey> [8 July 2013]

NHTSA. (2010) 'Preliminary Statement of Policy Concerning Automated Vehicles'. Technical Report [online] available from <www.nhtsa.gov/ staticfiles/rulemaking/.../Automated_Vehicles_Policy.pdf > [21 May 2014]

NHTSA. (2011) 'A Test Track Protocol For Assessing Forward Collision Warning Driver-Vehicle Interface Effectiveness'. Technical Report [online] available from <www.nhtsa.gov/DOT/NHTSA/NVS/Crash%20Avoidance/.../ 811501.pdf> [16 July 2013]

NHTSA. (2013a) 'Three-Reasons-Everyone-Should-Wear-A-Seat-Belt'. Article [online] available from <www.nhtsa.org/2013/04/08/three-reasons-everyone-should-wear-a-seat-belt> [16 July 2013]

NHTSA. (2013b) 'What we are and What We Do'. Article. [online] available from < <www.nhtsa.gov/About+NHTSA/Who+We+Are+and+What+We+Do> [10 January 2013]

NHTSA. (2013c) 'National Automotive Sampling System (NASS)'. Technical Database [online] available from < www.nhtsa.gov/NASS> [8 July 2013]

NHTSA. (2013d) 'NHTSA Vehicle Crash Test Database'. Technical Database. [online] available from <www.nhtsa.gov/Research/Databases+and+Software> [10 January 2013]

OM4IS. (2011) 'Occupant Model For Integrated Safety'. Research project website [online] available from <secure.om4is.at/. /.> [18 March 2012]

Oxford English Dictionary, [online] available from <oxforddictionaries.com> [16 July 2013]

Paver, J.G. Friedman, D. (2010) 'The development of IARV's for the HYBRID III neck modified for dynamic rollover crash testing'. ICRASH2010 international crashworthiness conference proceedings. Held 20-21 September 2010 at Washington DC

PE. (2011a) 'Vehicle Platooning Demonstrated For The First Time. Research Project Proves That Cars Linked In Convoys Is A Possibility'. Professional Engineering article published on 18/01/2011 [online] available from <profeng.com/tech/vehicle-platooning-demonstrated-for-the-first-time> [1 February 2011]

PE. (2011b) 'Vehicle Platooning. I have no doubt that the technology can and will work, and the issues highlights in the article can be overcome'. Professional Engineering article published on 30/08/2011 [online] available from <profeng.com/transport/vehicle-platooning> [1 September 2011]

PE. (2012) 'California to usher in era of driverless cars. State legislation to be amended to allow test and operation of autonomous vehicles on its roads and highways'. Professional Engineering article published on 26/09/2012 [online] available from <profeng.com/news/california-to-usher-in-era-of-driverless-cars> [10 January 2013]

PE. (2013a) 'Convoy offers alternative to HS2'. Professional Engineering article published on 01/05/2013 [online] available from <connection.ebscohost.com/c/letters/87714518/convoy-offers-alternative-hs2> [1 June 2013]

PE. (2013b) 'Driverless Cars 20 years away'. Professional Engineering article published on 7/05/2013 [online] available from <profeng.com/news/driverless-cars-20-years-away> [30 June 2013]

PRISM. (2002) 'Proposed Reduction of Car Crash Injuries through Improved Smart Restraint Development Technologies'. Research Project website [online] available from <www.prismproject.com> [15 November 2013]

PRISM. (2003a) 'Driver Dynamic Response Study. Technical Report [online] available from <www.prismproject.com/PRISM%20Task%201.5_TRL_simulator%20study_final.pdf> [15 March 2012]

PRISM. (2003b) 'Investigate Occupant Position By Photographic Studies'. Technical Report [online] available from <www.prismproject.com/Task%201.4%20R4A%20Final%20report_a.pdf> [15 March 2012]

Prüggler, A., Huber, P. (2011a) 'Implementation Of Reactive Human Behaviour In A Numerical Human Body Model Using Controlled Beam Elements As Muscle Element Substitutes'. ESV2011 International Conference [online] available from <www-nrd.nhtsa.dot.gov/pdf/esv/esv22/22ESV-000154.pdf>. Held 13-16 June 2011 at Washington DC [12 January 2012]

Prüggler, A., Huber, P. (2011b) 'Detailed Analysis Of 3d Occupant Kinematics And Muscle Activity During The Pre-Crash Phase As Basis For Human Modelling Based On Sled Tests'. ESV2011 International Conference [online] available from <www-nrd.nhtsa.dot.gov/pdf/esv/esv22/22ESV-000162.pdf>. Held 13-16 June 2011 at Washington DC [12 January 2012]

Ray, P., Newbery, T., Koziol, J. (2006) 'Quantifying the Change in Ride Height Due to Braking: Brake Dive Test Data'. Case Forensics, SAE Technical Paper Series, 2006-01-1563, Society of Automotive Engineers

Richard, M.G. (2013) 'Nissan Gives Rides in Self-Driving Electric LEAF at Japan's CEATEC Show (Videos)'. Article [online] available from <www.treehugger.com/cars/semi-autonomous-nissan-leaf-electric-car-cleared-road-testing-japan.html> [31 October 2013]

Rodarius, C., Van Rooij, L., de Lange R. (2007) 'Scalability Of Human Models'. ESV2007 International Conference, Paper number: 07-0314 [online] available from <www-nrd.nhtsa.dot.gov/pdf/esv/esv20/07-0314-O.pdf>. Held 18-21 June 2007 at Lyon, France [12 January 2012]

Rubens, P. (2013) 'Crash tests – Not for dummies'. Article [online] available from <www.bbc.com/future/story/20130408-crash-tests-not-for-dummies> [9 April 2013]

Ruff, C., Eicehnberger, A., Jost, T. (2006) 'Simulation of an airbag deployment in Out-of-Position', LS-Dyna European Conference [online] available from <online.tugraz.at/tug_online/voe_main2.getVollText?pDocumentNr=52507&pCurrPk=30190>. Held at Ulm, Germany [12 January 2012]

SARTRES. (2011) 'Safe Road Trains For the Environment'. European Project [online] available from <www.sartre-project.eu/en/Sidor/default.aspx> [1 July 2013]

SARTRES. (2012) 'Platooned traffic can be integrated with other road users on conventional highways'. Article [online] available from <www.sartre-project.eu/en/press/Documents/SARTRE%20final%20partner%20release.pdf> [1 July 2013]

Schneider, L., Olson, P., Anderson C., Post D. (1979) 'Identification of Variables Affecting Driver Seated Position'. MVMA Project No: 4.38. November 1979 [online] available from < deepblue.lib.umich.edu/bitstream/handle/2027.42/510/44894.0001.001.pdf?sequence=2> [30 September 2010]

Stubbs, D. (2010) 'Development of A Simulation Failure Method To Represent Airbag Fabric Failure'. Unpublished MSc thesis. Coventry University

Stubbs D. (2013) 'Vehicle Signal Analysis'. Unpublished Course Notes. Coventry University

Subramanian, J.K. (2010) 'Airbag Permeability Correlation Using MADYMO". Unpublished MSc thesis. Coventry University

TASS. (2010) 'MADYMO 7.0 Theory and User Manual'. Printed user manual. Delft, NL, TASS International

TASS. (2013) 'MADYMO Quality report. Active Human 50th Facet Q Model, Version 1.1 (R7.5). Report number: QAHM50FC-290813'. Technical Report [online] available from <0eca4fe331aaaa0387ab-39017777f15f755539d3047328d4a990.r16.cf3.rackcdn.com/active_human_50th_QR_conf_v3.pdf> [10 September 2013]

TEXTEST. (2010) 'Air Permeability'. Hardware Technical Information [online] available <www.aticorporation.com/textest.jsp> [17 February 2010]

Thatcham. (2011) 'Autonomous Emergency Braking'. Unpublished seminar presentation. Held 17 June 2011 at MIRA, Nuneaton, UK

Thatcham. (2013a) 'Thatcham Insight Stop the Crash! '. Technical Report [online] available from <www.thatcham.org/files/pdf/Thatcham_Insight_2nd_AEB.pdf> [8 July 2013]

Thatcham. (2013b) 'Auto Braking Cars: Government should meet motorist halfway '. News and Press Release [online] available from <www.thatcham.org/news-and-events/news-and-press-releases-reader/items/stop-the-crash > [16 May 2014]

Thatcham. (2014), 'Auto Braking Cars: Government Should Meet Motorists Halfway'. Press Release [online] available from <www.thatcham.org/ news-and-events/news-and-press-releases-reader/items/stop-the-crash> [14 June 2014]

The AA (2011) 'Active Safety'. News and Press Release [online] available from <www.theaa.com/motoring_advice/car-buyers-guide/cbg_safety.html> [18 June 2014]

TNO. (2011) 'user_instructions_active_human.pdf". [Computer file]. Unpublished User manual for initial setup file provided before the proposed amendments, September 2011

TNO. (2012) 'MADYMO, Human Body Models Manual, Release 7.4.1'. User Manual [online] available from <8bd730766c473bba5f62-39017777f15f755539d3047328d4a990.ssl.cf3.rackcdn.com/downloads/Human Models.pdf> [1 June 2012]

Toyota. (2010) 'THUMS (Total Human for Safety)'. Technical Information [online] available from < www.toyota-global.com/innovation/safety_technology/ safety_measurements/thums.html> [1 June 2011]

Traffic Technology International. (2013) 'Ready or Waiting '. Press Release [online] available from <zmags.com/publication/38bd52e3#/38bd52e3/6> [17 January 2013]

TRW. (2011) 'TRW Defines New Level of Safety with Integration of Active Seatbelt and Automatic Emergency Braking Systems'. Press Release [Online] available from < Ir.Trw.Com/Releasedetail.Cfm?Releaseid=550539> [6 March 2012]

UNECE. (2008) 'Global Technical Regulation 9. Pedestrian Safety'. Legislative Report [Online] available from < www.unece.org/trans/main/wp29/wp29wgs/wp29gen/wp29registry/gtr9.html > [14 June 2014]

USPTO. (2013) 'United States Patent and Trademark Office'. Patent database [online] available from < patft.uspto.gov/netahtml/PTO/index.html> [10 October 2013]

VCA. (2013) 'Vehicle Certification Agency', Vehicle Legislation Approvers [online] available from <www.dft.gov.uk/vca> [16 July 2013]

Vezin, P., Verriest, J.P. (2005) 'Development of a Set of Numerical Human Models for Safety', ESV2005 International Conference [online] available from <www-nrd.nhtsa.dot.gov/pdf/esv/esv19/05-0163-O.pdf>. Held 6-9 June 2005 at Washington DC [12 January 2012]

Vicon. (2012). 'Vicon Software'. Technical Information [online] available from <www.vicon.com/> [22 March 2012]

Vignau, R. (2011) 'Integrating systems inside and outside the vehicle', CARHS conference proceedings. Held 25 May 2011 at Aschaffenburg, Germany

WHO. (2013) 'Global Status Report On Road Safety 2013'. Technical Report (World Health Organisation) [online] available from <www.who.int/violence_injury_prevention/road_safety_status/2013/report/en/> [1 June 2013]

Vislab. (2013) 'PROUD-Car Test 2013'. Technical information [online] available from <vislab.it/vislab-events-2> [4 September 2013]

VTC2013-Fall. (2013) 'From ADAS to ADAS'. Technical information (IEEE 78th Vehicular Technology Conference) [online] available from <www.ieeevtc.org/vtc2013fall/plenary.php> [1 November 2013]

Wilson, G., Kingdom, C., Bastien, C., Christensen, J. (2013) 'Intelligent Design: The Multifunctional Design Method as Applied to Vehicular Light Weighting'. EVS27 International Symposium Proceedings. Held 17-20 November 2013 at Barcelona, Spain

Appendix A: List of Publications

As part of the research undertaken, this thesis has generated the following publications:

- C. Bastien, Blundell M, Stubbs D., Christensen J., Hoffmann J., Freisinger M., Van der Made R., "Correlation of Airbag Fabric Material Mechanical Failure Characteristic for Out of Position Applications", ISMA 2010, Leuven, September 2010.
- C. Bastien, Investigation into injuries of Out-of-Position (OoP) posture occupants and their implications in active safety measures, ICRASH2010 International Crashworthiness Conference, paper 2010-023, Washington DC, September 2010.
- Bastien C., Blundell M., Hoffmann J., Freisinger M., Van der Made R., Neal-Sturgess C., "Investigation Of Pre-Braking On Unbelted Occupant Position And Injuries Using An Active Human Body Model (AHBM)", ESV 2011, Washington DC, June 2011.
- C. Bastien, A. Diederich, M. Freisinger, J. Hoffmann, R. Van Der Made, M. V Blundell, C. Neal-Sturgess, P. Huber, A. Prueggler, " Influence of human bracing on occupant's neck, head and thorax injuries in emergency braking combined with an FMVSS208 impact scenario ", ICRASH2012, International Crashworthiness Conference, Milano, July 18th, 2012.
- Bastien C., Neal-Sturgess C., Blundell M., "Influence of vehicle secondary impact following an emergency braking on an unbelted occupant's neck, head and thorax injuries", International Journal of Crashworthiness, March 2013.
- Bastien C., Neal-Sturgess C., Blundell M., Hoffmann J., Freisinger M., Van der Made R., "Safety Assessment Of Autonomous Emergency Braking Systems On Unbelted Occupants Using A Fully Active Human Model", ESV2013, Korea, June 2013.

1

Appendix B: MADYMO Command Lines

Positioning of the Active Human Model

In order to perform a positioning run, the state of the flexible bodies in the thorax and the abdomen should be set to rigid. To achieve this, the following XML instructions are needed (only in the gravity loading case) and must be removed later on when equilibrium has been achieved.

```
<STATE.BODY
    BODY_LIST="
    Abdomen1_flexbod
    Abdomen2_flexbod
    Abdomen3_flexbod
    Abdomen4_flexbod
    Thorax1_flexbod
    Thorax2_flexbod
    Thorax3_flexbod
    Thorax4_flexbod"
    SWITCH="lock_switch"
 />
<SWITCH.TIME
    DESCRIPTION="switch is always 0, to lock joints"
    ID="99"
    NAME="lock_switch"
    TIME="0"
    INVERT="ON"
 />
```

As can be seen, at t=0s all the ***_flexbod**ies are locked at the beginning of the simulation (**TIME="0").**

Once the joint re-mapping is performed after the gravity loading, the lines above must be moved to <DISABLED>.

Creating Contracts between the Active Human Model and Multi-Body Components.

In the example provided, the Master surface is the sled model which is a group of multi-body entities (can be planes, ellipsoids), depicted in the command **MASTER_SURFACE="/sled_gmb"**. It is good practice to have the rigid structure (sled) as the Master segment and the deformable structure as Slave (human).

The deformable part is the human model which contact type is set to **SLAVE_SURFACE="/HumanMale50%/HumanBody_gfe"**. In the example given, the friction value between the seat and the human model is set to 0.3.

```
<CONTACT.MB_FE
    ID="1"
    NAME="human_to_sled_cmbfe"
    MASTER_SURFACE="/sled_gmb"
    SLAVE_SURFACE="/HumanMale50%/HumanBody_gfe"
    >
    <CONTACT_FORCE.CHAR
      CONTACT_TYPE="SLAVE"
      FRIC_FUNC="/occupant_to_interior_frict_fun"
      >
      <FUNC_USAGE.2D
        FUNC="/occupant_to_interior_frict_fun"
        Y_SCALE="0.3"
      />
  <FUNCTION.XY
    ID="6"
    NAME="occupant_to_interior_frict_fun"
    >
    <TABLE
      TYPE="XY_PAIR"
      >
<![CDATA[
| XI     YI  |
       0.0    1.0
       50.0   1.0
]]>
    </TABLE>
  </FUNCTION.XY>
```

Creating Contracts between the Active Human Model and Finite Element Components

In the example provided, the Master surface is the sled model which is a group of multi-body entities (can be planes or ellipsoids), depicted in the command **MASTER_SURFACE="/…/steering_wheel_gfe**", which is a group of finite element entities. It is good practice to have the rigid structure (steering wheel) as the Master segment and the deformable structure as Slave (human neck).

The deformable part is the human model whose contact type is set to **SLAVE_SURFACE= "/HumanMale50%/Neck_gfe"**.

The contact stiffness is ruled by the stiffness of the stiffness of the Slave, here the Neck.

```
<CONTACT.FE_FE
  ID="28"
  NAME="neck_to_strg_wheel_cfefe"

MASTER_SURFACE="/steering_wheel_sys/steering_wheel_fem/steering_wheel
_gfe
  SLAVE_SURFACE=""/HumanMale50%/Neck_gfe"
  >
  <CONTACT_METHOD.NODE_TO_SURFACE_CHAR
    FACE_TYPE="FRONT"
    >
    <CONTACT_FORCE.CHAR
      CONTACT_TYPE="MASTER"
      FRIC_FUNC="steeringwheel_to_occupant_friction_fun"
    />
    <INITIAL_TYPE.CHECK/>
  </CONTACT_METHOD.NODE_TO_SURFACE_CHAR>
</CONTACT.FE_FE>
```

Output of Active Human Model Finite Element nodes kinematics

Some key bio-mechanical marker positions on the AHBM can be output in a CSV (Comma Separated Variable) file. The typical chin (node 1601) position output.

```
<OUTPUT_NODE
    ID="1"
    NAME="chin_node_out"
    NODE_LIST="16011"
    BODY="/frame_sys/frame_bod"
    >
    <SELECT.POS
      WRITE_ALL="ON"
    />
  </OUTPUT_NODE>
```

The Chin point is attached to node 16011 for which all positions X, Y, Z and the resultant will be output in a CSV file for later analysis.

The following flags can be added if wished for more specific outputs (Rotations, Velocities and Accelerations as listed below).

```
<SELECT.ROT
WRITE_ALL="ON"
/>
<SELECT.ACC
WRITE_ALL="ON"
/>
<SELECT.VEL
WRITE_ALL="ON"
/>
<SELECT.ACC
WRITE_ALL="ON"
/>
```